SYNTHESIS AND CHARACTERIZATION OF BENTONITE CLAYS MODIFIED WITH CETYLTRIMETHYLAMMONIUM BROMIDE FOR THE TREATMENT OF CRUDE OIL POLLUTION IN WATER

BY

EMEKA THOMPSON NWANKWERE

DEPARTMENT OF CHEMISTRY
AHMADU BELLO UNIVERSITY, ZARIA

APRIL 2015

SYNTHESIS AND CHARACTERIZATION OF BENTONITES MODIFIED WITH CETYL TRIMETHYLAMMONIUM BROMIDE FOR THE TREATMENT OF CRUDE OIL POLLUTION IN WATER

BY

Emeka Thompson NWANKWERE,
BSc INDUSTRIAL CHEMISTRY (ABSU) 2005,
MSc ANALYTICAL CHEMISTRY (ABU) 2010
PhD/SCI/14246/2011-2012

A THESIS SUBMITTED TO THE SCHOOL OF POSTGRADUATE STUDIES, AHMADU BELLO UNIVERSITY IN PARTIAL FULFILMENT OF THE REQUIREMENTS FOR THE AWARD OF DOCTOR OF PHILOSOPHY IN CHEMISTRY

DEPARTMENT OF CHEMISTRY,
FACULTY OF SCIENCE
AHMADU BELLO UNIVERSITY, ZARIA
NIGERIA

APRIL, 2015

DECLARATION

I declare that the work in the thesis entitled **Synthesis and characterization of bentonites modified with cetyl trimethylammonium bromide for the treatment of crude oil pollution in water** has been performed by me in the Department of Chemistry, under the supervision of Professor C. E. Gimba, Professor G. I. Ndukwe and Dr. K A. Isuwa. The information derived from the literature has been duly acknowledged in the text and a list of references provided. No part of this Thesis was previously presented for another degree or diploma at this or and other Institution.

Emeka Thompson NWANKWERE ---------- ----------

Signature Date

CERTIFICATION

This project thesis entitled SYNTHESIS AND CHARACTERIZATION OF BENTONITES MODIFIED WITH CETYL TRIMETHYLAMMONIUM BROMIDE (CTAB) FOR THE TREATMENT OF CRUDE OIL POLLUTION IN WATER by Emeka Thompson NWANKWERE meets the regulation governing the degree of PhD Analytical Chemistry of the Ahmadu Bello University, and is approved for its' contribution to knowledge and literary presentation.

Prof. C. E. Gimba	_____	_____
Chairman, Supervisory Committee	Signature	Date
Prof. G. I. Ndukwe	_____	_____
Member, Supervisory Committee	Signature	Date
Dr. K. A. Isuwa	_____	_____
Member, Supervisory Committee	Signature	Date
Prof. V. O. Ajibola	_____	_____
Head of Department	Signature	Date
Prof. A. Z. Hassan	_____	_____
Dean, School of Postgraduate Studies	Signature	Date

DEDICATION

This Thesis is dedicated to my country, Nigeria

ACKNOWLEDGEMENT

My deep gratitude goes to my mentor, Professor C. E. Gimba. I am amazingly blessed to have a supervisor who gave me the liberty to explore on my own and at the same time the guidance to recover when my steps faltered. Also to my second supervisor Professor G. I. Ndukwe who, filled with wisdom and Organic Chemistry, gave me a thorough breakdown on the go about of this work and constantly reminds me the aphorism "it is well". His support helped me stay strong when research became frustrating and things seemed like they were falling apart. I am also grateful to Dr. K. A. Isuwa, my third supervisor, for his patience in going through this bulky details and his significant contribution to the completion of this work.

I am thankful to my lecturers and senior colleagues, Dr. N. B. Afolabi-Balogun of Centre for biotechnology research and training, Ahmadu Bello University Zaria, who gave me the "CTAB" used in the research; Dr. Calvin O. Nwokem, of the Department of Chemistry, Kaduna state University, who gave me lots of advice and the Borno Bentonite with all kindness. Dr. Daniel J. Adeyemo, of Centre for Energy Research and Training (CERT) Zaria, who personally took care of the radioanalytical aspect of this research. I am also indebted to Mr Oche Ochigbo of the Analytical Chemistry Lab, Ahmadu Bello University Zaria, of course, without him this research may have taken ages to complete.

I deeply appreciate all my colleagues and lab-mates. To Dr. Moses Yilleng who helped greatly in the XRD and BET analysis and interpretation in this research. Edwin Ogwuche (Schro), David Ebuka Arthur, Oluwaseye Adedirin, Adedayo Adebiyi, Ahmed Adetoro, Zaharadeen Garba and also Kenneth Alau for the philosophical discussions, the sleepless nights to meet deadlines, the hope for good results and the shared disappointments with each failed attempt. It is true that Iron sharpens Iron. I am particularly thankful to Stan Njiga and Uche Ndidi for their constant motivation. To John Anyam, my brother and an alternative to google.com, who is always liberal with his knowledge and academic resources. To Ifeanyi Nduka an extraordinary fellow who always knows what to say to keep one advancing. I think every researcher should talk with him.

I am also grateful to all my friends who helped me stay sane through these difficult years, supporting with good advice, company, chemicals, food and other helpful resources.To begin with, I must thank my friends Muyideen Babalola Bolarin and Yahaya Shuaib, who on several occasions gave me their place to stay (and their food too) when I could not sleep in the laboratory. To Lekan Habeeb, Gideon Soremekun, Justina John, Isaac Audu, Mbavan Ingya, Uzoma Ogelle, Nnamdi Idam, Nonso Ojiude, Theophilus Arebame and Gloria Joseph. I greatly value their friendship and deeply appreciate their belief in me. I am strongly convinced that their contributions and prayers played a great role in this research.

I am mostly grateful to my parents, my backbone- Barr. Thompson and Mrs Chidi Nwankwere- for providing me with an adequate blend of patience and impatience towards

the completion of this work and for all the financial and moral support they provide. Also to Alaba Nwankwere for all her cheer and help with the massive print work. Much appreciation goes to my brothers, Dr. Bob, Dr. Ndy, Mr Chima and Barr. Ifeanyi, for their slow but steady financial support, open ears and prayers. Their support and care helped me overcome stress and stay focused on the PhD program.

Finally and most importantly, my deepest gratitude goes to God Almighty, the First and the Last, who made it possible that all these people be available at the point, provided me with good health and technical support, protected me from laboratory hazards and gave me the wisdom to use the opportunity. I am eternally thankful.

ABSTRACT

Three types of Nigerian bentonite based nanoclays – Potassium (sample A), Calcium (Sample B) and Sodium (Sample C) bentonites– were investigated for their potential as oil spill sorbents after modification with Cetyltrimethylammonium Bromide (CTAB). The nanoclay samples were purified and subjected to hydrothermal ion exchange reaction to synthesize organoclays under mild reaction conditions. Changes in the microstructural, morphological and physicochemical properties of the modified clays caused by the intercalation of CTA^+ cations before and after the synthesis procedure were investigated. The changes in the chemical profile of the clays were studied by X-Ray Flouresence (XRF) and Neutron Activation Analysis (NAA). Crystallographic studies by X-Ray Diffraction (XRD), show higher intercalation time and surfactant loading, produce organoclays with higher basal spacing and more efficient oils sorption capacities. These observations were further explained by Fourier Transform Infrared (FTIR), Scanning Electron Microscopy (SEM) and Thermal Gravimetric Analysis (TGA). The presence of new (organic) groups in the characteristic bentonite structure of the nanoclays is prime evidence of successful synthesis. The organoclays were further tested in a simulated oil spill situation to assess their potential as oil sorbents and sorbed about 5 times their weight in water. To understand the manner and mechanism of the sorption procedure, batch kinetic and equilibrium studies were carried out using kinetic and equilibrium isotherm models. The kinetic data was best described by the Pseudo-second-order rate model (R^2 = 0.999, 0.990 and 0.9975 for the organoclay Samples 2, 5 and 15 respectively) demonstrating that the sorption procedure and mechanism was by chemisorption and that more than one process may have occurred during the procedure. The Langmuir isotherm model best described the manner of crude oil sorption (R^2 = 0.9968, 0.997 and 0.9936 for samples 2, 5 and 15 respectively) as predominantly monolayer. The results showed that these natural clays can be modified and used for the treatment of oil spillage. The organoclays present a cost effective and a suitably environmentally friendly alternative for the remediation of oil spill polluted lands in the Niger Delta region of Nigeria.

TABLE OF CONTENTS

Title Page i

Declaration ii

Certification iii

Dedication iv

Acknowledgement v

Abstract vii

Table of Contents viii

List of Tables xiv

List of Figures xv

List of Appendices xix

List of Abbreviations xxi

1.0 INTRODUCTION 1

1.1 Clay Minerals 4

1.2 Organoclays 5

1.3 Statement of the Problem 6

1.4 Justification for the Research 7

1.5 Aim and Objectives 9

2.0 Literature Review 11

2.1 Oil Spillage 11

2.2 Oil spillage in the Nigerian Niger-Delta 11

2.3 Effect of Oil Spillage in the Environment 14

2.4 The Toxic Contents of Crude Oil 17

2.4.1 Toluene 18

2.4.2 Benzene 19

2.4.3 Cresols (a group of Phenolic compounds) 20

2.4.4 Polynuclear Aromatic Hydrocarbons (PAH) 21

2.5 Oil Spill Response Techniques 23

2.5.1 Mechanical recovery 24

2.5.2 Chemical methods 26

2.5.3 In-situ burning 28

2.5.4 Bioremediation 29

2.5.5 Natural removal 30

2.6 Sorbent for Oil Spillage Treatment 31

2.6.1 Types of Sorbents 32

2.7 Clays 34

2.7.1 Smectite Clays 35

2.7.2 Bentonites 36

2.8 Organoclays 38

2.8.1 Application of organoclays 40

3.0 MATERIALS AND METHODS 42

3.1 Materials 42

3.2 Methods 44

3.2.1 Sample Preparation 44

3.2.2 Physicochemical characterization of clay samples 45

3.2.2.1 Bulk density determination 45

3.2.2.2 Moisture content (MC) determination 45

3.2.2.3 Volatile matter content (VMC) determination 46

3.2.3 X-Ray Florescence (XRF) Analysis 47

3.2.4 Scanning Electron Microscopy (SEM) 48

3.2.5 Thermal Gravimetric Analysis 48

3.2.6 Brauner-Emmet-Teller (BET) Analysis 49

3.2.7 X-ray Diffraction (XRD) Analysis 50

3.2.8 Fourier Transform Infra-Red (FTIR) Analysis 51

3.2.9 Neutron Activation Analysis 51

3.2.10 Purification of Clays 53

3.2.11 Organoclay synthesis 54

3.2.12 Removal of hydrocarbon spill from water surface 56

4.0 RESULTS 57

4.1 Physicochemical properties of raw and organically modified bentonites 57

4.1.1 Effect of intercalation properties on weigh on Bulk Density 61

4.2 X-Ray Fluorescence Analysis 65

4.3 Neutron Activation Analysis 67

4.4 X-Ray Diffraction Analysis 72

4.5 Fourier Transform Infrared Spectral Analysis 81

4.6 Thermal Gravimetric Analysis 91

4.7 Scanning Electron Micrographs of Raw and Modified Bentonites 99

4.8 Sorption Studies of Crude Oil on Bentonites and Organoclays 106

4.8.1 The effect of sorbent dosage on oil sorption capacity 107

4.8.2 The effect of initial oil concentration on oil sorption capacity 108

4.8.3 The effect of contact time on the oil sorption capacity 109

4.8.4 Equilibrium sorption studies 110

4.8.5 Kinetic Isotherm studies 116

5.0 DISCUSSION 122

5.1 Physicochemical Characterization of Raw and Modified Nanoclays 122

5.1.1 Proximate characteristics 122

5.1.2 Brauner-Emmet-Teller (BET) Analysis 123

5.1.3 pH in solution 124

5.1.4 Bulk Density 124

5.2 X-Ray Florescence (XRF) Analysis 127

5.3 Neutron Activation Analysis (NAA) 128

5.3.1 Interlayer/Exchangeable cations. 128

5.3.2 Octahedral Sheet Cations 129

5.3.3 Trace elements content 130

5.4 X-Ray Diffraction (XRD) Analysis 130

5.4.1 The effect of reaction time on the d(001) spacing 131

5.4.2 The effect of surfactant loading on d(001) spacing 132

5.4.3 The effect of temperature on intercalation 133

5.4.4 The effect of surfactant type on intercalation 134

5.5 Fourier Transform Infrared (FTIR) Analysis 135

5.6 Thermo-Analytical Studies 137

5.7 Scanning Electron Microscopy 140

5.8 Sorption Studies 141

5.8.1 Sorption of crude oil on clay and organoclay samples 142

5.8.2 Equilibrium Sorption Studies 145

5.8.3 Kinetics Sorption Studies 150

6.0 SUMMARY, CONCLUSION AND RECOMMENDATIONS 156

6.1 Summary 156

6.2 Conclusion 157

6.3 Recommendations 158

REFERENCES 159

APPENDICES 183

LIST OF TABLES

Table 3.1. Design of the experimental conditions for organoclay synthesis 55

Table 4.1. Physicochemical properties of raw and organo-modified clays 59

Table 4.2. Physical conditions for the synthesis of organoclays 60

Table 4.3. Regression statistics of the linear (predicted) residual plots of time and concentration on bulk density 64

Table 4.4. Analysis of variance for time and concentration effect on bulk density 64

Table 4.5. The chemical composition raw and modified clay samples by XRF analysis 66

Table 4.6. Results of Instrumental Neutron Activation Analysis 68

Table 4.7. Assignment of IR Bands for functional groups 83

Table 4.8. Results TGA and DSC analysis 93

Table 4.9. The regression parameter of the equilibrium isotherm models 115

Table 4.10. The regression parameters describing the kinetic models 121

LIST OF FIGURES

Figure 1.1:	Typical crystalline structure of layered silicates nanoclays	5
Figure 2.1:	Structure of toluene	19
Figure 2.2:	Structure of benzene	20
Figure 2.3:	Structures of cresols	21
Figure 2.4:	Structures of selected polyaromatic hydrocarbons	22
Figure 3.1:	Map of sampling location of bentonites	42
Figure 3.2:	Structure of Cetyl trimethylammonium bromide	43
Figure 3.3:	Structure of Cetyl trimethylammonium chloride	43
Figure 4.1:	Linear and non-linear regression plots for the effect of time on bulk density	62
Figure 4.2:	Linear and non-linear regression plots of the effect of concentration on bulk density	63
Figure 4.3:	Concentrations of interlayer/exchangeable ions in samples as determined by NAA	69
Figure 4.4:	Concentrations of octahedral sheet minerals in samples as determined by NAA	70
Figure 4.5:	Concentrations of trace metals in samples as determined by NAA	71
Figure 4.6:	XRD crystallographic pattern for sample A	73
Figure 4.7:	XRD crystallographic pattern for sample B	74

Figure 4.8:	XRD crystallographic pattern for sample C	75
Figure 4.9:	Superimposition of the XRD patterns of samples A, B and C	76
Figure 4.10:	Effect of time on intercalation: XRD diffractograms of samples A, 2, 10, 11 and 13	77
Figure 4.11:	The effect of surfactant loading on intercalation: XRD diffractograms of samples C, 14, 15, 16 and 17	78
Figure 4.12:	Effect of temperature on intercalation: XRD diffractograms of samples B, 4, 5, 6 and 9	79
Figure 4.13:	Effect of salt type on intelrcalation: XRD diffractograms of samples A, B, C, 1, 2 and 15.	80
Figure 4.14:	FTIR Spectra of sample A	84
Figure 4.15:	FTIR Spectrum of sample B	85
Figure 4.16:	FTIR spectrum of sample C	86
Figure 4.17:	FTIR spectra of clays and their corresponding organoclays, illustrating the effect of intercalation (samples A, B, C, 2 and 5)	87
Figure 4.18:	FTIR spectra of sample A and organoclay samples 2, 10 and 11 intercalated over the time range of 1 to 12 hours, illustrating the effect of time on intercalation	88
Figure 4.19:	Infrared spectra of sample C and organoclays 15, 16 and 17 intercalated over CTAB concentration range of 0.2 to 4.0 w/w of clay, illustrating the effect of surfactant loading on intercalation	89
Figure 4.20:	FTIR spectra of sample B, 4 and 6 illustrating the effect of temperature on intercalation	90
Figure 4.21:	Thermogram of sample A	94

Figure 4.22: Thermogram of sample B 95

Figure 4.23: Thermogram of sample C 96

Figure 4.24: Thermogram of sample 2 97

Figure 4.25: Thermogram of sample 5 98

Figure 4.26: SEM micrograph of sample A 100

Figure 4.27: SEM micrograph of sample 2 101

Figure 4.28: SEM micrograph of sample B 102

Figure 4.29: SEM micrograph of sample 5 103

Figure 4.30: SEM micrograph of sample C 104

Figure 4.31: SEM micrograph of sample 8 105

Figure 4.32: Effect of sorbent dosage on the sorption capacity 107

Figure 4.33: Effect of initial oil concentration on oil sorption capacity 108

Figure 4.34: Effect of contact time on the oil sorption capacity 109

Figure 4.35: The linearized Langmuir isotherm for organoclay samples 112

Figure 4.36: The linearized Freundlich sorption model for organoclay samples 113

Figure 4.37: The linearized Dubinin Radushkevich model for organoclays samples 114

Figure 4.38: The pseudo-second-order rate equation model for organoclay samples 118

Figure 4.39: The Elovich kinetic model for the sorption of crude oil 119

Figure 4.40: The Weber and Morris diffusivity model 120

LIST OF APPENDICES

Appendix I:	X-Ray diffractogram of sample 1	183
Appendix II:	X-Ray diffractogram of sample 2	183
Appendix III:	X-Ray diffractogram of sample 3	184
Appendix IV:	X-Ray diffractogram of sample 6	184
Appendix V:	X-Ray diffractogram of sample 5	185
Appendix VI:	X-Ray diffractogram of sample 6	185
Appendix VII:	X-Ray diffractogram of sample 9	186
Appendix VIII:	X-Ray diffractogram of sample 10	186
Appendix IX:	X-Ray diffractogram of sample 11	187
Appendix X:	X-Ray diffractogram of sample 12	187
Appendix XI:	X-Ray diffractogram of sample 13	188
Appendix XII:	X-Ray diffractogram of sample 16	188
Appendix XIII:	X-Ray diffractogram of sample 17	189
Appendix XIV:	X-Ray diffractogram of sample 15	189
Appendix XV:	FTIR spectra of sample 2	190
Appendix XVI:	FTIR spectra of sample 3	190

Appendix XVII: FTIR spectra of sample 4 191

Appendix XVIII: FTIR spectra of sample 5 191

Appendix XIX: FTIR spectra of sample 6 192

Appendix XX: FTIR spectra of sample 9 192

Appendix XXI: FTIR spectra of sample 10 193

LIST OF ABBREVIATIONS

ANOVA	Analysis of Variance
API	American Petroleum Institute
ASTM	American Standards for Testing and Materials
ATSDR	Agency for Toxic Substances and Disease Registry
BD	Bulk Density
BET	Brunauer Emmet Teller
BTEX	Benzene, Toluene, Ethylbenzene and Xylene
CEC	Cation Exchange Capacity
Conc	Concentration
CTA^+	Cetyltrimethylammonium cation
CTAB	Cetyltrimethylammonium Bromide
CTAC	Cetyltrimethylammonium Chloride
DCB	Dithionite, Citrate and Bicarbonate
DPR	Department of Petroleum Resources
D-R	Dubinin-Radushkevich
DTG	Differential Thermal Gravimetry

FEN	Friends of the Earth Netherlands
FTIR	Fourier Transform InfraRed
$HDTMA^+$	HexaDecylTrimethylAmmonium ion
HMW	High Molecular Weight
K_F	Freundlich constant
KRPC	Kaduna Refining Petroleum Corporation
MC	Moisture content
MNSR	Miniature Neutron Source Reactor
n	degree of favourability in adsorption
NAA	Neutron Activation Analysis
NAPL	Non Aqueous Phase Liquids
NIRR-1	Nigerian Research Reactor 1
OSC	Oil Sorption Capacity
PAH	Polycyclic Aromatic Hydrocarbons
PSOR	Pseudo-second-order rate
qD	Weber and Morris Diffusion coefficient
Qe	Equilibrium sorption Capacity

Qo	Initial sorbate concetration
R^2	Coefficient of Regression
R_L	Langmuir separation factor
SA	Surface Area
SPDC	Shell Petroleum Development Company
Temp	Temperature (T)
TGA/DSC	Thermal Gravimetric Analysis/Differential Scanning Calorimetry
UNDP	United Nation Development Program
USACE	United States Army Corps of Engineering
USDOA	United States Department of Agriculture
USEPA	United States Environmental Protection Agency
VMC	Volatile Matter Content
WMIDM	Weber and Morris Intra Diffusion Model
XRD	X-Ray Diffraction

1.0 INTRODUCTION

Oil is the life blood of our modern industrial society. It fuels the machineries and lubricates the wheels of the world's production (Tahir and Mustaque, 2005; Adebiyi and Adeyemi, 2010). It is one of the most important energy and raw material resource for synthetic polymers and chemicals worldwide (Annunciado *et al.,* 2005). However, when this vital resource is out of control, it can destroy lives and devastate the environment and economy of a particular region (Aynechi, 2004; Tahir and Mustaque, 2005).

An oil spill is the release of a liquid petroleum hydrocarbon into the environment due to human activity, and is a form of pollution (Rusu, 2010; Adelana *et al.*, 2011). The term often refers to marine oil spills, where oil is released into the ocean or coastal waters. The oil may be a variety of materials, including crude oil, refined petroleum products (such as gasoline or diesel fuel) or by-products, oily refuse or oil mixed with waste. Spills take months or even years to clean up (Adelana *et al.,* 2011). Due to its destructive properties, once an area has been contaminated with oil, the whole character of the place is damaged and when it encounters something to cling to, whether it be a beach, a rock, the feathers of a duck or a bathers hair, it does not readily let go (Aynechi, 2004). Hence, pollution by petroleum oils affects sea life, economy, tourism and leisure activities because of the coating properties of these materials (Hussein *et al.,* 2008).

There are countless opportunities for oil to go out of control (Al Malek and Mohamed, 2005). Many are due to mechanical failure of the equipment, to deliberate act or due to human carelessness or mistakes (Anderson and LaBelle, 2000; Aynechi, 2004; Al Malek and Mohamed, 2005; Adelana *et al.*, 2011). According to the United Nations Development

Program (UNDP, 2006), Niger Delta human development report, spills occur accidentally and also through the deliberate actions of the local people, who sabotage pipelines in protest against the action of the Federal Government and oil companies. There are also risks implicated in the materials involved and the means of transporting the oil. The risks involve terminals, loading docks, refineries, tankers, freighters and pipelines, tanks, trucks, filling stations, just to name a few (Aynechi, 2004, Wang *et al.*, 2013). In addition, the changing pattern of refining location has significantly increased the proportion of crude products moved over greater distances (Jagger, 1970). The increasing movement and storage of products has also increased the risk of instant water contamination (Jagger, 1970; Yammama, 1997).

The environmental effects of oil pollution are well known. They include the degradation of forest and depletion of aquatic fauna. Long term impacts are also possible, as in cases where mangrove swamps and ground water resources are harmed. In aquatic habitat, oil can be toxic to the frogs, reptiles, fish, water fowl and the animals that live in or other wise use the water (United State Environmental Protection Agency -USEPA, 2004a). Oiling may affect not only wild life but also plants that are rooted in or float in water, harming both the plants and the animals that depend on them for food and shelter. The implications of these findings are frightening, given that human health is tied to the food web (UNDP, 2006).

Spilled oil has an undesirable taste and odour and causes several environmental damages on water fowl, material life and affects tourisms and economy (Kingston, 2002). They harm the beauty of polluted sites; the strong odour can be felt miles away and the excessive growth of green algae alters sea colour and the landscape (Annunciado *et al.*, 2005). Cleaning up an oil contaminated area is time consuming, difficult and very costly. The term costly does not refer

only to the amount of money needed for the clean-up, but also to the destruction of wild life and fish, damage to properties, contamination of public water supplies and many other losses. These losses may extend for months or years (Stanley, 1969).

The adverse impact to ecosystems and the long term effect of environmental pollution call for an urgent need to develop a wide range of materials for cleaning-up oil from oil impacted areas especially as the effectiveness of oil treatment varies with time, the type of oil and spill, the location and weather conditions (Adebajo *et al.,* 2003). Thus, various processes are being developed to remove oil from contaminated areas by use of booms, dispersants and skimmers, oil water separators or by use of different kinds of sorbents (Nahla, 2008).

Sorbents are used in different arrangements to collect spilled oil and oil products (Sirotkina and Novoselova, 2005). Absorbents materials are attractive for some applications because of possibility of collection and complete removal of the oil from their oil spill site. The addition of absorbents to oil spill areas facilitate a change from liquid to semi-solid phase and once this change is achieved, the removal of the oil by the removal of the absorbent structure then becomes much easier. Furthermore these materials can in some cases be recycled (Adebajo *et al.,* 2003).

Oil sorbents can be categorized into three major classes: Inorganic mineral products, organic synthetic products and organic vegetable products (Hussein *et al.,* 2008). Sorbents with large surface areas and affinity to organic compound could be developed from cost effective and readily available natural materials and by-products (Diya'udeen *et al.,* 2008; Tiwari *et al.,* 2008; Site, 2001).

1.1 Clay Minerals

Clays are naturally occurring minerals with variability in their constitution depending on their groups and sources (Batra *et al.*, 2007). These minerals are hydrous aluminium phyllosilicates, sometimes with variable amounts of iron, magnesium, alkali metals, alkaline earths, and other cations. Clays form flat hexagonal sheets, similar to the micas, containing water trapped in the structure, hence good plasticity (Singh and Arbad, 2014). They are very common in fine grained sedimentary rocks such as shale, mudstone, siltstone and in fine grained metamorphic slate and phyllite (Merriman *et al.*, 2003).

Clay minerals can be classified as 1:1 or 2:1, this originate from the fact that they are fundamentally built of tetrahedral silicate sheets and octahedral hydroxide sheets. A 1:1 clay would consist of one tetrahedral sheet and one octahedral sheet, and examples would be kaolinite and serpentine. A 2:1 clay consists of an octahedral sheet sandwiched between two tetrahedral sheets, and examples are talc, vermiculite and montmorillonite (Uddin, 2008). Clays are widely used in industrial products and processes. The use of clay suspensions is important in ceramic industry as well as in the production of paper, detergent and paints, foundry, civil engineering and in drilling operations (Yurudu *et al.*, 2005).

The hydration of inorganic cations present in clay and the nature on Si-O groups impart a hydrophilic nature to the mineral surface and this property make them to absorb water but very difficult to disperse in polymer matrices, that is, organic compound cannot bond with adsorption site on the clay surfaces (Celis *et al.*, 2000). As a result, natural clays are ineffective sorbents for poorly water soluble organic contaminants (Jaynes and Boyd, 1991). The surface of the clay may be modified greatly to make it strongly organophilic, however,

by neutralizing the anionic framework of layer silicates by using positively charged organic species such as primary aliphatic amine salts and alkyl ammonium ion (Yurudu *et al.*, 2006). In the modified form the clay surface may show organophilic nature and can bond strongly with organic compounds (Manocha, 2008).

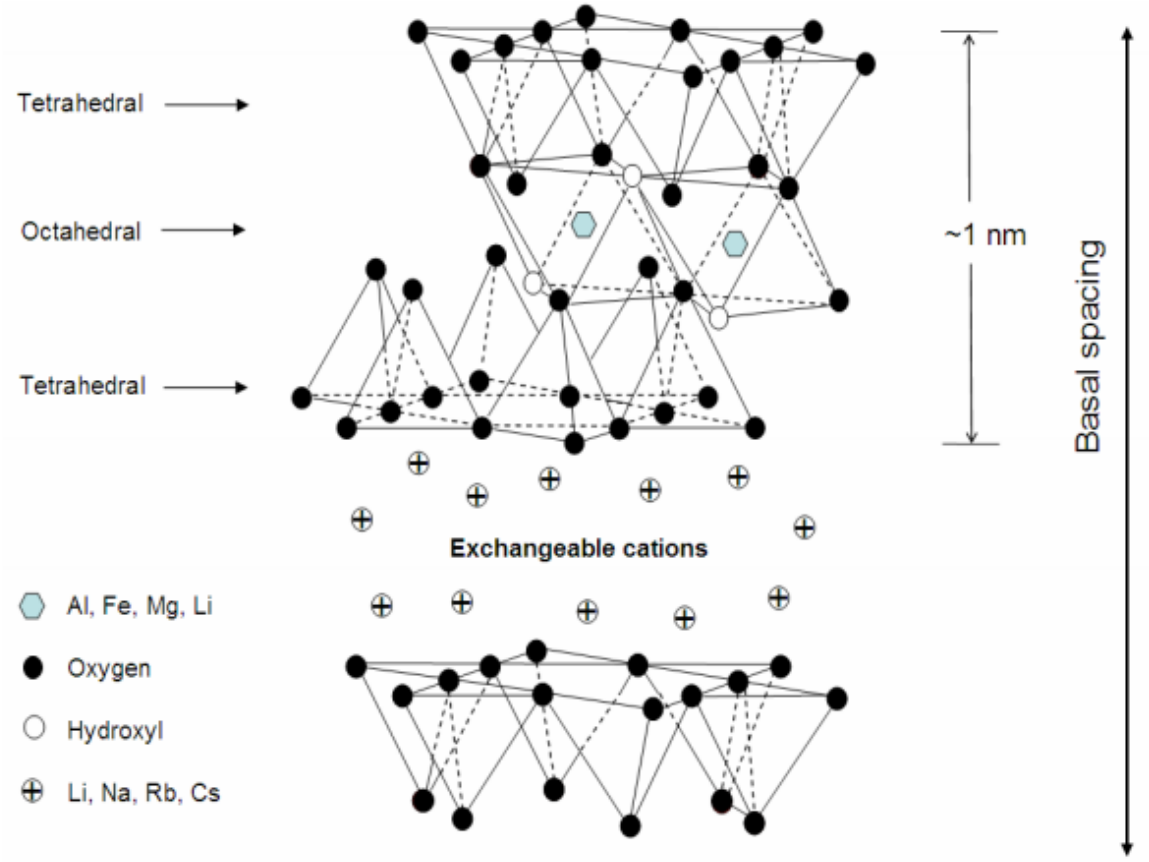


Figure 1.1: Typical crystalline structure of layered silicates nanoclays

1.2 Organoclays

The clay materials have layered structure and layer thickness is around 1 nm, as shown in Figure 1.1. The lateral dimension may vary to a few micron or more depending upon the particular layered silicates. Stacking of the layered silicates lead to irregular layered van der

Waal's gap between the layers called interlayer or gallery (Patel *et al.*, 2006). The clays used for the preparation of organoclays belong to the smectite group clays which are also known as 2:1 phyllosilicates, the most common which are montmorillonite and hectonite. The generic term layered silicate refers to natural clay as well as synthetic clays such as montmorillonite, laponite and hectonite (Bokopza, 2004). Organoclays can be obtained simply by the ion exchange reaction of hydrophilic clay with an organic cation such as an alkyl ammonium or phosphonium ion. The organic cation may enter into ion-exchange with exchangeable cations between the layers (Alemdar *et al.*, 2005; Yurudu *et al.*, 2006). In the modified form, the clay surface may show organophilic nature and can bond strongly with organic compounds.

1.3 Statement of the Problem

Residents of wetlands, like the Nigeria's Niger-Delta, are concerned about the environmental impact of reoccurring and residual oil spill into receiving surface waters and land (Nwankwere, 2010). Hundreds of oil spills occur in Nigeria every year, causing significant harm to the environment, destroying local livelihoods and placing human health at serious risk (Amnesty International, 2013). The adverse impact of oil spillage to the ecosystem and the long term effect of environmental pollution call for an urgent need to develop a wide range of materials for cleaning up oil from oil impacted areas (Adebajo *et al.*, 2003). Treating oil spillage could be costly and time consuming. Research into less costly and less time consuming technology calls for the need to investigate available natural resources that can remediate the environment. The most limiting problem with most natural materials is that they are generally highly hydrophilic in nature. Bentonite nanoclays can find application in oil spill treatment because of their nanostructured layer arrangement.

1.4 Justification for the Research

The possibilities of cleaning oil pollution however, have not yet been sufficiently investigated (Nenkova *et al.,* 2004) and there is still no suitable means of completely removing runoff in the water (Sirotkina and Nevoselova, 2005), pointing to a need for low-cost natural materials that are easy to dispose or biodegrade at the end of their service life. Absorbent materials are attractive for some applications because of the possibility of collection and complete removal of the oil from the oil spill site.

One important consequence of the charged nature of clays is that they are generally highly hydrophilic species and therefore naturally incompatible with wide range of non-polar systems (Patel *et al.*, 2006). The conversion of natural clays to organically modified clays has two consequences, first the gaps between the single sheet is widened, enabling organic cations chain to move in between them and second, the surface properties of each single sheet are charged from being hydrophilic to organophillic (Patel *et al.*, 2006). Organically modified layered silicate or nanoclays have become an attractive class of organic-inorganic hybrid materials because of their potential use in a wide range of applications such as polymer nanocomposites, rheological modifiers in paints, adsorbents for toxic gases, effluent treatment and drug delivery carrier (Patel *et al.*, 2006).

It is also known that commercially available synthetic sorbents are very costly and not readily available, mostly due to the fact that a lot has been spent and to increase the sorption capacity of the synthetic product and they, unlike the natural sorbents, can hardly be reused nor are they biodegradable. A lot of research is therefore being carried out to develop natural potential sorbent materials for oil spill clean-up. Improved techniques for control and

removal of oil slicks is one area of research under active development (Lee *et al.*, 1999). Within the last decade, several methods were developed and used for modification of natural materials because natural materials on their own are not sufficient to treat oil spills. Modified natural resources have shown very high capacity to sorb oil from spill sites. In more recent times, researchers have focused on the use of nanohybrid materials, whose fundamental starting materials are nanoclays to remove oil residues from aqueous environments.

Nanoclays are abundant in Nigeria, especially in the North-Eastern zones. They exist in their impure form and are also very inexpensive. Research into the investigation of the potentials of these clay minerals for environmental remediation is limited. Very little work has been done on the modification of Nigerian nanoclays for the purpose of sorption of organic matter from aqueous solutions. Also, the chemical role of clay materials in sorption of crude oil hydrocarbons has not been fully understood. The potential input to the environment from this research includes:

i. Treatment of water resources from oil spillage, thereby conserving the natural mangroves, wildlife and water supply.
ii. Reduced incidence and severity of forest wildfires through reduced accumulated crude oil residue in mangroves.
iii. Protection of water resources from accumulation of excessive amounts of poisonous crude oil runoff, such as benzene, toluene, cresols and polynuclear aromatic hydrocarbons.
iv. Utilization of undervalued natural clay minerals to valuable sorption media which has the potential of providing economic incentives.

v. Conversion of materials to biodegradable materials for oil spill clean-up to provide sustainable operations and development.
vi. A better understanding of sorption procedures (using natural materials) which will cause optimal use of sorption materials/processes.
vii. Application of the chemistry of the modification procedure in the development and improvement of other natural resources for similar applications.

1.5 Aim and Objectives

The aim of this research is to modify selected Nigerian bentonite clays, using Cetyl trimethylammonium cations under mild reaction conditions for subsequent application as sorbents for oil spill clean-up. The aim centres not only to provide an environmentally acceptable method of cleaning up oil spill but also to get an easily deployable and applicable technique which allows recovery for contingency. This aim is to be achieved via the following objectives:

i. Collection of three different bentonite based Nigerian clays
ii. Seperation and purification of the bentonite nanoclays
iii. Synthesis of organoclays by hydrothermal intercalation under several mild conditions using tertiary alkyl ammonium salts and investigation of the effect of those conditions, observing the optimum conditions that would produce the most efficient sorbents.
iv. Investigation of the influence of intercalation on the oil sorption capacity of the raw and modified samples.
v. Physico-chemical characterization of the raw and modified clay samples

vi. Structural and morphological characterization of the raw and organically modified nanoclays by statistical, gravimetric, microscopic, crystallographic, thermal and spectrophotometric methods.

vii. Estimation the amount of spilled oil that can be treated by the nanoclays in a typical spill situation by applying sorption models.

viii. Development and recommendation of environmentally acceptable methods of cleaning up and recovery of spilled oil.

2.0 LITERATURE REVIEW

2.1 Oil Spillage

Whenever oil is explored, transported and stored, and its derivates are used, there is a risk of oil spillage with the potential to cause significant environmental impact (Hussein *et al.*, 2008). Pollution by petroleum oils affects sea life, economy, tourism and leisure activities because of the coating properties of these materials. Oil spills harm the beauty of polluted sites; the strong odour can be felt miles away and excessive growth of green algae alters the sea and the landscape (Annunciado *et al.,* 2005). The nature and magnitude of oil spills on water habitats depend on the rate of water flow and the habitat's specific characteristics. Where there is proximity of high density human population, when these spills occur, human health and environmental quality are put at risk (Frost *et al.,* 2007).

2.2 Oil spillage in the Nigerian Niger-Delta

Nigeria is Africa's largest oil producer, and it is the eleventh largest producer and the eighth largest exporter of crude oil in the world (Umokoro, 2013). As at 2011, Nigeria is estimated to hold 37.2 million barrels (mbbl) of proven oil reserves (Ike *et al.*, 2013). Petroleum and derivatives dominate the Nigerian economy making about 98 percent of government annual revenue, 80 percent of foreign exchange revenue and 70 percent of budgetary expenditure. Today, the Niger Delta is best known as the region that sustains much oil exploration and exploitation by the agents of western economic powers (Oviasuyi and Uwadiae, 2010; Oshwofasa and Anuta, 2012). The Niger-Delta basin is considered the mainstay of the Nigerian economy to its significantly high level of oil reserves (UNDP, 2006; FEN, 2009). The Niger Delta is situated in the south of Nigeria and is a huge fertile wetland. Subsistence

farming and fishing is the mainstay of the people. Inhabited by more than 3000 long settled communities, the present population figures of the Niger Delta is estimated to be 27 milion. The region is also naturally endowed with viable deposits of hydrocarbons and gas reserves but air, water, soil and forest resources have been devastated by the exploitation of oil and gas resources, particularly from gas flares and oil spills (UNDP, 2006).

For decades, oil spill have devastated the environment of the fertile Niger-Delta. Oil spill incidences have occurred in various parts and at different times along the Niger Delta coast. According to available statistics (Shell Petroleum Development Company Report - SPDC, 2006), in the last 30 years, more than 400,000 tons of oil have been spilled into creeks and soils of southern Nigeria. According to the Department of Petroleum Resources (DPR), between 1976 and 1996, a total of 4647 incidents resulted on the spill of approximately 2,369,470 barrels of oil into the environment (Badejo and Nwilo, 2004). More recent records show that a total of 6817 oil spills occurred between 1976 and 2001 with a loss of approximately 3 million barrels of oil. More than 70 percent was not recorded. Shell Petroleum Development Company (SPDC), in their 2009 annual report, went further to project an increase in oil spill incidences in Nigeria.

Some major spills in the coastal zones are the COCON's Escravos terminal tank failure in 1978 of about 580,000 barrels and Texaco funiwa-5 blowout in 1980 of about 400,000 barrels. The most publicized of all oil spills in Nigeria occurred on January 17, 1980 when a total of 37 million liters of crude oil got spilled into the environment. The spill occurred as a result of a blow out at funiwa-5 offshore station (Badejo and Nwilo, 2004). Other oil spill incidences are those of Abudu pipeline in 1982 of about 18,818 barrels, the Jesse fire incidence which claimed about a thousand lives and the Idaho oil spill of January 1998.

Recently, Agip has reported a total of 471 oil spills due to sabotage and theft between January and the end of September 2013, with the total estimated quantity of oil spilt being 4,014 barrels. Shell also recorded 138 spills for the same period (less than half the number reported by Agip), but with total volume spilt of just over 16,000 barrels amounting to over 33,000 tonnes (Amnesty International, 2013; Uba, 2013).

The number and frequency of oil spills in the Niger Delta is staggering. Hundreds of spills occur every year and this has gone on for decades (Amnesty International, 2013). Some 70 percent of the oil has not been recovered (UNDP, 2006). In the period of 1997-2006, according to its own report, Shell Nigeria experienced about 250 oil spills each year (SPDC, 2006). Shell claims some 60 percent are consequences of sabotage. In January 2008, the Nigerian National Oil Spill Detection and Response Agency (NOSDRA) declared it had so far located more than 1130 oil spill sites abandoned by various oil companies within the Niger Delta (Anonymous, 2008).

With the expansion of oil production, the incidences of oil spills have increased considerably in the region. Approximately 6 percent spilled on land and 25 percent in swamps and 69 percent in offshore environments. The vast majority of the spills are consequently of aging facilities and human errors. In recent times, oil spill appears to be caused more by wilful damage to facilities than by accidents (UNDP, 2006). According to Badejo and Nwilo (2004), fifty percent of oil spills is due to corrosion, twenty eight percent to oil productions operations. One percent to oil drill is due to engineering drills, inability to effectively control oil wells, failure of machines and inadequate care in loading and unloading oil vessels.

2.3 Effect of Oil Spillage in the Environment

Depending on its form and chemistry, oil can cause an array of physiological and toxic effects, for example; benzene is a carcinogen and is toxic to humans and wildlife (United States Army Corps of Engineers - USACE, 2005). Some hydrocarbons are toxic to organisms but less persistent in the environment, while others tend to be less toxic, but more persistent and more likely to result in long term environmental effects (UNDP, 2006). The environmental effects of oil spillage are well known. They include the degradation of forest and the depletion of aquatic fauna. Long term impacts are also possible, as in the case where mangrove swamps and ground water resources are harmed (Lee, 1999).

Although the situation is improving with more stringent environmental regulations for the oil industry, marine pollution is still a serious problem. The harmful effects on the environment are many. Oil kills plants and animals in the estuarine zones. Oil settles on beaches and kills organisms that lie there. It also settles on oceans floors and kills benthic (bottom dwelling) organisms such as crabs (Badejo and Nwilo, 2004; UNDP 2006).

Oil poison algae, disrupts major food chains and decreases the yield of edible crustaceans. It also coats birds, impairing their flight and reducing the insulative properties of their feathers, thus making the birds more vulnerable to cold. Oil endangers fish hatcheries in coastal areas as well as contaminates the flesh of commercially valuable fish (Badejo and Nwilo, 2004). Oil is "acutely lethal" to fish, that is it kills fish quickly, at a concentration of 4000 parts per million (ppm) (Prasad and Kumari, 1987).

The spilled oil contributes an undesirable taste and odour to drinking water and causes severe environmental damage. Contaminated water cannot be used for municipal water supply, for

industry nor irrigation. Public concern for sustaining a healthy environment has resulted in stronger environmental regulations regarding water quality and use of hazardous chemicals and substances (Lee, 1999). The implication of these findings is frightening given that human health is tied to the food web. Udoette (1997) reported, for example, that ingestion of hydrocarbon directly or indirectly through contaminated food, leads to poisoning. Some researchers (Kanoh *et al.*, 1990; Snyder and Hedlim, 1996; Eyong *et al.*, 2004) have documented toxic and carcinogenic effects of exposures to high concentrations of hydrocarbons (UNDP, 2006).

Soil and water contamination by hydrocarbons from leaking storage tanks and improper disposal of hazardous waste are of concerns worldwide. Petroleum hydrocarbons are responsible for 65 % of all contaminated groundwater sites (Ramos-Vianna, 2004). If proper remediation measures are not taken, the organic pollutants released from gasoline spills can lead to surface and ground water contamination, which can be potentially toxic to biota and humans.

Oil spill clean-up in wetlands is problematic because of the limited remediation techniques that can be applied in such environments (Chung and Vennosa, 2008). Remediation of wetland ecosystems impacted by crude oil spills is a challenging task because often times, the response can be more destructive than the spill itself (Vennosa *et al.*, 2002). Implications of these findings are important for the clean-up of oil contaminated wetlands.

Also, it is clear from spills and also field and laboratory studies (Wardrop *et al.*, 1996; Duke *et al.*, 2000; Shigenaka, 2002), that at least in many circumstances, oil harms or kills mangroves. What is less obvious is how that harm occurs and the mechanism of toxicity.

Although there are some consensus that oil causes physical suffocation and toxicological or physiological impacts, researchers disagree as to the relative contribution of each mechanism which may vary with type of oil and time since the spill (Proffitt *et al.,* 1997). Investigations from many spills event around the world have shown that mangroves suffer both lethal and sub lethal effects from oil exposure.

One of the universal challenges faced by researchers when dealing with oil impacts is the fact that oil is a complex mixture of many kinds of chemicals (Pichon and Lynch, 2005; Venkatesan *et al.,* 2005; Ayotamuno *et al.,* 2006). The oil spilled in one incident is almost different from that spilled in another. In addition, oils within broad categories like "crude oil" or diesel can be vastly different, depending on the geological source of the original material, refining processes and additives incorporated from transportation in barges or tankers (Shigenaka, 2002). Even if we could somehow stipulate that all spilled oil was to be of a single fixed chemical formulation, petroleum products released into the environment are subjective to different processes of weathering that immediately begin altering its original physical and chemical characteristics. As a result, samples of oil of exactly the same source can be different in composition after being subjected to a different mix of environmental influences (Wang and Fingas, 2003).

Similar to the oil toxicity situation for many other intertidal environments, the mangrove-related biological resources at risk in a spill situation can be affected in at least two principal ways: First from physical effects; second, the true toxicological effects of the petroleum (Shigenaka, 2002). The crude oil is a very complex mixture of many different chemicals, consequently the effect of an oil spill on the marine environment is dependent on the exact nature and quantity of the oil spilled as well as such other factors as the prevailing conditions

and the ecological characteristics of the effected region (Sayed *et al.,* 2004). Many oil products are highly viscous. In particular, crude oils and heavy fuel oils can be deposited on shorelines and shoreline resources in thick, stick layers that may either disrupt or completely prevent normal biological process of exchange with the environment (Naik, 2009). These hydrocarbon spills damage marine ecosystem and cause wide spread contamination of the surrounding environment. The contamination of shorelines generally has the greatest environmental and economic impact due in part to the difficulties of clean-up measures (Frost *et al.,* 2007).

Even if a petroleum product is not especially toxic in its own right, when oil physically covers plant and animals they may die from suffocation, starvation or other physical interferences with normal physiological function. The lighter or lower molecular weight aromatic hydrocarbons often are major components of oil mixtures and are also known to damage the cellular membranes in subsurface roots: this in turn could impair salt exclusion in those mangroves that have the root filters. Genetic damage is a more subtle effect of oil exposure but can cause significant impact at the population level. For example, researchers have linked the presence of polynuclear aromatic hydrocarbons (PAH) in soil to an increased incidence of a mangrove mutation in which chlorophyll is deficient or absent (Shigenaka, 2002).

2.4 The Toxic Contents of Crude Oil

Crude oil is a mixture of many different kinds of organic compounds, many of which are highly toxic and carcinogenic (cancer causing) (Prasad and Kumari, 1987; Baek *et al.*, 2004). The chemical composition of each crude oil and petroleum product varies significantly, and can have diverse effects on different organisms within the same ecosystem (Overton *et al.*,

1994). Though the toxicity of each individual component may be known, the toxicity of complex mixtures such as crude oils and refined products is extremely difficult to assess, because researchers know little about the additive, synergistic, or antagonistic effects of the various mixtures (Baek *et al.*, 2004; Ayotamuno *et al.*, 2006). It has been noted by some people assisting in the clean-up operations that their health has been affected. The obvious effect of the spill is odour (many of these compounds have very low odour threshold), however, the other effects noted such as headaches or fatigues are all symptoms of the exposure of compounds such as polynuclear aromatic hydrocarbons (PAH) (Mobbs, 1996). Eyong *et al. (*2004) reported that the ingestion of crude oil directly or indirectly, results in toxicity targeted at the hematopoietic system. These differences in toxic effects are due to qualitative compositional differences in the various products, as well as concentration differences of the chemical constituents (Albert, 1995; Sverdrup *et al.*, 2003). There are a number of toxic compounds which are of concern since they are present in significant quantities within the oil (Mobbs, 1996), for example:

2.4.1 Toluene

Toluene is a known constituent of crude oil (Mobbs, 1996). The structure of toluene is presented in Figure 2.1. Crude oil is by far the largest source of toluene (USEPA, 1994). The most important health concern for humans from either intentional or occupational exposures to toluene is its harmful effects on the nervous system. These effects of toluene depend on both the amount and length of exposure. Short term exposure to moderate amount of toluene, such as in elevated workplace exposures can produce fatigue, confusion, general weakness, drunken type actions, memory loss, nausea and loss of appetite, these symptoms disappear when exposure is stopped (ATSDR, 2008a).Teratological and epidemiological evidence

relating toluene exposure to reproductive outcomes have also been reported (Wilkins-Haug, 1997; Bukowski, 2001). Effects on fertility such as abortion were reported in rabbits by inhalation (Vee Gee scientific, 2004).

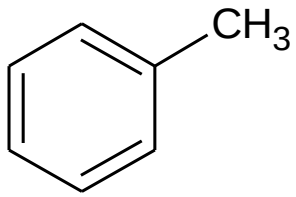


Figure 2.1: Structure of Toluene

2.4.2 Benzene

The major sources of benzene in water are at atmospheric deposition, spills from petroleum and other petroleum products and chemical plant effluents. The structure of benzene is presented in Figure 2.2. Benzene is an established human and animal carcinogen (Khan, 2007). Benzene is known to be a human carcinogen based on sufficient evidence in humans (IARC, 2005). Exposure to benzene has been associated with leukaemia in humans and several types of malignancies in animals (Khan, 2007). Benzene is harmful, especially to the tissues that form blood cells. The effect of this toxicity manifests as lowered blood counts (hematotoxicity), even in individuals occupationally exposed to low levels of benzene (Smith *et al.*, 2011). A significant decrease in almost all blood cell counts, was identified as a phenotypic effect of benzene that occurred even below 1 ppm benzene exposure (Zhang *et al.*, 2010). In addition, human and animal studies indicate that benzene is harmful to the immune system, increasing the chance for infections and perhaps lowering the body's defence against tumour (Mobbs, 1996). Later studies reported that when administered,

benzene by gauge, mice developed head and neck, thoracic cavity and subcutaneous sarcomas (French *et al.*, 2001; Hulla *et al.*, 2001). Certain benzene metabolites are genotoxic and mutagenic (Khan, 2007). Biological plausibility for a causal role of benzene in these diseases comes from its toxicity to hematopoietic stem cells (HSC) or progenitor cells, from which all leukemias and related disorders arise (Smith *et al.*, 2011). The United States Agency for Toxic Substance and Disease Registry (ATSDR) (1997) lists benzene as one of its top twenty toxic chemicals (Mobbs, 1996). Through its metabolites, benzene induces multiple alterations that likely contribute to the leukemogenic process, and appears to operate via multiple modes of action (Smith *et al.*, 2011). The exact mechanism of benzene-induced toxicity is poorly understood (Khan, 2007; Zhang *et al.*, 2010).

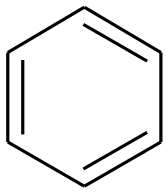
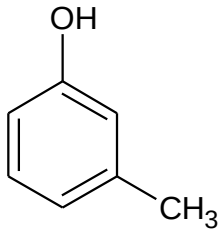


Figure 2.2: Structure of Benzene

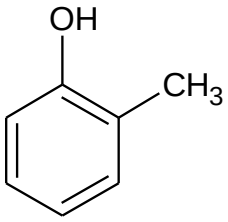
2.4.3 Cresols (a group of Phenolic compounds)

Cresols (monomethyl derivatives of phenol, exist as three isomers - ortho, meta, and para or o, m, and p) and are produced commercially by chemical synthesis or by distillation from petroleum or coal tar (Kirk-Othmer, 2004). The structures of cresols are presented in Figures 2.3. Cresols are known respiratory irritants in animals and humans (ATSDR, 2006). When cresols are breathed, ingested or applied to the skin at very high levels, they can be very harmful. The United States ATSDR (1997) has determined that cresols are possible

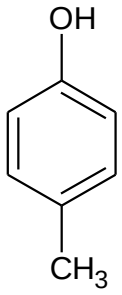
carcinogens. In addition to being highly toxic and potential carcinogen, cresol causes, even at very low concentration, adverse effects on the central nervous system, cardiovascular system, lungs, kidney, and liver resulting in CNS depression (Singh *et al.*, 2008). Effects observed in people include irritation and burning of skin, eyes, mouth, and throat; abdominal pain and vomiting; heart damage; anaemia; liver and kidney damage; facial paralysis; coma and even death (Mobbs, 1996). Further, Vernot *et al. (*1977) determined that cresols (and individual isomers) were corrosive to the skin of rabbits (Sanders *et al.*, 2009). It is not known what the effects are from long-term ingestion or skin contact with low levels of cresols (ATSDR, 2008b). Phenolic compounds generated by petroleum and petrochemicals, coal conversion and phenol producing industries are common contaminants in waste water (Ramos-Vianna, 2004).



o-cresol (*o*-methylphenol)



m-cresol (*m*-methylphenol)



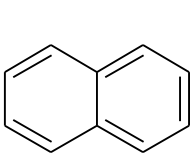
p-cresol (*p*-methylphenol)

Figure 2.3: Structures of cresols

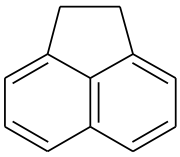
2.4.4 Polynuclear Aromatic Hydrocarbons (PAH)

The quantities of PAH's in crude oil is uncertain as are particular types of PAH. As a pollutant, they are of concern because some have been identified as carcinogenic mutagenic and teratogenic (European Commission, 2002). The structures of selected PAH's are

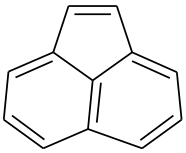
presented in Figure 2.4. Drinking water or swallowing food, soil or dust particle that contain PAH are other routes for these chemicals to enter the body. Under normal conditions of environmental exposure, PAH could enter the body if skin comes into contact with soils that contains high level of PAH. The department of health and human services had determined that PAH may reasonably be anticipated to be carcinogens. Several of the PAH's have caused tumours in laboratory animals when they ate them, when they were applied to skin and when they breathed them in air for long periods of time. Similar effects occur in humans.



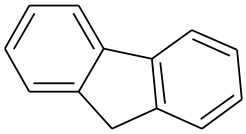
1. Naphtalene



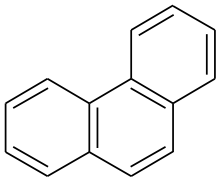
2. Acenaphthene



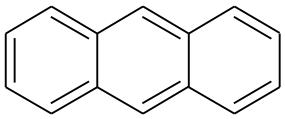
3.Acenaphthylene



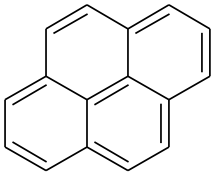
4. Fluorene



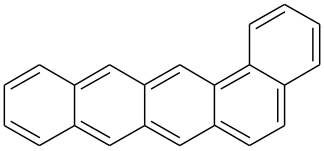
5. Phenanthrene



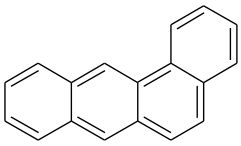
6. Anthracene



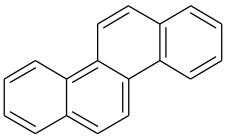
7. . Pyrene



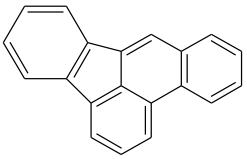
8. Dibenzo(a,h)anthracene



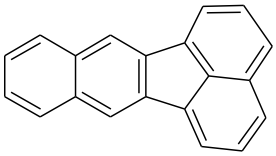
9. Benzo(a)anthracene



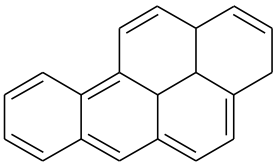
10.Crysene



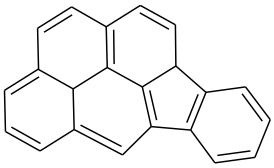
11.Benzo(b)fluoranthene



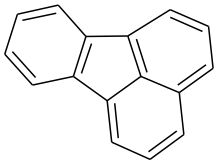
12.Benzo(k)fluoranthene



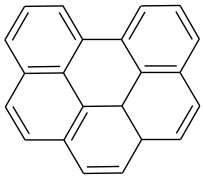
13. Benzo(a)pyrene



14. Indeno(1,2,3·c,d)pyrene



15. Fluoranthene



16. Benzo(g,h,i)perylene

Figure 2.4: Structures of selected Polyaromatic Hydrocarbons

The effect of these compounds may be showing up in those people most exposed to the oil slick and the accompanying air pollution – for example problems of fatigue, headache, nausea and skin rashes. It is important to note also that these substances are not only harmful by ingestion or inhalation, if the skin is exposed, they can be absorbed into the body – an obvious problem for those coming into direct contact with the oil (Mobbs, 1996).

2.5 Oil Spill Response Techniques

The serious environmental consequences of oil spills have long been recognized and considerable research and technological development has been carried out to develop appropriate remediation techniques (Suni *et al.*, 2004; Ventikos *et al.*, 2004). The objective of spill response in any habitat is to minimize the damage caused by the accidental and released oil (Yender, 2002). In clean-up operations, after oil spills, the first requirement is to contain the spills in as small an area as possible and prevent it from reaching water courses and thus contaminating their environment (Greene *et al.,* 1975). When significant deposits of oil were discovered in the 19thcentury, this fossil fuel appeared to offer a limitless source of energy to drive development. Oil spills and leaks along coastline pose risk to marine life and fishes and can threaten the livelihood of human communities (Burgeir *et al.*, 2002). Each year, 0.75-1.8 billion gallons of crude oil are unintentionally released into the environment (Burgeir *et al.*, 2002). Variables such as oil types, weather, location and availability of response equipment will determine initial spill response options. In the best case scenario, oil is prevented from moving into and contaminating mangrove areas. Promising on-water responses that can help prevent oil from reaching mangrove forest include chemical dispersant and in-situ burning. Potential benefits of oil removal must be weighed against the

risk of potential harmful impacts from the clean-up techniques (Yender, 2002). There are five major options for responding to oil spills.

i. Mechanical containment

ii. Chemical treatment Methods

iii. In-Situ Burning

iv. Bio remediation and

v. Natural removal (Mullin and Champ, 2003)

2.5.1 Mechanical recovery

Mechanical recovery is the most commonly used oil spill response technique (Broje and Keller, 2006). It is the transfer of oil from the water surface to some transportable form of temporary storage by the help of booms to contain or divert oil, skimmers or solvents to recover or remove it from the water surface, hoses and pumps (Yender, 2002). Mechanical methods for oil spill remediation have been utilized for a long time with varying degrees of success (Wei *et al.*, 2003). This technique physically removes oil from the water surface, even in the presence of ice (Jensen and Mullin, 2003). Mechanical containment and collection of spilled oil on water using equipment such as booms and skimmers clean-up methods is used at many spills (Yender, 2002). Booms are employed to prevent oil from spreading on the water's surface and surround the spill close to the source (ITOPF, 2004). However, different from booms, skimmers are designed to recover oil from the surface of water. There are different skimming techniques such as weir skimmer, oleophilic skimmer and suction

skimmer (USEPA, 2004a). The use of booms and skimmers is still a primary option for combating marine oil spills (Mullin and Champ, 2003) since it is fairly quick and easy. Barriers can be used along mangrove shorelines and inlets to prevent oil entry. Proper strategic booms deployment in sheltered lagoon areas may be highly effective in trapping large quantities of mobile oil and reducing oil impacts to interior mangroves. To be effective, barriers must be deployed immediately after a spill before oil moves into mangrove areas (Yender, 2002).

Manual removal, using hand tools and manual labour, is often conducted to remove bulk oiling by heavier oils such as crude oil or bunker oil stranded in mangroves. Manual removal help prevent other areas from becoming contaminated as the oil moves around and helps limit long term sediment contamination (Yender, 2002). Performance of any of these however can be severally limited by oceanic conditions and weather, including currents, waves and wind and by the nature of oil slick. Research has shown, though, that mechanical recovery alone usually cannot adequately deal with very large spills offshore. Weather and sea conditions, the nature of the oil and other factors may limit the effectiveness of mechanical recovery.

Another important method is the use of sorbents. Mechanical recovery by the help of oil sorbents is one of the most important countermeasures in oil spill response (Wei *et al.*, 2005). There are numerous compounds and material available as sorbents to collect oil slicks. Today the sorbents in use can be classified as either: natural organic products such as saw dust, rice husks or maize husk, synthetic organic products such as Plastic or polyurethane foam or natural inorganic products such as zeolite and goethite (Deschamps *et al.*, 2003). Sorbent booms or other sorbent materials can be placed at the fringe of oiled mangroves forest to passively recover any mobile oil including sheens. Sorbents are oleophilic and either absorb

or adsorb oil. They can be composed of either synthetic or natural materials and they come in variety of forms, including sausage boom, "pom-pom" or snare boom, sheet rolls and loose particulates. Sorbents vary in their effectiveness depending upon type, degree of oil weathering and absorption capacity. Sorbent materials must be placed and removed (when they are saturated and no longer needed) carefully to minimize disturbance of sediments and injury to mangrove roots (Yender, 2002).

2.5.2 Chemical methods

Chemical methods are best methods for removing small spills; widely spread thin layers of oil, oil rough seas and oil spills immediately threatening damage to property and life (Yender, 2002). Chemical methods involve the use of: dispersants, sinking agents, demulsifiers, gelling agents and neutralization agents. Chemical shoreline cleaners are sprayed on oil coated surfaces to loosen the oil from the surface so it can be flushed off with ambient water. Tidal waters or water sprays alone cannot effectively wash away heavy oil. Shore line cleaning products vary in their toxicity and recoverability of the treated, mobilized oil (Yender, 2002). Chemical shoreline cleaners can be very helpful in cleaning of oiled shorelines by improving the efficiency of water washing. The improvement results from loosening of the oil coating which makes it easier to remove from shoreline surfaces. The benefits is reduced washing time and effectiveness at lower water temperature needed (Lane, 1995).

Chemical dispersants are products applied to oil on the water surface to enhance formation of tiny oil droplets, which mix into the water column and are dispersed by currents (Yender, 2002). Dispersants simply disperse the oil to accelerate the oil and separate it from the water

by absorption (Adebajo *et al.*, 2003). When used judiciously and in the right circumstances, the application of chemical dispersants can be an effective means of accelerating the dispersion of water into water columns (Chapman *et al.*, 2007). Dispersants break spilt oil into tiny particle, of different sizes (IPIECA, 2001) that can be easily degraded by bacteria. Most oil physically disperse naturally to some degree due to agitation created by wave action and ocean turbulence. The key components of a chemical dispersant are one or more surface-active agents, or surfactant-sometimes called "detergents". They contain molecules with both water-compatible (hydrophilic) and oil compatible (hydrophobic) portions. Most chemical dispersants also contain a solvent that reduces viscosity and facilitates dispersal (Lane, 1995; Yender, 2002).

Chemical dispersants enhance and speed up this natural dispersion process, minimizes impact in wildlife at the water surface (e.g. birds and marine mammals) and reduces the amount of floating oil that reaches sensitive near shore and shoreline habitats (Yender, 2002). Moreover using dispersant in oil spill remediation does not create any wastage (NOAA, 2004), although the use of chemical dispersant in addition to being less effective and expensive, introduces more pollutant in the system (Ayotamuno *et al.*, 2006, Odokuma *et al.*, 2003).

Typical sinking agents include sand, brick dust, fly ash, china clay, coal dust and cement. However, sinking is seldom completely effective initially, and some oil tends to surface. Other chemical materials have also been used in the combat against oil spills with a less extensive scale. They include emulsion breakers (Nordvick *et al.*, 1996; Buist *et al.*, 1999) and gelling agents or solidifiers (Delaune *et al.*, 1999; Reynolds *et al.*, 2001; USEPA, 2004b) and neutralizing agents (Ventikos *et al.*, 2004).

2.5.3 In-situ burning

In-situ burning is an oil spill response technique that involves the controlled ignition of the oil at or near the spill on the surface the spill site on the surface of the water or in marsh (Mullin and Champ, 2003). In-situ burning involves the ignition and controlled combustion of the spilled oil (USACE, 2005). In situ burning of oil spills has the benefit of minimizing contamination of coastal marine environments. In order for oil on water to burn, the slick must be relatively fresh and at least 3mm thick. It is a response technique in which spilled oil is burned in a place. When viewed appropriately, in-situ burning can remove large quantities of oil quickly and efficiently with minimal logical support (Aurell and Gullett, 2010). Like dispersants, in-situ burning can help minimize impacts to wildlife at the water surface and reduce the amount of oil that reaches sensitive near shore and shoreline habitats including mangroves.

Since volatile components in the oil begin to evaporate as soon as the spill occurs, the potential for burning decrease with time. Burning is usually 95-98 % efficient, but does cause black smoke. The smoke is not more toxic than if the oil were burned as intended in fuels. However, burning oil is not an environmentally friendly method as it causes air pollution and leaves residual unburnt particles (Christodoulou, 2002). Probably the largest detriment is the emissions from the incomplete combustion of the oil, as indicated by the copious volumes of black, particle-laden smoke (Aurell and Gullett, 2010). One gallon of oil burned this way creates the same pollutions as tree logs in fire place and woodstove. Burning can also be dangerous for the personnel conducting operations (Buist *et al.*, 1999).

2.5.4 Bioremediation

Constituents of oil degrade naturally when attacked by bacteria, algae, protozoa and marine fungi. Enhancement of biological degradation has been proposed using specially bioengineered microbes (Yender, 2002). Primary factors affecting hydrocarbon bioremediation in marine sediments as well as in soils are: the presence of hydrocarbon degrading bacteria (HDB); the optimal environmental conditions stimulating bacterial activity; the chemical composition of spilled petroleum and its relative toxicity, and the bioavailabilty of hydrocarbons to HDB (Palletier *et al.,* 2004). Biodegradation can take place both in the presence and absence of oxygen. If molecular oxygen is present, the biodegradation is aerobic or oxic but if it proceeds in the complete absence of oxygen with other substances (such as nitrates and sulphates), the biodegradation is anaerobic or anoxic (Kanaly and Harayama, 2000; Gieg and Suflita, 2005). There could be a combination of both oxic and anoxic biodegradation in some systems as have been reported to take place in near surface accumulations of tar sands (Connan *et al.*, 1997; Head *et al.*, 2003). However, microbes that degrade hydrocarbons are readily available everywhere in nature, except in polar waters where the rates of breakdown are very slow and variable.

Nutrients addition can enhance biodegradation of oil under nutrient-limited conditions. Microbes and essential nutrients for oil degradation generally are not limited to mangrove habitats, so enrichment may not offer much benefit. Burns *et al. (*1999) concluded that aeration of contaminated sediments may be effective in enhancing biodegradation of oil in the mangrove sediments, since mangrove sediments are usually anaerobic below surface layers. The researchers suggest a bioremediation strategy that employs selective aeration to promote the survival of trees vital to maintaining the structural integrity of the mangrove

forest. Burns *et al. (*1999), points out that aeration is not necessarily a strategy to be used over large areas. Bioremediation methods have also been studied by Tsutsumi *et al. (*2000). Bioremediation is time consuming (USEPA, 2004c) since the rate is normally equal to the half-lives of the hydrocarbons (Wang *et al.*, 2001). Another method is the use of plants and their associated microorganisms for remediation. This is known as phytoremediation. Phytoremediation is proving effective for a wide variety of contaminants including petroleum and hydrocarbons (Fingas and Charles, 2001).

2.5.5 Natural removal

Natural process will eventually remove oil. Tidal actions and precipitation can help physically flush sanded oil out of contaminated mangrove areas. Weathering processes degrade the oil, gradually reducing quantity and toxicity. There are several circumstances under which it is appropriate to do nothing. When no cleaning is conducted, oil will slowly degrade and can be removed naturally, assisted by natural and storm generated flushing.

Spills of light oils, which will naturally evaporate and break down very rapidly, do not require clean up. Such light oils are usually gone within five days. Furthermore, light fuel oils such as gasoline and jet fuels typically impart their toxic impact immediately and clean up can do little to reduce the damage. The only light refined product that might warrant some clean-up is diesel (if sediment could be contacted) (Yender, 2002). Clean-up is not recommended for small accumulation of oil regardless of product type. Impacts caused by light accumulations, regardless of product type, generally do not warrant the trade-offs associated with clean-up activities. Even for major oil spills, there may be cases for which it is best to take no action,

depending on the nature of oiling and characteristics of the mangrove forest affected (Yender, 2002).

2.6 Sorbent for Oil Spillage Treatment

One of the most economic and efficient means of cleaning up hydrocarbon spill on the shoreline and on water is the use of sorbents (Choi and Cloud, 1992; Teas *et al.*, 2001; Adebajo *et al.*, 2003; Frost *et al.*, 2007). The use of sorbents to clean-up oil spill presents nearly many advantages due to simplicity of approach and the inexpensive nature of the materials (Chung *et al.*, 2008). Recently, increasing concerns about pollution of ground water by organic chemicals has led to research on the use of various sorbents (Ramos-Vianna, 2004). Once a sorbent is applied to an impacted wetland, it absorbs the contaminating oil. It retains the oil for a sufficient length of time to allow biodegradation of hydrocarbon by indigenous bacteria under aerobic conditions (Chung *et al.*, 2008).

Sorbents for oil spill in water are materials that soak up the oil. Sorbents work by either absorption or adsorption (Ghalambor, 1995). Absorbents operate like sponges and collect oils by capillary action or suction. They rely on large surface area, the chemical affinity of the sorbent for the spilled oil and chemical constituents including their porosity, molecular structure and changes in volume. Absorbents work best on light, less viscous oil. In some cases, a sorbent material may utilize both techniques for oil recovery (Aboul-Gheit, 2006). They can be used to recover oil through the mechanism of absorption and adsorption or both. Absorbents allow oil to penetrate into pore spaces in the material they are made of, while adsorbent attract oil to their surfaces but do not allow it to penetrate into the material (Aboul-Gheit *et al.*, 2006). Once sorbents have been used to recover oil, they must be removed from

water and properly disposed on land or cleaned for reuse. Any sorbent that is removed from the sorption system must also be disposed off or recycled (Aboul-Gheit *et al.,* 2006).

2.6.1 Types of Sorbents

Sorbents can be natural organic, natural inorganic, synthetic substances or a mixture of the three (Ventikos *et al.,* 2004; Bayat *et al.,* 2005; Frost *et al.,* 2007).

2.6.1.1 Natural organic sorbents

This first category include peat moss (Balternas and Vaisis, 2005; Ohtsubo *et al.*, 2011), straw (Sun *et al.*, 2002), hay, barley straw (Hussein *et al.,* 2009), sawdust (Akonye and Onwudiwe, 2004; Banerjee *et al.*, 2006), bark (Huassard *et al.*, 2003; Saito *et al.*, 2003), grown corncobs (Olufemi *et al.*, 2014), rice husks (Thompson *et al.,* 2010), wool (Choi and Moreau, 1992; Choi, 1996), feathers (Coxeter, 1994), groundnut shell (Nwokoma and Anene, 2010) and other wood based products. They are relatively inexpensive and generally readily available. Organic sorbents can absorb three to fifteen times their weight of oil but they also present some disadvantages. Some organic sorbents are loose particles such as sawdust and are difficult to collect after they spread on water (Ghalambor, 1995). In addition, plant derived organic sorbents are biodegradable thus leaves no permanent residue. Poile (1990) discussed the collection and cleaning methods available in oil spill. He found that natural and biodegradable sorbents have particular advantages over synthetic sorbents. Choi *et al. (*1992; 1993) conducted further studies on milkweed and cotton fibers. The results showed that milkweed and cotton sorb oil more efficiently but cannot be reused as often as polypropylene.

The disadvantage of organic sorbents is that organic sorbent are loose particles and are difficult to collect after they have spread on water (Sayed *et al.,* 2004). The use of sorbents

combined with bioremediation represents an environmentally friendly, simple and cost effective remediation technology for the clean-up of oil from wetlands. The idea is to sorb or wick the oil from the anaerobic subsurfaces for hydrocarbon biodegradation (Chung and Venosa, 2008). Organic substances are inexpensive and readily available. Most organic materials can only be used on land and not adaptable to water use for oil spill clean-up.

2.6.1.2 Natural inorganic sorbents

These include silica (Ametov *et al.*, 1998; Daughney, 2000), graphite (Toyoda and Inagaki, 2000; Toyoda and Inagaki, 2003; Yue *et al.*, 2009), diatomite (Tang and Kovscek, 2004), perlite (Teas *et al.*, 2001; Roulia *et al.*, 2003), zeolites (Sakthivel *et al.*, 2013), vermiculite (Hitzman and Okia, 1968; Mysore *et al.*, 2005), glass (Akhlaq *et al.*, 1997), glass wool and volcanic ash(Xi, 2006). They can sorb four to twenty times their weight of oil. These materials are used in the oil spill clean-up in the light of the fact that they are inexpensive and are available in large quantities. One of their advantages is that they have low sorption capacity for non-polar hydrocarbons (Ribeiro *et al.*, 2001).

2.6.1.3 Synthetic sorbents

Synthetic products include man-made, polymeric materials such as polypropylene (Wei *et al.*, 2003), nylon fibres (Johnson *et al.*, 1973) and polyurethane foams (Teas *et al.*, 2001, Duong and Burford, 2006) which are commonly used sorbents in oil spill clean-up due to their oleophilic and hydrophobic characteristics. Most synthetic sorbents can absorb as much as seventy times their weight of oil (Adebajo and Frost, 2004). Synthetic sorbents that cannot be cleaned after use can present difficulties because they must be stored temporarily until they can be disposed of properly. They are best suited to absorb lighter viscosity oils that can penetrate or wick into its fibre (Aboul-Gheit *et al.*, 2008). Recently, research into synthetic

organic-inorganic hybrids is becoming an area of high interest for example, organo-clays and coal/mineral complex were used by Ramos-Vianna (2004) and found out that organoclays can be utilized effectively as liners for controlling pollution from petroleum contaminated waters. Aboul-Gheit *et al. (*2006) conducted adsorption studies on waste plastics (polyethylene and propylene powder) and concluded that they absorb heavier crude oil more strongly than lighter crude oil and have the property of reusability. Synthetic products have high oleophilic and hydrophobic properties and are the most widely used sorbents in the remediation of oil spills. However these materials degrade very slowly relative to mineral and vegetable products (Lee, 1999).

2.7 Clays

Natural clay minerals are well known and have been familiar to mankind from the earliest days of civilization (Nayak *et al.*, 2007). They are inexpensive, readily available and environmentally stable, and have high adsorptive and ion exchange properties (Sarkar *et al.*, 2010, Mehta *et al.*, 2007). Clay is composed mainly of silica, alumina and water, frequently with appreciable quantities of iron, alkalis and alkali earths (Nayak *et al.,* 2007). Generally speaking, clay minerals are essentially hydrous aluminosilicates with very fine particle size. They possess a layered structure and their layer thickness is around 1 nm with lateral dimension that may vary to a few microns or more (about 200-300 nm), depending upon the particular layered silicates (Manocha *et al.*, 2008; Mallakpour, 2013). Two structural units are involved in the atomic lattices of most clay minerals. One unit consists of closely packed oxygen and hydroxyls in which aluminium, iron and magnesium atoms are embedded in an octahedral combination so that they are equidistant from six oxygen or hydroxyls. The second unit is built of silica tetrahedrons. The silica tetrahedrons are arranged to form a hexagonal

network that is repeated indefinitely to form a sheet of composition, $Si_4O_6(OH)_4$ (Nayak *et al.*, 2007). Stacking of the layered silicates leads to regular van der Waal gap between the layers called interlayer or gallery (Manocha *et al.*, 2008). Clay minerals are classified by the differences in their layered structures (Nayak *et al.*, 2007).There are several classes of clays such as smectites (montmorillonite, saponite), mica (illite), kaolinite, pylophyllite (talc), vermiculite and sepiolite (Shichi and Takagi, 2000).

2.7.1 Smectite Clays

The smectite group of clay minerals has abroad compositional range. At present, the best-known clay minerals of the 2:1 layer type are the smectite group which are the most studied and widely used in various branches of industry due to their high cation exchange capacity, swelling ability and high surface area (He *et al.*, 2004; Mallakpour and Dinari, 2011;Haraguchi *et al.*, 2006; Mehta *et al.*, 2007). These clays have been noted to being abundant in soils and sediments, besides having high specific area, properties of ionic exchange and thermal and chemical stability (Jaber *et al.*, 2005).These properties are critical for the successful development of sorbents. In the smectite group an octahedral alumina layer is sandwiched between two tetrahedral silicate layers. In this group, the most common dioctahedral smectite is montmorillonite (MMT), a hydrated magnesium aluminium silicate, whose octahedral sites are occupied mainly by Al^{3+} but partially substituted by with Fe^{3+} and Mg^{2+}. Because of an isomorphic substitution within the layers, by metal cations, the clay layers have perpetual negative charges, which are counterbalanced by exchangeable cations such as Na^{+}, Ca^{2+} and Mg^{2+}in the interlayer space (Xi, 2006; Patel *et al.*, 2008; Batra *et al.*, 2011). The knowledge of such properties is important to fundamental research. Montmorillonite clay has the largest surface area and highest cation exchange capacity.

Cation exchange capacity, that is, the ability to exchange ionic species is probably the most important physicochemical characteristic of smectite-rich clays. This property is linked to their chemical activity and common cation substitution (Pˇrikryl, 2006). Its current market price is considered to be 20 times cheaper than that of activated carbon (Babel and Kurniawan, 2003).

2.7.2 Bentonites

Bentonites are naturally occurring absorbent aluminium phyllosilicates, essentially pure clays of chemically altered volcanic ash, belonging to the smectite group and consists mostly of montmorillonite (Hosterman and Patterson, 1992; Cheskis *et al.*, 1991). The term "bentonite" was originally suggested for the plastic clays from Fort Bentor, Wyoming, USA (Gonzaga *et al.*, 2007). They are light-colored clays that expand in water, plentiful, inexpensive and available in many countries. They are known for having layered structure and to be quite porous materials (Nguyen *et al.*, 2013), usually rich in organic matters, which colour them black or grey (Ahmed *et al.*, 2012). It has however, been reported that Grin in 1972 redefined bentonite along a more general line as a clay body consisting essentially of montmorillonite minerals, regardless of origin or occurrence (Ahmed *et al.*, 2012). It is widely used in a large number of many fields. In environmental treatment, bentonite is often used as a natural adsorptive material (Nayak and Singh, 2007). It has also been used for oil drilling mud formulation mud (Ahmed *et al.*, 2012; Dolz *et al.*, 2007), fillers for paper (Yun, 1993), pharmaceutical products (Viseras and Lopez-Galindo, 1999; Iborra *et al.*, 2006; López-Galindo *et al.*, 2007), adsorbents (Banat *et al.*, 2000; Naseem and Tahir, 2001; Brezovska *et al.*, 2004) and catalyst (Divakar *et al.*, 2008; Rožić *et al.*, 2011; Soetaredjo *et al.*, 2011) in the chemical process industries. There are different types of bentonite, each

named after the respective dominant element, such as potassium (K), sodium (Na) and calcium (Ca). According to Ahmed *et al. (*2012), there are three principal types of bentonite, namely:

2.7.2.1 Natural sodium bentonite or sodium montmorillonite

Natural sodium bentonite is a high swelling clay composed mainly of sodium montmorillonite (P˘rikryl, 2006). As the name suggests, they occur with sodium as the predominant exchange cation. It is characterized by excellent colloidal properties such as high swelling (expands when wet, absorbing as much as several times its dry mass in water), high liquid limit, thixotropic ability and high thermal durability, and finds application as oil and gas drilling mud (Ahmed *et al.*, 2012; Dolz *et al.*, 2007). Sodium MMTs are widely used in various science fields due to their good cation-exchange capacity, high specific surface area, good swelling capacity, high platelet aspect ratio and ease with which their surface can be modified (Hackman and Hollaway, 2006).

2.7.2.2 Natural calcium bentonite or calcium montmorillonite

Majority of bentonites occurring worldwide are of the calcium type. Calcium bentonite has lower swelling and liquid-limit values compared to natural sodium bentonite. It is the main active ingredient of fuller's earth, probably one of the earliest industrial cleaning agents. It is a useful adsorbent of ions in solution (Legaly, 1995), as well as fats and oils. It is used as a bleaching agent in cooking oil industries, and lubricant oil recycling, as a catalyst, absorber, filler, etc.

2.7.2.3 Potassium bentonites

Also known as potash bentonite or K-bentonite or metabentonite, potassium bentonite is a non-swelling, potassium-rich illitic clay formed from alteration of volcanic ash. It is of less commercial interest due to the presence of mixed (Smectite-illite) structures that decrease the unique properties of true bentonites (Pˇrikryl, 2006).

There are also the magnesium and lithium types. Their chemical composition as well structure is not always same and varies from place to place (Manocha *et al.*, 2008,). In Nigeria, Bentonite tuffs have been reported to occur in the Benue trough and around the Jos Plateau. Bentonitic clays also exist in the North-east quadrant of Nigeria (Borno, Yobe, Taraba, Gombe, Bauchi and Adamawa States) where a probable reserve of more than 700 million tonnes has been indicated. Similarly, over 90 million tonnes have been reportedly found in Afuze, Ekpoma-Igueben road, Ovibiokhuan and Okpebho areas of Edo State. Some occurrences have also been reported in Abia, Ebonyi and Anambra States (Ahmed *et al.*, 2012).

2.8 Organoclays

The hydration of the inorganic exchange ions present in clays and the nature on Si-O groups impart a hydrophilic nature to the mineral surfaces and this property makes them easy to absorb water but very difficult to disperse in organic matrices, i.e., organic compounds cannot bond with adsorption sites on the clay surfaces (Manocha *et al.*, 2008). As a result natural clays are ineffective sorbents for poorly water-soluble organic contaminants (Muhammad *et al.*, 2012; Manocha *et al.*, 2008). However, the surface properties of these clays can be

modified greatly by neutralizing the anionic framework of layer silicates by using positively charged organic species such as primary aliphatic amine salts and alkyl ammonium ions.

In the modified form, the clay surface may show organophilic nature and can bond strongly with organic compounds (Manocha *et al.*, 2008). Among nanohybrid materials, organoclays compose a multitalented area of exploration, which is due in particular to the accessibility of natural clay minerals and their ability to incorporate a large variety of functional molecules, including polymers (Ruiz-Hitzky and Van Meerbeeck, 2006). Surface modifications of clay minerals have received attention because it allows the creation of new materials and new applications (De Paiva *et al.*, 2008). When the surfaces of these clays are modified with organic molecules, the resulting products are called organoclays. The main focus of surface modification of clays is materials science, because organoclays are essential to develop polymer nanocomposites (De Paiva *et al.*, 2008).

Organoclays are manufactured by modifying clays with quaternary amines, a type of surfactant that contains a nitrogen ion. The nitrogen end of the quaternary amine (i.e. the hydrophilic end) is positively charged and ion exchanges onto the clay platelet for sodium or calcium (Alther, 2002). Intercalation of organic guest species into smectites is a way of constructing ordered inorganic–organic assemblies with unique microstructures controlled by host–guest and guest–guest interactions (Kakegawa and Ogawa, 2002). These materials combine the structural and textural properties of the host matrix with the chemical functionality of the organic guest (Mallakpour and Dinari, 2011). Ion exchange with alkylammonium ions is well-known and is the preferential method to prepare organoclays (De Paiva *et al.*, 2008). Numerous studies on organoclays have extensively been carried out

for their unique sorption behaviour towards various hydrophobic organic contaminants in the environment (Nayak and Singh, 2007).

In recent years, there has been an increasing interest in utilizing clay minerals such as bentonite, kaolinite, diatomite, hectorite (Vougaris and Petridis, 2002), synthetic fluoro-hectorite (Gorassi *et al.*, 2003; Tamura and Nakazawa, 1996), sepiollite (Akyüz and Akyüz, 2003; Arroyo *et al.*, 2003) synthetic micas (Tamura and Nakazawa, 1996; Klapyta *et al.*, 2001; Chang *et al.*, 2003; Klapyta *et al.*, 2003) and fullers earth for their capacity to absorb not only inorganic but also organic molecules (Nayak and Singh, 2008; Mallakpour and Dinari, 2011). Among the clay minerals, smectites, especially bentonites, have been extensively used to prepare organoclays because of its excellent properties, such as high cation exchange capacity, swelling behaviour, adsorption properties and large surface area. Bentonites are naturally capable of adsorbing organic substances; however, the adsorption capacity is not high enough to be applied in practice. Hydrocarbon chain inserted into layers can increase interlayer distance and hydrophobic property of the clays leading to higher affinity toward organic substances (Juang *et al.*, 2002; Yildiz *et al.*, 2005).

2.8.1 Application of organoclays

The uses of organoclays range from industrial, to domestic, to environmental applications. Organoclays also have been used in several applications. These applications include adsorbents, rheological control agents, paints, grease, cosmetics, personal care products, oil well drilling fluids, etc (Santos,1989; Beall and Goss, 2004; Xi *et al.*, 2005; Araújo *et al.*, 2005). The various industrial uses of these organoclays are due to their physical and chemical properties, being applied in oily well drilling muds (Cardoso *et al.*, 2007; Silva *et al.*, 2014),

catalysts (Wang *et al.*, 2006; Scheuermann *et al.*, 2009; Ghiaci *et al.*, 2011), sorbents (Liu *et al.*, 2007; Patel *et al.*, 2008; Masooleh *et al.*, 2010; Sarkar *et al.*, 2010), emulsion stabilizers (Bayer *et al.*, 2013; Zhang *et al.*, 2014), loading agents (Gonzaga *et al.*, 2007), pharmaceutical industry (Egbon *et al.*, 2013; Rodrigues *et al.*, 2013), cosmetics (Powell, 1983; Patel *et al.*, 2006) , adhesives (Jeong *et al.*, 2007; Bayer *et al.*, 2009; García del Cid *et al.*, 2014) and so on, in the midst of other applications (Murray, 2000). At present, there are many applications of organoclays, especially as sorbents in pollution prevention and environmental remediation such as treatment of spills, waste water, hazardous waste landfills, etc (Masooleh *et al.*, 2010).

Organoclays, prepared by intercalating clays with surfactant cations, have been considered as potential sorbents for removing organic pollutants from water (Dabrowski, 2001; Bartelt-Hunt *et al.*, 2003; Chen *et al.*, 2005; Kim *et al.*, 2006; Nguyen *et al.*, 2010). The use of clay modified by quaternary ammonium salts has been shown to remove efficiently organic compounds of low solubility in water. They also effectively remove chlorinated phenols and other hydrophobic, sparingly chlorinated, soluble compounds, e.g., PAHs and PCBs (Mortland *et al.*, 1986). Studies have shown that these materials exhibited good capacity to adsorb organic solvents when tested in gasoline, diesel, methanol, ethanol, toluene and acetone. Organoclays are particularly useful in water purification e.g. by the removal of oil and toxic chemicals from water (Alther, 2000; Volovicheva *et al.*, 2001; Xi, 2006; Zhou *et al.*, 2007; Tiwari *et al.*, 2008). Remediation of industrial waste waters is enabled through the use of organoclays (Tiwari *et al.*, 2008; Sulaymon *et al.*, 2010; Cavalcanti *et al.*, 2012). These types of materials are useful for the remediation of contaminated soils (Brixie and Boyd, 1994, Sarkar *et al.*, 2010; Moyo *et al.*, 2014) and they are also applied as clay liners in landfills (De Paiva *et al.*, 2008).

3.0 MATERIALS AND METHODS

3.1 Materials

Smectite clay samples were collected from the National Geosciences Research Laboratory, Kaduna, Kaduna State on 14 May, 2013 and were identified to be from Yola, Adamawa State (9º33'N 12º43'E); Dikwa, Borno State (11º30'N 13º00'E) and Gujba, Yobe State (12º00'N 11º30'E) and were coded as samples A, B and C respectively.



Figure 3.1: Map of sampling location of bentonites. Sourced from "Google Maps" (Map data @2015 Google) 15 March, 2015. Illustrating positions of Dikwa, Yola and Gujba.

All chemicals used were analytical grade reagents. Sodium dithionite, sodium bicarbonate, sodium acetate and Hydrogen peroxide were used for purification of the clay samples. Properties of the clays were modified through the hydrothermal intercalation with alkyl ammonium surfactants cationic surfactants, cetyltrimethylammonium bromide (CTAB) ($(C_{16}H_{33})N^{+}(CH_3)_3Br^{-}$, Molar mass = 364.45 g/mol; melting point = 237-243 °C; boiling point (bp) = 235 °C) and cetyltrimethylammonium chloride (CTAC) ($(C_{16}H_{33})N^{+}(CH_3)_3Cl^{-}$, Molar mass = 320.00 g/mol), involving ion exchange. The structural formulae of CTAB and CTAC are presented in Figures 3.2 and 3.3 respectively.

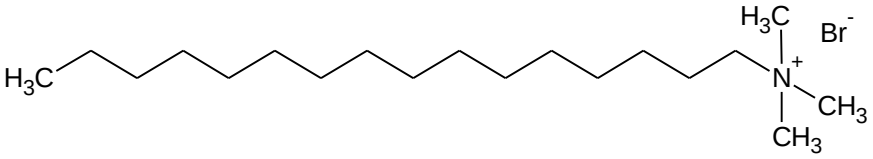


Figure 3.2: Structure of Cetyl Trimethylammonium Bromide

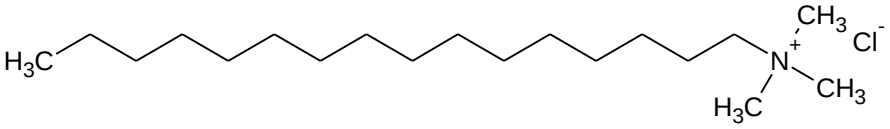


Figure 3.3: Structure of Cetyl Trimethylammonium Chloride

Distilled water used was produced and collected from the Department of Chemistry, Ahmadu Bello University Zaria. Urals Crude oil samples were collected from Kaduna Refining Petroleum Corporation (KRPC), Kaduna state.

3.2 Methods

All experiments were carried out at ambient temperature at the Department of Chemistry, Ahmadu Bello University, Zaria except where otherwise stated. All glassware were washed in tap water, rinsed with 5 % HNO_3 solution and oven dried before use.

3.2.1 Sample Preparation

3.2.1.1 Clay sample preparation

The bulky bentonite samples were pulverized by continuous rubbing and grinding in a ceramic laboratory morter using a pestle. The pulverized samples were sieved through a 200 µm BS410/1986 laboratory sieve to attain homogeneity and to allow easy dispersion in distilled water. The samples were stored in dry air tight containers for subsequent use.

3.2.1.2 Crude oil wethereing

In order to effectively simulate an oil spill situation and to minimize experimental variations, the crude oil samples were weathered for 24 hours, as described in Hussein *et al. (*2009), with some modifications. The samples were held in thin layers for 24 hours in open air, using watch glasses, and then safely transferred to a laboratory oven set at 100 ^{o}C to release emulsified water and very volatile hydrocarbon content so as to achieve gravimetric stability. Crude oil contains low boiling fractions that evaporate rapidly after a spill and often before significant clean-up operations can begin, in the early stages of an oil spill, lighter hydrocarbons evaporate before any possible clean-up operations can take place (Satish, 2003). The wethered samples were collected in beakers and kept in dessicators for subsequent use.

3.2.2 Physicochemical characterization of clay samples

The physicochemical properties of clays that were carried out before and after treatment include

3.2.2.1 Bulk density determination

The bulk density of the sorbents were carried out in the laboratory based on the method described in the European Committee for Standardization, *CEN/TS 13040:2007*. Where an empty cylinder with known volume (V_a) was was preweighed to the nearest 1 g (M_1) using an analytical balance. Using a scoop and a funnel abouve the cylinder, the homogenized samples were each transferred into the cylinder. The cylinder is periodically shaken and its content compacted with a pluger. Once the cylinder was overfilled, the excess clay was removed from the cylinder avoiding further compaction or disturbance. The material and the cylinder were weighed to the nearest 1 g (M_2) using the balance.The weight of the clay (M_a) in the cylinder were calculated by subtracting M_1 from M_2. The results were recorded and the Record the result (mX).An empty cylinder was calculated using the formula:

$$B_D = M_a/V_a \ g/cm^3 \qquad (3.1)$$

where B_D is the bulk density, M_a and V_a are the weight and volume, respectively, of the materials used.

3.2.2.2 Moisture content (MC) determination

About 2 g each of the samples was weighed into preweighed watch glass using an analytical balance. The samples in the watch glass were placed in the oven for 24 hours at 105 ^oC. After

24 hours, the oven dried samples were reweighed and the moisture content determined with the formula:

$$M_c = [(W_o - W_2)/W_o] \times 100 \quad (3.2)$$

where M_c is the moisture content; W_2 is the new weight after drying; W_o is the initial weight of the dry samples (ASTM, 1994).

3.2.2.3 *Volatile matter content (VMC) determination*

About 2 g of each sample were heated to about 300 ^oC for 20 minutes in a partially closed porcelain crucible placed in a muffle furnace. The crucible and its content were retrieved and cooled in a dessicator. The difference in weight was recorded and the volatile content determined thus

$$V_c = [(W_a - W_o)/W_o] \times 100 \quad (3.3)$$

where V_c is the volatile component in percentage; W_a is the weight of matter after cooling and W_o is the original weight of dry sorbent (ASTM, 1994).

3.2.2.4 pH (10%) determination

The pH of the samples were measured by weighing out about 5 g of the samples and transferring to a 100 ml beaker containing 50 mls of distilled water of known pH. The mixture ws\as properly stirred with a clean glass rod until all sediments are properly dispersed in water. The pH of the material was then tested using a handheld *HANNA* pH instrument. The pH was noted and recorded.

3.2.2.5 Cation Exchange Capacity (CEC)

The CEC of the clay samples were determined by the $BaCl_2$ Compulsive Exchange Method as described in Ross and Ketterings (1996). This method determines CEC as the pH and ionic

strength of the soil. In the procedure, about 2 g of clays was transferred to a funnel containing low grade filter paper and slowly leached with 20 cm^3 of 0.1 M $BaCl_2.2H_2O$ allowing each addition to soak into the soil before adding more. The clay samples were further leached with 60 cm^3 of 2 mM $BaCl_2.2H_2O$ in six 10 cm^3 portions. The pH of the last 10cm^3 of leachate was determined and recorded. After leaching, the filter paper plus samples were transferred to a pre-weighed 125 cm^3 flask and 10.0 cm^3 of 5 mM $MgSO_4$ added and stirred occasionally for 1hour. The conductivity of the 1.5 mM $MgSO_4$ solution and the samples were determined. Distilled water was added with mixing, until the sample solution's conductivity is that of the 1.5 mM $MgSO_4$. The pH of the sample solutions was determined and if it was not within 0.1 units of the previous measure, 0.05 M H_2SO_4 was added drop-wise until pH was in the appropriate range. The pH and conductivity were adjusted alternately until the endpoints were reached. The CEC of the clays were calculated thus:

Total solution (cm^3) = final tube weight (g) - tube tare weight (g) - 2 g [a] (3.4)

Mg in solution, not on CEC (meq) = total solution (cm^3) x 0.003 (meq/cm^3) [b] (3.5)

Total Mg added (meq) = 0.1 meq + meq added in 0.1 M $MgSO_4$ [c] (3.6)

CEC (meq/100g) = ([c] – [b]) x 50 (3.7)

3.2.3 X-Ray Florescence (XRF) Analysis

The chemical composition of the clay minerals before and after refining was measured by XRF using an Oxford Instrument (X-supreme 8000) with a tungsten X-ray tube and powder sample holder at the Ahmadu Bello University Multiuser Research Laboratory. About 2 g of each sample was weighed and transferred to the sample cups. The sample cups were gently

shaken to ensure uniform distribution of samples and kept for analysis. For each set of sample, it took abour 3.1 minutes which included 60 seconds acquisition time for the metal conditions as well as 66 seconds 'dead time' during which the XRF will establish each measurement condition. Scans were conducted in sample cups assembled from 21 mm diameter and the cup combined with polypropylene inner cups was sealed at one end with 4 µm Poly-4 XRF sample film. Concentration was expressed in percentages (%).

3.2.4 Scanning Electron Microscopy (SEM)

To determine the size and surface morphology of the samples, before and after modification, Scanning Electron Microscopy (SEM) was carried out at the Department of Chemical Engineering, Ahmadu Bello University, Zaria, using a Phenon™ X-pro Scanner. Minimal preparation includes the acquisition of the sample and placing it on a clean carbon strap that will be attached on the sample holder, which fit into the SEM chamber, and some accommodation to prevent charge build-up and also prevent the sample from making contact with the Detector.

3.2.5 Thermal Gravimetric Analysis

TGA/DSC was used to investigate the thermal and energy profile of the clay and organoclays materials. A Mettler-Toledo TGA/DSC1 Star® (Mettler-2012) instrument with heating rate of 20 ^{o}C/min in Nitrogen (N_2) atmosphere was employed in determining the thermal characteristics of the raw and modified clay samples and carried out at the School of Chemistry and Chemical Engineering, Queens University, Belfast, UK. All of the samples were heated up to 450 °C. The test samples were dried under a vacuum at 120 °C for 24 h before DSC. Thermal Analysis (TGA and DSC) detects the interatomic and inter-/intra-

molecular interactions as related to an imposed external change in temperature. The Nitrogen gas was set as the inert gas and Oxygen gas as the oxidative. The gas environment is preselected for thermal decomposition (inert nitrogen gas) and an oxidative decomposition (air or oxygen). The required flow rates was adjusted to provide the appropriate environment for the tests. Then the clays and organoclay samples were placed in the specimen holder and the temperature of the furnace was raise to 500 °C. The initial weight was set to read 100 % before the heating program was initiated.

3.2.6 Brauner-Emmet-Teller (BET) Analysis

The Brunauer–Emmett–Teller (BET) was carried out at the School of Chemistry and Chemical Engineering, Queens University, Belfast, U.K. The surface area, porosity and pore sizes of the clays and their corresponding CTAB organoclays were measured from N_2 sorption isotherm at 77 K using a Micrometrics Tristar II BET analyser. The samples were degassed under flowing nitrogen at 250 °C for 4 hours using the Smart Prep™ 065. The degassing unit removes adsorbed contaminants from the surface and pores of a sample in preparation for analysis. The sample tube in the analysis port was again degassed before the Dewar containing liquid nitrogen was automatically elevated upwards to submerge the sample tube. A predetermined pressure of nitrogen was bled into the manifold above the analysis port. The sample analysis port valve was then opened, exposing the sample to nitrogen. The quantity of adsorbed nitrogen was determined by the difference in the recorded pressure. The sample analysis port was then closed and the manifold filled with a slightly higher pressure of nitrogen before re-exposure to the sample followed by calculation of the next value. The process was repeated to generate isotherms. The surface area of the sample

was then calculated from the isotherm using the Brunauer–Emmett–Teller (BET) equation and N_2 cross-sectional area of 0.162 nm^2.

$$\frac{P_e}{(P_o - P_e)V_{ads}} = \frac{1}{CV_m} + \frac{(C-1)}{CV_m} * \frac{P_e}{P_o} \quad (3.8)$$

where P_e is the equilibrium pressure (i.e. after sample is exposed to N_2 in manifold), P_o the saturation pressure, V_{ads} the volume of nitrogen adsorbed, V_m the volume of nitrogen monolayer and C is a constant.

3.2.7 X-ray Diffraction (XRD) Analysis

XRD is a widely used analytical instrument for the identification and analysis of crystalline materials. XRD analysis was used to probe the crystal lattice structure and basal spacing of the clay and organoclay powders. XRD pattern is a known effective way to characterize the formation of a nanocomposite. A Philip X'pert 3 analytical Diffractometer (Philips X'pert-PRO, PW3064 fitted with an X'Celerator and a secondary monochromator, Copper Kα radiation (λ = 1.54180 Å) at 40 kV/40 mA, with a goniometer velocity of 2 °/min and a step size of 0.05°, with 2θ ranging from 2° to 69°) was used to probe the crystal lattice structure and basal spacing of the clay and organoclay powders, and also to examine the materials for the presence mineral phases. The samples were prepared for XRD measurement by orienting the clays in a glass slide following standard procedure. The slides were air dried and placed in a desiccator containing silica gel to prevent rehydration. Glycolated and heat treated (300 ^oC) samples were also prepared following standard procedure. Fixed anti-scatter and divergence slits of ¼^o were used together with a beam mask of 10mm. All scans were carried

out in ‘continuous’ mode using the X’Celerator RTMS detector. The d(001) spacing (Å) was determined using the Bragg’s equation:

$$Å = \lambda / 2 \sin (2\theta/2) \quad (3.9)$$

Where λ is theKα wavelength and 2θ is the peak value at the $^{o}2\theta$ axis. The XRD data were interpreted with PANanalytical X'Pert HighScore (Version 2.0a) and Jade (version 5.0).

3.2.8 Fourier Transform Infra-Red (FTIR) Analysis

To determine whether a chemical reaction took place between organic compounds and the clay samples and also to investigate the position and presence of characteristic organic groups in the sample’s structure, FTIR Analysis was carried out using KBr. The FTIR spectra were recorded on a Shimatzu Fourier Transform Infrared Spectrometer (FTIR) at the National Research Institute for Chemical Technology (NARICT), Zaria. The sample was mixed with Potassium bromide (KBr) and then ground to a homogeneous blend and compressed to give a small transparent disc of 13 mm diameter. A background spectrum of pure KBr was run before the spectrum of any sample to account for any absorption due to impurities in the KBr. The disc containing the sample was then placed in the infrared spectrometer and the spectrum of the samples were collected. 20 scans were collected for each measurement over the spectral range of 4000-400 cm^{-1} with a resolution of 4 cm^{-1}. All spectra were presented without baseline correction or normalization.

3.2.9 Neutron Activation Analysis

Neutron Activation Analysis of the clay and organoclay samples was carried out at the Centre for Energy Research and Training (CERT), Ahmadu Bello University, Zaria, using the

Nigeria Research Reactor-1 (NIRR-1). The NIRR-1 is a Miniature Neutron Source Reactor (MNSR) with highly enriched Uranium as fuel, light water as moderator and Beryllium as reflector; and has a tank-in-pool structural configuration with a nominal thermal power rating of 31 kW. Data processing was done with gamma ray spectrum analysis software WISPAN 2004 developed at CIAE, China. For irradiation, four schemes (S1, S2, L1 and L2) were adopted based on the half-life of the product nuclide. For element leading to short-lived activation products (S1 and S2) the samples were each packed and sealed in $7cm^3$ rabbit capsules and sent for irradiation in turn in an outer radiation channel B_4 where the neutron spectrum is "soft". The choice of the outer irradiation channel is to eliminate corrections, notable Mg in the presence of Al; Al in the presence of Si; and Na in the presence of P. This is due to the proximity of the inner channels of MNSRs to the core leading to relative higher ratio of fast-to-thermal neutron. For elements leading to short lived activation products (L1 and L2), sample wrapped in polyethylene films were then irradiated for 6 hours in any of the small inner irradiation channels (A_1, B_1, B_2 or B_3) to take advantage of the maximum value of thermal neutron flux in the inner channels. The neutron flux variability over irradiation volume was determined experimentally to be less than 2 % through the measurement of specific activities of irradiated Cu wires arranged axially and radially inside the vial. Radioactive measurement of induced radio nuclides were performed by the PC-based gamma ray spectrometry set up. Samples were counted on a Plexi-glass holder designated as H1, corresponding to a source-detector geometry of 1 cm. The neutron setting for the short irradiation of the materials was raised to 5×10^{11} n/cm/s sensitivities for analysis of elements using procedures S1 and S2.

3.2.10 Purification of Clays

The bentonite samples were purified using the three stage treatment procedure described in Manocha *et al. (*2008). In the first stage, the heavy impurities such as quartz and free Iron present in raw clay samples were reduced by dispersing the clay powder in distilled water and slowly decanting the suspension. The residue containing the heavy impurities were discarded. The suspension was centrifuged and the settled clay was dried at 100-110 °C. The dried clays were grounded and sieved to have clay particles of <75 μm size.

In the second stage, the free iron oxide and organic matters present in clay structure were reduced by heating about 150 g each of the clay samples for four hours in a mixture of 1.0 g sodium dithionite ($Na_2S_2O_4$), 75.3 g/L citrate ($C_6H_5Na_3O_7$) and 8.3 g/L bicarbonate ($NaHCO_3$) solution, also referred to as DCB, at 80 ^oC in a 500 ml beaker. The mixture was centrifuged to separate the treated clay from the DCB solution. The clay were rinsed with distilled water and centrifuged again. The rinsing step was repeated till the deep yellow-brown colour of DCB was removed.

After this stage, the rinsed clay was further treated with a mixture of 136 g/L sodium acetate ($C_2H_3NaO_2$) and 30 % hydrogen peroxide (H_20_2) respectively to remove organic impurities from the clay materials for 4 hours after which the clay slurry was centrifuged. Settled clay was washed with distilled water (2-3 times) and dried at 100-110 °C. The dried clay was grounded using a mortar and pestle, and sieved to collect particles with less than 75 μm fractions.

3.2.11 Organoclay synthesis

Syntheses of Organoclays were carried using the hydrothermal intercalation method as described in Zhou *et al. (*2007) and Manocha *et al. (*2008). Cetyltrimethylammonium bromide (CTAB) and cetyltrimethylammonium chloride (CTAC) were used in the reactions as intercalants. About 100 g each of the purified clay samples were dispersed in about 200 cm^3 of dionized water in a 500 cm^3 beaker. The surfactant was slowed added to the clay suspension in a concentration of 50 % w/w of clay sample. The reaction mixtures of aqueous suspensions of the layered silicates and organic salts were stirred constantly for about 10 hours at an optimum temperature of 80 °C in a thermostated water bath. The experiments were repeated varying the concentrations (5, 10, 20 and 30 % w/w of clay sample), time (2.5, 5.0, 7.5, 10 and 12.5 hours) and temperature (30, 40, 60, 80 and 90 ^oC). The conditions for synthesis of the orgaoclays and their corresponding organoclay sample Identity/codes used in the research are presented in Table 3.1. The resulting solution is centrifuged to collect organoclays. A solution of 0.01 M silver nitrate ($AgNO_3$) is added to the supernatant solution after each centrifuging stage to indicate the presence or absence bromide and chloride ions in clay suspension. All products obtained were washed 3-8 times with portions of 1000 cm^3 hot distilled water until the washing water is free of bromide or chloride anions and confirmed using $AgNO_3$, as no white precipitate or cloudiness was formed in washing water. The resulting organoclays were then centrifuged at 70 °C and ground in an agate mortar to pass through a 200 µm-mesh sieve and kept in desiccators for further analysis.

Table 3.1: Design of the experimetal conditions for organoclay synthesis

S/N	clay	Salt	T(°C)	t (hrs)	Conc (% w/w clay)	sample ID
1	A	CTAC	80	10.0	50	1
2	A	CTAB	80	10.0	50	2
3	C	CTAC	80	10.0	50	3
4	B	CTAB	30	10.0	50	4
5	B	CTAB	80	10.0	50	5
6	B	CTAB	50	10.0	50	6
7	B	CTAC	80	10.0	50	7
8	C	CTAB	80	10.0	50	8
9	B	CTAB	90	10.0	50	9
10	A	CTAB	80	2.5	50	10
11	A	CTAB	80	5.0	50	11
12	A	CTAB	80	7.5	50	12
13	A	CTAB	80	12.5	50	13
14	C	CTAB	80	10.0	30	14
15	C	CTAB	80	10.0	20	15
16	C	CTAB	80	10.0	10	16
17	C	CTAB	80	10.0	5	17

T (°C) represients the Temparature (in °C); t (hrs) represents the interaction time (in hours); Conc is the concentration of the surfactant used; Clay indicates the type of clay used; sample ID represents the codes used in identifying each organoclay sample.

3.2.12 Removal of hydrocarbon spill from water surface

The crude oil sorption tests on the bentonite and organoclay samples were carried out using a modified method described in Thompson *et al. (*2010), based on the Standard test methods for sorbent performance of adsorbents in ASTM F726-99 (2004). The focus of this method concerns the evaluation of sorbents performance for removing non-emulsified oils and other floating, immiscible liquids from the surface of water bodies and also gives idealized laboratory data which can be used to compare the oil adsorbing capacity of one adsorbent with another and relative cost effectiveness. To 100 g of distilled water in a 200 cm^3 beaker, 5 g of crude oil was added to attain a concentration of about 0.005 g/L. A 0.5 g sorbent dose was placed in a 200 mesh stainless steel basket, which was lowered into the beaker with the hydrocarbon so that the sorbent was completely covered by the liquid. After 1 minute of immersion, the basket with the sorbents was removed manually in a vertical direction and allowed to drain for about 30 mins. The saturated sorbents were then transferred to preweighed watch glasses (W_1). The weight of the sorbents in the watch glasses were recorded (W_2). The glasses were transferred to an oven set at 95^{o}C for another 1hour to ensure that all water molecules escapes the clay structure. The sorbents were removed from the oven and kept in a desiccator to cool. The weight of the clay and the sorbent (W_3) were measured and recorded. The crude oil pick-up ratio on a weight basis was calculated as follows:

Weight of oil sorbed $W_s = W_3 - W_1 - 0.5$ (3.8)

The amount of water removed $W_W = W_2 - W_3 - W_1 - 0.5$ (3.9)

Sorption capacity (g oil/g sorbent) $= W_s/0.5$ (3.10)

The experiment was repeated, varying time and initial oil concentration to explain the kinetics and equilibrium of the sorption pattern.

4.0 RESULTS

4.1 Physicochemical properties of raw and organically modified bentonites

The physiochemical tests carried out on the clays samples A, B, C and their corresponding organoclays samples 2, 5 and 8 respectively are presented in Table 4.1. From the results, all samples used in the experiments were below 200 µm in size as a results of the sieve mesh size used. The Bulk density of the materials reduced from 1.508 g/cm^3 to 1.004 g/cm^3 in sample A, 1.432 g/cm^3 to 0.912 g/cm^3 in sample B and from 1.508 g/cm^3 to 1.016 g/cm^3 in sample C after intercalation. The Moisture Contents (MC) of the materials were determined and only sample B had moisture of 2%. The Volatile Matter Content (VMC) of the samples carried out at 300 ^{o}C showed 0 % volatile matter for samples A and B and 4 % for samples C. After intercalation there was an increase in VMC contents as a results of the alkane chains in the clay lattices. The VMC of samples 2, 5 and 8 were 24 %, 18 % and 16 % respectively. The pH of the clay samples indicated the samples were all slightly alkaline, with pH of B > C > A. The results show a decrease in pH of all clay samples A, B and C were decreased from 7.66, 8.9 and 8.02 respectively to 7.00 after intercalation. The pore size, pore volume and BET surface area of all samples as recorded on the BET analyser have also been presented in Table 4.1. The pore volumes of the clay samples were observed to be decreased after intercalation. The pore volumes of sample A, B and C decreased from 0.166 cm^3/g, 0.037 cm^3/g and 0.053 cm^3/g to 0.054 cm^3/g, 0.017 cm^3/g and 0.026 cm^3/g respectively. Except for sample A, the pore sizes of the clay material increased after intercalation. Sample A decreased from 137.396 4V/A to 124.392 4V/A in sample 2, while samples B and C increased from 54.219 4V/A and 58.355 4V/A to 148.449 4V/A and 136.778 4V/A respectively. The BET surface area were contrary to the pattern of Pore sizes. Except for

sample A, there was a decrease in the surface areas of the clay samples after intercalation. The pore sizes of sample A increased from 5.113 m^2/g to 18.256 m^2/g, while it reduces in samples B and C from 39.472 m^2/g and 47.728 m^2/g to 4.515 m^2/g and 6.324 m^2/g respectively, after intercalation. Another important character of clay samples is there position on the XRD 2θ scale. The resulting d(001) spacing in Å has been calculated using the Bragg's equation. The d(001) of A < B < C. A shift to the left in the XRD diffractogram corresponds with an increase in d(001) afrter modicication. The d(001) of the clay samples show an increase from 11.57, 13.25 and 15.25 to 20.27, 17.23 and 17.85 respectively after intercalation. The crude oil sorption capacity of the clay and organoclay samples have also been reported in Table 4.1. The organoclay samples showed higher oil sorption capacities than the raw clay samples. The Oil Sorption Capacity (OSC) of samples A, B and C were 1.36 g/g, 2.02 g/g and 1.43 g/g respectively, while those of their corresponding organoclays were 7.46 g/g, 7.56 g/g and 7.62 g/g of sorbent respectively.

The physical conditions used for the identification and synthesis of organonclay and their corresponding bulk density and d(001)mean values are presented in Table 4.2. The values are used subsequently to determine the effect of time, surfactant loading and temperature during intercalations on bulk density and d(001) spacing.

Table 4.1. Physicochemical paroperties of raw and organo-modified clays

S/N	Properties	Raw Samples			Organoclay Samples		
		A	B	C	2	5	8
1	Size (µm)	<200	<200	<200	<200	<200	<200
2	BD (g/cm^3)	1.508	1.432	1.584	1.004	0.912	1.016
3	MC (%)	0	2	0	0	0	0
4	VMC (%)	0	0	4	24	18	16
5	pH (10 %)	7.66	8.9	8.02	7.00	7.00	7.00
6	Pore Volume (cm^3/g)	0.166	0.037	0.053	0.054	0.017	0.026
7	Pore Size (4V/A)	137.396	54.219	58.355	124.392	148.449	136.778
8	BET SA (m^2/g)	5.113	39.472	47.728	18.256	4.515	6.324
9	CEC (Meq/100g)	98.24	106.7	92.6	ND	ND	ND
10	d(001) spacing (Å)	11.57	13.25	15.25	20.27	7.23	17.85
11	OSC	1.36	2.02	1.43	7.46	7.56	7.62

BD represents Buk Dnsity value; MC stands for moisture content; VMC, volatile matter content; BET SA, Bruner Emmet Teller Surface Area; CEC, cation exchange capacity; and OSC stands for the Oil soption capacity of the materials.

Table 4.2. Physical conditions for the synthesis of Organoclays

Sample ID	clay	Salt	T(°C)	t (hrs)	Conc	BD (g/cm^3)	d(001) (Å)
1	A	CTAC	80	10	50	0.97	11.74
2	A	CTAB	80	10	50	1.004	20.27
3	C	CTAC	80	10	50	0.736	16.70
4	B	CTAB	30	10	50	1.06	7.15
5	B	CTAB	80	10	50	0.912	7.23
6	B	CTAB	50	10	50	0.968	7.05
7	B	CTAC	80	10	50	1.023	7.01
8	C	CTAB	80	10	50	1.016	17.14
9	B	CTAB	90	10	50	0.912	7.13
10	A	CTAB	80	2.5	50	1.148	16.52
11	A	CTAB	80	5	50	1.116	17.51
12	A	CTAB	80	7.5	50	1.056	18.05
13	A	CTAB	80	12.5	50	0.921	19.59
14	C	CTAB	80	10	30	1.996	15.79
15	C	CTAB	80	10	20	1.092	17.85
16	C	CTAB	80	10	10	1.132	16.62
17	C	CTAB	80	10	5	1.168	15.89

T(°C) represients the Temparature (in °C); t(hrs) represents the interaction time (in hours); Conc is the concentration of the surfactant used; BD is the bulk density of the material after intercalation and $\delta_{(001)}$(Å) is the interlayer spacing of the materials (in Å).

4.1.1 Effect of intercalation properties on weigh on Bulk Density

The effect of time and surfactant loading on the mean Bulk Density (BD) values of the organoclays are graphically illustrated in Figures 4.1 and 4.2 respectively. From Table 4.2, the values of samples 2, 10, 11, 12 and 13 have been used to explain the effect of intercalation time on the bulk density of the organoclays while, the values of samples 8, 14, 15, 16 and 17 have been used to explain the effect of surfactant loading on bulk density of the organoclay. In the chart of Figures 4.1 and 4.2, the blue lines markers define the values of the bulk density with respect to time and surfactant concentration, while the red marker define the predicted bulk density by linear regression. The straight line equation gives a predictive relationship of the bulk density of the organoclays. For Figure 4.1, $BD = -0.04t + 1.37$ and for Figure 4.2, $BD = -0.08C + 1.32$ with R^2 values of 1. Where, t and C are the time and surfactant concentration respectively. The slope, intercept and R^2 values are listed in Table 4.3. Table 4.4 is the table of the results of the analysis of variance (ANOVA) showing significant P values of 0.015 and 0.112 respectively at 95 % confidence level.

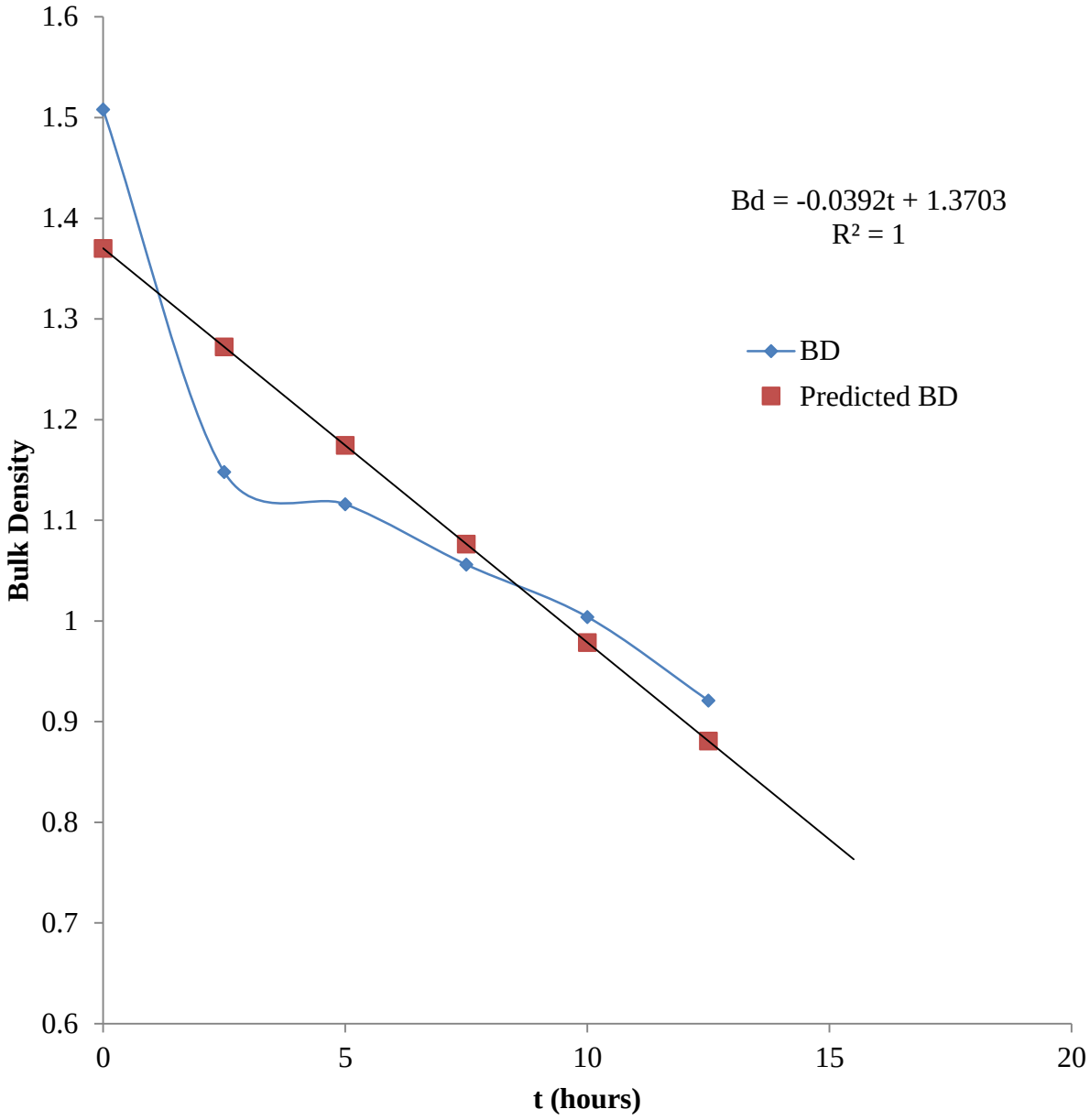


Figure 4.1:Linear and non-linear regression plots of the effect of time on bulk density

Where BD represents Bulk density and t is time (hours).

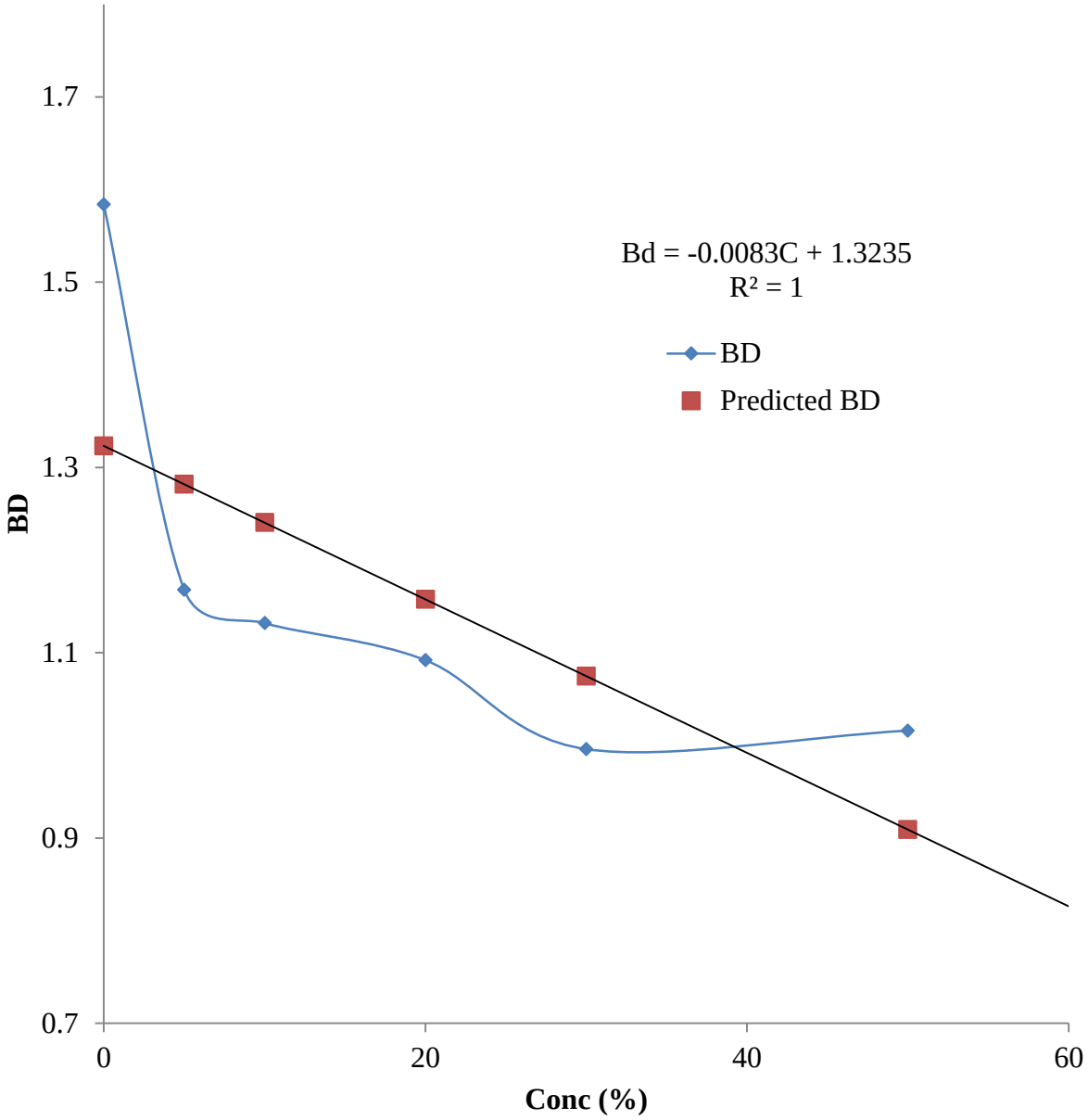


Figure 4.2: Linear and non-linear regression plots of the effect of concentration on bulk density

BD represents the bulk density of the samplw and Conc (%) is the concentration of the surfactant loading used in the synthetic process.

Table 4.3. Regression statistics of the Linear (predicted) residual plots of time and concentration on bulk density

Regression Statistics	Time	Concentration
R Square	1	1
Intercept	1.3703	1.3234
Slope	-0.0392	-0.0083

Table 4.4. Analysis of Variance for Time and Concentration Effect on Bulk Density

ANOVA

		df	*SS*	*MS*	*F*	*Significance P*
Time	Regression	1	0.1678	0.1678	16.5544	0.0152*
	Residual	4	0.0405	0.0101		
	Total	5	0.2083			
Concentration	Regression	1	0.1181	0.1181	4.1213	0.1122
	Residual	4	0.1146	0.0287		
	Total	5	0.2327			

*Significant difference between the samples at $P < 0.05$

4.2 X-Ray Fluorescence Analysis

Table 4.6 shows the chemical composition of the samples by X-Ray Fluorescence (XRF) analysis. The results gives the percentages of the Oxides of 14 metals and Cl in the samples. The major octahedral sheet minerals include Al_2O_3 and SiO_2. The values of Al_2O_3 in the clay samples A, B and C increased from 29.141 %, 16.619 % and 25.797 % respectively to 39.353 %, 25.335 % and 27.638 % for organoclay samples 2, 5 and 8 respectively. Except for sample A which reduced from 65.53 % to 54.093 % after intercalation to sample 2, Samples B and C showed an increase in the SiO_2 percentages after intercalation, from 40.884 % and 53.002 % to 51.838 % and 55.692 % respectively. Other octerhedral sheet minerals include Fe_2O_3, MgO and TiO_2. The amount of Fe_2O_3 in clay samples A, B and C all increase after intercalation from 1.318 %, 11.626 % and 12.124 % to 2.361 %, 9.660 % and 11.207 % respectively. For MgO, there is a change from 0.523 %, 5.863 %, 1.831 % to 0.616 %, 3.795 % and 1.574 % respectively for samples A, B and C after intercalation. A similar trend is observed in TiO_2 amounts from 2.211 %, 1.476 %, 1.520 % to 2.789 %, 1.155 % and 1.659 % resectively for samples A, B and C after intercalation.

The oxides of the major exchangeable cations in the tetrahedral layer of the clay minerals are NaO, CaO and K_2O. Contrary to the increasing tendency of the octahedral sheet minerals after intercalation, the exchangeable cations tend to reduce after intercalation except for the values of sample C in CaO and K_2O. NaO reduced from 0.077 %, 0.000 % and 2.959 % to 0.000 %, 0.000 % and 0.519 % respectively for organoclsys of samples A, B, C after intercalation. The amount of CaO changed from 0.019 %, 20.473 % and 0.465 % to 0.028 %, 1.155 % and 1.659 % for the organoclays of samples A, B and C respectively. In a similar

fashion, the K_2O concentration changed from 0.411 %, 1.293 % and 0.706 % to 0.375 %, 0.944 % and 0.859 % respectively for organoclays of samples A, B and C.

Table 4.5. The chemical composition raw and modified clay samples by XRF analysis

S/N	Oxides (%)	A	B	C	2	5	8
1	Na_2O	0.077	0.000	2.959	0	0.000	0.516
2	MgO	0.523	5.863	1.831	0.616	3.795	1.574
3	Al_2O_3	29.141	16.619	25.797	39.353	25.335	27.638
4	SiO_2	65.538	40.884	53.002	54.093	51.838	55.692
5	P_2O_5	0.000	0.000	0.000	0.000	0.000	0.000
6	SO_3	0.585	1.203	0.357	0.333	0.347	0.224
7	Cl	0.037	0.082	1.118	0.012	0.033	0.005
8	K_2O	0.411	1.293	0.706	0.375	0.944	0.859
9	CaO	0.129	20.473	0.465	0.028	6.677	0.512
10	TiO_2	2.211	1.476	1.520	2.789	1.155	1.659
11	Cr_2O_3	0.011	0.030	0.022	0.019	0.013	0.024
12	Mn_2O_3	0.010	0.358	0.073	0.015	0.145	0.070
13	Fe_2O_3	1.318	11.626	12.124	2.361	9.660	11.207
14	ZnO	0.000	0.024	0.016	0.003	0.024	0.014
15	SnO	0.009	0.068	0.012	0.004	0.034	0.005
	Total	100	100	100	100	100	100

4.3 Neutron Activation Analysis

The concentrations in g/1000g of the elements detected by the Instrumental Neutron Activation Analysis in the clay and organoclay samples are listed in Table 4.6. The Elements with the highest concentration in the clay and organoclays are the octahedral sheet minerals Al, Fe, Ti and Mg. After intercalation, the values of Al increased from 66850 g/1000g in sample A to 75750 g/1000g in sample 2, but decreased from 11180 and 6508 g/1000g in samples B and C to 78220 g/1000g and 108400 g/1000g in samples 5 and 8 respectively. The same pattern is observed in Fe. Samples A increased from 6952 g/1000g to 11330 g/1000g while samples B and C increased in concentration from 40830 g/1000g to 58060 g/1000g to 35930 g/1000g to 49390 g/1000g after intercalation. All concentrations of Ti decreased after intercalation especially in sample that decreased from 4316 g/1000g to 0 g/1000g. The major interlayer cations are Na, K and Ca. Na concentrations in samples A, B and C reduced from 183 g/1000g, 2165 g/1000g and 21770 g/1000g respectively to 180 g/1000g, 655 g/1000g and 3559 g/1000g in the modified samples 2 g/1000g, 5 g/1000g and 8 g/1000g. Similar reduction trend is observed in the K values, except for sample C that increased from 6508 to 8963. Br concentration was observed to have also increased in the clay samples after intercalation from 3.05, 3.71 and 3.5 in samples A, B and C respectively to 1155, 9198 and 8963 g/1000g in samples 2, 5 and 8 respectively. The concentrations of trace elements Cr, Mn, Zn, V, La, U, Ho, Sc, Cr, Co, Zn, Rb, Ba, Cs, Nd, Eu, Tb, Yb, Lu and Ta are also listed in Table 4.6. The results have been used to compare the concentrations of the samples and graphically illustrated in Figures 4.3 to 4.5. Figure 4.3 compares the exchangeable ion concentrations, Figure 4.4 compares the octahedral sheet minerals concentrations and Figure 4.5 compares the concentrations of selected trace metals in the samples

Table 4.6. Concentrations (g/1000g) of elements detected by neutron Activation Analysis

Elements	Raw samples			Organoclay samples		
	A	**B**	**C**	**2**	**5**	**8**
Na	183	2165	21770	180	655	3559
Mg	0	10190	4060	0	7087	6157
Al	66850	79400	117500	75750	78220	108400
Br	3.05	3.71	3.5	1155	1996	730
K	2260	11180	6508	2178	9198	8963
Ca	0	83670	0	0	27870	5256
Ti	6540	4316	5890	5530	0	5843
Cr	45	103	93	79	80	97
Mn	45	1328	241	33	377	268
Fe	6952	40830	58060	11330	35930	49390
Zn	0	117	98	0	0	90
V	35	139	106	38	140	268
La	80	32	62	65	N	57
U	3.5	1.7	BDL	BDL	N	N
Ho	1.8	1.8	BDL	BDL	N	N
Sc	1.8	1.8	BDL	BDL	N	N
Cr	45	103	93	79	80	97
Co	1.5	39	16	41	67	44
Zn	BDL	117	98	BDL	BDL	90
Rb	BDL	65	109	BDL	78	109
Ba	BDL	170	255	BDL	B	90
Cs	BDL	B	6.5	BDL	4	4
Nd	67	37	41	BDL	22	B
Eu	1.5	2.2	1.7	1	1.8	1.5
Tb	1.2	1.2	0.9	BDL	BDL	1.1
Yb	3.7	2.9	2.5	1.5	BDL	1
Lu	0.53	0.46	0.37	0.4	BDL	0.37
Ta	2.9	1	1.9	3.7	BDL	2.1

BDL- Below detectable limits; N- Not detected. All elemets are measured in g/1000g of samples used.

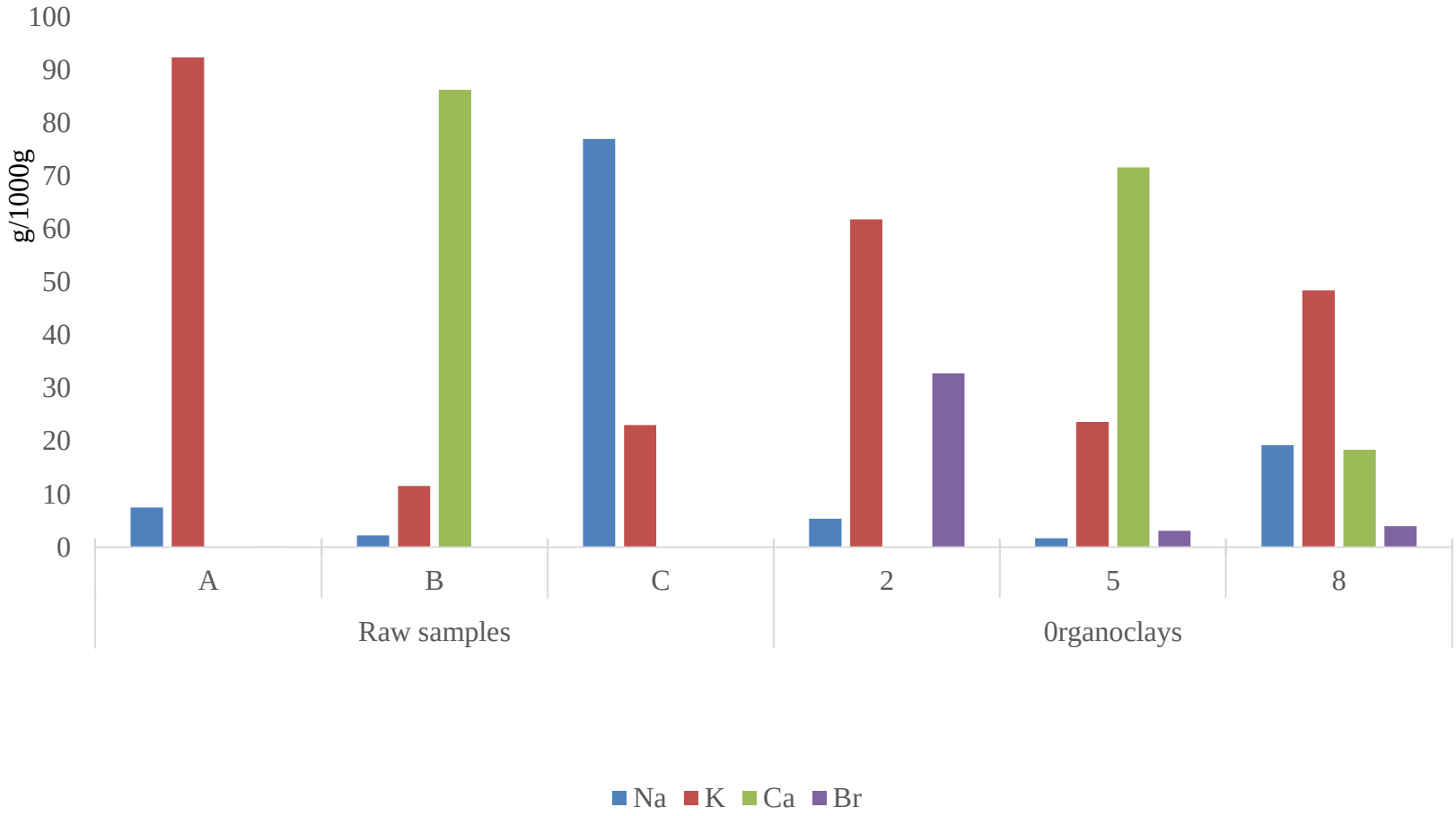


Figure 4.3: Concentrations of interlayer/exchangeable ions in samples as determined by NAA

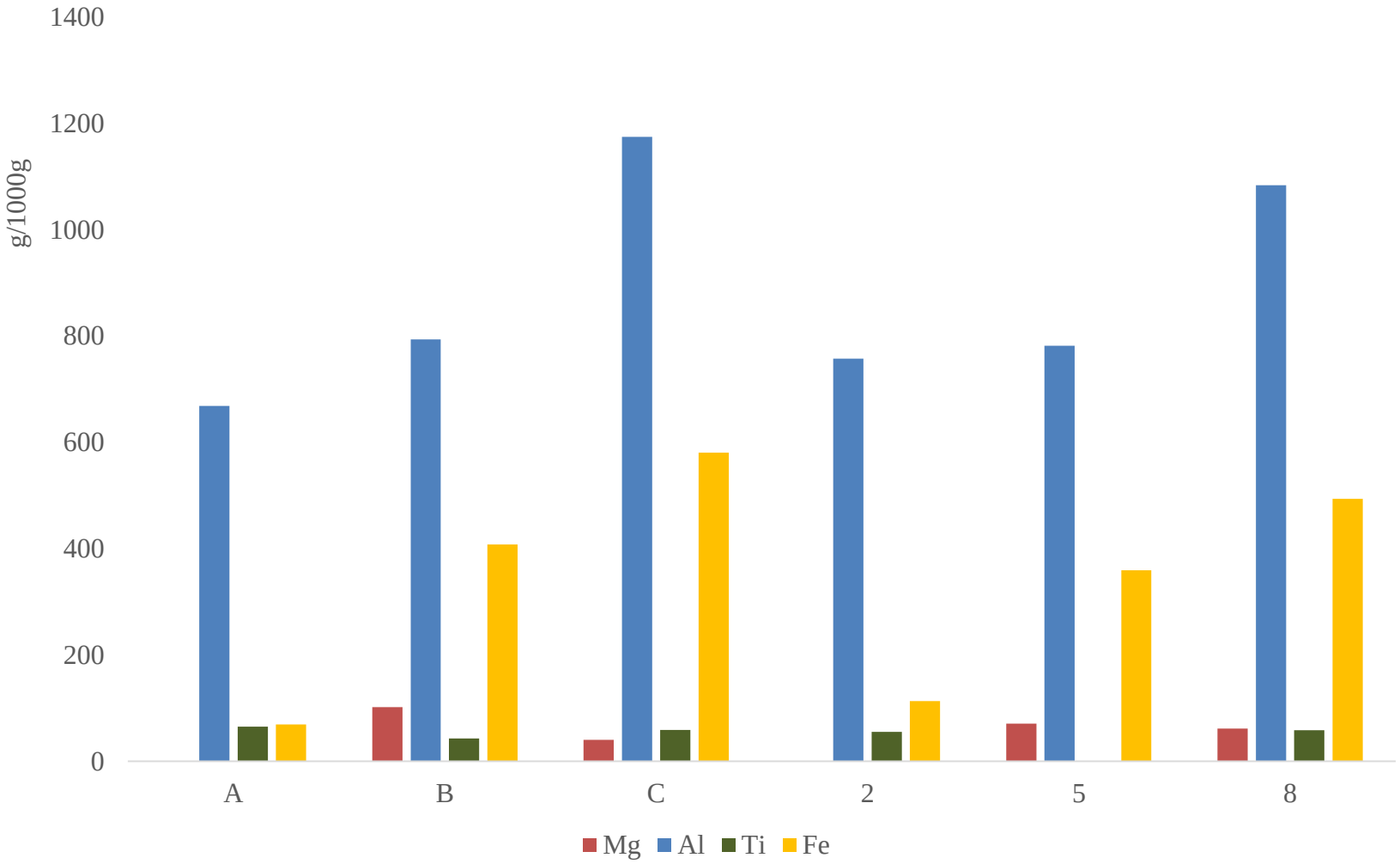


Figure 4.4: Concentrations of octahedral sheet minerals in samples as determined by NAA

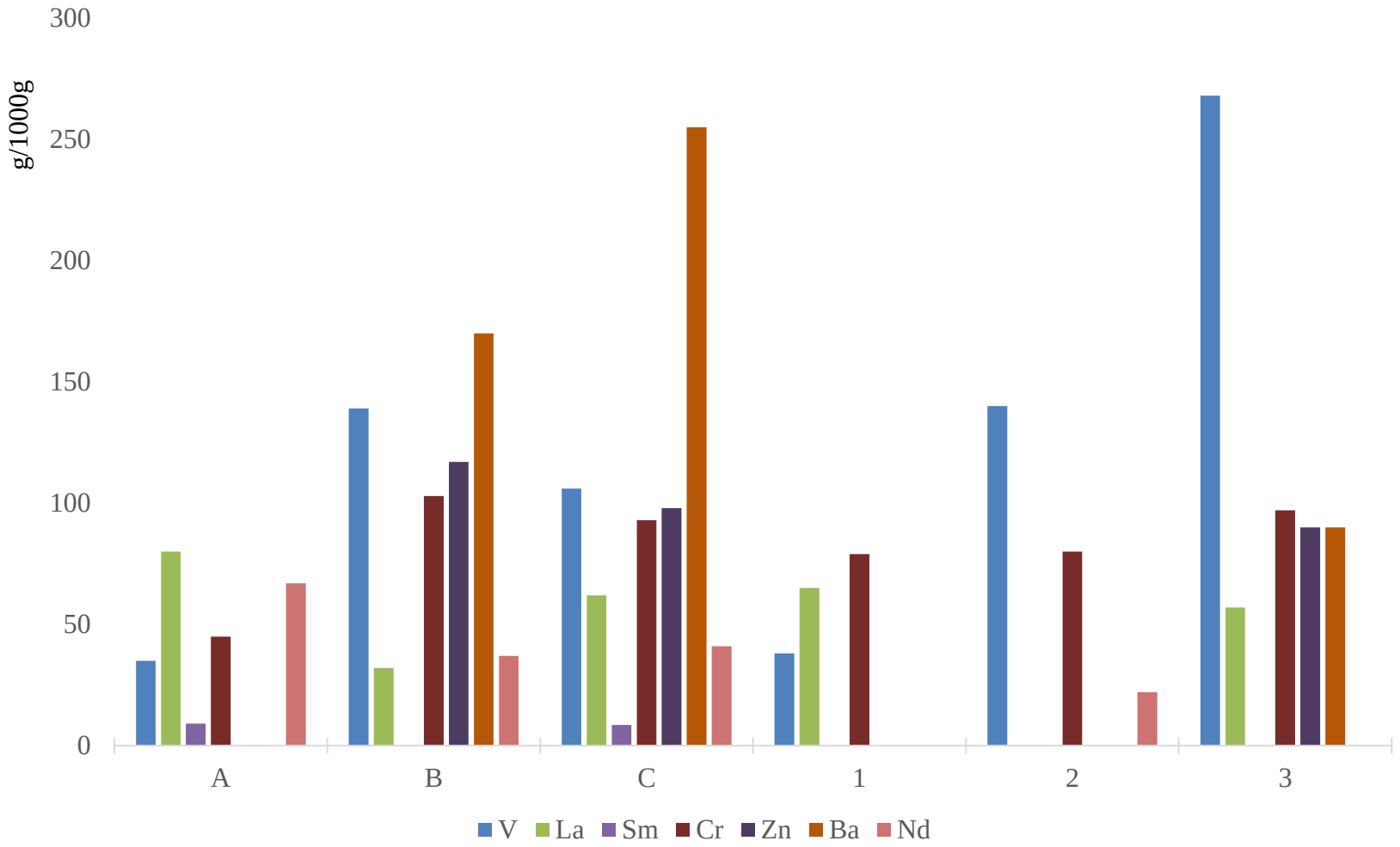


Figure 4.5: Concentrations of selected trace metals in samples as determined by NAA

4.4 X-Ray Diffraction Analysis

The diffractograms of the clay and organoclay samples have been presented in Figures 4.6 to 4.13. Figure 4.6 shows the crystallographic pattern of clay sample A. Characteristic d(001) peak for montmorillonite containing samples is reflected at 7.63 $^{o}2\theta$ (11.57 Å) with the d(001) peaks of Quartz (SiO_2) reflected at around 27 $^{o}2\theta$. Figure 4.7 shows the d(001) reflection of montmorillonite at 6.67 $^{o}2\theta$ (13.25 Å) and the peaks for silica at about 27 $^{o}2\theta$ with shoulder bands around 30 and 32 $^{o}2\theta$. Figure 4.8 shows the diffractogram of sample C. The d(001) peak for montmorillonite is reflected at 5.79 $^{o}2\theta$ (15.25 Å), again with peaks for silica at about 27 $^{o}2\theta$. Figure 4.9 is a superimposition of Samples A, B and C indicating the differences in the crystal properties of the natural clays. The d(001) spacing (Å) of A < B < C and is seen in their position in the 2θ axis of the diffractorgrams. Figure 4.10 accounts for the effect of time on the d(001) spacing of the organoclays. The XRD pattern of samples A, 2, 10, 11 and 13 have been superimposed to illustrate the effect of time on d0001 spacing. Figure 4.11 accounts for the effect of surfactant loading on d(001) spacing of using samples C, 14, 15, 16 and 17. Figure 4.12 also accounts for the effect of temperature on the d(001) spacing of samples B, 4, 5, 6 and 9. The chart of Figure 4.13 explains the effect of salt type and also clay type on intercalation. A shift to the left after intercalation with CTAB and CTAC is noticed. The d(001) peaks CTAB are relatively more to the left than the d(001) peaks of CTAC.

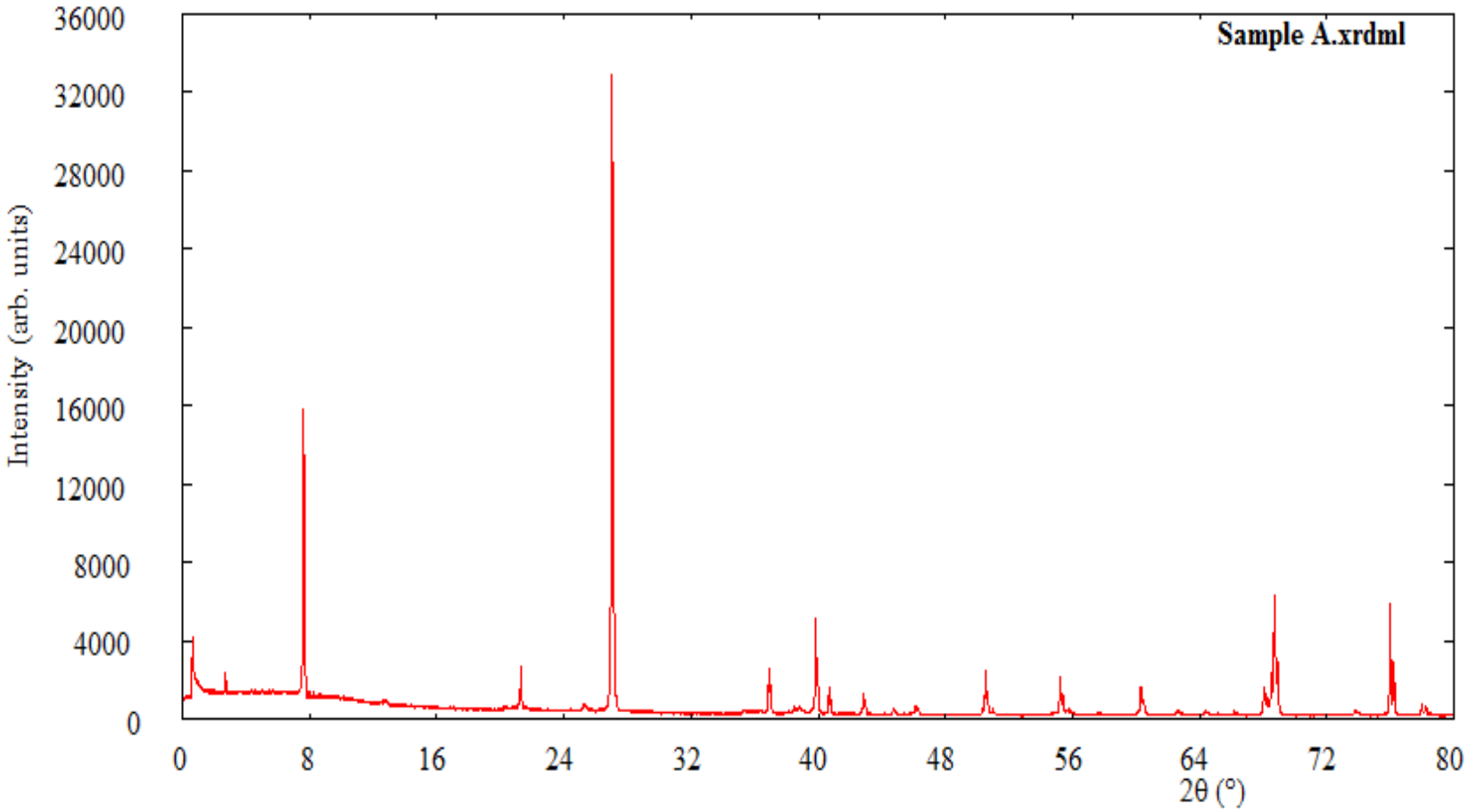


Figure 4.6: XRD crystallographic pattern for sample A.

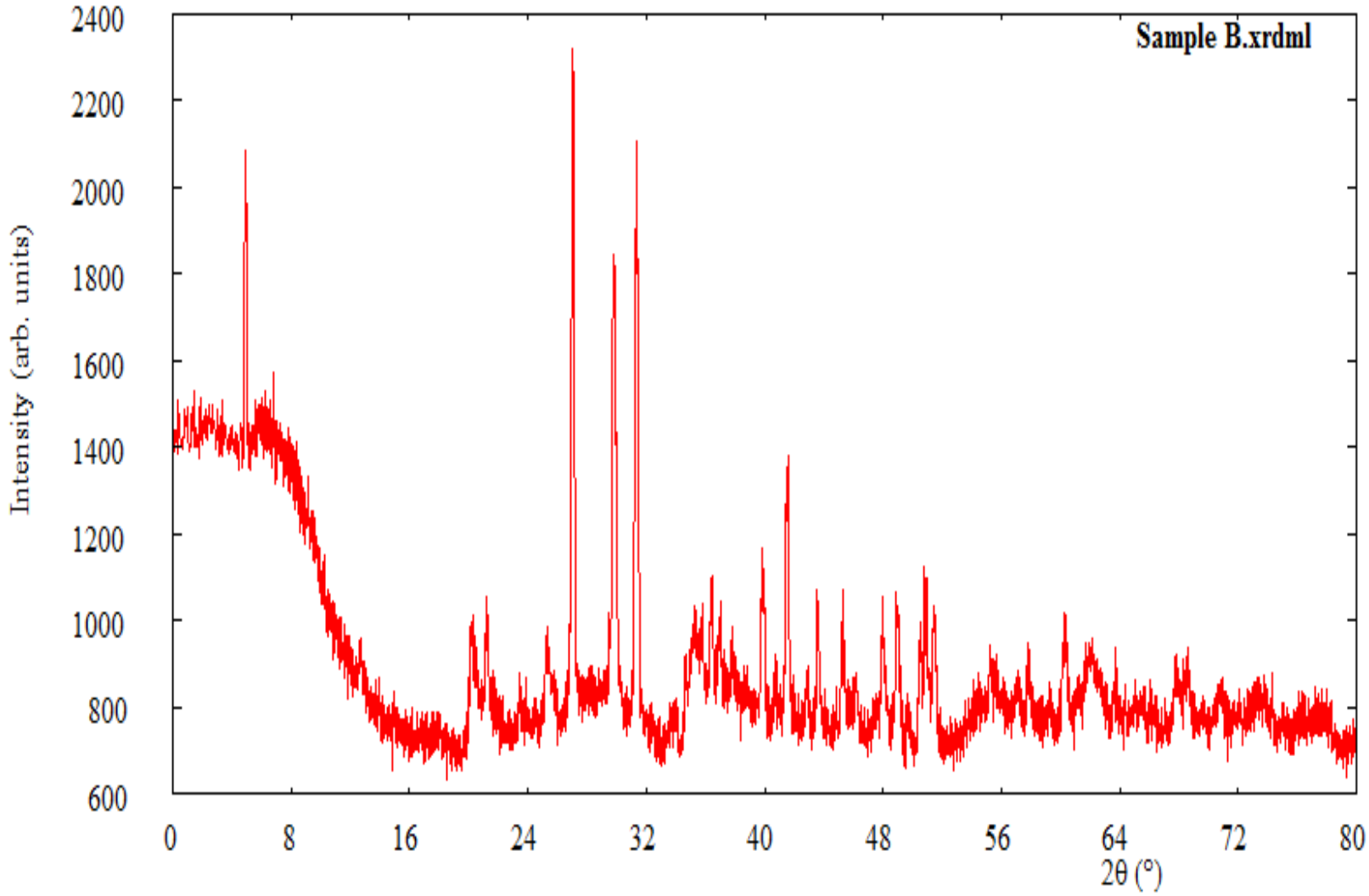


Figure 4.7: XRD crystallographic pattern for sample B

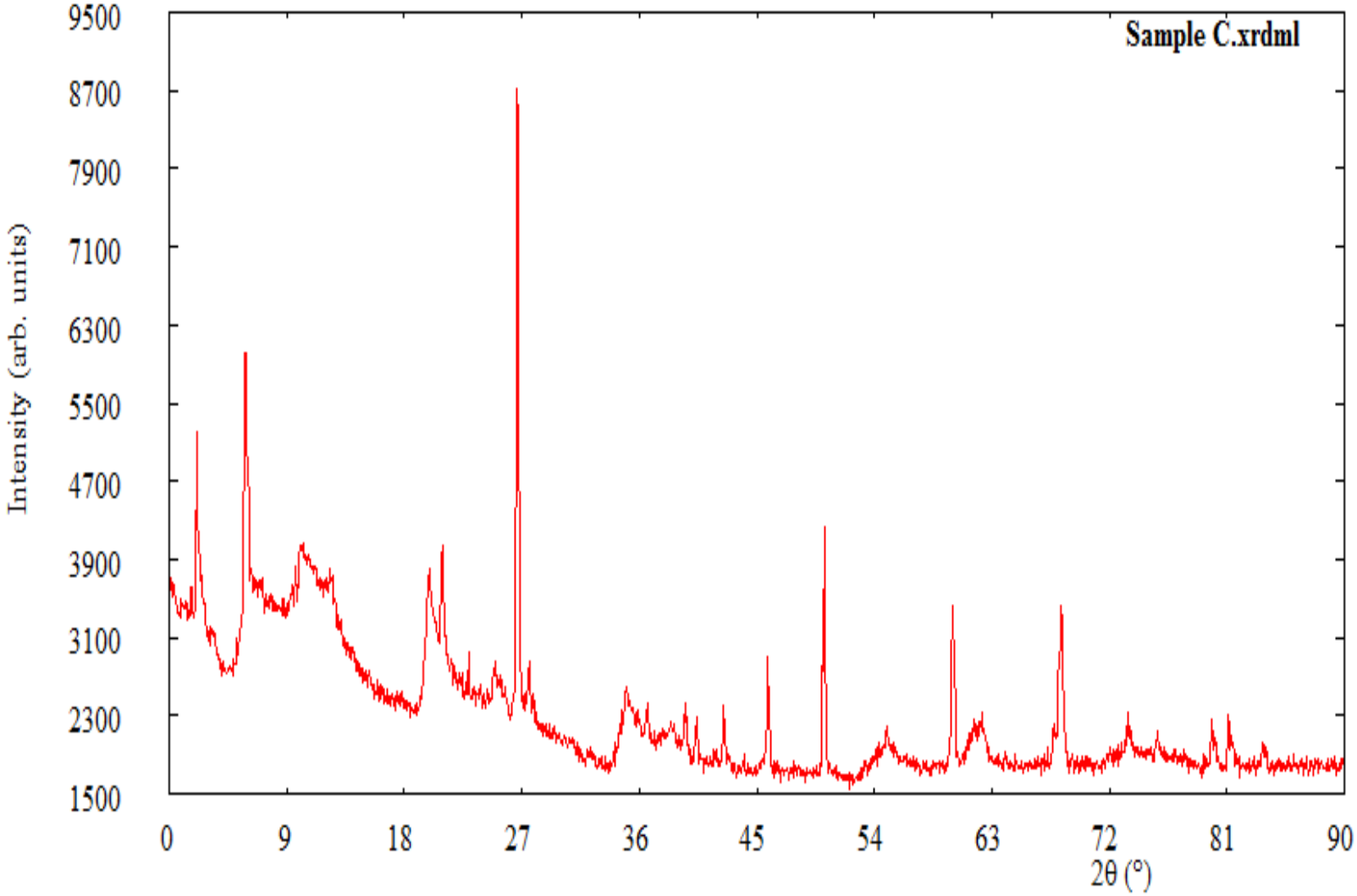


Figure 4.8:XRD crystallographic pattern for sample C

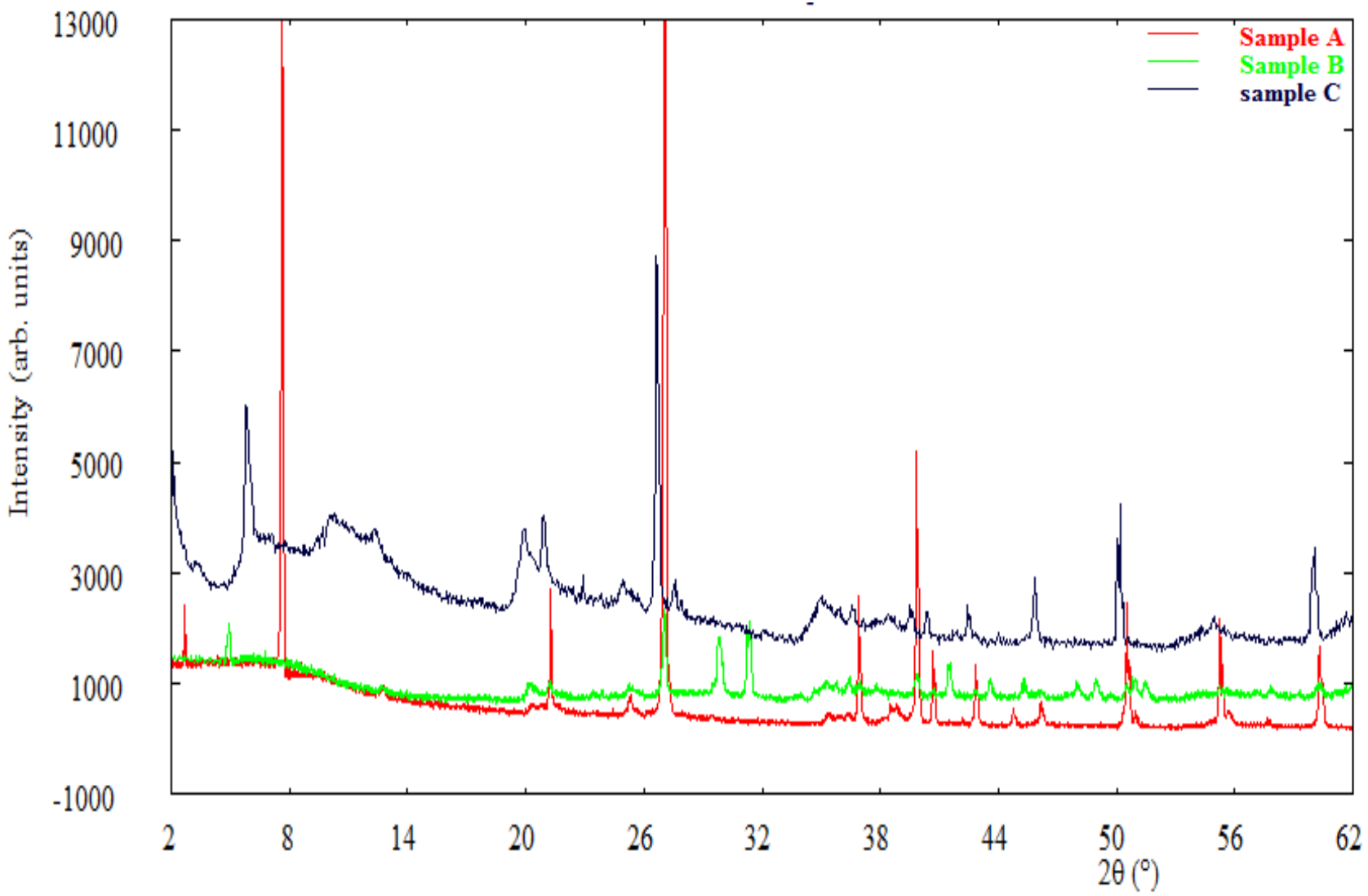


Figure 4.9: Superimposition of the XRD patterns of samples A, B and C

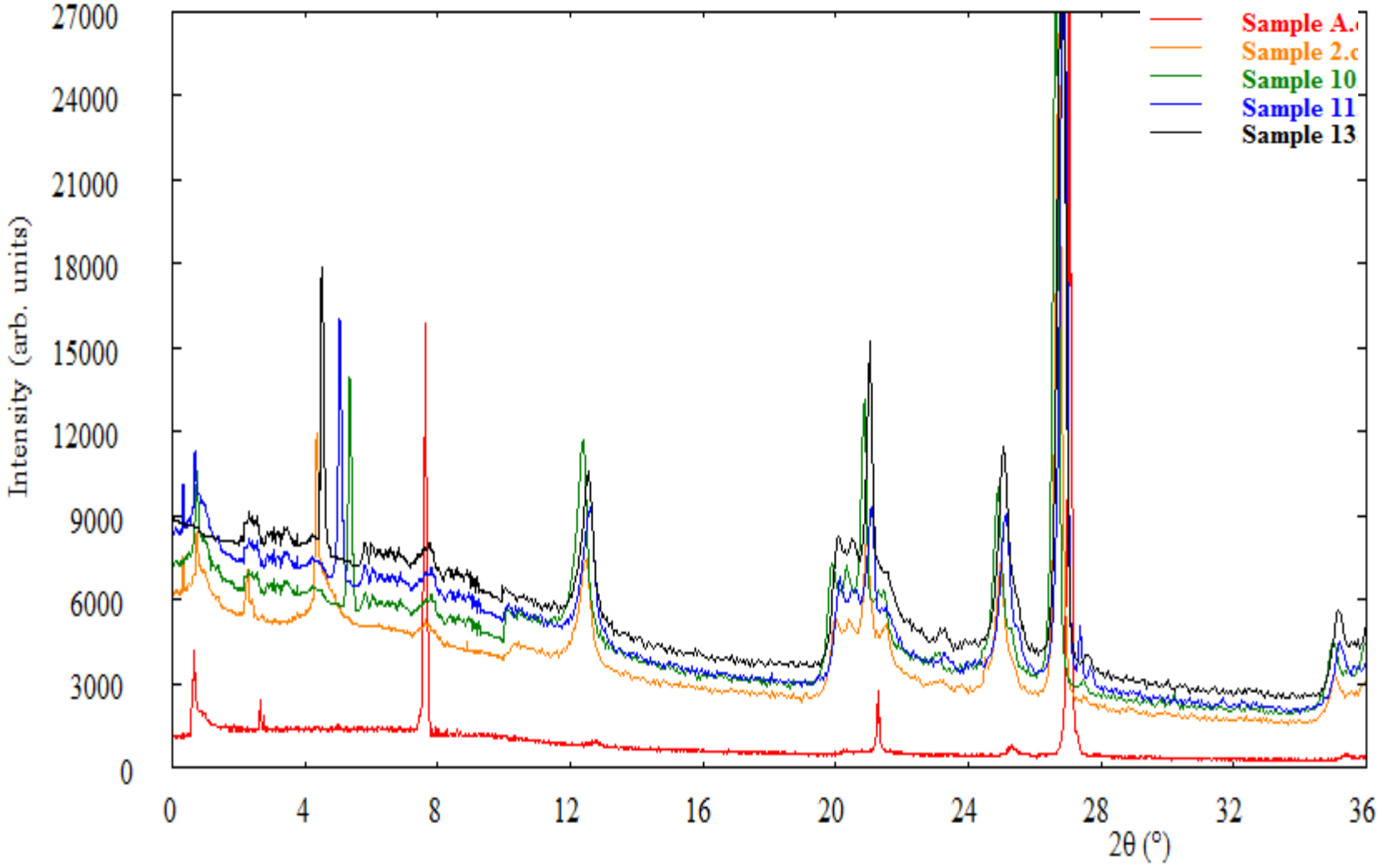


Figure 4.10: Effect of time on intercalation: XRD diffractograms of Samples A, 2, 10, 11 and 13

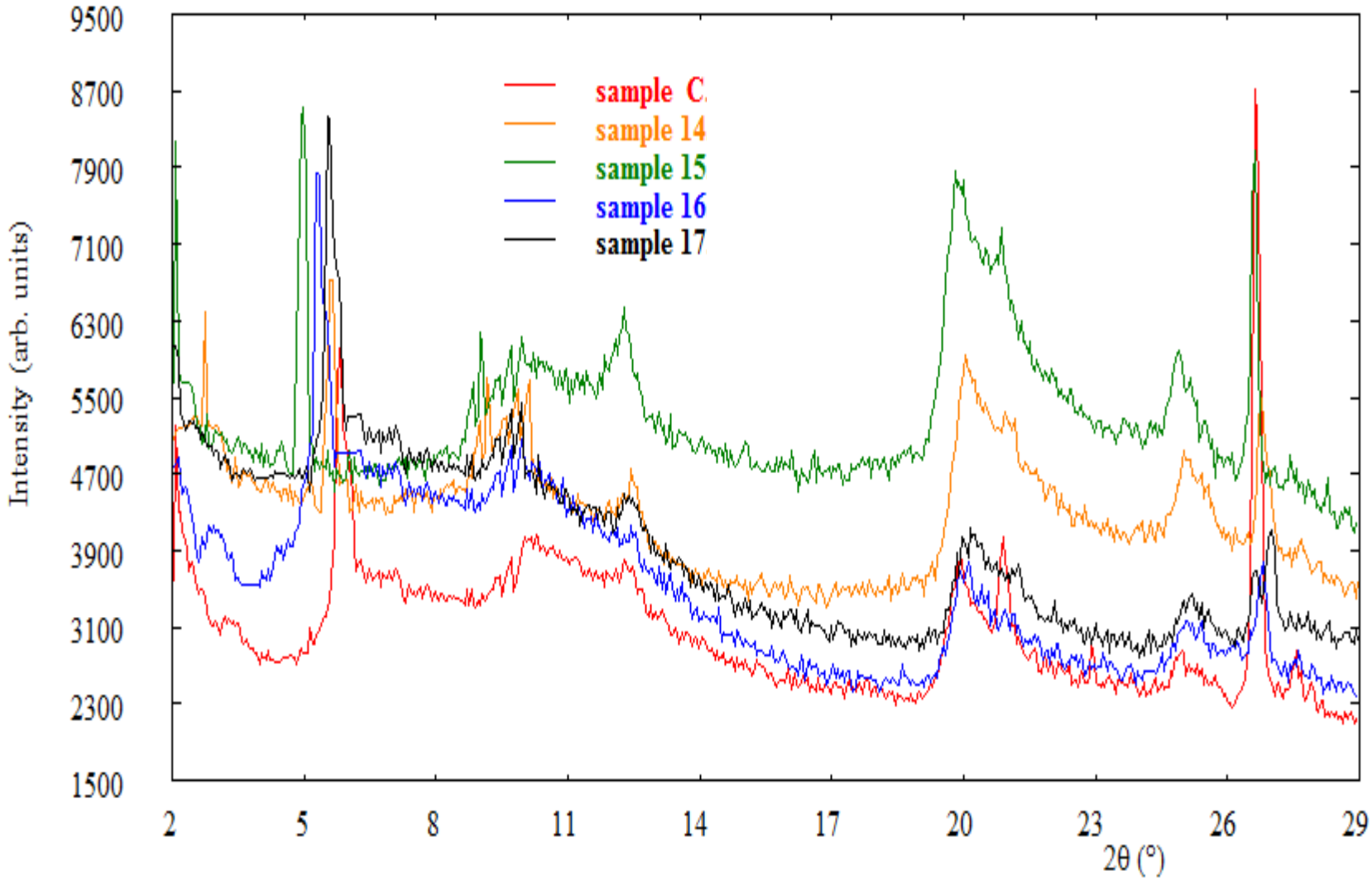


Figure 4.11: The effect of surfactant loading on intercalation: XRD diffractograms of Samples C, 14, 15, 16 and 17

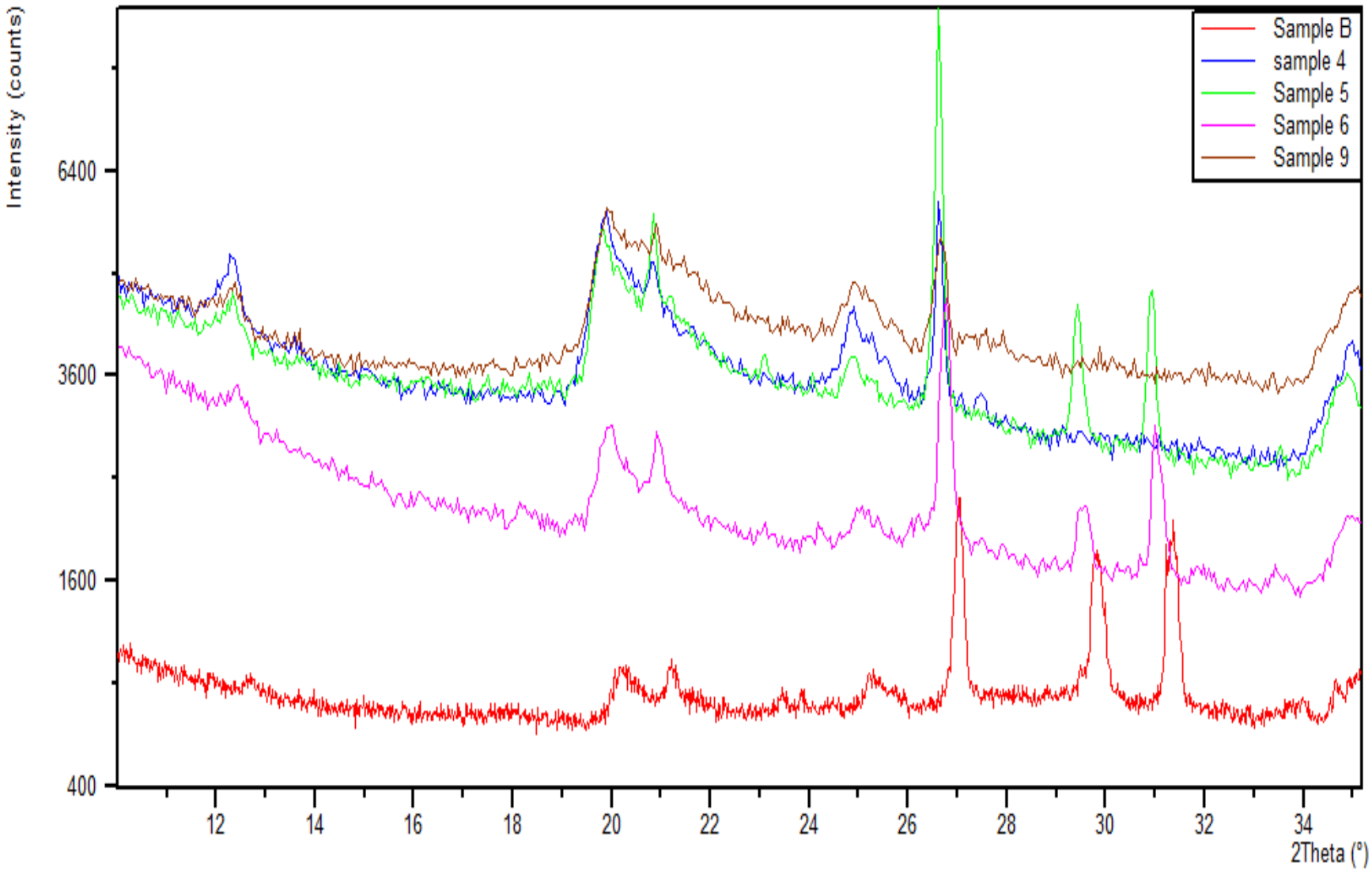


Figure 4.12: Effect of temperature on intercalation: XRD diffractograms of Samples B, 4, 5, 6 and 9

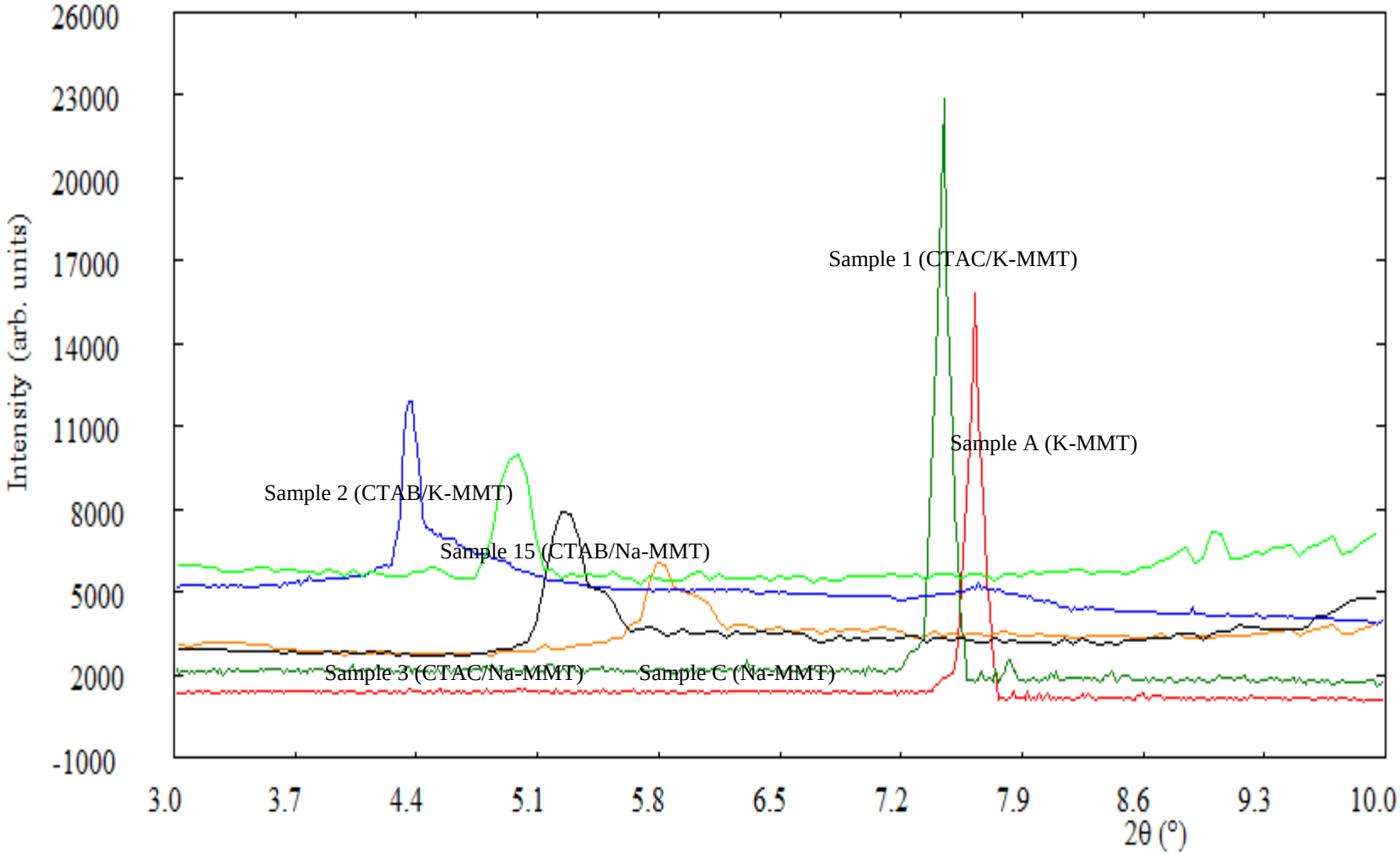


Figure 4.13: Effect of salt type on intelrcalation: XRD diffractograms of Samples A, B, C, 1, 2 and 15.

4.5 Fourier Transform Infrared Spectral Analysis

The FTIR spectral bands positions and there vibration mode over the spectral range of 4000 – 400 cm^{-1} are summarized in Table 4.7. Bands at 470-420 cm^{-1} are vibrational modes for Si-O and Al-O bending from the clay minerals. Bands at 550-510 are attributed to Si-O-Al tetrahedral bending of octahedral smectites. Band at 900-600 cm^{-1} indicate Mg-Al-OH bending of smectite clays. The distinct peaks at 914 cm^{-1} are indicative of Al-Al-OH bending of interlayer Aluminium. Bands at 1060-1000 cm^{-1} are attributed to Si-O (out-of-plane) vibrations of smectites/layered-silicates. The bands at 1480-1400 cm^{-1} reflect CN stretching and CH bending due to Angular deformation of CH_3 groups from the surfactants. Bands at 1660-1620 cm^{-1} are O-H bending modes of clay interlayer water. Bands between 3000-2800 cm^{-1} have been attributed to C-H Stretching modes and CH_2 absorption bands from organic ammonium cation. The bands at 3600-3440 cm^{-1} are attributed to O-H stretching from Interlayer hydration in clays and organoclays. The distinct band at 3622 cm^{-1} are attributed to Al-Al-OH (and Si-OH-Al) Stretching vibration of clay interlayer water while the 3655 cm^{-1} position is indicative of Si-O-H stretching vibration of Silica.

Figure 4.14 is the FTIR spectra of sample A over the range of 400 and 4500 cm^{-1}. The strong bands around 3670 cm^{-1}, 3442 cm^{-1},1031 cm^{-1}, 530 cm^{-1} and 458 cm^{-1} are reflected in the spectra of Sample A. Figure 4.15 is the FTIR spectra of sample B, over the range of 400 to 4500 cm^{-1}. Strong bands are observed around 3620 cm^{-1}, 3428 cm^{-1}, 1433 cm^{-1}, 1030 cm^{-1} and 443 cm^{-1}. Figure 4.16 is the FTIR spectra of sample C, over the range of 400 to 4000 cm^{-1}. Strong bands are observed around 3622 cm^{-1}, 3416 cm^{-1}, 1241 cm^{-1}, 1033 cm^{-1}, and 470 cm^{-1}. Figure 4.17 shows the spectra of the clay samples A, B and C and organoclay samples 2 and 5, illustrating the effect of intercalation on the structural properties of the clay samples.

New bands have been observed to appear around 2922 cm^{-1}, 2852 cm^{-1} and 1470 cm^{-1} also the broadening and increase intensity of bands around 2354 cm^{-1} is observed. The effect of intercalation time on the structural properties of the clays samples is shown in Figure 4.18. Where the spectra of samples A, 2, 10 and 11 are presented. Sample A, 2, 10 and 11 were intercalated for 0.0, 10.0, 2.5 and 5 hours respectively. The chart confirms the presence of increasing peaks around 3662 cm^{-1}, and new peaks around 2900 cm^{-1}, 2800 cm^{-1} and 1400 cm^{-1}. The effect of CTAB surfactant loading on intercalation and structural properties of clays is also illustrated in Figure 4.19 using samples C, 15, 16 and 17. Samples C, 15, 16 and 17 were respectively intercalated with 0, 20, 10 and 5 % w/w surfactant concentration. The chart confirms the presence of increasing peaks around 3662 cm^{-1}, and new peaks around 2900 cm^{-1}, 2800 cm^{-1} and 1400 cm^{-1}. In Figure 4.20, sample B, 4 and 6 have been used to illustrate the effect of temperature on intercalation and structural properties of clays. Samples 4 and 6 were intercalated at 30 and 50 ^{o}C respectively. The chart confirms the presence of increasing peaks around 3662 cm^{-1}, and new peaks around 2900 cm^{-1}, 2800 cm^{-1} and 1400 cm^{-1}.

Table 4.7. Assignment of IR Bands for functional groups

Position (cm^{-1})	**Vibration**	**Inference**
470-420	Si-O and Al-O bending	Clay minerals
550-510	Si-O-Al tetrahedral bending	Octahedral smectite
900-600	Mg-Al-OH bending	Smectite
914	Al-Al-OH bending	Interlayer Aluminium
1060-1000	Si-O (out-of-plane)	Smectites/layered-silicates
1480-1400	CH bending	Angular deformation of CH_3 groups
1660-1620	O-H bending	Interlayer water
3000-2800	C-H Stretching, CH_2 absorption bands	Organic ammonium cation
3600-3440	O-H stretching	Interlayer hydration
3622	Al-Al-OH (and Si-OH-Al) Stretching	Interlayer water
3655	Si-O-H stretching	Silica

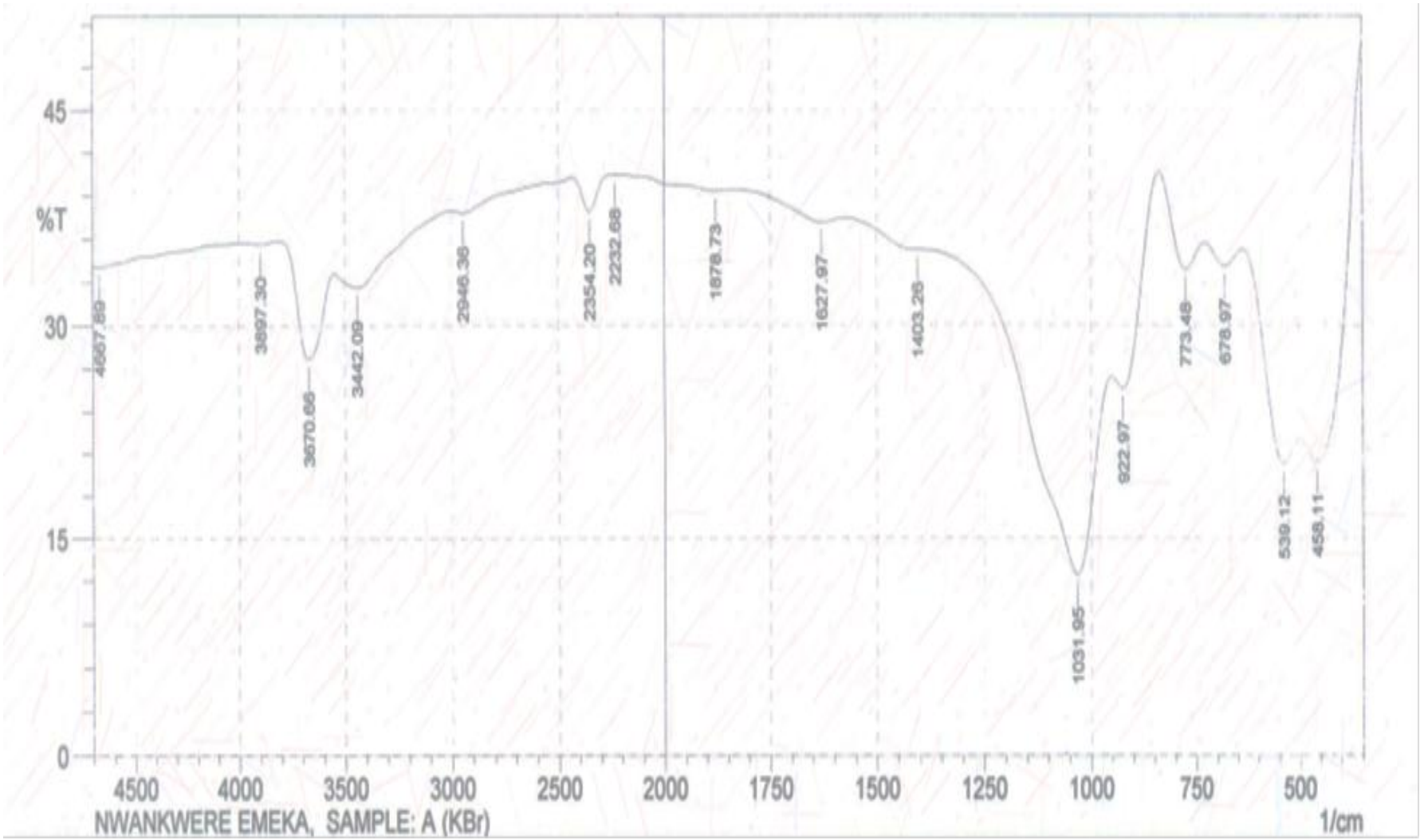


Figure 4.14: FTIR Spectra of Sample A

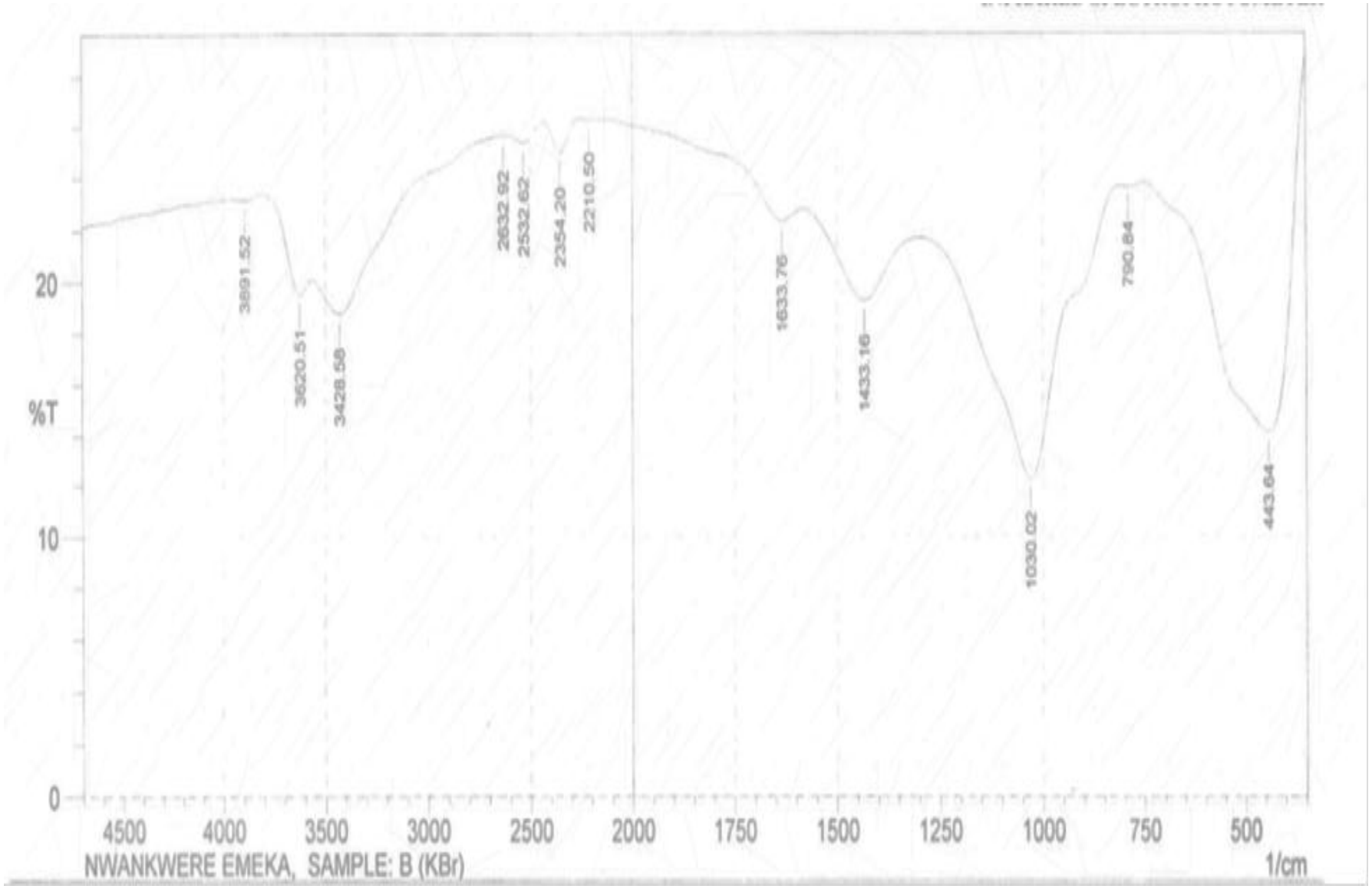


Figure 4.15: FTIR Spectrum of Sample B

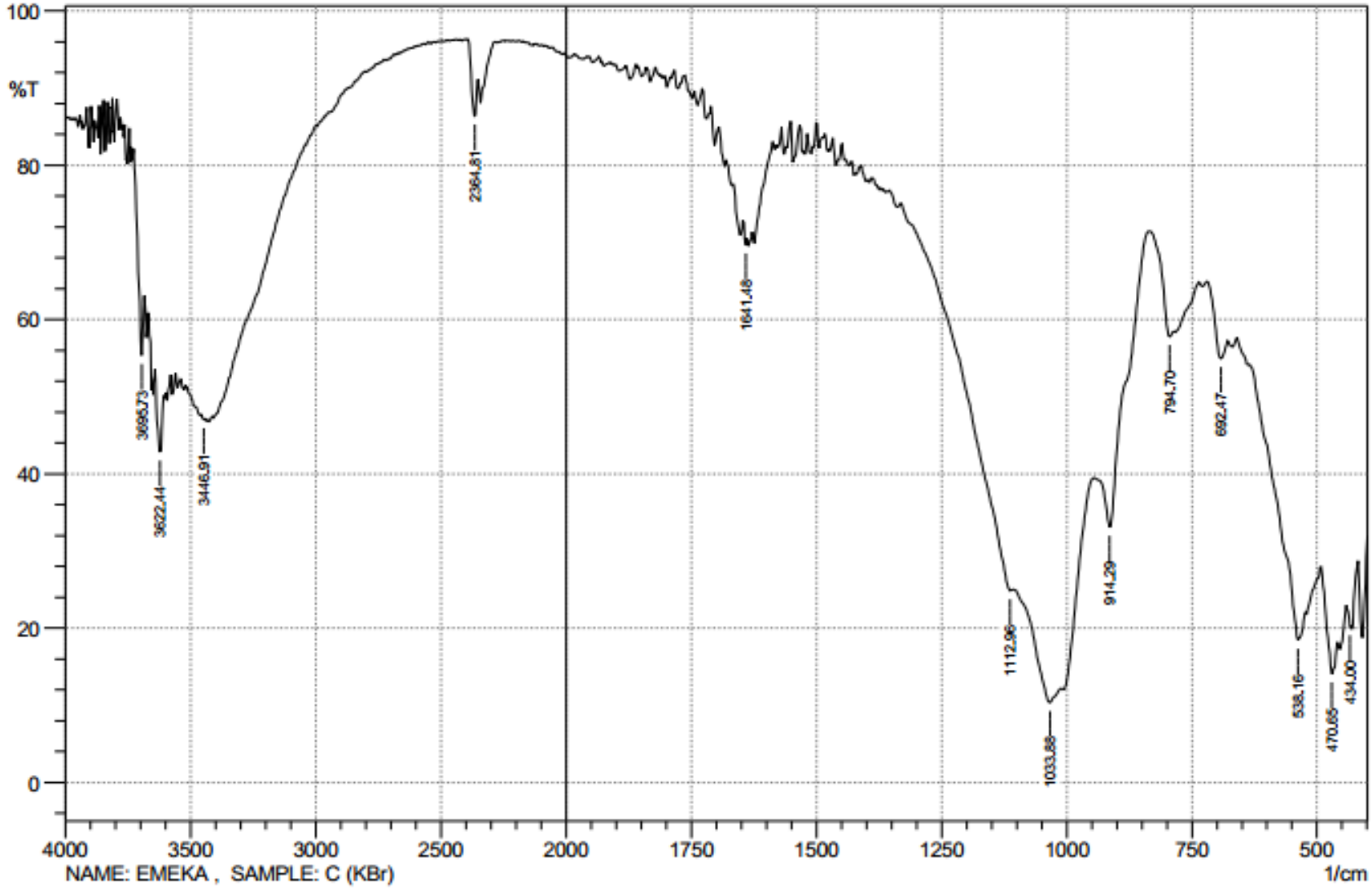


Figure 4.16: FTIR spectrum of sample C

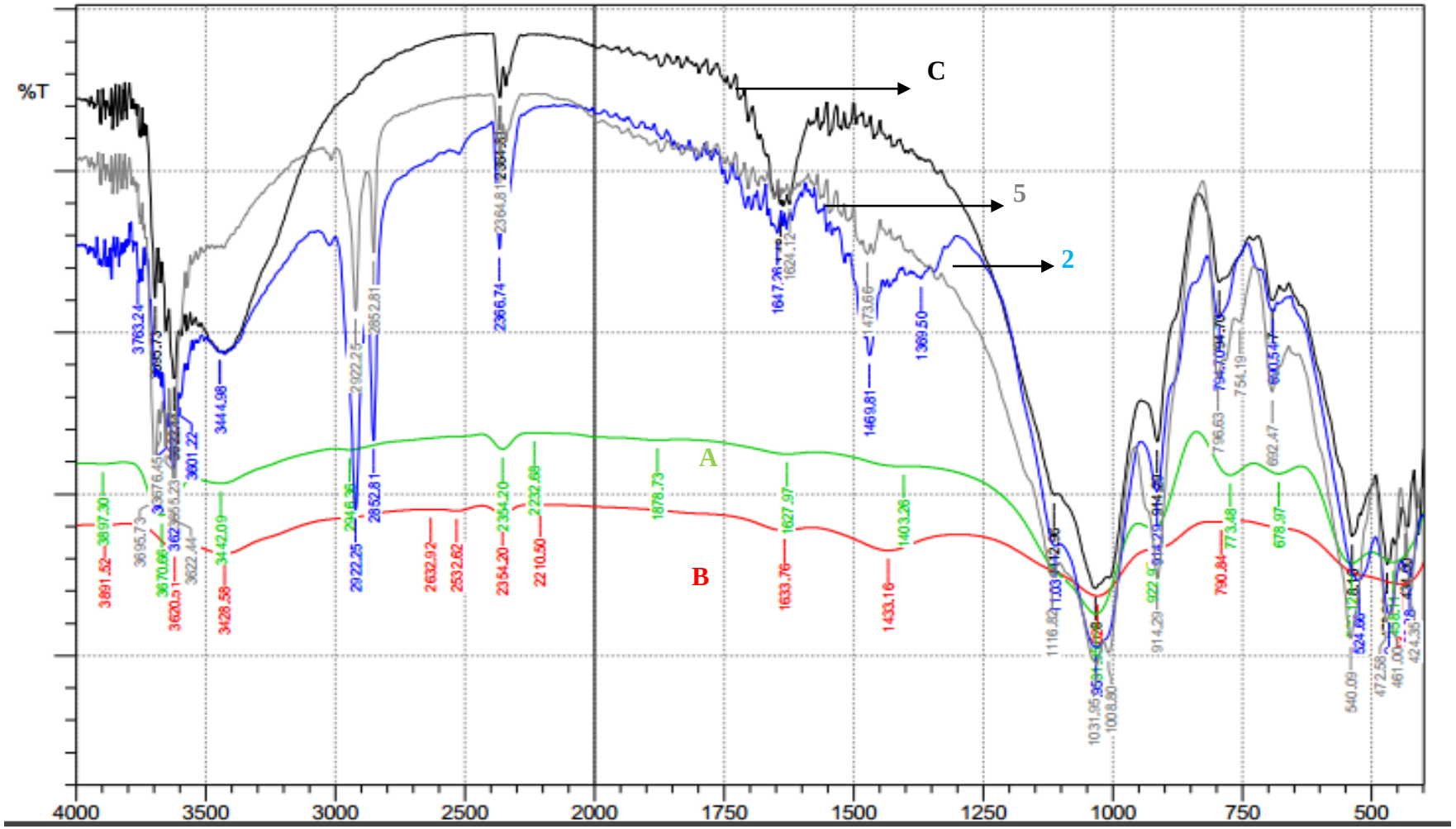


Figure 4.17: FTIR spectra of clays and their corresponding organoclays, illustrating the. Effect of intercalation (samples A, B, C, 2 and 5)

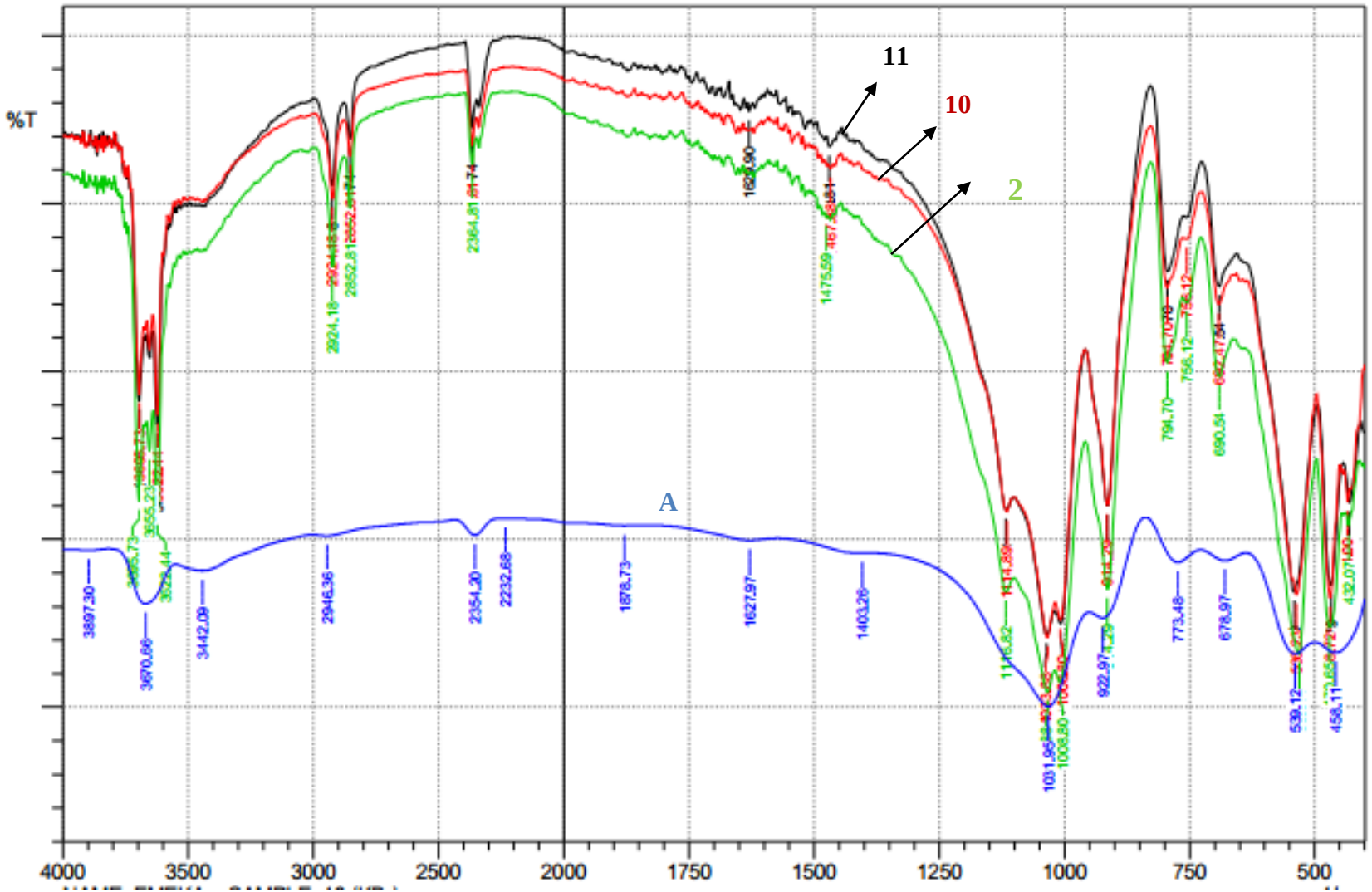


Figure 4.18: FTIR spectra of sample A and organoclay samples 2, 10 and 11 cation exchanged clays over the time range 1 to 12 hours, illustrating the effect of time on intercalation

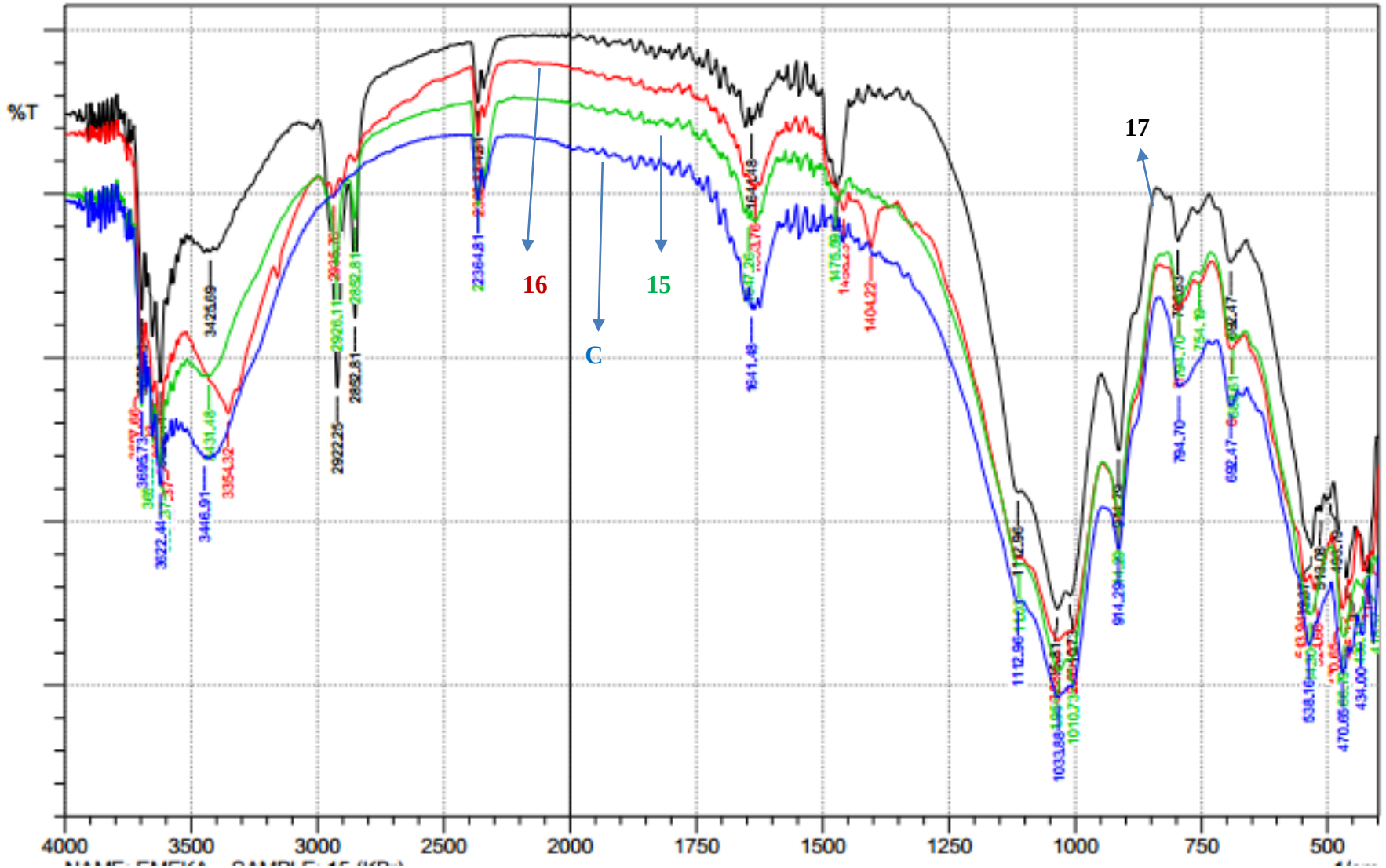


Figure 4.19: Infrared spectra of sample C and corresponding organoclays 15, 16 and 17 over the CTAB concentration range 0.2 to 4.0 w/w of clay, illustrating the effect of surfactant loading on intercalation

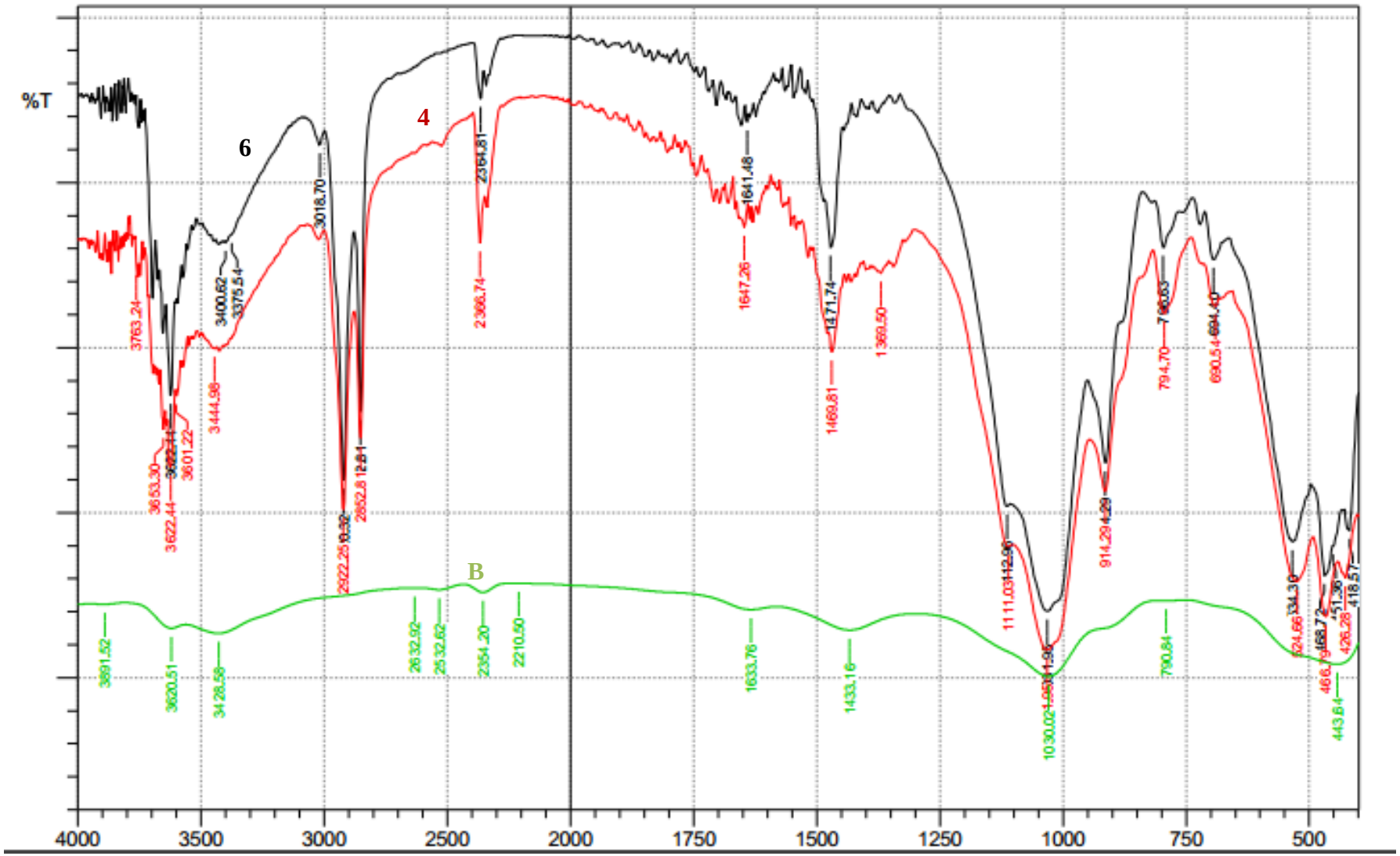


Figure 4.20: FTIR spectra of Sample B, 4 and 6 illustrating the effect of temperature on intercalation

4.6 Thermal Gravimetric Analysis

Table 4.8 shows summarizes the changes in the stages involved during the thermogravimetric and differential scanning calorimetric analysis of the clay and organoclay samples. The analysis has been divided into four stages. Stage 1 involves mass loss at 80 to 120 ^{o}C. Changes were observed in the TG studies of the raw clay samples but not in those of the organoclay samples. Samples A reduced by 0.1 % starting at 86 ^{o}C, sample B decreased in mass by 1.4 % starting from 84.5 ^{o}C and sample C decreased by 3.3 % starting from 83.5 ^{o}C. In stage 2 and 3, the mass loss of samples A, B and C were 0.3 %, 3.8 % and 0.0 % respectively. In the final stage the mass loss of the samples increased significantly by 1.78 % in sample A, 6.2 % in sample B, 7.3 % in sample C, 10.5 % in sample 2 and 22.8 % in sample 5. The peak values in the thermograms of the samples were 125.25 ^{o}C, 82.92 ^{o}C, 246.35 ^{o}C and 256.75 ^{o}C for samples B, C, 2 and 5 respectively. The peak value reduction rate were -62.69 mg/min, -64.31 mg/min, -0.16 mg/min and -0.2 mg/min for samples B, C, 2 and 5 respectively.

The themogram of sample A is presented in Figure 4.21. The initial weight of the sample used was 2.52 mg and reduced by 1.743 % to 0.044 mg at the midpoint of 445.2 ^{o}C. The DSC scan showed instability in the heat profile of the clay material till 500 ^{o}C. The thermogram of sample B is presented in Figure 4.22. The initial weight of sample used was 8.55 mg and was reduced 6.15 % to about 8.02 mg at midpoint of 302.33 ^{o}C. The differential thermal scans showed instability in the clay samples with maximum peaks at 86.36 and 125.25 ^{o}C. The thermogram of sample C is also presented in Figure 4.23. The initial weight of sample used was 8.46 mg and was reduced by 7.20 % to 7.85 mg at midpoint of 439.32

^{o}C. The differential thermal scans showed instability in the clay samples with maximum peaks at 82.92 ^{o}C.

The thermogram of sample 2, which represents the organoclay of Sample A is presented in Figure 4.24. The initial weight of sample introduced was 7.98 mg and was reduced by 10.54 % to 7.14 mg at midpoint of 458.21 ^{o}C. The differential thermal scans showed sample 2 to be stable till about 241 ^{o}C. The thermogram of sample 5, which is the organoclay of sample B is also presented in Figure 4.25. The initial weight of sample introduced was 4.93 mg and was reduced by 22.75 % to about 3.81 mg at midpoint of 270.70 ^{o}C. Sample 5 showed good thermal stability for the first 292 ^{o}C.

Table 4.8. Results TG and DSC of analysis

Samples	Stage 1 (100±20^{o}C)		Stage 2-3 (120-375 ^{o}C)		Final stage (375-500 ^{o}C)		DTG	
	M loss (%)	*Inflt pt. (^{o}C)*	*M loss (%)*	*Inflt pt. (^{o}C)*	*M loss (%)*	*Inflt pt. (^{o}C)*	*Peak (^{o}C)*	*peak value (mg/min)*
A	0.1	86	0.3	150	1.78	474.8	-	-
B	1.4	84.5	3.8	124	6.2	392	86.36, 125.25	-57.58, -62.69
C	3.3	83.5			7.3	475.55	82.92	-64.31
2	-	-	5.8	246.0	10.5	489.7	246.35	-0.16
5	-	-	10.8	128	22.8	254	256.75	-0.2

M loss (%) represents the weight loss of the samples during combustion. Inflt pt. stands for the inflection point during the TGA analysis

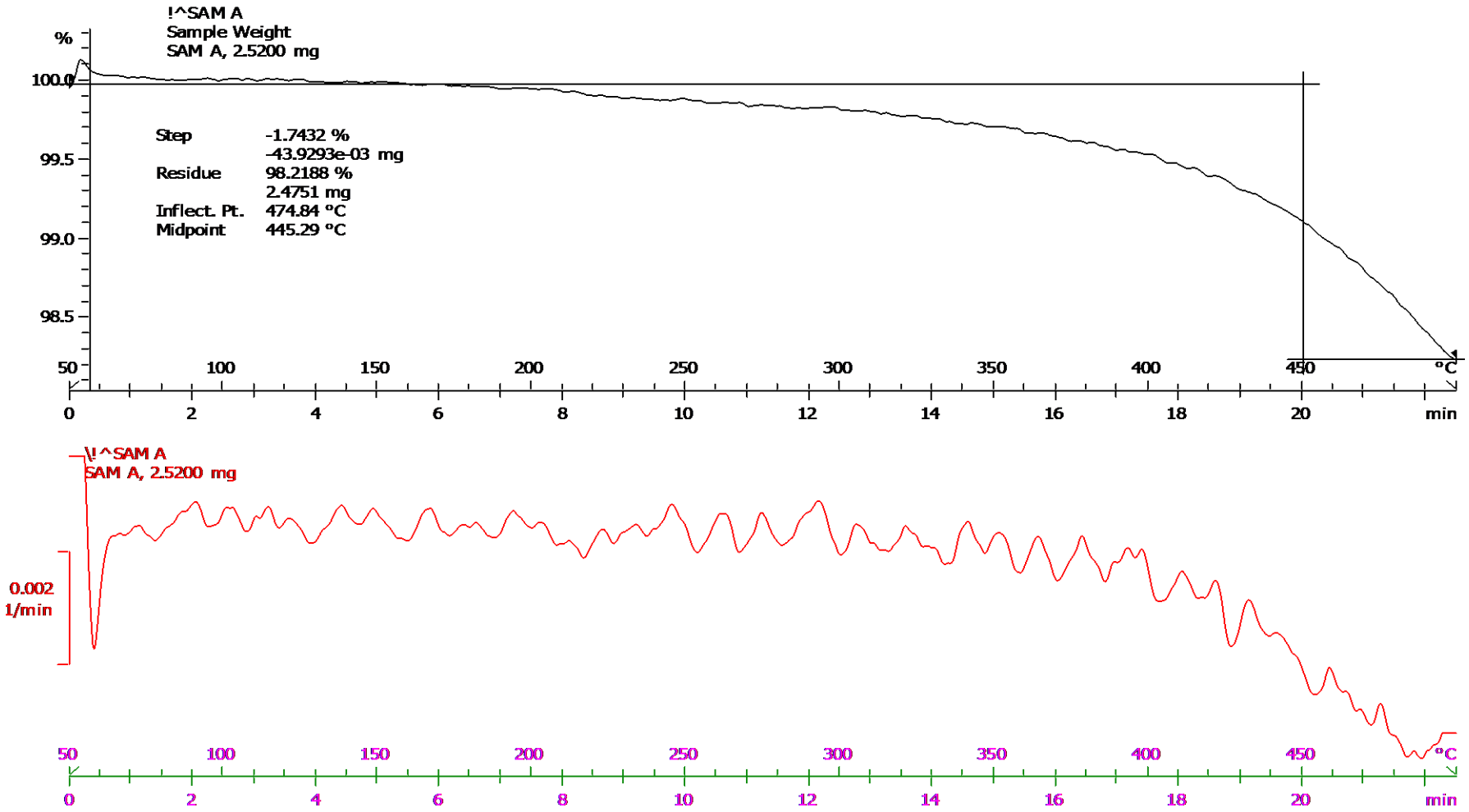


Figure 4.21: Thermogram of sample A

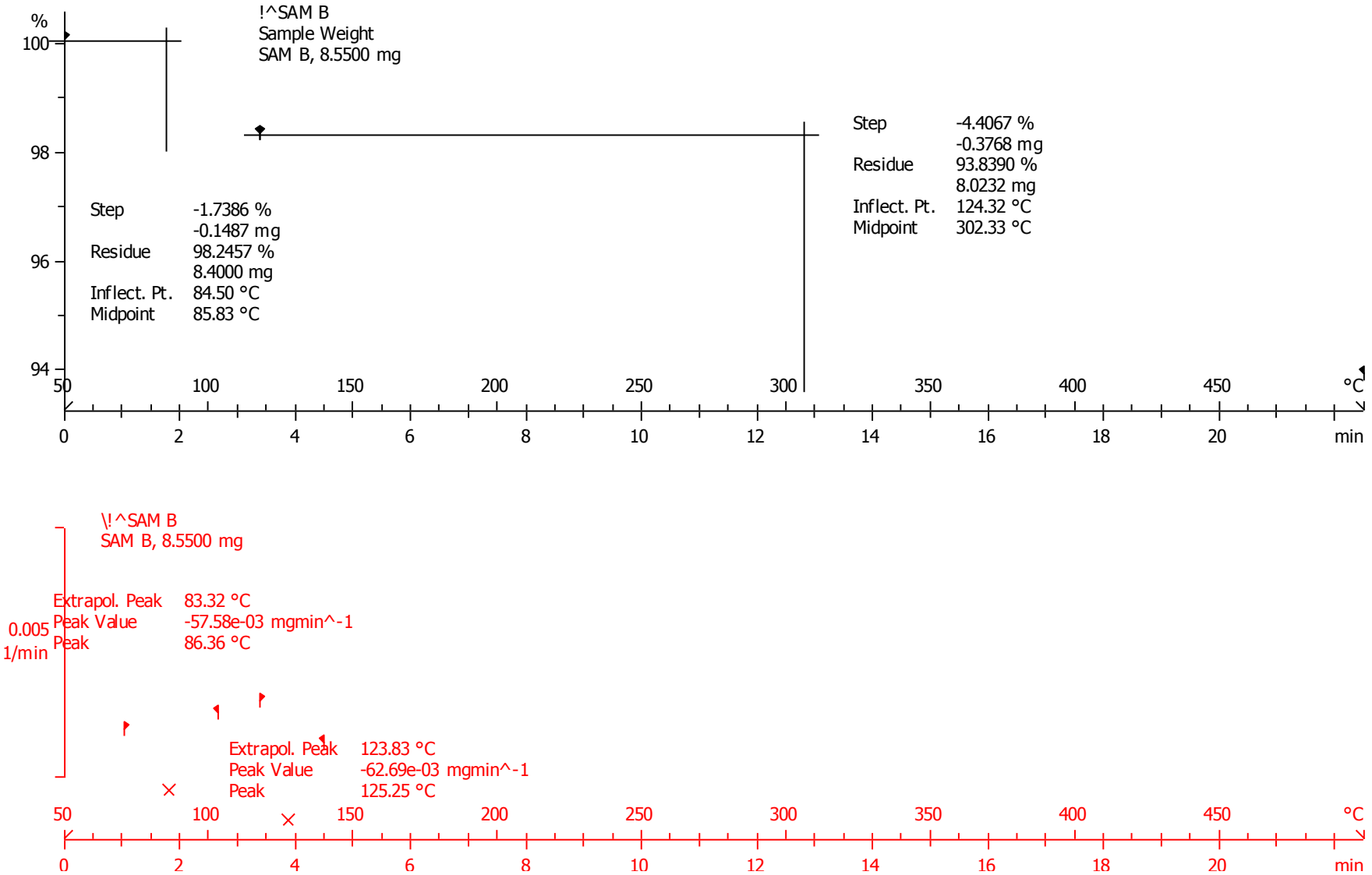


Figure 4.22: Thermogram of sample B

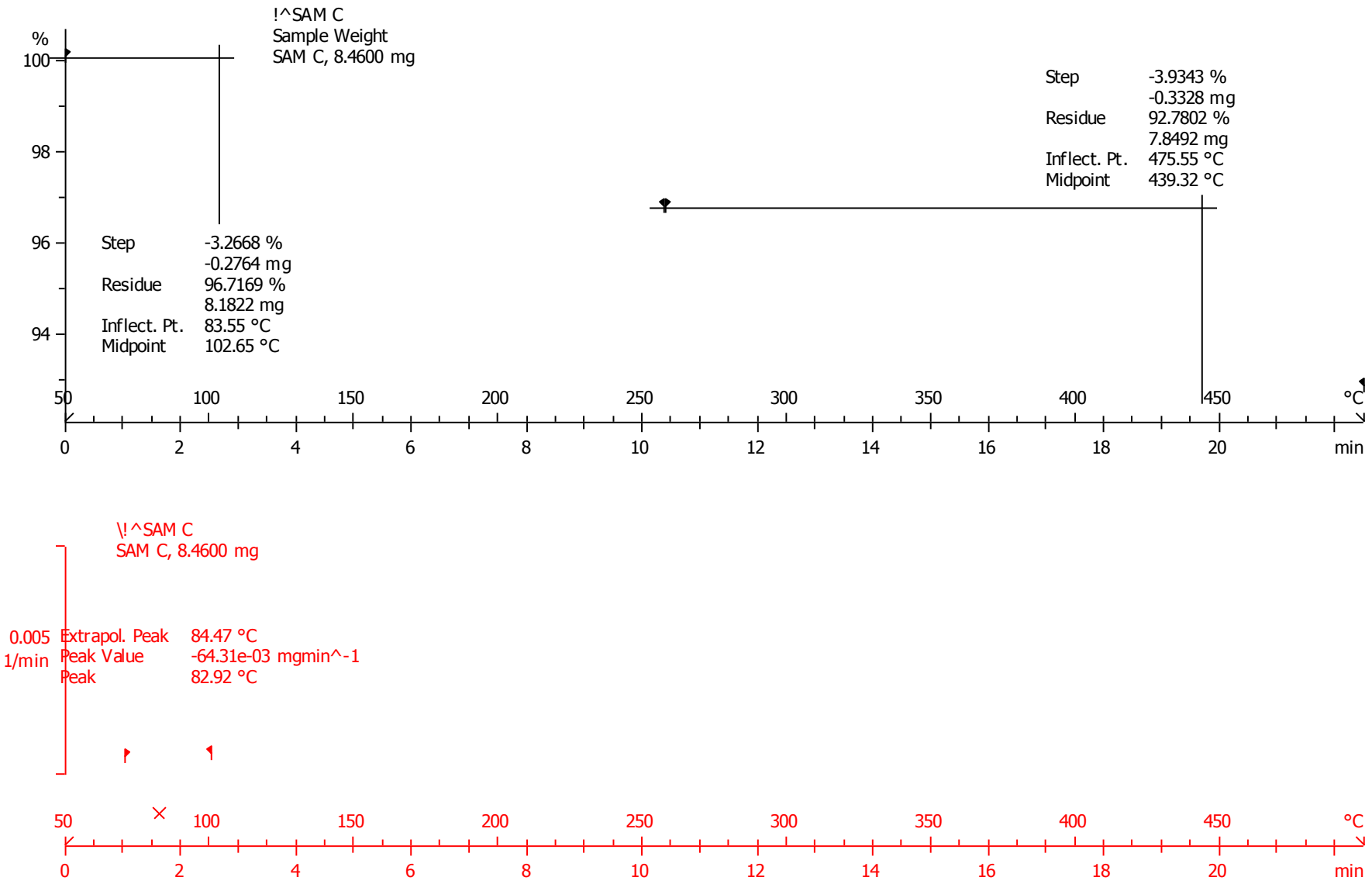


Figure 4.23: Thermogram of sample C

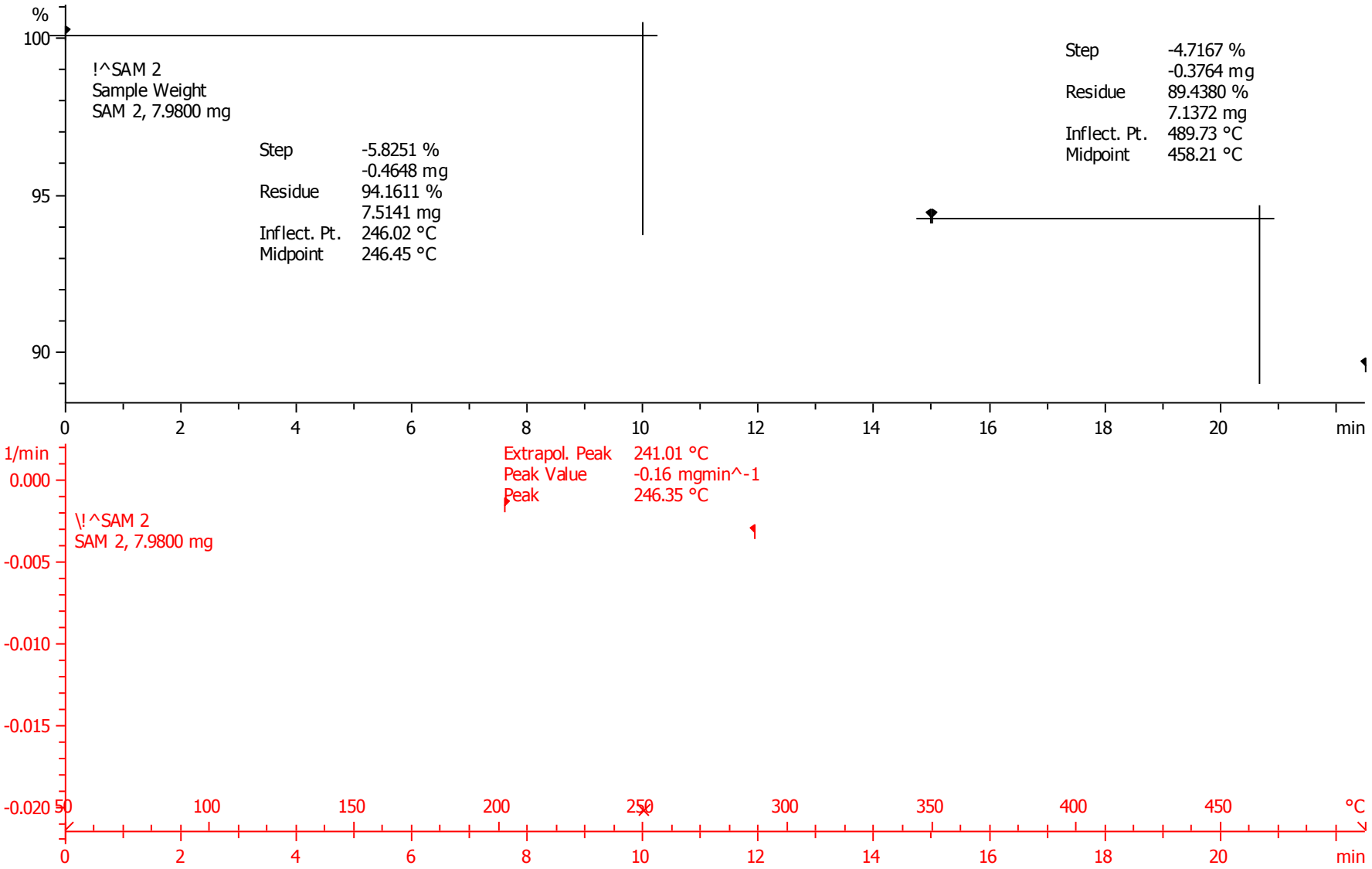


Figure 4.24: Thermogram of sample 2

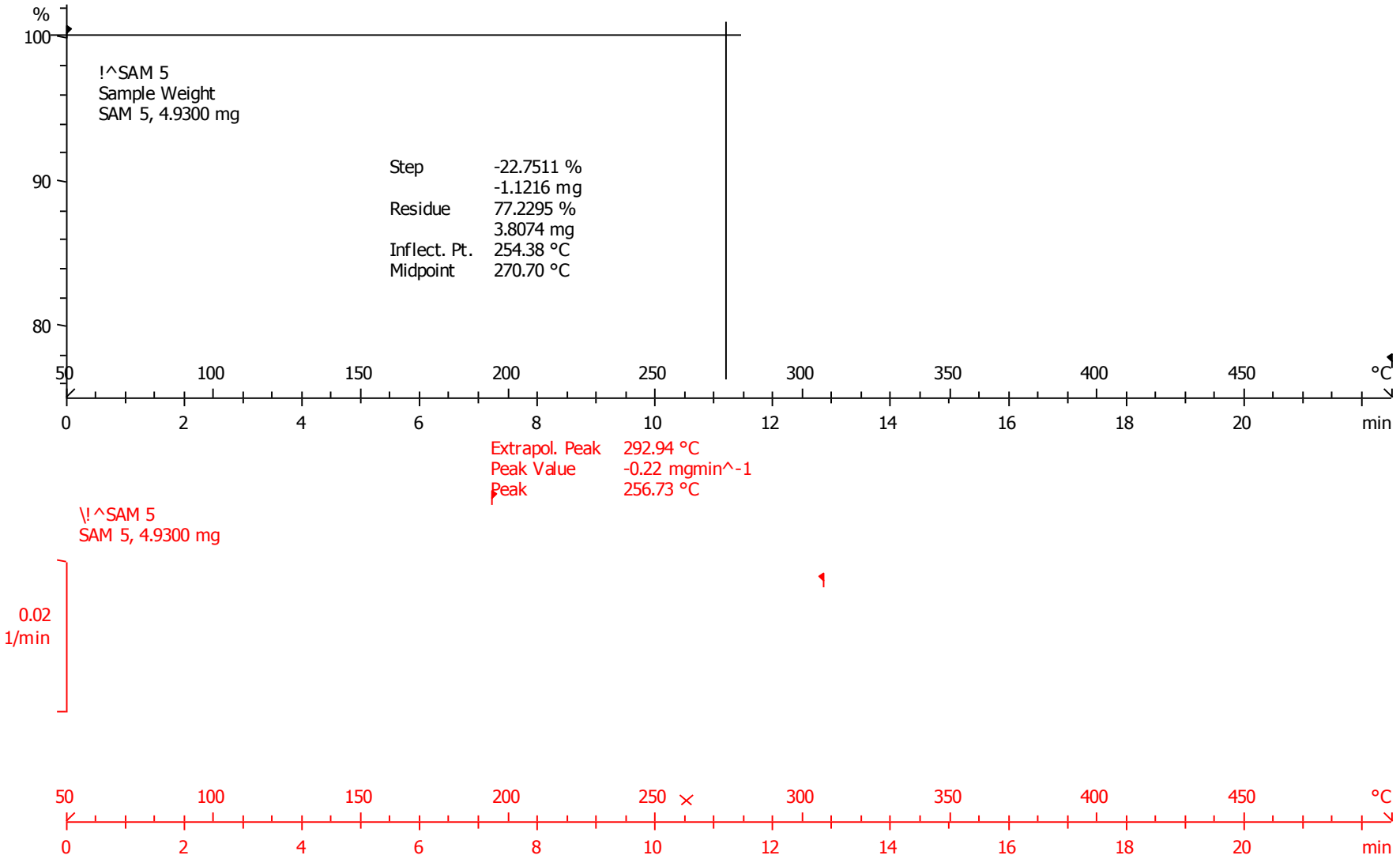


Figure 4.25: Thermogram of sample 5

4.7 Scanning Electron Micrographs of Raw and Modified Bentonites

Figure 4.26 is the SEM micrograph of sample A. The micrograph, which was taken on 13 December, 2013 at 2:17 pm, shows a magnification of sample A by 1903x at 50 μm. The micrograph shows sample A to be bulky and large in morphology. Figure 4.27 shows the SEM micrograph of sample 2, which was taken on 23 May, 2014 at 8:43 am, shows a magnification by 2100x at 30 μm. The micrograph shows that sample 2 has become smaller and aggregated in morphology.

Figure 4.28 shows the micrograph of sample B determined by SEM analysis. The micrograph, which was taken on 13 December, 2013 at 2:58 pm, shows a magnification of sample A by 2691x at 50 μm as a bulky mass. Figure 4.29 is the micrograph of sample 5 which is the corresponding organoclay of sample B. The micrograph, which was taken on 23 May, 2014 at 8:59 am, shows a magnification of sample A by 2100x at 30 μm. The morphology of the clay is smaller and aggregated.

Figure 4.30 shows the micrograph of sample B determined by SEM analysis. The micrograph, which was taken on 13 December, 2013 at 3:37 pm, shows a magnification of sample A by 1902x at 50 μm is a bulky mass. Figure 4.31 is the micrograph of sample 8 which is the corresponding organoclay of sample B. The micrograph, which was taken on 23 May, 2014 at 10:04 am, shows a magnification of sample A by 2100x at 30 μm. The morphology of the clay is also aggregated.

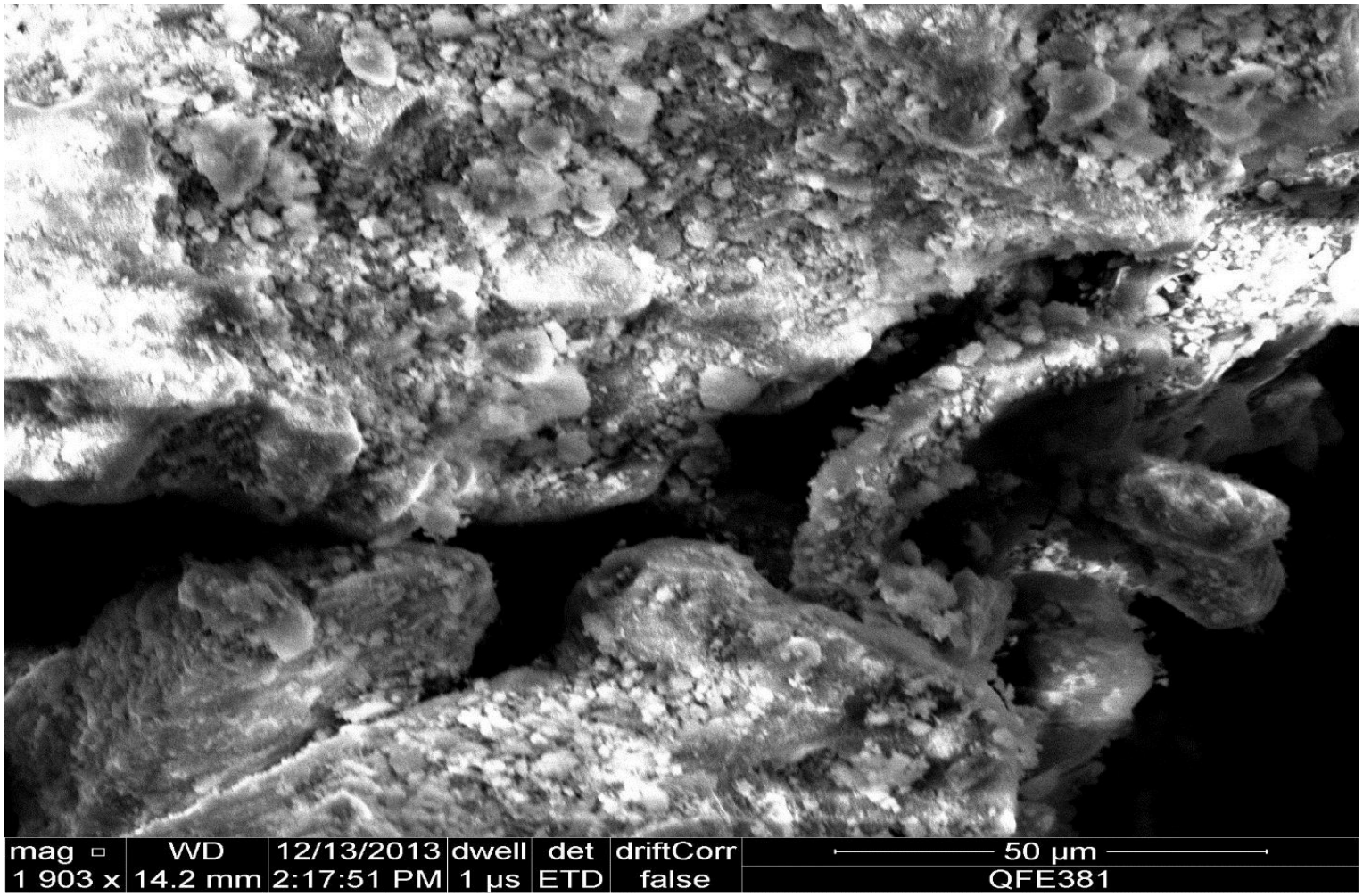


Figure 4.26: SEM micrograph of sample A.

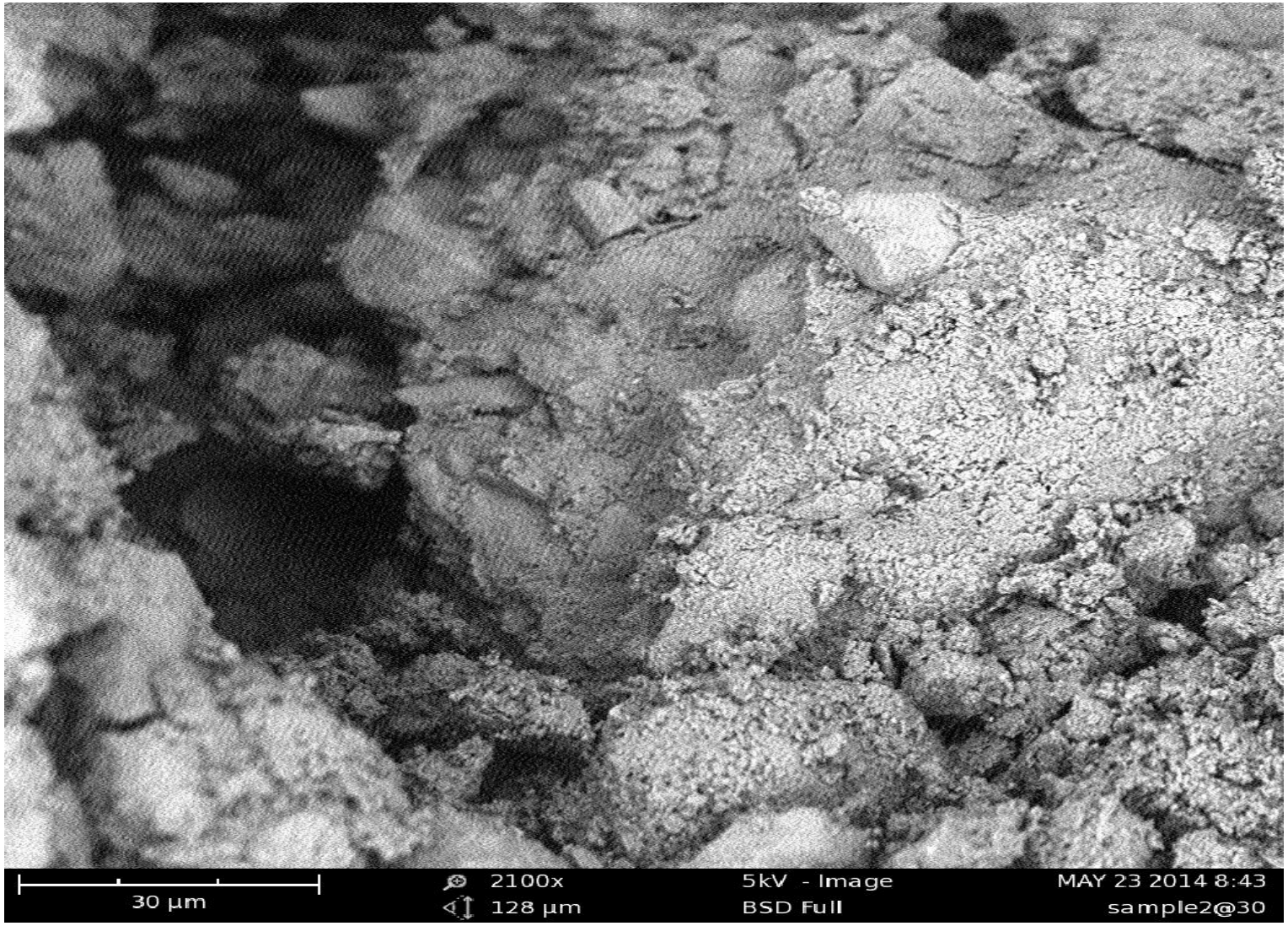


Figure 4.27: SEM micrograph of sample 2

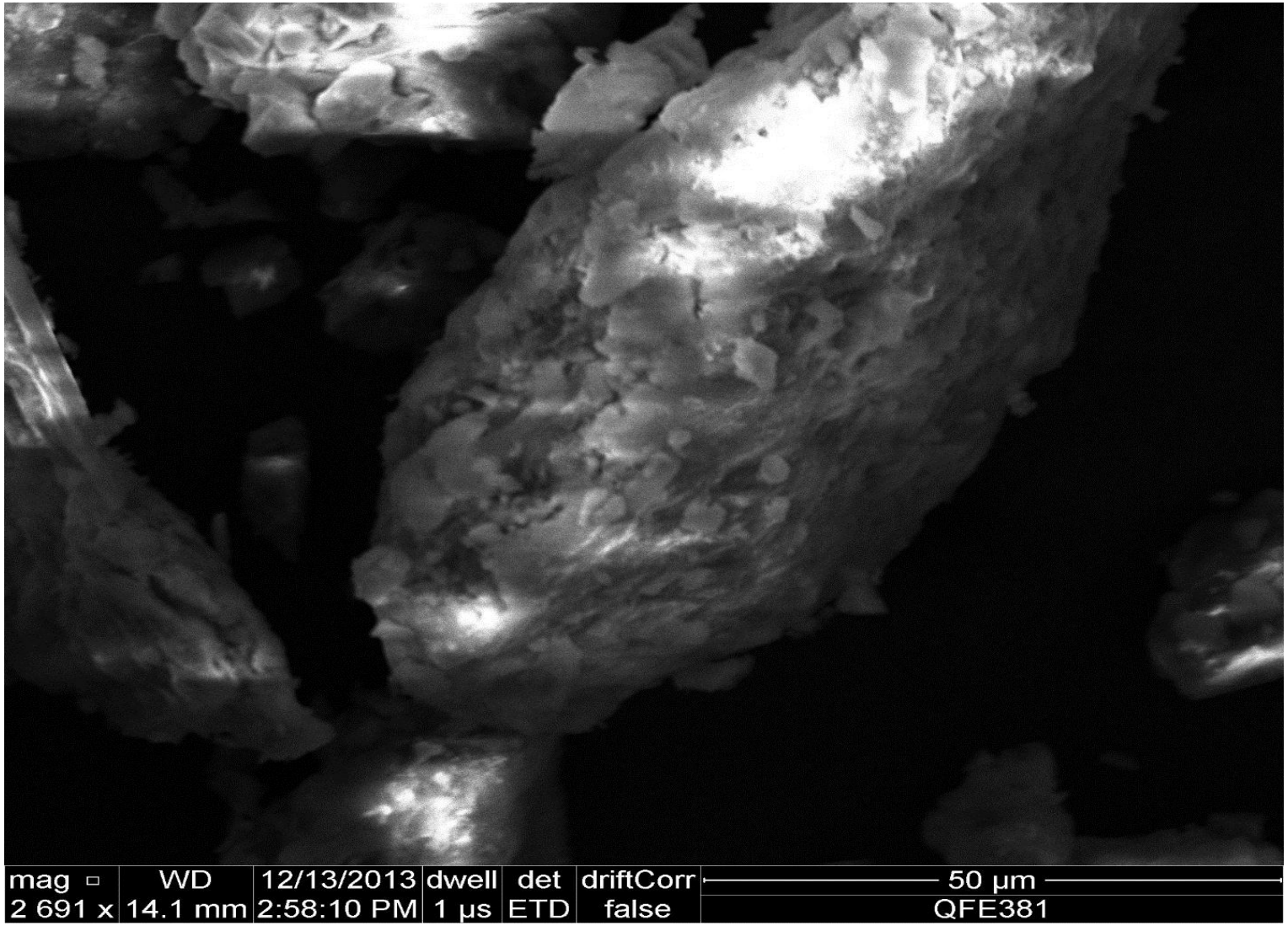


Figure 4.28: SEM micrograph of sample B

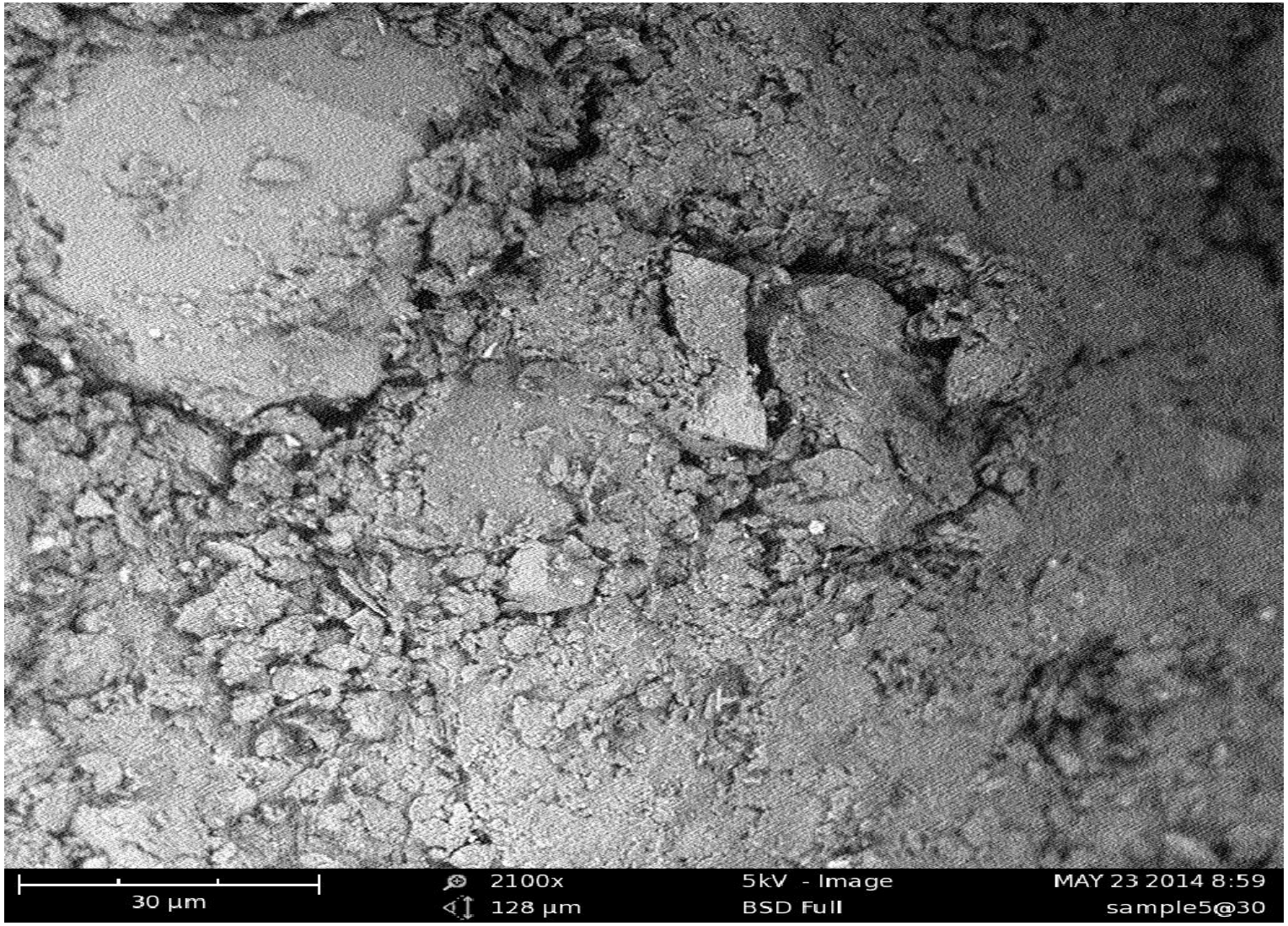


Figure 4.29: SEM micrograph of sample 5

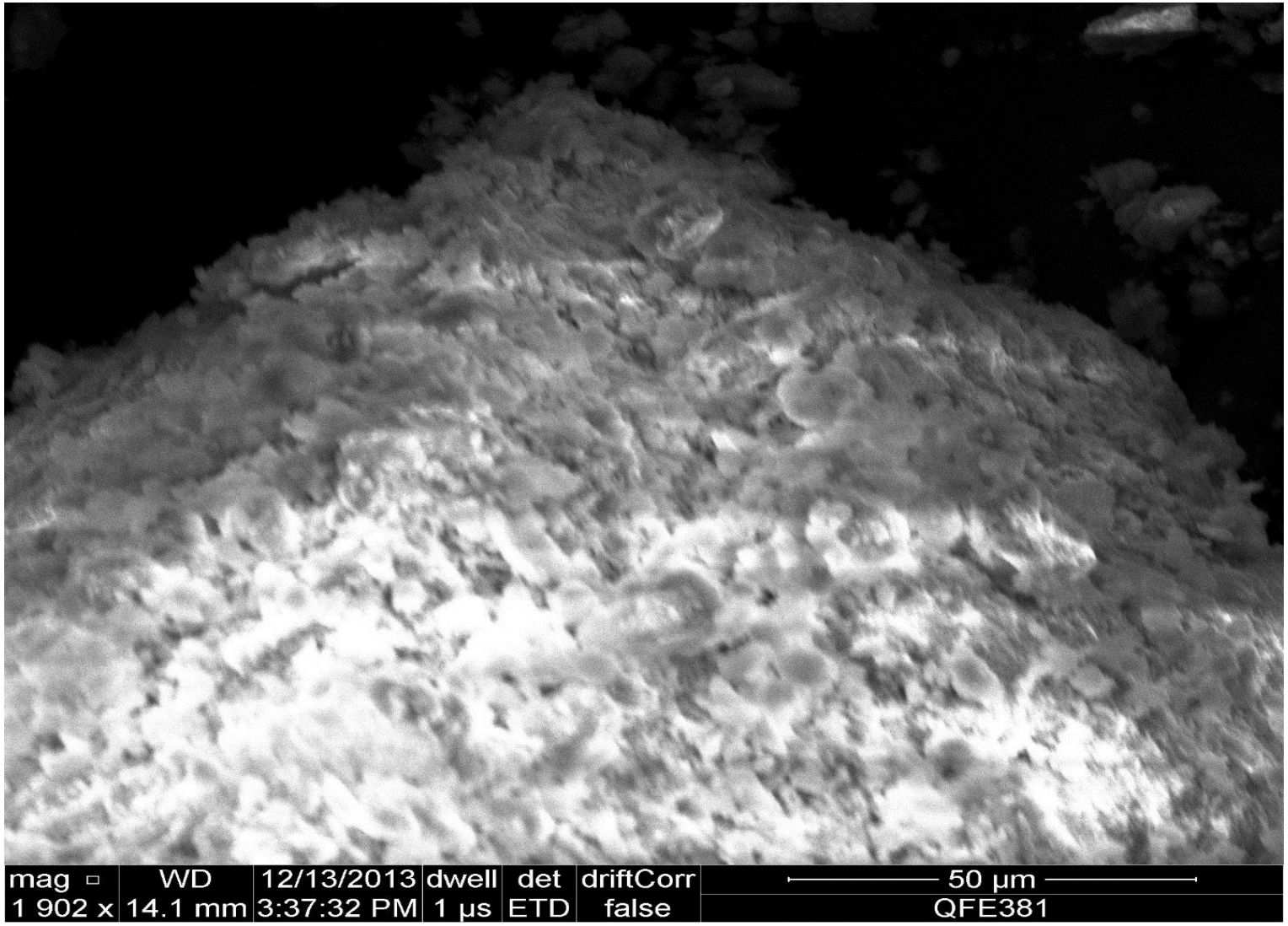


Figure 4.30: SEM micrograph of sample C

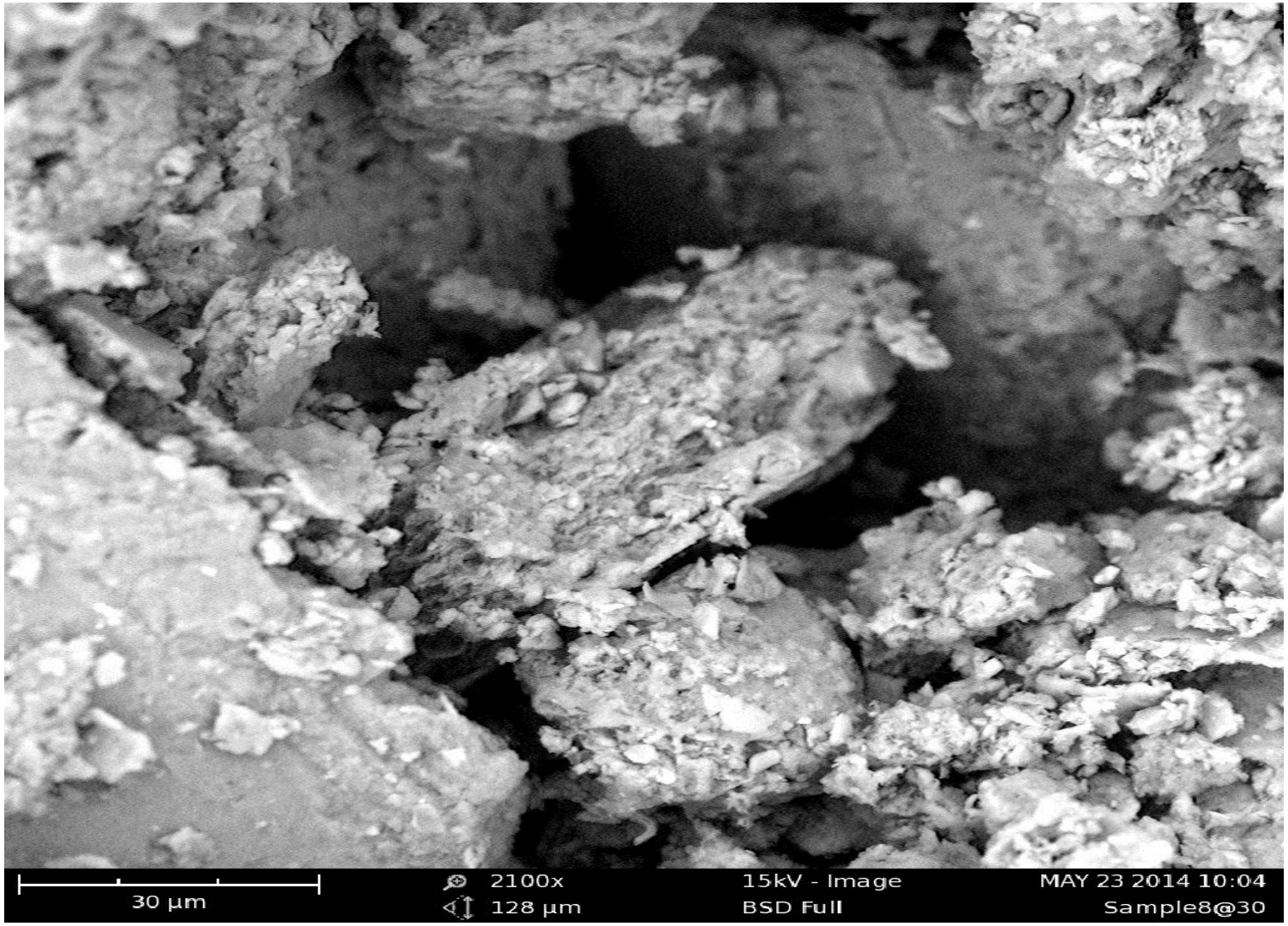


Figure 4.31: SEM micrograph of sample 8

4.8 Sorption Studies of Crude Oil on Bentonites and Organoclays

Figure 4.32 shows the effect of sorbent dosage on the oil sorption capacity of the clay and organoclay samples used. Samples A, B and C and their corresponding organoclay samples 2, 5 and 15 have been used to illustrate the change in oil sorption capacity as the sorbent dosage increases. For the clay samples A, B and C, there is an initial increase from the first 1.5 g of the sorbents, after that there seemed not to be any significant change in the sorption capacity of the materials. The sorption capacity of sample A < C < B. The organoclay samples showed a constant increase in oil sorption capacity as the dosage of the materials increased.

Figure 4.33 shows the effect of initial oil concentration on the oil sorption capacity of the clay and organoclay samples. The chart shows an increasing oil sorption ability for all samples as initial oil amount is increased. The oil sorption capacity of the materials increase in the order B < A < C < 5 < 2 < 15.

Figure 4.34 shows the effect of contact time on the oil sorption capacity of the clays and organoclay samples. 0.5 g each of the samples were used in the experiment. The demarcation between the clay samples A, B and C, and the organoclay samples 2, 5 and 15 is obvious. The samples showed an increase in the first one minute and afterwards became constant and showed no significant change. The clay samples sorbed less than 0.5 g of oil while the organoclays were able to sorb up to 3.5 g of oil.

4.8.1 The effect of sorbent dosage on oil sorption capacity

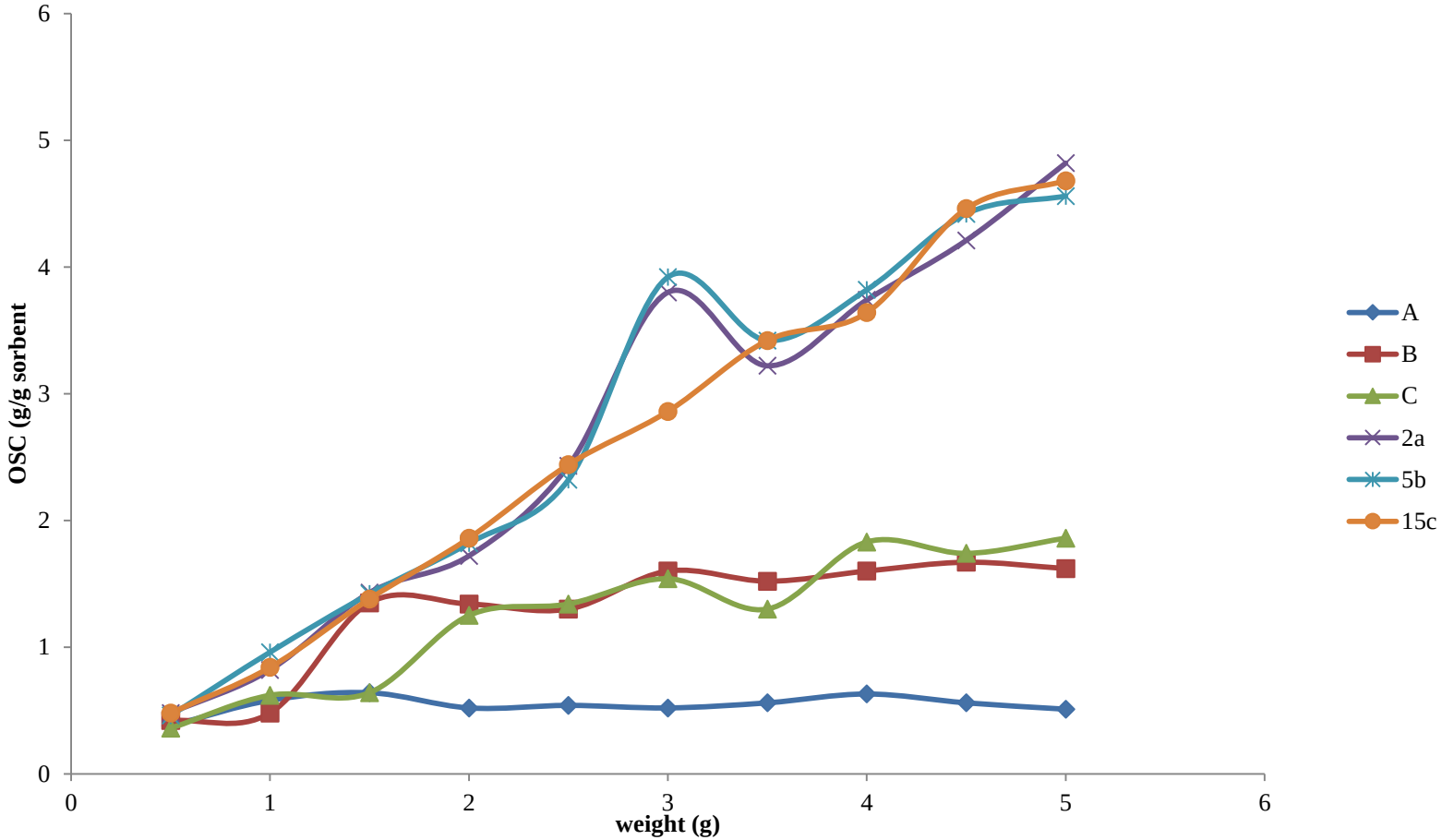


Figure 4.32: Effect of sorbent dosage on the sorption capacity of clay and organoclay materials

4.8.2 The effect of initial oil concentration on oil sorption capacity

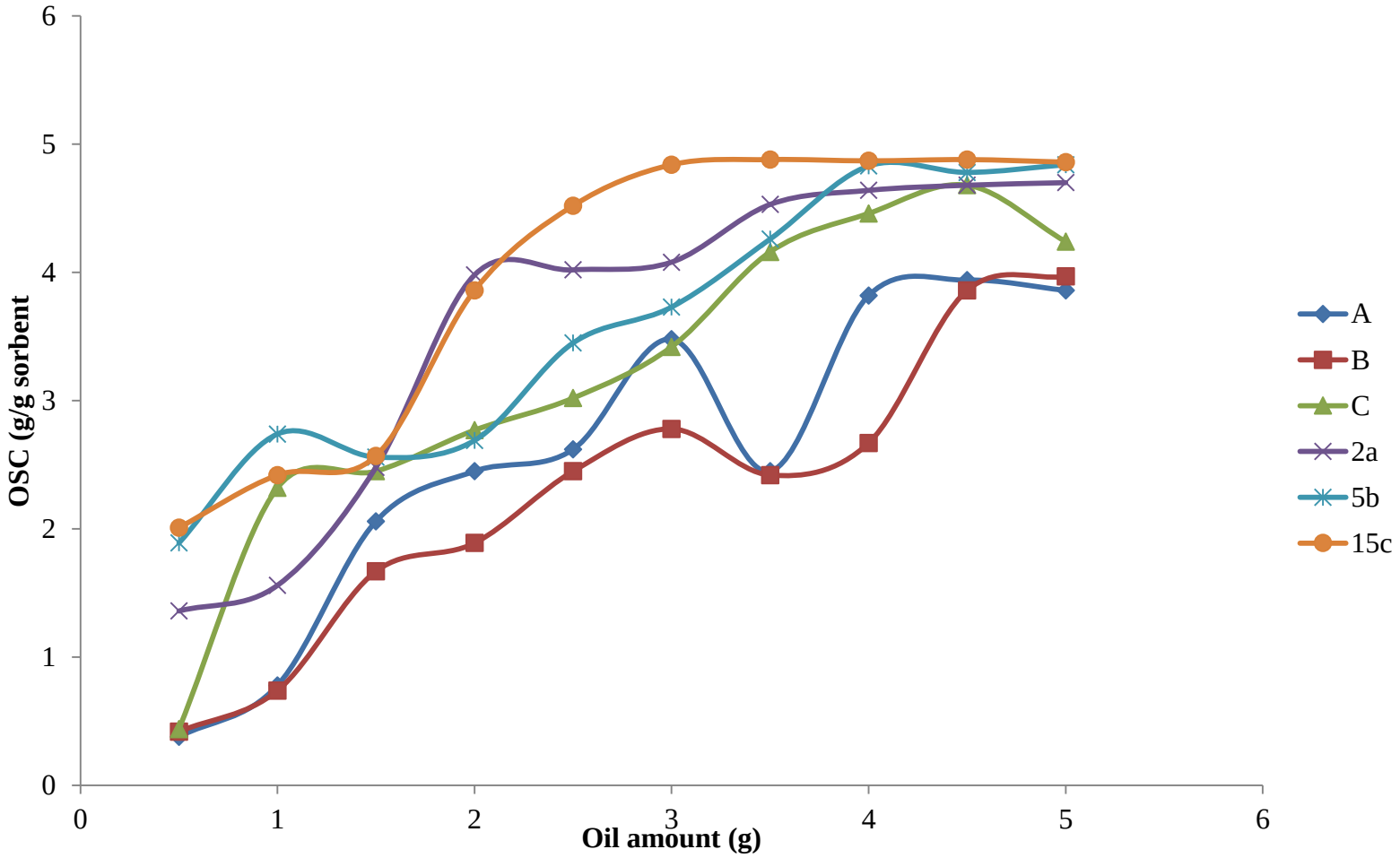


Figure 4.33: Effect of initial oil concentration

4.8.3 The effect of contact time on the oil sorption capacity

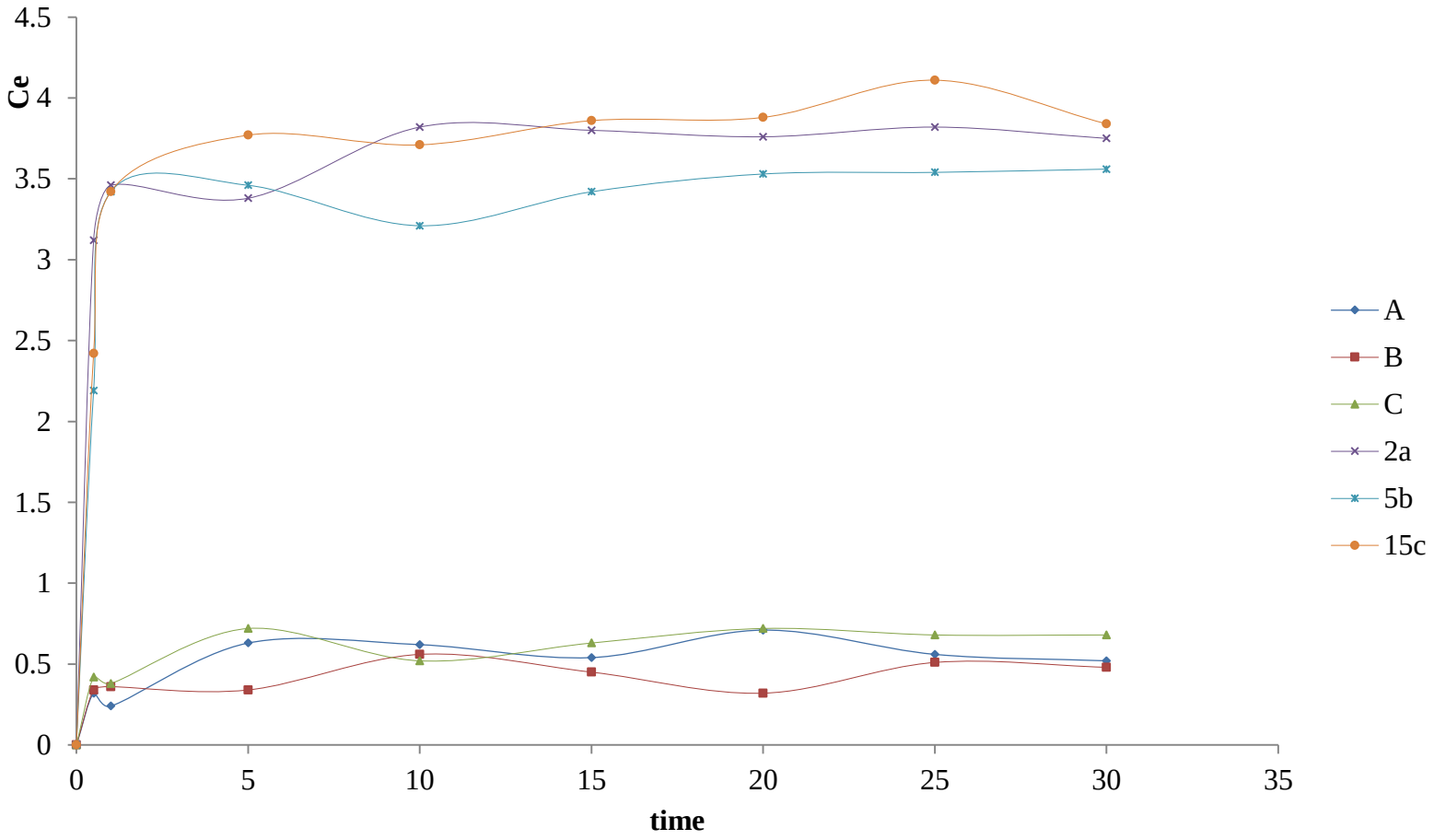


Figure 4.34: Effect of contact time on the oil sorption capacities of clays and organoclays

4.8.4 Equilibrium sorption studies

Figure 4.35 shows the chart of the linearized Langmuir isotherm models for the organoclay samples 2, 5 and 15. In the chart, plots of $1/q_e$ vs $1/C_e$ for samples have been used to linearize the equilibrium sorption data obtained for the organoclay samples. The linear plots are closely fit to themselves and can be differentiated by their equations and R^2 values. The R^2 values of samples 15 (0.9936) < sample 2 (0.9968) < sample 5 (0.997). The values of the slope and intercepts of the plots are used to calculate the Langmuir parameters presented in Table 4.9.

Figure 4.36 shows the chart of the linearized Freundlich sorption models for the organoclay samples 2, 5 and 15. The chart is defined by plots of $ln(q_e)$ vs $ln(C_e)$ used to linearize the equilibrium sorption data obtained for the organoclay samples. The linear data are closely fit to themselves and can be differentiated by their equations and R^2 values. The R^2 values of samples 5 (0.9771) < sample 15 (0.9798) < sample 2 (0.9862). The values of the slope and intercepts of the plots are used to calculate the Dubinin-Radushkevich parameters presented in Table 4.9.

Figure 4.37 shows the chart of the linearized Dubinin-Radushkevich models for the organoclay samples 2, 5 and 15. The chart is defined by plots of $ln(q_e)$ vs $RTln(1+1/C_e)$ is used to linearize the equilibrium sorption data obtained for the organoclay samples. The linear data are closely fit to themselves and can be differentiated by their equations and R^2 values. The values of the slope and intercepts of the plots are used to calculate the Freundlich parameters presented in Table 4.9.

Table 4.9 shows the regression parameters of the isotherm models used to describe the equilibrium behaviour of crude oil on organoclays. The data were obtained from the plots in Figures 4.36 to 4.38. The R^2 is the coeeficient of regression; n is the Freundlich parameter related to the sorption intensity; K_F is the Freundlich constant describing the sorption capacity; Q_m, is the maximum

specific uptake for a monolayer coverage corresponding to the site saturation; R_L is the Langmuir sepation factor indicating favourability of sorption; B_D is a Dubinin-Raduskevich constant related to the mean free energy of sorption per mole of the sorbate; q_D is the Dubinin-Raduskevich isotherm constant representing the theoretical saturation capacity; E is the apparent sorption energy.

4.8.4.1 The Langmuir sorption Isotherm model

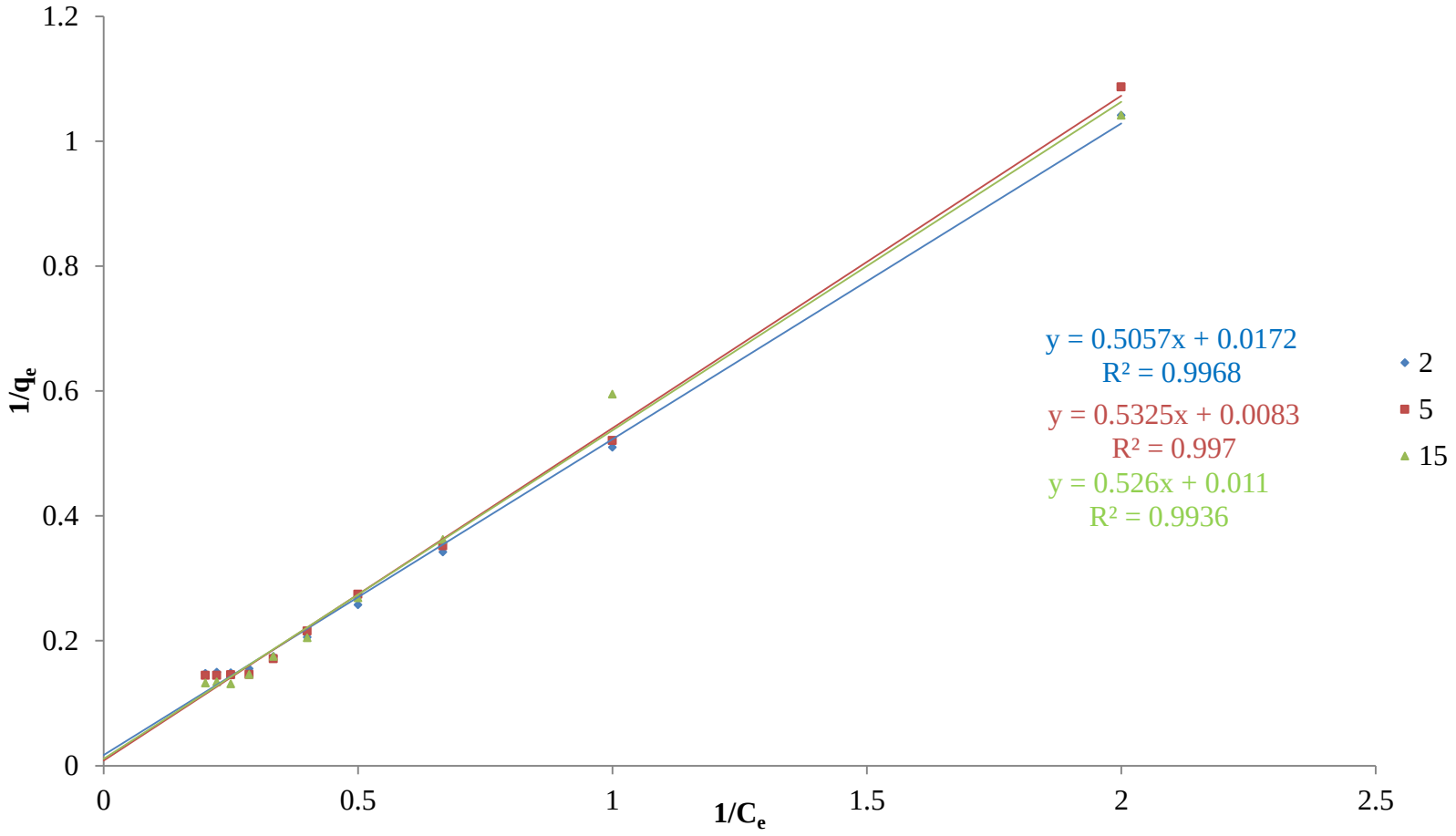


Figure 4.35: The linearized Langmuir isotherm for organoclay samples

4.8.4.2 The Freundlich sorption isotherm model

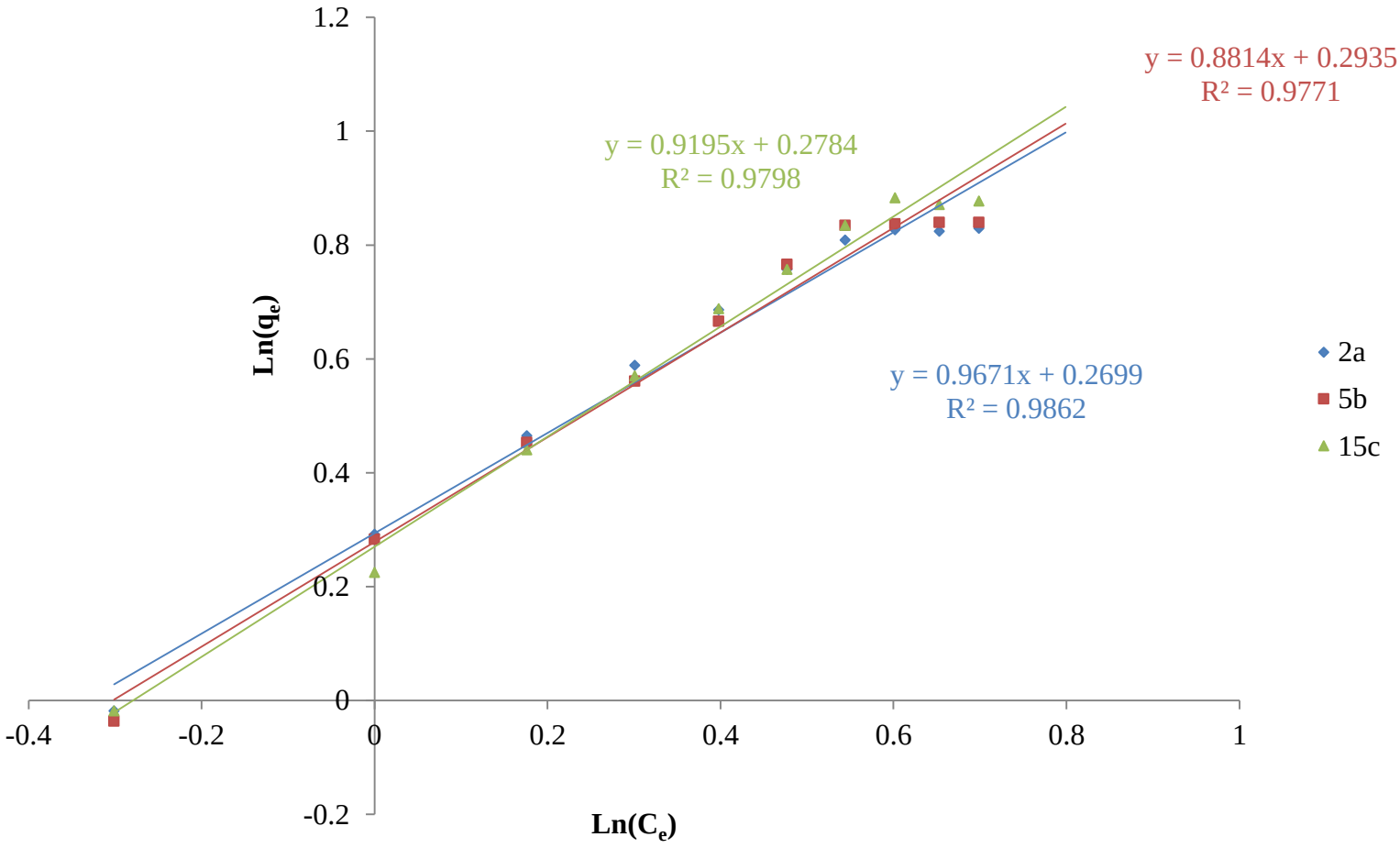


Figure 4.36: The linearized freundlich sorption model for organoclay samples

4.8.4.3 The Dubinin-Raduskevich (D-R) model

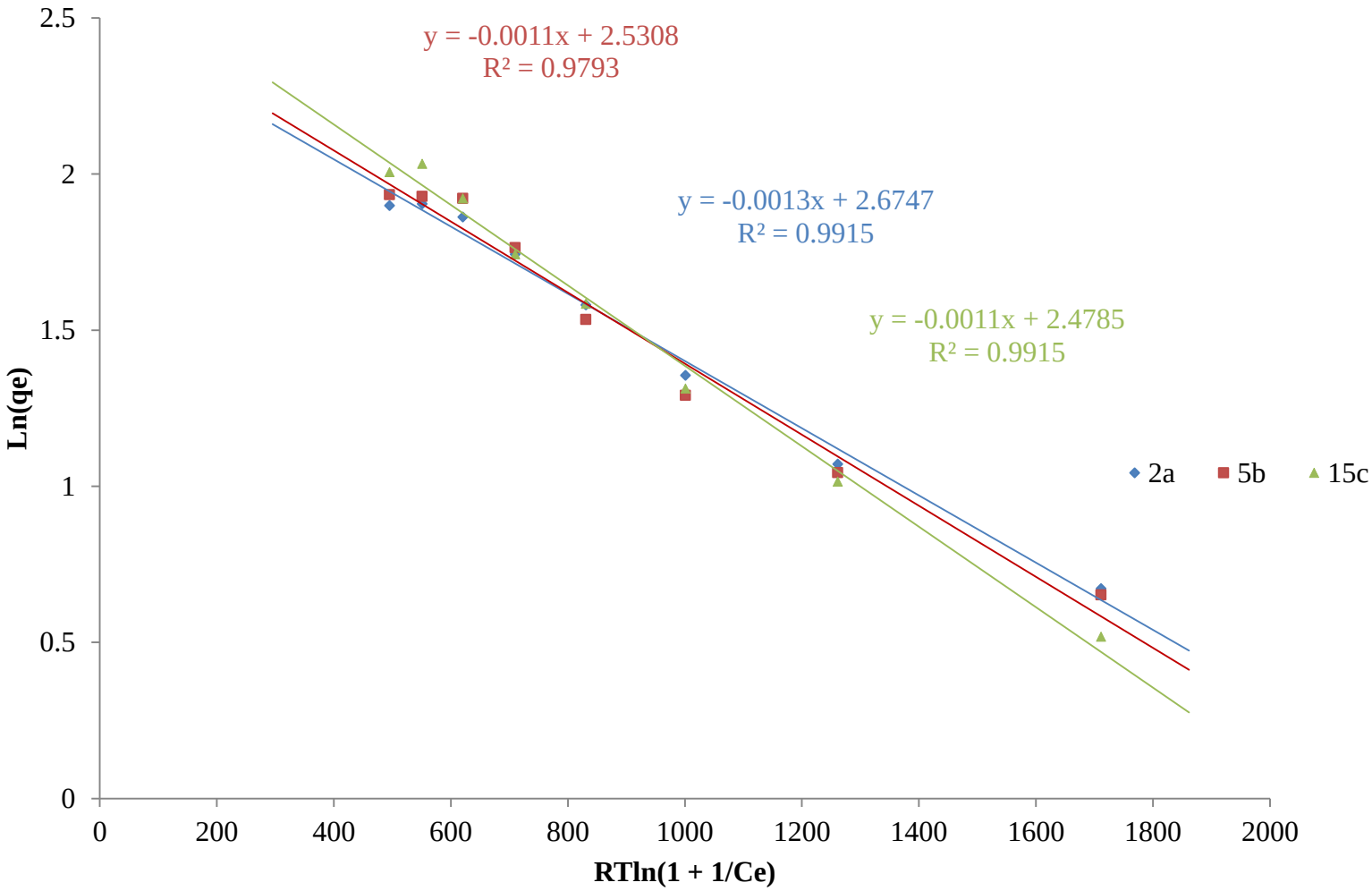


Figure 4.37: The linearized Dubinin Radushkevich model for organoclays samples

Table 4.9. The regression parameter of the equilibrium isotherm models employed

	Freundlich			Langmuir			Dubinin-Raduskevich			
samples	R^2	n	K_F	R^2	Q_m	R_L	q_D	R^2	$Bx10^{-4}$	E
2	0.9862	1.0340	1.8617	0.9968	1.9775	0.855	11.923	0.9915	5.5	30.15
5	0.9771	1.1346	1.9656	0.997	1.8779	0.928	12.564	0.9793	5.5	30.15
15	0.9798	1.0876	1.8985	0.9936	1.9011	0.905	14.508	0.9915	6.5	27.74

R^2 is the coeeficient of regression; n is the Freundlich parameter related to the sorption intensity; K_F is the Freundlich constant describing the sorption capacity; Q_m, is the maximum specific uptake for a monolayer coverage corresponding to the site saturation; R_L is the Langmuir sepation factor indicating favourability of sorption; B_D is a Dubinin-Raduskevich constant related to the mean free energy of sorption per mole of the sorbate; q_D is the Dubinin-Raduskevich isotherm constant representing the theoretical saturation capacity; E is the apparent sorption energy.

4.8.5 Kinetic Isotherm studies

Figure 4.38 shows the chart of the Pseudo-second-order rate model for the sorption of crude oil by organoclays. The linearized model is defined by a plot of t/q_e against t. The linear data are described by their equations and R^2 values. The R^2 values of samples 15 (0.9976) < sample 5 (0.999) < sample 2 (0.9995). The values of the slope and intercepts of the plots are used to calculate the Pseudo-second-order rate parameters presented in Table 4.10.

Figure 4.39 shows the chart of the Elovich kinetic model for the sorption of crude oil by organoclays. The linearized model is defined by a plot of q_t against $ln(t)$. The linear data are described by their equations and R^2 values. The R^2 values of samples 2 (0.9700) < sample 5 (0.9166) < sample 15 (0.9504). The values of the slope and intercepts of the plots are used to calculate the Elovich kinetic model parameters presented in Table 4.10.

Figure 4.40 shows the chart of the Weber and Morris Intraparticle Diffusion Model for the sorption of crude oil by organoclays. The linearized model is defined by a plot of q_t against $t^{1/2}$. The linear data are described by their equations and R^2 values. The R^2 values of samples 5 (0.5341) < sample 15 (0.582) < sample 2 (0.7137). The values of the slope and intercepts of the plots are used to calculate the Elovich kinetic model parameters presented in Table 4.10.

Table 4.10 is the table of the regression parameters describing the kinetic models used to explain the sorption of crude oil on the organoclays. The constants are determined from the plots of the Elovich, Pseudo-second-order rate and Weber and Morris Intraparticle Diffusion models for organoclay samples 2, 5 and 15. In the table, PSOR represents Pseudo-Second-Order Rate model and WMIDM represents the Weber and Morris Inter-Diffusion Model; α is the initial sorption rate; a is parameter related to the extent of surface coverage and activation energy; R_E^2 represents the

Elovich coefficient of determination; q_e is the value of the sorption capacity of the organoclays; $k_{2,}$ the pseudo-second-order rate constant; R^2 the coefficient of regression; k_{id} is the WMIDM rate constant; R_i^2 is the intraparticle coefficient of determination and C_i is the intraparticle diffusion coefficient accounting for the bonding effect between the clay layers.

4.8.5.1 The Pseudo-Second-Order kinetic rate model

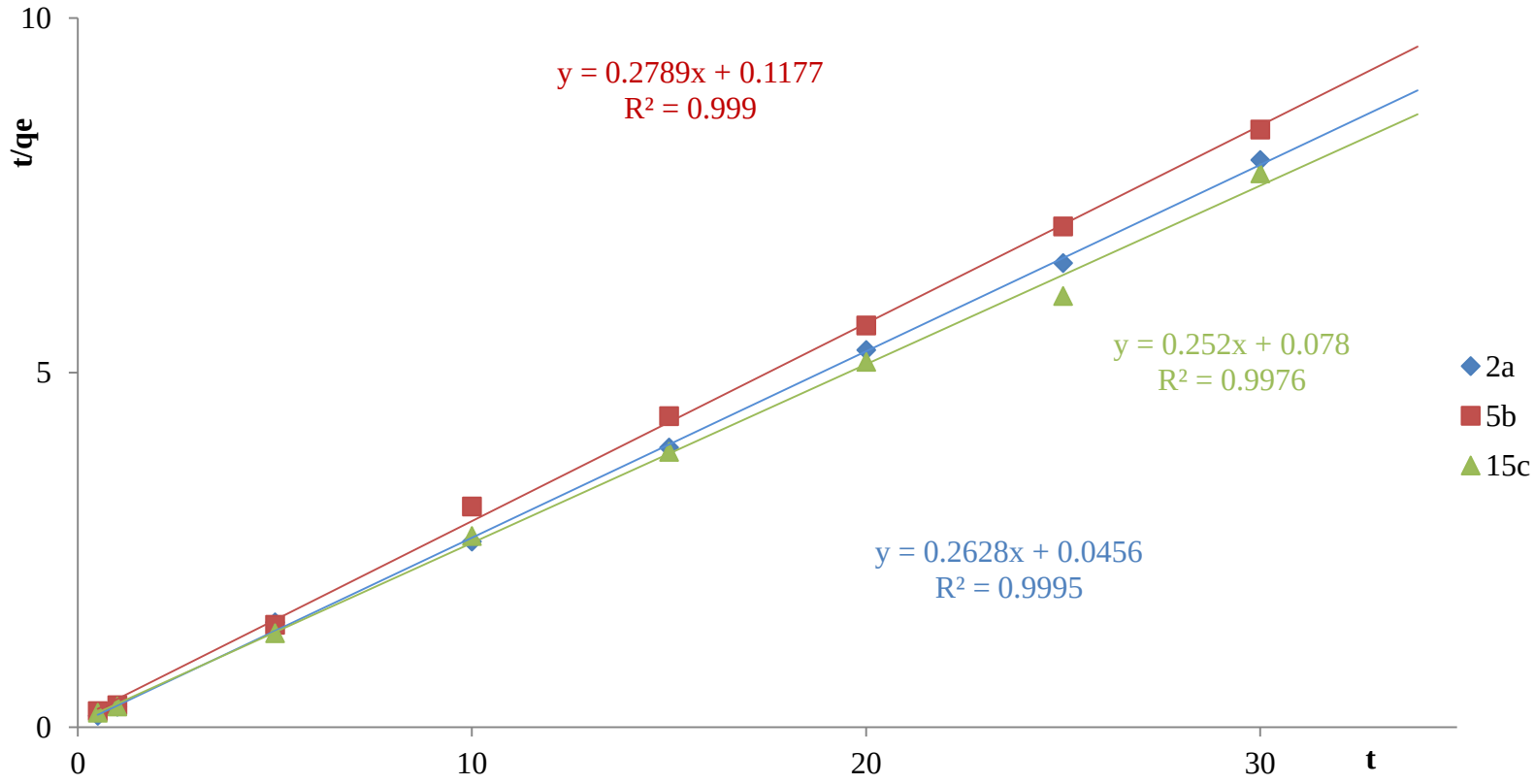


Figure 4.38: The Pseudo-second-order rate equation model for organoclay samples

4.8.5.2 The Elovich kinetic Model

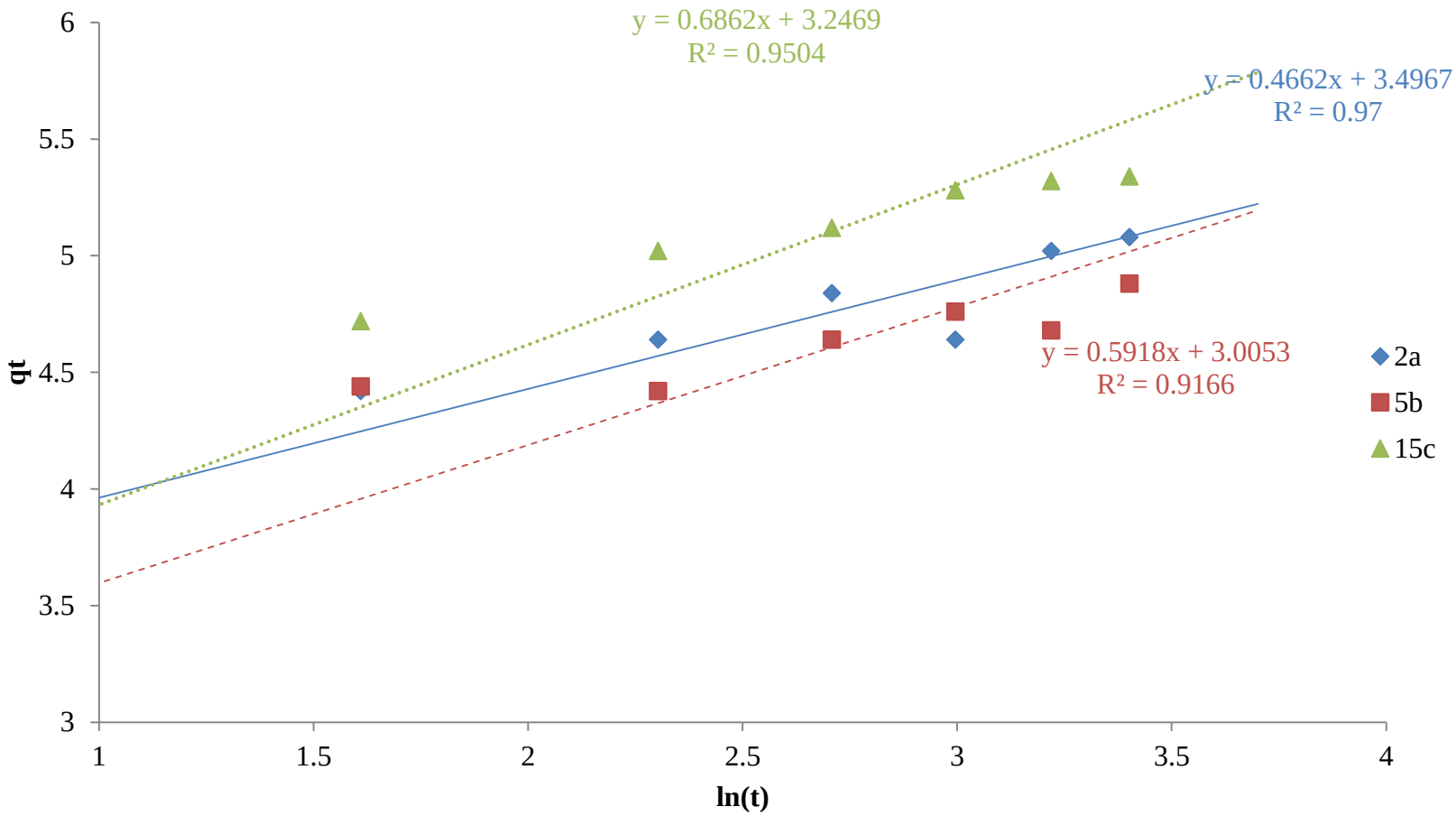


Figure 4.39: The Elovich kinetic model for organoclay samples

4.8.5.3 The Weber and Morris diffusivity Model

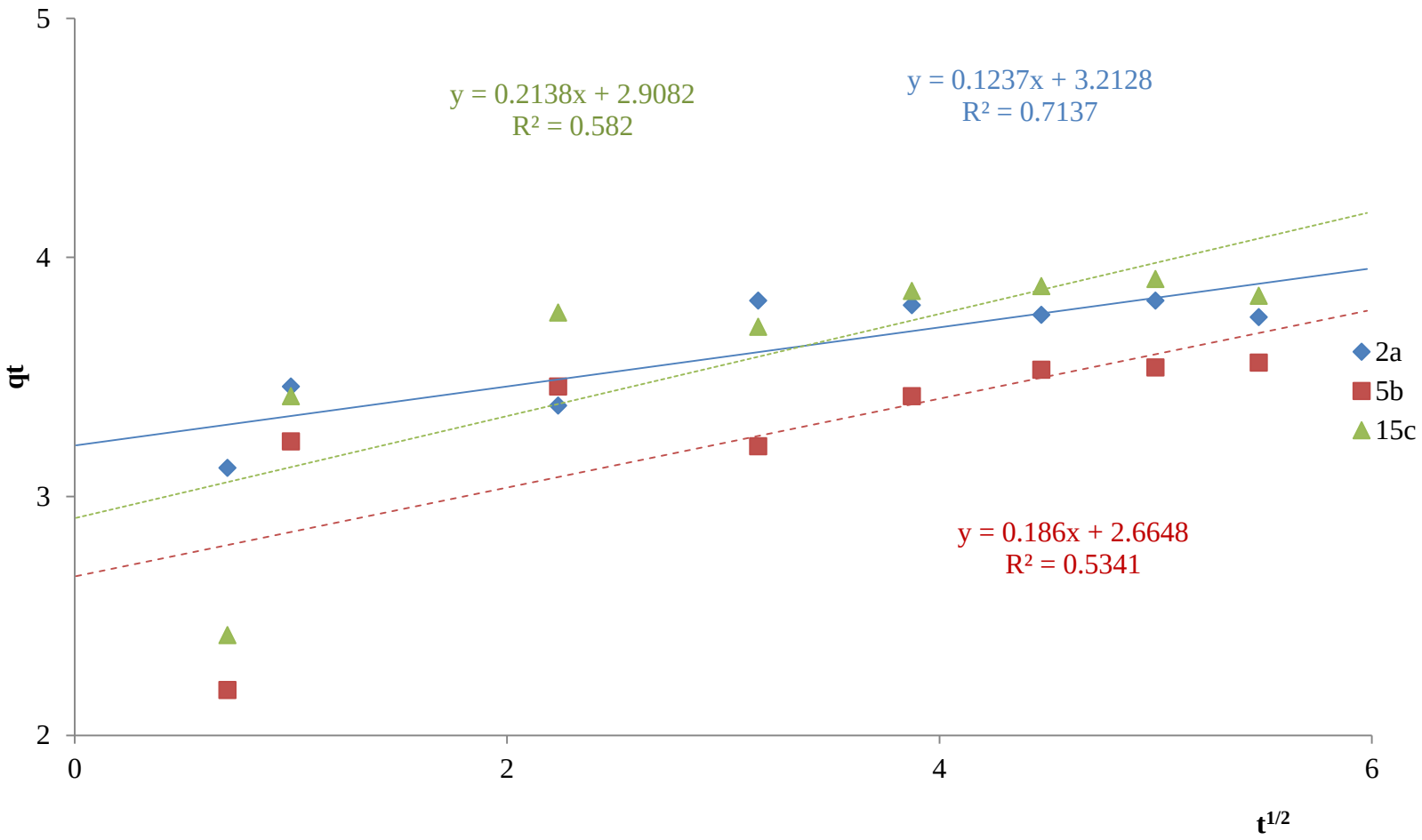


Figure 4.40: The Weber and Morris diffusivity model for orgaoclay samples

Table 4.10. The regression parameters describing the kinetic models

Sample ID	Elovich			PSOR			WMIDM		
	R_E^2	α	a	R^2	Q_e	K_2	R_i^2	K_{id}	C_i
2	0.9700	3.4967	0.3268	0.9995	3.8052	1.5146	0.7137	0.1237	3.2128
5	0.9166	3.0053	0.4052	0.9990	3.5856	6.6088	0.5341	0.186	2.6648
15	0.9504	3.2469	0.3805	0.9976	3.9683	0.8142	0.582	0.2138	2.9082

PSOR represents Pseudo-Second-Order Rate model and WMIDM represents the Weber and Morris Inter-Diffusion Model; α is the initial sorption rate; *a* is parameter related to the extent of surface coverage and activation energy; R_E^2 represents the Elovich coefficient of determination; q_e is the value of the sorption capacity of the organoclays; k_2, the pseudo-second-order rate constant; R^2 the coefficient of regression; k_{id} is the WMIDM rate constant; R_i^2 is the intraparticle coefficient of determination and C_i is the intraparticle diffusion coefficient accounting for the bonding effect between the clay layers.

5.0 DISCUSSION

5.1 Physicochemical Characterization of Raw and Modified Nanoclays

The results of the physicochemical properties of the raw and organically modified nanoclays are summarized in Table 4.1. The physicochemical tests were carried out before and after intercalation of the clay samples with Cetyltrimethylammonium bromide (CTAB). From data in Table 4.1, it is observed that the optimal ammonium salts dose to synthesize the organoclays is 80 % of the corresponding weight of the clay samples. Table 4.1 also shows the effect of the intercalation procedure on the physicochemical properties of the nanoclays. The results of the corresponding organoclay samples, samples 2, 5 and 8 (based on their high d(001) spacing values) as determined by X-Ray Diffraction analysis were selected to be compared with the results of their parent raw nanoclays. Generally, the results indicate significant improvement in the properties of the nanoclays after modification by intercalating with the CTA^+ ions. Table 4.2 summarizes the physical conditions for synthesis and the outcomes as bulk density and basal spacing *d(001)* values of the synthesized organoclays.

5.1.1 Proximate characteristics

The Moisture contents of the materials carried out at 105^{o}C were 0, 2 and 0 % for the raw samples A, B and C respectively; and 0, 0 and 0 % for corresponding organoclay samples 2, 5 and 8 respectively as shown in Table 4.1. For the organoclay samples, the zero moisture content values suggests that the material is hydrophobic. This is due to the removal of interlayer moisture/hydroxyl ions by the intercalation process. The volatile matter content for the raw samples A, B and C were obtained as 0, 0 and 4 % respectively while those of their corresponding organoclays samples 2, 5 and 8 were 24, 18 and 16 % respectively. The

increase in the volatile matter content are due to the presence of organic chains bound to the surface and interlayers of the clay galleries. This is an indication of success of the intercalation process.

5.1.2 Brauner-Emmet-Teller (BET) Analysis

BET analysis was carried out using Nitrogen gas adsorption isotherms to investigate the surface properties of the organoclays. The pore size, surface area and pore volumes of the clay materials are presented in Table 4.1. From Table 4.1, there were commonalities between the three organoclays namely: the low specific surface area; the limited pore volume and the relatively high pore size available for adsorption processes in the micropores (Table 4.1). By examining the results of the raw samples (B and C) against the organoclay samples, it is obvious that the intercalation process decreased the specific surface area and pore volume of the organoclay samples. In contrast, the pore sizes have increased from 54.219 4V/A and 58.355 4V/A in samples B and C to 148.449 4V/A and 136.778 4V/A in samples 5 and 8 respectively. The surface area of sample A (5.113 m^2/g) however, is relatively smaller than those of samples B and C. This is because the BET method requires dehydrating the clays at 120°C under vacuum, therefore removing the intramolecular/interlamellar water molecules and allowing the octahedral aluminosilicate sheets of sample A to collapse.

These results are unexpected since modification of the clay should ideally increase the basal spacing of the clay interlayer which implies more sorption sites are accessible are in agreement with the findings of Carmody *et al. (*2007). This also suggests that the main adsorption mechanism for the organoclays occurs on the external surface of the material in the diffusion region and/or capillaries.

5.1.3 pH in solution

From the results in Table 4.1, it is clear the pH (10 % in solution) of the raw sample have been reduced to neutral (7.00) after the cation exchange reaction. The modification mechanism is complex and presents many reasons for the change of the clay's pH. The pH of organoclay solutions in solvent change with each modification step (Kim, 2012). There are many stages in the modification process, for example: the exchange of interlayer cations and hydroxyl groups; the removal of surface ores and minerals by free amino and bromide groups; van-der-Waal's attractions and the process of washing, till free of detectable bromide ions, with distilled water. These processes contribute to the adjustment of the pH of the clay materials to pH 7.

5.1.4 Bulk Density

Bulk density is a measure of density including void pores and interstices and may vary depending on compaction. There is a relationship between the extent of intercalation of organoclays and the bulk density of the materials. A change in time, temperature and concentration of the organophilation procedure affects the bulk density of the materials.

5.1.4.1 Effect of intercalation time on bulk density

The exchange of inorganic cation by the CTA^+ cations is grossly affected by contact time as shown in the chart of Figure 4.1. The chart shows that as time increases the bulk density of the material reduces. As time increases, the density of the lighter surfactant molecules increases hence reducing the amount and density of heavier inorganic cations in the bulk material. This decrease is influenced by the available chain length of the alkyl ammonium cation at constant basal spacing, thus structures with a minimum deviation of the basal

spacing from the monolayer or bilayer are formed (De Paiva *et al.*, 2008). The initial change in bulk density (weight loss) within the first 2.5 hours was rapid, but as time increased the change in bulk density values also reduced. During the initial contact time, the alkanes form structures with a wide distribution of gallery heights, giving rise to very broad XRD peaks, by replacing heavier cations and their hydroxides and making the materials relatively lighter and thus more aggregated.

To further explain this behaviour, the data values have been treated by linear regression. The linear regression plot gives a more reliable and predictable relationship between the change in bulk density of the material and the intercalation time change. The predicted time linear plot is also seen in Figure 4.1. The values of the regression parameters and coefficients are presented in Table 4.3. The linear equation for the plot is given to be

$$BD = -0.0392t + 1.3703 \qquad 4.1$$

with an R^2 value of 1. Where *BD* represents the bulk density of the samples and *t* equals to time (hours). The coefficients of time (the slope, -0.0392) represents the rate of weight loss with time and also the kinetic rate of cation exchange within the surface and interlayers of the clays structure. The intercept indicates the maximum weight (or bulk density) that is available at the smallest contact time of intercalation. Analysis of variance was carried out to determine the statistical difference in the rate of change of bulk density with respect to time and presented in Table 4.4. The results confirm that there is always a significant change (Significant $P < 0.05$) in the values of the bulk densities as time changes during ion exchange. Thus, increasing time further than the experimental 10 hours used in this research will most likely further improve the physicochemical properties of the organoclays.

5.1.4.2 Effect of surfactant loading on Bulk Density

The bulk density of the organoclays is also influenced by the surfactant loading during the interaction procedure. Figure 4.2 vividly illustrates that the bulk density of the materials reduces as the surfactant loading increases. Increasing surfactant density gives rise to more cation exchange during the interaction procedure. Figure 4.2 shows a decrease in bulk density of the original clay sample from 1.584 to 1.132 g/cm^3 for the first 10 % w/w addition in surfactant loading. Subsequent increase was slow but constantly reduced the bulk density of the materials up to 1.016 g/cm^3 at 50 % w/w surfactant dosage, tending towards equilibrium between interlayer cations and the organic cations. The experimental data was also treated statistically by linear regression analysis and by Analysis of Variance. The regression statistics and the values of the ANOVA results are presented in Tables 4.3 and 4.4 respectively. The concentration linear plots are also represented in Figure 4.2 as predicted bulk density. The plot is defined by the linear equation:

$$BD = -0.008C + 1.3235 \qquad 4.2$$

with the coefficient of regression, R^2 as 1. *BD* and *C* represents bulk density and concentration respectively. The coefficient of concentration (the slope, -0.008) is a factor for the equilibrium replacement of interlayer cations within the clay materials while the intercept shows the maximum bulk density that is available as soon as intercalation starts. The results of the ANOVA show that there is no significant in density changes as the concentration increases (significant P > 0.05). This is because of the large chain lengths of the incoming cations which tend to saturate the interlayer galleries of the clay materials thus making equilibrium a fast process. This explains why the value of the decreasing slope is very small.

5.2 X-Ray Florescence (XRF) Analysis

The elemental oxide composition of the bulk samples were investigated using X-ray fluorescence spectroscopy. Table 4.5 shows the result of the percentage metal oxide/ore composition of the clays samples before and after characterization. Certain properties of the bentonites can be observed from the results. Sample B is a Calcium Montmorillonite clay and also contains a relatively high amount of iron and magnesium oxides. Calcium content reflects both the interlayer cation and the calcite content of the samples (Carlson, 2004). Sample C can be described as low Sodium Montmorillonite clay and also contains relatively high amount of Iron impurities. The XRF analysis does not differentiate between divalent and trivalent Iron and the Fe_2O_3 in the tables represents total iron content of the samples.

A close study of the values of the cation composition in the samples by the XRF results shows that there was a significant increase in the values of the silica and aluminium present in the clays. This increase in the total percentage is as a result of the decrease in the metal cations that once existed on the surface and between the lamella of the clay samples. All the metals present showed a significant decrease by at least 10 %. There was no reduction in the values of Cr_2O_3 in the organophilated samples, it has been reported by Sakar *et al. (*2010) that organoclays show strong affiliation toward hexavalent chromium. There were other instances of increased presence of metals in the organoclay samples for example in sample 2, Mn_2O_3, MgO, SnO, TiO, and ZnO did not reduce. Rather, there was a corresponding decrease in the amount of silica present as a result. For sample C, all metal ions except Cr as discussed earlier, showed a significant decrease by the procedure. Sample 8 showed increase in the values of K, Ca, Ti and also in Cr. A reduction in the chloride and sulphur contents of the

material indicated that there must have been some level of anion exchange with free organic groups.

The ratios of the SiO_2 to Al_2O_3 content (Si:Al) show that Samples A, B, C, 4 and 5 prove that the clay types are 2:1 alumino-silicate clays and are an indication that they are Smectite/Montmorillonite clay minerals. The Si:Al ratio of sample 2 reduced, indicating a decrease in the integrity of the crystal structure after the organophilation process. This may be due to the relative lack of cations within the interlayers of the 2:1 structure of the clay for cation exchange.

5.3 Neutron Activation Analysis (NAA)

The clay materials were also studied for the quantification of the major interlayer/exchangeable cations (Na, Ca and K), octahedral sheet cations (Fe, Ti, Mg, Mn and Al), Trace elements and possible bromide (Br^-) ion loads using the INAA technique. There are many trace elements usually found in the interlayers and surface of clay and their abundance depends on the origin and also the mixture levels of the clay material. Prevailing concentration of the studied elements in g per 1000g samples using INAA are presented in Table 4.6. The final concentrations are reported on dry weight basis and are the averages of triplicate determinations.

5.3.1 Interlayer/Exchangeable cations.

The interlayer cations found in smectite clays are majorly Na, Ca and K. A comparison of the values of Br ions and, Na, Ca and K cation, in the samples are presented in their percentages graphically in Figure 4.3. Also, Figure 4.3 confirms the predictive description of

the clay types in the XRF analysis and also the qualitative examination of the clay types by the XRD analysis. Although K is present in all samples it is the predominant exchangeable cation in sample A, defining it as a K-bentonite. Calcium is only present in sample B and its corresponding organoclay, sample 5. The abundance of Ca in sample B defines it as a Ca-montmorillonite confirming the results of the XRF results. Na is present in all clay samples, though its abundance is reflected in sample C, which has already been defined as a Na-bentonite. The effect of intercalation on the organoclay samples is vividly illustrated in Figure 4.3 by the reduction of exchangeable cations in the corresponding raw samples. There was a reduction in Na for all three samples after intercalation. Although K did not show a significant reduction in samples B and C, all other interlayer cations present were vividly reduced. The effect of intercalation can also be seen by the increase in Br ions on the surface and interlayers of the raw samples. The Br level is quite low relative to the cations present and is an indication that the Br ions samples were not completely washed of the samples after intercalation. The source of the Br detected is from the CTAB surfactant used in the intercalation process.

5.3.2 Octahedral Sheet Cations

The major elements in the octahedral layer are Mg, Fe, Al and Ti. Unlike the interlayer minerals, these metals are not readily exchangeable. The removal of the interlayer cations from the bulk material affects the concentration of the octahedral layer metals and hence the structure of the materials. The extent of change in the concentration (g/1000g) of the octahedral layer cations are graphically presented in Figure 4.4. As seen from Figure 4.4, the values of the octahedral layer metal content of the clays decreases upon intercalation except for sample 2 which did not show any significant decrease. Al is the most abundant metal in

the octahedral layer of clay minerals, Mg in the samples represents the level of smectite present in the material. The Mg load is more significant in the XRF analysis than it is in the NAA analysis. The samples prove significant decrease in Mg load in the samples. The NAA method does not differentiate Fe^{2+} from Fe^{3+} and are collectively reported as Fe. The reduction in the octahedral sheet metal load is an indication of other mineral phases in the clay mixture.

5.3.3 Trace elements content

Other trace elements in the material have been detected by the NAA technique as reported in Table 4.6 and presented in Figure 4.5. These metals are usually present in the surface or interlayers of the clay and can also exist in other mineral phases found on the clay. Figure 4.5 shows the level of trace metals in the clay samples in g/1000g. The reduction in the level of trace metals present in all three clays shows that the cation exchange reaction was successful. It is possible that the selective interaction of CTAB with these element grossly affects the manner in which the surfactant removes the cations of interest in the clay materials. Generally there was a reduction in all trace metals except for V in sample C.

5.4 X-Ray Diffraction (XRD) Analysis

XRD can give the basal spacing information of the organoclays which is very important for explaining the intercalation and configuration of organic surfactant into the clays (Xi, 2006) and also enables the determination of the expansion to be determined as well the crystal size of the clay (Mallakpour and Dinari, 2011). The XRD patterns of the raw bentonites and the modified bentonites under specific conditions are summarized in Tables 4.1 and 4.2. Figures 4.6, 4.7, 4.8 and 4.9 show the XRD patterns of the raw clay samples. Figure 4.9 is a

superimposition of the three bentonite types for the purpose of comparison. The XRD pattern of the samples A, B, C clearly indicates strong peaks at 11.57, 13.29 and 15.25 Å respectively corresponding to the characteristic d(001) peaks, indicative of montmorillonite mineral at 2θ position of approximately 7 $^{o}2\theta$ and interlayer spacing of approximately 12.5 (±3.0) Å (Ahmadi *et al.*, 2004; Sarker *et al.*, 2005; Zidelkheir and Abdelgoad, 2008). The clay sheets are bound with in-plane covalent bonds and therefore, their crystal structure is stable, but clay layers are held loosely with van der Waal's bonds and therefore, expansion of interlayers is commonly seen when water or organic molecules are introduced between the layers (Yürüdü *et al.*, 2005). During intercalation with quaternary ammonium compounds, the bulk alkanes form structures with a wide distribution of gallery heights giving rise to broad XRD peaks. The configuration of the organic molecule into the clays can also be predicted from the results of the XRD patterns summarized in Table 4.2. Generally speaking, in adsorptive clays, the organic cations only form monolayers. In the case of organophilic clays, the organic cations may form monolayers, bilayers, pseudotrimolecular layers or paraffin complexes (Xi, 2006).

5.4.1 The effect of reaction time on the d(001) spacing

The effect of reaction time on the organophilation process was investigated. The modification process was carried out under mild conditions using 50 % *wt.* CTAB as intercallants and allowed to run for 2.5, 5, 7.5, 10 and 12.5 hours. Figure 4.10 shows the effect of increasing surfactant time on the XRD patterns of the synthesized organoclays. The XRD pattern of the natural bentonite (sample A) showed a characteristic reflection at about 7.6 $2\theta^{o}$ which corresponds with a basal spacing of 11.5Å. After organophilation, the reflection peaks shifted leftward from this first characteristic peak towards lower angles, indicating increase in the

interlayer/basal spacing of the materials as observed in Figure 4.10. Figure 4.10 shows evidently the increase in basal spacing with increasing temperature from 11.53 Å for sample A to 20.27, 16.53, 17.51, 18.05, and 19.60 Å for the modified samples 2, 10, 11, 12 and 13 respectively. These values indicate that the CTA^+ cations form a bilayer arrangement within the clay galleries.

The modification process induced noticeable effect on interlayer spacing after 2.5 hours (16.53 Å), but the maximum interlayer spacing (20.27 Å) was obtained after 10 hours. Furthermore, no further increase in spacing was observed after the 10 hour process. Instead there was a decrease in the basal spacing to 19.6 Å when the process was allowed to stay for 12.5 hours. The shift of the XRD peak as time progressed can be attributed to re-orientation of the long organic salt chain between MMT layers (Lapides *et al.*, 2002). The basal spacing of alkylammonium montmorillonite changes in a characteristic way with the length of the alkylammonium (de Paiva *et al.*, 2008). This is the characteristic property of smectites (Manocha *et al.*, 2008).

5.4.2 The effect of surfactant loading on d(001) spacing

Figure 4.11 shows the XRD spectra of sample C and its corresponding modified samples measured at 2θ between 0 and 25^o, illustrating the effect of surfactant concentration on the organophilation process. As was expected, the values of the d(001) spacing varied and increased as the modifier was intercalated between the layers. XRD reflections of the clay shifted to new positions with increase in surfactant loading confirming that intercalation and surface modification of sample C had taken place. However upon increasing the concentration of CTAB, additional increase in spacing was observed. The interlayer spacing

increased from 15.25 Å to 19.43 Å in response to increase in the surfactant concentration from 5 to 50 percent. As shown in the XRD spectra of the samples in Figure 4.11, little effect was observed in the change in the d(001) values from 15.25 Å in sample C to 15.89 Å in sample 17 (5 % CTAB) of cationic surfactant into the interlayer of Montmorillonite (Jaynes and Boyd, 1991). The layers of the clay were propped open upon swelling in water in the presence of the surfactant. After the ion exchange process, the cationic head groups of the intercalation agent molecule would preferentially reside at the layer surface and the aliphatic tail will radiate away from the surface (Hoidy *et al.*, 2009) expanding the d-spacing by the CTA molecules in comparison with that of the original clay (Mallakpour and Dinari, 2011).

5.4.3 The effect of temperature on intercalation

Temperature is an important parameter in the successful interaction of nanoclays. Samples 4, 5, 6 and 9 at intercalation temperatures of 30, 60, 80 and 90 ^{o}C were chosen for the study of the effect of intercalation temperature on the synthesis of organoclays. Figure 4.12 shows a graphical superimposition of the XRD pattern of Samples B, 4, 5, 6 and 9. It can be seen from Figure 4.12 that the interlayer distance of the studied organoclays, using optimal concentrations of the CTAB salts, does not depend significantly on temperature. In Figure 4.12, the introduction of new peaks at about d(001) and increased counts on the materials compared to sample B is observed. This change is evident of the successful intercalation of sample B and due to the expansion of the clay crystal lattice by CTAB cations. Sample 4 had the highest basal spacing with d(001) value of 7.18 Å, followed by samples 9, 5 and 6 with d(001) values of 7.08, 7.08 and 7.03 Å respectively. This shows that small temperature increase does significantly affect the rate of intercalation reaction.

5.4.4 The effect of surfactant type on intercalation

The effect of the nature and of quaternary ammonium salts on interlayer distances of organoclay with different quaternary ammonium salts and clay types obtained from XRD patterns are shown in Figure 4.13. It is clear that interlayer distance of organoclay depends on nature and amount of organic ammonium salts. Samples 2 and 15 intercalated with CTAB cations have larger distances than their corresponding samples 1 and 3, intercalated with CTAC respectively. In details, interlayer distances of samples 1, 2, 3 and 15 with 80 % w/w organic ammonium salt are 11.74 Å, 20.16 Å, 16.70 Å and 17.64 Å, respectively. The difference in the influence of quaternary ammonium bromides and chlorides on nanoclays has not yet been fully understood. In homogenous mixtures, organobromides undergo displacement reactions approximately 50 times faster than organochlorides. Also, depending on the layer charge of the clay mineral and the chain length of the organic ion, different arrangements of organic molecules between the layers can be formed. The geometry of the surface and the degree of exchange can also be of influence (De Paiva *et al.*, 2008).

According to Hackett *et al. (*1998), Heinz *et al. (*2007) and De Paiva *et al. (*2008), for organoclays with interlayer distance of about 13.5 Å, organic cations lie between bentonite layers as monolayers while interlayer distances < 22.7 Å corresponds to bilayer arrangements of the organic cations in the bentonite layers. The d(001) values of (CTAC) intercalated samples 1 and 3 implies intercalation was successful and that the CTA^+ cations lay parallel to the bentonite planes forming a lateral monolayer arrangement of hydrocarbon tails. While the d(001) values of the CTAB intercalated samples correspond to lateral bilayer arrangement of the surfactant molecules with the long alkyl chains lying down on the clay surface. This is in agreement with the findings of Heinz *et al. (*2007) and Oliveira *et al. (*2012).

5.5 Fourier Transform Infrared (FTIR) Analysis

The FTIR spectra of the clay samples and their resultant organoclays, within the range of 4000 to 400 cm^{-1}, are shown in Figures 4.14 – 4.19. Table 4.7 is a table of the assignments of the key spectral bands present in the sample as determined by the FTIR technique. FTIR characterization has been proven to be an effective method for exploring the microstructures of organoclays (Hoidy *et al.*, 2009; Frost *et al.*, 2006; Yurudu *et al.*, 2005; Zhu *et al.*, 2005). Since FTIR spectroscopy measures the molecular vibrations and determines in the molecular structure of the organoclays, any change in the structure of the organoclay will be observed through alterations in the infrared spectra (He *et al.*, 2006; Mallakpour and Dinari, 2011). The infrared spectra of the unmodified clays show major peaks that are characteristic of montmorillonite clays. Bands in the 600-400 cm^{-1} region are attributed to Si-O and Al-O bending vibration with interlayer deformation around 1630 cm^{-1}. The tetrahedral bending modes were near 430 cm^{-1} for Si-O-Si and 540 cm^{-1} for Si-O-Al (Van der Marel and Beutelspacher, 1976). Si-O bending modes was also observed at 790 and 690 cm^{-1} indicating the presence of quartz in the materials (Nayak and Singh, 2007). The intense broad bands observed between 1100 and 1020 cm^{-1} were those for Si-O stretching vibrations of montmorillonite. The band in the 3600-3440 region are ascribed to OH stretching of hydroxyl groups present in the interlayer of the clay material by covalent attachment to the silane molecules. The spectra shows prominent peaks between 3622 and 3695 cm^{-1} indicating the possibility of hydroxyl linkage due to OH stretching vibration of structural OH group from Al-Al-OH and Si-OH-Al stretching (inter-octahedral), attributed to montmorillonite, with the bending frequency was at 914 cm^{-1} and 922 cm^{-1}. These are considered characteristics of dioctahedral smectites (Akçay and Yurdakoç, 1999).

Common features in the spectra of the organoclays are the appearance of bands frequency at/near to 3655 cm^{-1}, 2852 cm^{-1}, 2922 cm^{-1},1470 cm^{-1}, 1010 cm^{-1}, 752 $cm^{-1}$and 432 cm^{-1}. The organic clays do not only have characteristic montmorillonite bands, but also have characteristic alkyl or aryl and acid group bands as seen on Figures 4.17 to 4.20. The absorption band at about 1470 cm^{-1} is attributed to a characteristic C-H bending vibration of the asymmetric angular deformation of the CH_3 groups from $(CH_3)_4N^+$ (Madejova, 2003; Zhou *et al.*, 2008). The IR peaks that appear at the 3000-2800 cm^{-1} region are the signature of CH_2 infrared absorption bands. These bands are indicative of the ordering (gauche/trans conformer ratio), packing density of the surfactants in organoclays and the interactions between the alkyl chains (Zhu *et al.*, 2005). The bands at 2922 cm^{-1} are also due to asymmetric C-H stretching vibration of CH_2 aliphatic and the absorption band at 2852 cm^{-1} corresponds to symmetrical CH_3 stretching (Oliveira *et al.*, 2012). According to previous reports (Masooleh *et al.*, 2010; Frost *et al.*, 2007), the CH_2 infrared absorption bands on FTIR patterns, especially the $v_{as}(CH_2)$ mode, are sensitive to the packing density of the sorbed surfactants on clays, and the absorption frequencies of $v_{as}(CH_2)$ are believed to be inversely related to the packing density of the adsorbed surfactants (Zhu *et al.*, 2005). Peaks due to asymmetric and symmetric modes do not appear in the case of unmodified clay due to absence of organic molecules therein (Sarkar *et al.*, 2010). In the spectra of the organoclays, bands in the 3500-3000 cm^{-1} region for the amine chains are observable. The weak bands near to 3260 cm^{-1} and at 3230 cm^{-1} corresponds with N-H in NH_4^+ stretching vibration of intercalated primary aliphatic ammonium.

Upon organophilation, CTA^+ is intercalated into layer silicates of the clays, broadening the absorption peaks origins. The FTIR spectra of the organoclays showing the effect of time,

ammonium salt concentration and temperature are vividly illustrated in Figures 4.18, 4.19 and 4.20 respectively. The presence of -CH_3, CH_2 and NH_4^+ transmission bands in organoclays confirms the alkyl ammonium intercalation in the interlayer spaces of MMT and the systematic decrease in intensity of OH (free) band shows that the organoclays become more and more organophilic with increasing concentration of organic compounds. It is evident that there is a shift for these bands towards a lower frequency as the surfactant loading rates increase from 25 % to 70 % clay-surfactant (*w/w*) as seen in Figure 4.19. It is also evident from the XRD results in this study that increasing surfactant packing density causes additional expansion of the clay interlayer spaces. By monitoring the frequency shifts of the CH_2 stretching and scissoring vibrations as a function of interlayer packing density, chain length, and temperature, it has been found that the intercalated molecules exist in states with different degrees of order (de Paiva *et al.*, 2008). Figure 4.20 shows the changes in the structure of Sample B after intercalation at relatively higher temperatures. This is indicative of the fact that higher temperatures favour disordered conformation. Therefore, these results are attributable to the progressively developing conformation of the adsorbed surfactant molecules from low packing density and ordering (liquid like) to high packing density and ordering (solid like) (Zhu *et al.*, 2005).

5.6 Thermo-Analytical Studies

Thermal stability plays an essential role in determining both technological applications and processing conditions of the clay materials (Hoidy *et al.*, 2009). Thermal gravimetry is essentially a means of observing the weight of a sample as a function of temperature (dynamic heating) or time (isothermal heating). Often thermoanalytical studies can lead to new insights into the structure of intercalated clays (Apinion *et al.*, 2006). The

thermogravimetric and respective differential thermometric profiles of the raw and modified bentonites are shown in Figures 4.21 to 4.25. The results of the thermogravimetric analyses are reported in Table 4.8. Table 4.8 summarizes the weight % loss due to the cation exchange with the surfactants. Figure 4.21, 4.22 and 4.23 display the Thermo-Gravimetric Analysis (TGA) and Differential Scanning-Calorimetry (DSC) results for the bentonite clays without intercalation with the surfactant while Figures 4.24 and 4.25 show the TG and DTG for modified bentonites samples 2 and 5 respectively.

The way in which the mass loss steps occur can provide information on the properties of the inserting molecules (Xi *et al.*, 2005). At a given temperature the bentonite and organoclays weight loss is directly related to the rate of the material decomposition process (Hoidy *et al.*, 2009). The organoclay decomposition occurs in very different ways from those of the raw bentonite clays. The curves in thermogravimetric analysis show a four step weight loss covering 50 to 500ºC. In this way the use of TG techniques enable a better understanding of the organoclays.

The first step form the ambient to 100 °C temperature range and is attributed to desorption of water from the clay (Magaraphan *et al.*, 2001). Bentonic clays are usually highly hydrated due to its large hydrophilic internal surface (Xie *et al.*, 2001). Hence, free water (water between particles and water sorbed on the external surfaces of crystals) are released at the temperature of below 100°C (Magaraphan *et al.*, 2001) as shown in Figures 4.21 – 4.23. Sample A reduces from 100 % at ambience to 99.95 % at 130 ºC while samples B and C decreases to about 98 % at 85ºC and 102ºC respectively. The TGA curves shows that the losses are endothermic. This is only possible due to the loss of physisorbed water and organics and loss of chemisorbed water (Venkatathri, 2006).

In the organoclay samples the desorption of water step is not very visible because the clay material is now hydrophobic and does not contain as much OH groups as was in the initial samples. The proof of hydrophobicity is reflected in the thermal stability of the organoclay samples within the first 200 ºC on the DTG scans. There are at least two reasons why organoclays contain less water than inorganic parent material. The larger size of the organic cations physically take up room that would be occupied in an inorganic system and much lower hydration energy of the cation. As a result, the amount of water in organoclays is considerably reduced (Madejova, 2003).

The second step occurs from about 120 to 210 °C temperature range and is assigned to the loss of hydration water or dehydroxylation, of bonded OH, of the layer crystal lattice structure (Magaraphan *et al.*, 2009) dehydration of the hydrated cation in the interlayer and the dehydroxylation of the montmorillonite respectively (Xi *et al.*, 2005).

The third mass loss step is attributed to the removal of the surfactant. This step corresponds to decomposition of the alkyl ammonium ions present in the Organo bentonite samples. The modification process occurred in such a way that the alkyl ammonium ions were adsorbed in the interlamellar space of the clays. The adsorption was through an exchange reaction between the inorganic cations on the clay and the alkyl ammonium ions in the solution (Manocha *et al.*, 2006). The percent weight loss at this point depends on the amount of the surfactant cation exchanged and the surfactants adsorbed to the surface of the clay crystals.

This decomposition stage is split into two steps which are mainly attributed to the chemical decomposition of the bonded structure of the organic modifier. The latter temperature simply represents desorption of the surfactant molecules from the surface of the clay particles. The

onset for decomposition of organic matter occurs around 200 °C with the maximum decomposition around 250 °C – 275 °C. The DTG curve of the surfactant shows an inflection from stability at 200 °C which is the escape of surfactant and its content. This temperature is very close to the melting point of CTAB which is 253 ºC. This indicates two types of bonding of surfactant molecules in the organoclays. One type of bonding is to the silica surface and the second to other surfactant molecules. It is to be noted that organics on decomposition will give exothermic weight loss (Venkatathri, 2006).

The final mass loss step in the TG curves is assigned to the loss of structural hydroxyl groups from within the clay. According to Arroyo *et al. (*2003) water in the interlayer space usually is removed at the temperature of around 350 °C.

5.7 Scanning Electron Microscopy

SEM has been used to investigate the morphology of the raw and modified bentonite samples. Figures 4.26 to 4.30 show the SEM surface morphology of the samples A, B and C before and after modification. The unmodified clays (Figures 4.26 to 4.28) show massive, aggregated morphology, and in some instances, there are some bulky flakes. It can be seen that the original clays have massive and curved plates. On the other hand, the organoclay (Figures 4.29 to 4.31) are discrete, pile up and gather together much easier than those of the raw samples. They are characterized by several small and aggregated particles and the plates become relatively flat. It can be observed that the modified samples showed a more heterogeneous agglomeration in terms of dimension and particle size (polydispersity), comprising many irregular lamellae very likely because of the interactions between the alkyl groups of surface exchanged molecules belonging to different particles. The layered structure

of clay can be seen distinctively showing the retention of characteristic properties of clay after giving the chemical treatment. These results are in agreement with the findings of Gonzaga *et al. (*2007) and, Mallakpour and Dinari (2011). It is of importance to reveal that the organoclays show significant change in morphology compared to their original nature yet there are not many morphologic differences observed between the organoclays despite the obvious variation observed in the XRD measurements. The layered structures as seen in the micrograph are no more continuous and the scattered platelets show an increase in the interplanar distance (Manocha *et al.*, 2008).

These observations support the FTIR and XRD data indicating that with increase in time or surfactant concentration during organophilation, the curved plates in the clay transforms to flat layers. Showing that not only the basal spacing but also the morphology of the organoclays depends on the density of surfactants within the montmorillonite interlayer space.

5.8 Sorption Studies

Sorption studies were carried out on both the raw and organically modified clay samples. It was observed that the organically modified samples sorbed more oil than their clay counterparts as explained in the subchapters below. An important consequence of replacing inorganic with organic cations is that the clay surface takes on hydrophobic character, which greatly enhances their affinity for non-polar organic pollutants. (Madejova, 2003).

5.8.1 Sorption of crude oil on clay and organoclay samples

5.8.1.1 Effect of Sorbent dosage on crude oil sorption capacity

To study the effect of increasing sorbent weight on the absorption of different oil types, different weight (from 0.5 to 5.0 g) were investigated. The curves of Figures 4.32 explain the effect of varying the sorbent weight or dosage on the sorption capacity of the sorbents. Figure 4.32 illustrates that the amount of oil sorbed increases with increase in weight of sorbent. As expected for samples A, B, C, 2, 5 and 15, the amount of oil sorbed increases with increase in dosage of sorbent used. The curves of Figure 4.32 showed the increase in sorption capacity of sorbent with increase in sorbent weight for the six sorbent types at 0.5 to 1.5 g after which they tend to become more stable. This stability may be due to compacting of the nanoclays as weight increases which may inhibit the ability of oil to evenly penetrate the crystal lattice efficiently over a short period of time. It is also observed from Figure 4.32 that the organoclay samples happened to sorb more oil than the raw clay samples.

5.8.1.2 Effect of initial oil concentration

The initial concentration study is very important because the initial concentration of the oil residue in solute can strongly affect the sorption kinetics and more specifically, the mechanism that controls the overall kinetic coefficient. Figure 4.33 explains the relationship between initial concentration and the amount of oil sorbed by the materials, showing the effect of initial oil concentration on sorbing power the materials. The charts on Figure 4.33 show that the sorption of oil increases with increasing initial oil concentration up to a certain level and then tends to attain equilibrium. It is also evident from the Figure 4.33 that the sorption capacities of the organoclays were higher than those of the raw nanoclays. This is

because the raw nanoclays are hydrophilic in nature. They also easily form dispersions in the water and later settle at the base of the beaker after a while, making sorption of the oil difficult. The high sorption capacity of organoclays were due to the presence of hydrophobic groups from the quaternary ammonium cations that were intercalated within the layers of the nanoclays during the organophilation process which consequently enhance the hydrophobic character of the nanoclay particles. This is an indication of success in the intercalation of clays by the surfactant. At higher initial concentrations, the surface of the hydrophobic organoclays enhances oil residue diffusion through the film surrounding the materials and into the porous network of the organoclays.

5.8.1.3 Effect of contact time on oil sorption capacity

The effect of time on the sorption of oil by the nanoclays was studied by varying the time used in the sorption of the crude oil from a water mixture. The relationship between the oil uptake per gram of raw and modified nanoclays (q_e) as a function of the contact time (t) from 1-30 minutes is illustrated in Figure 4.34. As expected, the plots show that the sorption of crude oil increases with time until it reaches an equilibrium beyond which no significant increment was observed. The plots of the effect of time on oil sorption show that sorption capacity slightly increases with the contact time for the first one minute after which no further oil removal from the solution was observed. This implies that the process was of a fast and stable nature as only slight differences were observed between the initial and final contact time. The sorption process was rapid at the initial stages of the contact period and thereafter it became slower towards equilibrium. This phenomenon is due to the fact that a large number of vacant surface sites and microscopic voids were available for sorption during the initial stages, and after a lapse of time, the remaining vacant surface sites were difficult to be

occupied due to repulsive forces between the oil molecules on the solid and bulk phases (Amer *et al.*, 2007; Sokker *et al.*, 2011; Eman, 2013). As time goes by, the sorbed oil residue starts to clog the pores near the outer surface so oil residue can no longer diffuse to the active sites deep within the interior surface.

It is also evident from the plots of Figure 4.34 that the sorption capacities of the organoclays were higher than those of the raw nanoclays. The difference in the sorption behaviour of the sorbent groups is ascribed to the hydrophilic character of their surface properties. These hydrophilic surfaces of nanoclays give them affinity towards water, making them to easily form dispersions in the water and swell at the base of the beakers after a few moment, thus making sorption of the oil difficult. This is because the liquids are held on surfaces either within the sorbent material such as pores, capillaries of interstices or on external surfaces of plastic fibres or mineral granules. Also, the small interlayer spacing of the clay structures may not allow the oil particles to be trapped by the clay material as the oil droplets are usually larger than the pores sizes of the raw clays and cannot be trapped in the layers of the clays unlike those of the modified clays (Eman, 2013). This is somewhat logical, regarding that a molecule cannot enter a pore which is smaller than the molecule itself. The higher sorption capacity of the modified clays are as a result of the effect of the available surface area subjected to the oil (Nwankwere *et al.*, 2010), and the ability for the oil molecules to form covalent bonds with the alkylammonium cations on the surface and layers of the organoclays. Sorption is a surface phenomenon that is directly related to surface area. Therefore increasing the surface area increases the specific sorption. Also surface area affects the sorption of the material to a certain extent. As the surface area increases, it increases the capillaries that are being formed and hence increases the absorption (Hussein *et al.*, 2009). The hydrophobic

character of the modified clays was due to successful intercalation of the ammonium quaternary cation of CTA^+ within the layers of the clays. These results are consistent with the findings of Hussein *et al. (*2008) and Thompson *et al. (*2010). Oliveira *et al. (*2010) in the sorption of oil by hydrophobic and hydrophilic porous materials. This is evidence that the organoclays are suitable materials for the removal of oil from oil-water interactions.

5.8.2 Equilibrium Sorption Studies

The existence of equilibrium between the liquid and solid phase is well described by sorption isotherms (Roopa *et al.*, 2014). Equilibrium studies that give the capacity of the sorbent and the equilibrium relationships between sorbent and sorbate are described by sorption isotherms which are usually the ratio between the quantity sorbed and the remaining in solution at fixed temperature and at equilibrium (Igwe and Abia, 2007). Sorption isotherms are important in describing how solutes interrelate with the sorbents and so is critical in optimizing the use of sorbents (Foo and Hameed, 2010). Correlation of isotherm data by empirical or theoretical equations is thus essential for the operating of sorption systems and practical design. Equilibrium data collected were fitted into the well-known Langmuir, Freundlich, and Dubinin-Raduskevich sorption isotherm models which were used to analyse data. These isotherm models are depicted in Figures 4.35, 4.36 and 4.37. The isotherms yield constants whose values express the affinity of sorbate for the surface of sorbent.

5.8.2.1 The Langmuir Isotherm Model

The Langmuir Isotherm model which was originally developed to describe the sorption of gas on to solid surface is used for monolayer sorption onto a surface containing a finite number of identical binding sites (Langmuir, 1918). The model represents the equilibrium

distribution of sorbates molecules between the solid and liquid phases, suggesting the formation of monolayer sorption and also energetically homogeneous surfaces (Arivoli, 2009; Itodo *et al.*, 2009; Thompson *et al.*, 2010). Sorption isotherms of the organoclays were studied using the linearized form of the Langmuir isotherm model expressed as

$$1/q_e = 1/C_e q_m b + 1/q_m \qquad 5.3$$

The linearized form of the Langmuir isotherm allows the calculation of sorption capacities and the Langmuir constants by plotting $1/q_e$ against $1/C_e$ as shown in Figure 4.35. Where q_e is the amount of oil (g) accumulated per gram of organoclay material used; C_e is the residual amount of oil in water at equilibrium, q_m, a constant related to sorption capacity (mg/g), is the maximum specific uptake for a monolayer coverage corresponding to the site saturation and *b*, the Langmuir constant related to energy of sorption, is the ratio of sorption and desorption rates. The constant *b* expresses the affinity between the sorbent and sorbate (Dawodu *et al.*, 2012). q_m and *b* were obtained from the slopes and intercepts respectively of the plots shown in Figure 4.35. The Langmuir isotherm parameters are given in Table 4.9. The high values of q_m and the low values of *b* obtained suggest that the organoclays have high affinity for crude oil and subsequently large organic molecules. The essential characteristics of Langmuir isotherm can be expressed by dimensionless separation factor, R_L (Manocha *et al.*, 2002; Satish, 2003).

$$R_L = 1/[1 + bC_o] \qquad 5.4$$

Where C_o is the highest initial concentration of sorbate ($mg \cdot \ell^{-1}$), and *b* ($\ell \cdot mg^{-1}$) is the Langmuir constant. The value of R_L indicates the shape of the isotherm to be either

unfavourable (R_L>1), linear (R_L =1), favourable (0 < R_L< 1) or irreversible (R_L = 0) (Sunil and Arti, 2010). The R_L values given in Table 4.9 for this sorption process were in between 0 and 1, indicating the favourable sorption of crude oil on the organoclays took place. This suggests that the organoclays are suitable sorbents for the pickup of crude oil in water. The R^2 values of the Langmuir Isotherm are all greater than 0.99 and higher than the R^2 values of the Freundlich and D-R isotherms. Indicating that the manner of sorption in monolayer and that the surfaces of the organoclays are predominantly homogeneous.

5.8.2.2 The Freundlich sorption model

The Freundlich isotherm has been applied to estimate the sorption intensity of the sorbent towards the sorbate. One major characteristic of the Freundlich isotherm is its ability to give an appropriate description of equilibrium data over a restricted range of concentration (Dawodu *et al.*, 2012; Roopa *et al.*, 2014). The Freundlich isotherm is excellent for multicomponent systems (Li and Werth, 2002; Asaka and Ogino, 2005). Crude oil is a mixture of several chemical and therefore a multicomponent system of interest. The model assumes that the removal of crude oil molecules occurs on a heterogeneous sorbent surface and can be applied to multilayer sorption (Freundlich, 1906). The equilibrium data were treated with the linearized Freundlich isotherm was by plotting a chart of $\ln q_e$ against $\ln C_e$ as shown in Figure 4.36. The linearized form of Freundlich sorption isotherm was used to evaluate the sorption data and is represented as:

$$\ln q_e = \ln K_F + {}^{1}/_{n} \ln C_e \qquad 5.5$$

This isotherm is usually used in special cases of heterogeneous surface energy which is characterized by the heterogeneity factor *1/n*. *n* is an empirical parameter related to the

sorption intensity, where q_e is the solid phase sorbate concentration at equilibrium (g/g), C_e is the liquid phase sorbate concentration at equilibrium (g/L), K_F is a constant describing the sorption capacity (L/g), also called the Freundlich constant. A plot Lnq_e vs. LnC_o enables the constant K_F and exponent *1/n* to be determined. The calculated Freundlich isotherm parameters obtained are given in Table 4.9. The values of the constants n and K_F were obtained from the slope and intercept respectively. The magnitude of K_F and *n* shows easy separation of the crude oil from the contaminated water and high sorption capacity. The values of K_F and n determine the steepness and curvature of the isotherm. The '*n*' values should be in between 1and 10 for favourable sorption. In the present study values of n which is related to the distribution of bonded molecules on the organoclay surface were found to be positive and between 1 and 10 for the crude oil sorption. The values of the calculated n were 1.034 for sample 2, 1.135 for sample 5 and 1.088 for sample 15 which indicates the favourable sorption and also implies that the organoclays have a high affinity for crude oil and therefore the sorption capacity of the organoclays will be high at high sorbent dosages but will rapidly diminish at lower dosages of sorbent. Also, the higher the K_F value the greater the sorption intensity (Igwe and Abia, 2007). The K_F values for sample 5 (1.966) seemed to be the highest and sample 15 (1.899) being the runner-up and slightly higher than sample 2 (1.862). The higher values of k indicate more sorption, so the results of sample 2 offered a maximum sorption capacity compared to the other sorbents. The Freundlich equation is also suitable for a highly heterogeneous surface and a sorption isotherm lacking a plateau, indicating a multi-layer sorption (Igwe and Abia, 2007). Analyses of the values of the regression coefficients (R^2) obtained for these isotherm plots reveal that Freundlich isotherm also describes the present system's sorption pattern as heterogeneous surface but within a restricted range only. The R^2 for each organoclay were high but relatively much lower than

their corresponding Langmuir and Dubinin-Radushkevich values. This shows that this isotherm gave a good but not a better fit to the experimental data compared to the Langmuir and Dubinin-Radushkevich isotherms. The results support the findings in the Langmuir Isotherm studies that the organoclays surfaces are predominantly homogenous.

5.8.2.3 The Dubinin-Radushkevich isotherm

The Dubinin-Radushkevich isotherm (D-R) is a most popular model for a single solute system, based on the distribution of solute between the solid phase and aqueous phase at equilibrium (Singh *et al.,* 1999). The D-R isotherm model was applied to the data in order to deduce the heterogeneity of the surface energies of sorption, the characteristic porosity of the sorbent and the apparent sorption energy (Dubinin *et al.*, 1947). The linear form of the D-R isotherm is expressed

$$ln\, q_e = ln\, q_e - 2B_D RT\, ln\left(1 + {}^{1}/_{C_e}\right) \qquad 5.6$$

Where, B_D (mol^2 /J^2) is a constant related to the mean free energy of sorption per mole of the sorbate as it migrates to the surface of the sorbent from infinite distance in the solution and the constant q_D (mol/g) is the D-R isotherm constant representing the theoretical saturation capacity or the degree of sorbate sorption by the sorbent surface. Usually, *R* is the ideal gas constant, (8.314 J/molK), *T (K)* is the temperature of sorption and *E* (kJ/mol) is the mean free energy of sorption per molecule of the sorbate. Plots of *lnqe* versus [*RTln(1 + 1/Ce)]* as shown in Figure 4.37, yielded straight lines and indicate a good fit of the isotherm to the experimental data. The coefficient of Regression-R^2, the apparent sorption energy-*E*, and the values of q_D and B_D are summarized in Table 4.9. The constants q_D and B_D were calculated from the intercept and slope respectively. E was calculated using $E = 1/(2B_D)^{\frac{1}{2}}$ when

transferred to the surface of the solid from infinity in solution (Kundu and Gupta, 2006). The higher the values of q_D, the higher the sorption capacity and the better are the sorbents (Igwe and Abia, 2007; Venkateswaran and Parimaladevi, 2011). The q_D values were in the order, sample 4 (14.51) > sample 5 (12.56) > sample 2 (11.92). This implies that the sample 4 is a better sorbent than the sample 5 which is consequently better than sample 2. When the value of *E* lies below 20 kJ/mol it indicates a physical sorption process (Atkins, 1999; Itodo and Itodo, 2010). The values of the apparent energy of sorption (*E*) were above 20 kJ/mol for all instances and indicated that chemisorption predominated physisorption between the organoclays and the crude oil molecules. As indicated from the plots, the value of the regression parameter-R^2 for the D-R isotherm is relatively higher than that of the Freundlich Isotherms. R^2 (0.9915-sample 2, 0.9792-sample 5 and 0.9915-sample 4) indicates suitability of the D-R isotherm on the equilibrium uptake data of the materials and proves a good model in explaining their sorption energies.

5.8.3 Kinetics Sorption Studies

Sorption is a mass transfer process involving transfer of sorbate from liquid phase into solid phase and apply on the basis of these three consecutive steps: (i) Boundary layer mass transfer across the liquid film around the particle, (ii) Internal diffusion /mass transport within the particle boundary as pore and /or solid diffusion, (iii) Sorption within the particle and or on the external surface (Qiu *et al.*, 2009; Nounou *et al.*, 2010; Adeyi *et al.*, 2014). The studies of sorption equilibrium are important in determining the effectiveness of sorption; however, it is also necessary to identify the types of sorption mechanism in a given system (Yakout and Elsherif, 2010).

5.8.3.1 The Pseudo-Second-Order Rate Model

The data for the time dependence of oil sorption on the organoclay samples were subjected to the linearized Pseudo-second-order rate model equation of Ho and McKay, (1998). Whereby this equation is based on the sorption capacity, it predicts the behaviour over the whole range of studies supporting the validity, and is in agreement with chemisorption being the rate-controlling step (Ho and McKay, 1998). Based on equilibrium sorption, the linearized pseudo-second-order kinetic equation is expressed as

$$\frac{t}{q_t} = \frac{1}{h} + \frac{t}{q_e} \qquad 5.7$$

Where q_t (mg/g) is the amount of sorbate retained at time, t (min). Plots of t/q_t versus t for the organoclay samples are presented in Figure 4.38. The value of the sorption capacity of the organoclays q_e, the pseudo-second-order rate constant k_2, (g/mg min) the initial sorption rate constant h (mg/g min), and the coefficient of determination R^2 were evaluated from the plot and presented in Table 4.10. The constants k_2 and h were calculated respectively from the intercept and slope of the linear plots obtained. The straight lines in the plots prove a good agreement of experimental data with the second-order kinetic model. According to Ho *et al. (*1995), if the plot is linear, then the sorption process may be described as chemisorption. The data showed that modification by CTA^+ enhances the equilibrium sorption capacity of the clay materials towards the crude oil. It can be seen that the kinetics of crude oil sorption onto organoclays follow this model with correlation coefficients higher than 0.99. These results imply that chemisorption mechanism may play an important role for the sorption of crude oil on organoclays. The sorbed molecules are held to the surface of the organoclays by covalent

forces of the same general type as those occurring between bound atoms in the oil molecules (Topallar, 1998).

5.8.3.2 The Elovich Model

Elovich equation was used successfully to describe second-order kinetics assuming that the actual solid surfaces are energetically heterogeneous though the equation does not propose any definite mechanism for sorbate–sorbent (Demibras *et al.*, 2008; Yakout and Elsherif, 2010). It has extensively been accepted that the chemisorption process can be described by this semi-empirical equation (Zhang and Stanforth, 2005). The analyses of the results outlined an inversely proportional relationship between C_o and the values of the parameter - *a*, which is related to the extent of surface coverage and the activation energy for chemisorption. Consequently, the number of active sites available for sorption was reduced due to the larger number of sorbate molecules at higher initial concentrations (Yeneva *et al.*, 2013). The linear form of this equation is given by

$$q_e = \alpha \ln a\alpha + \alpha \ln t \qquad 5.8$$

Where α is the initial sorption rate (mg/g min), and the parameter *a* is related to the extent of surface coverage and activation energy for chemisorption (g/mg). α and a were calculated from the intercept and slope of the straight-line plots of q_t against *lnt* and listed in Table 4.10. Figure 4.39 shows the Elovich kinetic models for the organoclays. From Table 4.10, the good correlation among the experimental points and the theoretical lines is observed. It implies that the Elovich model well describe the kinetic data over a short period of time. The possibility that the adsorption was occurring in the system water/oil/organoclay, also involving the participation of some other forces, beside the Van der Waal's, was estimated by applying the Elovich equation (Uzunova *et al.*, 2013). When the correlation between the

sorption capacity and the constant b is negative, it is accepted that the adsorbent does not retain the sorbate. The positive value of the constant gives evidence for occurring of sorption. The applicability of the simple Elovich equation for the present kinetic data indicates that the Elovich equation was able to describe properly the kinetics of crude oil sorption on organoclays.

5.8.3.3 The Intraparticle Diffusion Model

The possibility that the diffusion might be the rate limiting stage in regard to the entire process was evaluated by the linear dependence on the Weber-Morris Intraparticle diffusion model (Weber and Morris, 1963). Intraparticle diffusion is a transport process involving movement of species from the bulk of the solution to the solid phase (Uzunova *et al.*, 2013). The structure of the solid and its interaction with the diffusion substance influences the rate of transport. Sorbent may be in the form of porous barriers and solute movement by diffusion from one fluid body to the other by virtue of concentration gradient (Shrihari *et al.*, 2005; Srihari and Das, 2009). The pseudo-second-order and Elovich kinetic models may not be sufficient to give the certainty of the sorption mechanism and did not identify the diffusion mechanism, the kinetic results were further analysed using the intra-particle diffusion model. The intraparticle diffusion model has therefore been integrated to explain the diffusion and describe the sorption process occurring within the internal pores of the sorbent. The kinetic data were fitted into the linear equation of the diffusion model developed by Weber and Morris (1963), as shown in Figure 4.40.

$$q_e = k_{id} t^{1/2} + C_i \qquad 5.9$$

A plot of the amount of sorbate sorbed, q_t (g/g) and the square root of the time *t*, gives the rate constant k_{id} ($gg^{-1}\ min^{-1/2}$) which is the intraparticle diffusion rate coefficient as the slope of the plot and C_i (g/g) which is the intraparticle diffusion coefficient as the intercept of the line accounting the bonding effect between the clay layers. Larger k_{id} values illustrate better sorption which is related to improved bonding between sorbate and sorbent particles (Erhan *et al.*, 2004) and may simply be due to the fact that higher sorbate concentration adds to a greater driving force for diffusion of sorbate molecules into the pores (Sunil and Arti, 2010). K_{id} of 0.124, 0.186 and 0.2138 $g/gmin^{-1/2}$ were calculated for sample 2, sample 5 and sample 4 respectively. Sample 4 supports an enhanced rate of adsorption more than sample 5 and sample 2 and is in turn linked to improved bonding (Erhan *et al.*, 2004). The correlation coefficients ($R^{2)}$ for the intraparticle diffusion model were 0.7137, 0.5341 and 0.582 for sample 2, sample 5 and sample 4 respectively (Table 4.12). These poor values of R^2indicate that the kinetic Weber-Morris diffusion Model suggests that intraparticle diffusion may not be the only rate limiting step in the procedure. According to Itodo *et al. (*2010), the sorption mechanism assumes intraparticle diffusion if the following conditions are met: (i) High R_2 values to ascertain applicability; (ii) Straight line which passes through the origin for the plot area q_t vs. $t^{1/2}$; (iii) Intercept $C_i < 0$. A validity test which deviates from (ii) and (iii) above shows that the mode of transport is affected by more than one process which means that two or more stages occur. It was observed that the straight lines did not pass through the origin i.e. $C_i > 0$ for all cases, further indicating that the intra-particle diffusion is not the only rate-controlling step. According to Yakout and Elsherif (2010), when the plots do not pass through the origin, it is indicative of some degree of boundary layer control and this further show that the intra-particle diffusion is not the only rate-limiting step, but also other kinetic models may control the rate of sorption, all of which may be operating simultaneously. Probably, the

initial stages were controlled by external mass transfer or surface diffusion, followed by chemical reaction or a constant-rate stage, and diffusion causing gradual decrease of the process rate. It is likely that a large number of molecules diffuse into the pore before being sorbed.

6.0 SUMMARY, CONCLUSION AND RECOMMENDATIONS

6.1 Summary

Three Nigerian bentonite based clays have been successfully modified into organoclays that have shown potential as oil spill sorbents. CTAB was used to modify the bentonite clays in an attempt to create inexpensive materials that can be applied as agents for the removal of crude oil and organic pollutants in the environment and therefore as precursors for the synthesis of other nanocomposites. From the results obtained, synthesis of the organoclays with good high sorption capacity for organic pollutants was successfully achieved.

The results of the physicochemical analysis carried out on the raw and modified clay samples have clearly shown that intercalation was successful. The change in chemical composition of the clays were examined by XRF and NAA analysis. Morphological and microstructural properties of the clays have been analysed by FTIR, XRD, TGA and SEM techniques. The X-ray diffractograms of the organoclays showed that, the clay galleries were properly intercalated by the surfactant molecules. A shift to the left in the 2θ axis indicates an increase in the basal spacing of the montmorillonite clay as a result of the incorporation of surfactant chains in the interlayer galleries of the nanoclays thus making the originally hydrophilic bentonites organophilic. This finding was supported by the results of the FT-IR spectra of the organoclays which showed the presence of new organic groups on the characteristic bentonite structure. The introduction of new peaks at about 2920 and 2850 supported by broadening of peak intensities at about 1460 is indicative of new organic groups in the structure of the clay samples. Bands which are attributed to water stretching vibrations decrease in intensity as the ion exchange of the sodium from the montmorillonite occurs.

Further studies carried out using these techniques to investigate the effect the reaction conditions on the synthesized materials revealed that, while mild temperatures do not have a significant influence on intercalation, reaction time and surfactant loading had significant effect on the organoclays. The CTA^+ formed a bilayer arrangement within the layers of the bentonite layers and thus make them hydrophobic in nature. This makes the organoclays thermally stabile as reflected in the TGA scans until a temperature of about 233 ^oC, where inflection corresponds to the boiling point the surfactants. The layered structure of the synthesized materials were determined by the SEM technique. SEM images show that modification with surfactant reduces the clay particles size and aggregation. The combination of this techniques are therefore excellent for the structural and microstructural elucidation of organoclays which are complex compounds.

The potential of the modified clays to sorb crude oil from crude oil polluted was also investigated. As expected, the organoclays, unlike the raw bentonite nanoclays, were able to sorb crude oil up to five times their weight. Adsorption behaviour of the crude oil–organoclay systems was described well by Langmuir isotherm model and the Pseudo-second-order rate model. Langmuir maximum adsorption capacities of samples 2, 5 and 15 on crude oils had were quite high. The Pseudo-second-order rate model suggested that the mechanism of removal was rapid and by chemisorption. The rapid rate of adsorption process makes these materials a suitable candidate for absorption of organic materials from water.

6.2 Conclusion

From this study, it can be concluded that the Nigeria's natural bentonites deposits possess valuable resources that can be used as precursor materials to synthesize potential sorbents for

treating organic pollution in aqeous waste environment. The intercalated CTA^+ affects the physicochemical, microstructural, thermal and morphological properties of the synthesized materials. The degree of interaction between CTA^+ and the bentonite particles depends on the, reaction time, temperature and CTA^+ concentration in the suspension. The organoclays produce can sorb up to 7.5 % its weight of crude oil. The results obtained show that the organoclays developed are cost-effective, eco-friendly, and have the potential for numerous application in environmental remediation. The knowledge obtained from this research presents useful resources for control of the nanohybrid synthesis and performance and contributes to the development of other nano-structured (and polymerizable) sorbents.

6.3 Recommendations

Based on the results and the conclusions reached in this study, the following recommendations are therefore offered for further research and application.

1 The synthesized organoclay can be applied in drinking water treatment technology. More research geared into the drinking water treatment technology using organoclays should be promoted to explore the full potentials of our natural clay resources.

2 It is also recommended that organoclays be produced and kept readily available for oil spill contingy.

3 The results of the organically modified clays indicate the potential of these materials in the preparation of polymer nanocomposites and the possibility of removal of other emulsifiable and non-emulsifiable organic pollutants liquids. Research into the removal of other toxic pollutants from pesticides, organochlorines and poisonous gasses from towers.

REFERENCES

Aboul-Gheit, A-K., Khalil, F. H. and Abbdul-Moghny, T. (2006). Adsorption of spilled oil from sea water by waste plastic. *Oil and Gas Technology Rev- IFP*, 61(2), 259-268.

Adebajo, M. O. and Frost, R. L. (2004). Infrared and 13C-MAS Nuclear Magnetic Resonance Spectroscopic study of acetylation of cotton. *Spectrochimica Acta, Part A: Molecular and Biomolecular Spectroscopy*, 60(1-2), 449-453.

Adebajo, M. O., Frost, R. L., Kloprogge, J. T., Carmody, O. and Kokot, S. (2003). Porous Materials for Oil Spill Cleanup : A Review of Synthesis and Absorbing Properties. *Journal of Porous Materials*, 10(3), 159–170.

Adebiyi, F. M. and Adeyemi, A. F. (2010). Characterisation of the petroleum hydrocarbons-contaminated soils around a petroleum products depot. *Chemistry and Ecology*, 26(2), 137-146.

Adelana, S. O, Adeosun, T. A, Adesina, A. O. and Ojuroye, M. O. (2011). Environmental pollution and remediation: challenges and management of oil Spillage in the Nigerian coastal areas. *American Journal of Scientific and Industrial Research*. 2(6), 834-845.

Adeyi, A. A., Popoola, L. T., Yusuff, A. S. and Grema, A. S. (2014). Kinetics Analysis and Dosage Effects of Manganese Dioxide Adsorbent on Desulphurization of Crude Oil. *Journal of Bioprocessing and Chemical Engineering*, 2(1), 1–6. Retrieved from http://scienceq. org/Journals/JBCE.php

Agency for Toxic Substances and Disease Registry (ATSDR) (2006). *Draft Toxicological Profile for Cresols*. http://www. atsdr. cdc. gov/toxprofiles/tp34. pdf.

Agency for Toxic Substances and Diseases Registry (ATSDR) (2008-a). *Toxicological Profile for Toluene Update*. Atlanta GA. US department of health and human service, public health service.

Agency for Toxic Substances and Diseases Registry (ATSDR) (2008-b). *Toxicological Profile for Cresols.* Atlanta GA. US department of health and human services, public health service.

Ahmadi, S. J., Yudong, H. and Li, W. (2004). Synthesis of EPDM / Organoclay Nanocomposites : Effect of the Clay Exfoliation on Structure and Physical Properties. *Iranian Polymer Journal*, 13(5), 415–422.

Ahmed, A. S., Salahudeen, N., Ajinomoh, C. S., Hamza, H. and Ohikere, A. (2012). Studies on the Mineral and Chemical Characteristics of Pindiga Bentonitic Clay. *Petroleum Technology Development Journal*, 1, 1–8.

Akhlaq, M. S., Götze, P., Kessel, D. and Dornow, W. (1997). Adsorption of crude oil colloids on glass plates: measurements of contact angles and the factors influencing glass

surface properties. *Colloids and Surfaces A: Physicochemical and Engineering Aspects*, 126(1), 25-32.

Akonye, L. A. and Onwudiwe, I. O. (2004). Potential for the use of sawdust and leaves of *Chromolaena odorata* in the mitigation of crude oil toxicity. *Niger Delta Biologia*, 4(2), 50-60.

Akyüz, S. and Akyüz, T. (2003). FT-IR spectroscopic investigations of surface and intercalated 2-aminopyrimidine adsorbed on sepiolite and montmorillonite from Anatolia. *Journal of Molecular Structure*, 651–653, 205–210.

Akçay G. And Yurdakoç M. K (1999). Nonyl-and Dodecylamines Intercalated Bentonite and Illite From Turkey. *Turkish Journal of Chemistry*, 23, 105-113.

Albert, P. H. (1995). *Petroleum and Individual Polycyclic Aromatic Hydrocarbons*. In Handbook of Ecotoxicology; Hoffman, D. J., Rattner, B. A., Burton, G. A., Jr., Cairons, J., Jr., Eds. ; CRC Press: Boca Raton, FL, pp. 330–355.

Alemdar, A., Güngör, N., Ece, O. I. and Atici, O. (2005). The rheological properties and characterization of bentonite dispersions in the presence of non-ionic polymer PEG. *Journal of Materials Science*, 40(1), 171-177.

Alther, G. R. (2001). How to remove emulsified oil from wastewater with organoclays, *Water Engineering and Management*, 148(7), 27-29.

Al Malek, S. A., and Mohamed, A. M. O. (2005). Environmental impact assessment of off shore oil spill on desalination plant. *Desalination*, 185(1), 9-30.

Amensty International. (2013). Bad Information: Oil Spill Investigations in the Niger Delta. London, United Kingdom: Amnesty International Publications. Retrieved from www. amnesty. org/en/library/asset/AFR44/. . . /afr440282013en. pdf

Amer, A. A., El-Maghrahy, A., Malash, G. F., and Nahla, T. A. (2007). Extensive characterization of raw barley straw and study of the effect of steam pretreatment. *Applied Science Resources*, 3(1), 1336–1342.

American Standards for Testing and Materials (ASTM) (1994). Standard Test Method For Direct Moisture Content of Wood and Wood Based Materials: D4442-84. *ASTM*, 04-09: 514-518.

Ametov, I. M., Karakchiev, E. I. and Bench, A. R. (1998). Influence of adsorption of silica-gel/asphaltene fraction on heavy oil displacement factor. *Neftyanoe Khozyaistvo*, (6), 29-30.

Anderson, C. M. and LaBelle, R. P. (2000). Update of comparative occurrence rates for offshore oil spills. *Spill Science and Technology Bulletin*, 6(5/6), 303-321.

Annunciado, T. R., Sydenstricker, T. H. D. and Amico, S. C. (2005). Experimental investigation of various vegetable fibers as sorbents materials for oil spills. *Marine Pollution Bulletin*, 50(11), 1340-1346.

Anonymous (2008). Article: NOSDRA Detects 1150 Oil Spill Sites. *Newspaper This Day*, Jan. 25.

Apinon, N., Supachai, S., Suparerk, A. and Jantrawan, P. (2008). The Effect of Surfactant Concentration on the Interlayer Structure of Organoclay. *Chiang Mai Journal of. Science*, 35(1), 199-205. www.science.cmu.ac.th/journal-science/josci.htcm[3]

Araújo, S. S., Andrade, D. L. A. C. S., Carvalho, L. H., Gomes, A. S. and Silva, S. M. L. (2005). Quais são os efeitos da velocidade de processamento sobre as propriedades mecânicas de formulações PP/bentonita. *Plástico Industrial*, pp. 104–116.

Arivoli, S., Nandhakumar, V., Saravanan, S. and Sulochana, N. (2009). Sorption Dynamics of Copper ion by Low Cost Activated Carbon, *The Arabian Journal of Science and Engineering*, 34, 1-12.

Arroyo, M., Lopez-Manchado, M. A. and Herrero, B. (2003). Organo-montmorillonite as substitute of carbon black in natural rubber compounds. *Polymer*, 44, 2447-2453. DOI: 10. 1016/S0032-3861(03)00090-9.

Asakawa, T. and Ogino, K. (1986). Removal of trace organic compounds from multicomponent liquid mixtures. I. Adsorption of surfactant mixtures on activated carbon. *Colloid and Polymer Science*, 264(12), 1085–1089. doi:10. 1007/BF01410327.

Atkins, P. (1999). *Physical chemistry* (6th ed.). London: Oxford University press. pp. 857–864

Aurell, J. and Gullett, B. K. (2010). Aerostat sampling of PCDD/PCDF emissions from the Gulf oil spill in situ burns. *Environmental Science and Technology*, 44(24), 9431-9437.

Aynechi, N. (2004). *Oil Spill Response*, http://www. darwin. bio. uci. edu/- sustain/global. htcm (30 June 2004).

Ayotamuno, M. J., Kogbara, R. B., Ogaji, S. O. T. and Probert, S. D. (2006). Bioremediation of a crude-oil polluted agricultural-soil at Port Harcourt, Nigeria. *Applied Energy*, 83(11), 1249-1257.

Babel, S., and Kurniawan, T. A. (2003). Low-cost adsorbents for heavy metals uptake from contaminated water: a review. *Journal of hazardous materials*, 97(1), 219-243.

Badejo, O. T. and Nwilo, P. C. (2004). *Management of Oil Spill Dispersal along the Nigerian Coastal Areas*. Unpublished paper, 1-13.

Baek, K.-H., Kim, H.-S., Oh, H.-M., Yoon, B.-D., Kim, J. and Lee, I.-S. (2004). Effects of Crude Oil, Oil Components. and Bioremediation on Plant Growth. Journal of Environmental Science and Health, *Part A- Toxic/Hazardous Substances and Environmental Engineering*, 39(9), 2465–2472. doi:10. 1081/LESA-200026309.

Balternas, P. and Vaisis, V. (2005). Experimental investigation of thermal modification influence on sorption qualities of biosorbents, *Environmental. Engineering and. Landscape Management*, 13(1), 3-8.

Banat, F. A., Al-Bashir, B., Al-Asheh, S. and Hayajneh, O. (2000). Adsorption of phenol by bentonite. *Environmental Pollution*, 107(3), 391-398.

Banerjee, S. S., Joshi, M. V. and Jayaram, R. V. (2006). Treatment of oil spill by sorption technique using fatty acid grafted sawdust. *Chemosphere*, 64(6), 1026-1031.

Bartelt-Hunt, S. L., Burns, S. E. and Smith, J. A. (2003). Nonionic organic solute sorption onto two organobentonites as a function of organic-carbon content. *Journal of. Colloid Interface Science*, 266, 251–258.

Batra, M., Gotam, S., Dadarwal, P., Nainwani, R. and Sharma, M. (2011). Nano-Clay as Polymer Porosity Reducer : A Review. *Journal of Pharmaceutical Science and Technology*, 3(10), 709–716. Retrieved from http://www.onlinepharmacytech. info/docs/vol3issue10/JPST11-03-10-01.pdf

Batra, M., Gotam, S., Dadarwal, P., Nainwani, R. and Sharma, M. (2011). Nano-Clay as Polymer Porosity Reducer: A Review. *Journal of Pharmaceutical Science and Technology*, 3(10), 709–716.

Bayat, A., Aghamiri, S. F., Moheb, A. and Vakili-Nezhaad, G. R. (2005). Oil spill cleanup from seawater by sorbent materials. *Journal of Chemical Engineering and Technology*, 28, 1525-1528.

Bayer, I. S., Brown, A., Steele, A. and Loth, E. (2009). Transforming anaerobic adhesives into highly durable and abrasion resistant superhydrophobic organoclay nanocomposite films: a new hybrid spray adhesive for tough superhydrophobicity. *Applied Physics Express*, 2(12), 125003.

Bayer, I. S., Steele, A. and Loth, E. (2013). Superhydrophobic and electroconductive carbon nanotube-fluorinated acrylic copolymer nanocomposites from emulsions. *Chemical Engineering Journal*, 221, 522-530.

Beall, G. W. and Goss, M. (2004). Self-assembly of organic molecules on montmorillonite. *Applied Clay Science*, 27, 179–186.

Bodîrlău, R. and Teacă, C. A. (2009). Fourier Transform Infrared Spectroscopy and thermal analysis of lignocellulose fillers treated with organic anhydrides. *Romanian Journal of Physics*, Bucharest, 54(1-2), Pp 93-104.

Bokobza, L. (2004). Elastomeric composites:Silicone composites. *Journal of Applied Polymer Science*, 93(5), 2095-2104.

Brezovska, S. S., Marina, B., Panova, B., Burevski, D., Bosevska, V. and Stojanovska, L. (2004). The adsorption characteristics and porous structure of bentonite adsorbents, determined from the adsorption isotherms of benzene vapor. *Journal of the Serbian Chemical Society*, 69(2), 145-151.

Brixie, J. M. and Boyd, S. A., (1994). Treatment of contaminated soils with organoclays to reduce leachable pentachlorophenol. *Journal of Environmental. Quality,* 23, 1283–1290.

Broje, V. and Keller, A. A. (2006). Improved mechanical oil spill recovery using an optimized geometry for the skimmer surface. *Environmental science and technology*, 40(24), 7914-7918.

Buist, I., McCourt, J., Potter, S., Ross, S. and Trudel, K. (1999). In situ burning. *Pure Applied Chemistry,* 71(1), 43-65.

Bukowski, J. A. (2001). Review of the epidemiological evidence relating toluene to reproductive outcomes. *Regulatory Toxicology and pharmacology*. 33, 147-156.

Burgeir, J., Tseng, F., Jessup, D. and Clapp, R. (2002). *Oil: A Life Cycle Analysis of Its Health and Environmental Impacts*, the Center for Health and the Global Environment.

Burns, K. A., Codi, S., Pratt, C., Swannell, R. J. P. and Duke, N. C. (1999). Assessing the oil degrading potential of endogenous micro-organisms in tropical marine wetlands. *Mangroves and Salt Marshes,* 3, 67-83.

Cardoso, M. A. F., Ferreira, H. S., da Silva, I. A., Ferreira, H. C. and Neves, G. A. (2012). *Development of Organoclays for Use in Oil-Based Drilling Fluids*. In: Materials Science Forum, Vol. 727, pp. 1557-1562.

Carlson, L. (2004). *Bentonite Mineralogy*. Part 1: working report 2004, POSIVA, Finland. Pp 10-33.

Carmody, O., Frost, R., Xi, Y. and Serge, K. (2007). Surface characterisation of selected sorbent materials for common hydrocarbon fuels. *Surface Science,* 601, 2066–2076.

Cavalcanti, J. V. F. L., Abreu, C. A. M., Carvalho, M. N., Sobrinho, M. A. M., Benachour, M. and Baraúna, O. S. (2012). Removal of Effluent from Petrochemical Wastewater by Adsorption Using Organoclay. In D. V. Patel (Ed.), *Petrochemicals*, pp. 277–295. Rijeka: InTech. Retrieved from www. intechopen.com

Celis, R., Hermosin, M. C. and Cornejo, J. (2000). Heavy metal adsorption by functionalized clays. *Environmental Science and Technology*, 34(21), 4593-4599.

Chang, J. H., An, Y. U., Cho, D., and Giannelis, E. P. (2003). Poly (lactic acid) nanocomposites: comparison of their properties with montmorillonite and synthetic mica (II). *Polymer*, 44(13), 3715-3720.

Chapman, H., Purnell, K., Law, R. J. and Kirby, M. F. (2007). The use of chemical dispersants to combat oil spills at sea: A review of practice and research needs in Europe. *Marine Pollution Bulletin*, 54(7), 827-838.

Chen, B.,Zhu, L.,Zhu, J. and Xing, B. (2005). Configurations of the bentonite-sorbed myristylpyridinium cation and their influences on the uptake of organic compounds. *Environmental Science and Technology*, 39, 6093-6100.

Cheskis, H. P., Tungatt, P. D. and Tyler, D. E. (1991). *Technique for forming silicon carbide coated porous filters.*U. S. Patent No. 4,983,219. Washington, DC: U. S. Patent and Trademark Office.

Choi, H. and Cloud, R. M. (1992). Natural sorbent in oil spill cleanup. *Environmental Science and Technology*, 26 (4), 772-776.

Choi, H. M. (1996). Needle punched cotton nonwovens and other natural fibers as oil cleanup sorbents. *Environ. Sci. Health*, 31(6), 1441–1457.

Choi, H. M. and Moreau, J. P. (1993). Oil sorption behavior of various sorbents studied by sorption capacity measurement and environmental scanning electron microscopy. *J. Microscop. Research Tech.*, 25(5-6), 447-455.

Christodoulou, N. C. (2002). *Porous and Magnetic Inorganic Based Composite Materials Used as a Sorbent for Cleaning Water and the Environment from Oil Spill*, International patent: PCT/CY00/00003.

Chung, and Venosa, A. D. (2008). Effect of sand particle size, oil contamination and water table level on the effectiveness of sorbents in wicking oil from contaminated wetland. *2008 Intl Oil Spill Conference*, Ohio, 537-540.

Chung, S., Gandee, J., Suidan, M. T., and Venosa, A. D. (2008, May). Effect of sand particle size, oil contamination, and water table level on the effectiveness of sorbents in wicking oil from contaminated wetland. In International Oil Spill Conference (Vol. 2008, No. 1, pp. 537-539). American Petroleum Institute.

Connan, J., Lacrampe-Couloume, G. and Magot, M. (1997). Anaerobic biodegradation in reservoirs: A widespread phenomenon in nature. *8th international meeting on organic geochemistry*, September 22-26, Maastricht, The Netherlands, pp. 5-6.

Coxeter, R. (1994). Hope for oil spills is a thing with feathers. *Business Week*, 76. http://www.businessweek.com/archives/1994/b338184.arc.htm?campaign_id=search.

Dabrowski, A. (2001). Adsorption—from theory to practice, *Advances in Colloid Interface and Science*, 93. 135–224.

Daughney, C. J. (2000). Sorption of crude oil from a non-aqueous phase onto silica: the influence of aqueous pH and wetting sequence. *Organic Geochemistry*, 31(2), 147-158.

Dawodu, F. A., Akpomie, G. K. and Ogbu, I. C. (2012), Isotherm modeling on the equilibrium sorption of Cadmium (II) from solution by Agbani clay.*International Journal Of Multidisciplinary Sciences And Engineering*, 3(9), 9-14.

Dechamps, G., Carvel, H., Bonedom, M., Bonnin, C. and Vigroles, C. (2003). Oil removal from water by selective sorption on hydrophobic cotton fibers: study of sorption properties and comparism with cotton fiber-based sorbents. *Environmental Science Technology*, 37(5), 1013-1015.

Delaune, R. D., Lindau, C. W. and Jugsujinda, A. (1999). Effectiveness of "Nochar" solidifier polymer in removing oil from open water in coastal wetlands. *Spill Science and Technology Bulletin*, 5(5-6), 357-359.

Demirbas, E., Kobya, M. and Sulak, M. T. (2008). Adsorption kinetics of a basic dye from aqueous solutions onto apricot stone activated carbon, *Bioresource Technology*, 99, 5368.

De Paiva, L. B., Morales A. R. and Díaz, F. R. V. (2008). Organoclays: Properties, preparation and applications. *Applied Clay Science*, 42, 8–24.

Divakar, D., Manikandan, D., Kalidoss, G. and Sivakumar, T. (2008). Hydrogenation of benzaldehyde over palladium intercalated bentonite catalysts: Kinetic studies. *Catalysis letters*, 125(3-4), 277-282.

Diya'uddeen, B. H., Mohammed, I. A., Ahmed, A. S. and Jibril, B. T. (2008). Production of activated carbon and its utilization in crude oil spillage cleanup. *Agricultural Engineering International: the Cigr Ejournal*, 1-9.

Dolz, M., Jiménez, J., Hernández, M. J., Delegido, J. and Casanovas, A. (2007). Flow and thixotropy of non-contaminating oil drilling fluids formulated with bentonite and sodium carboxymethyl cellulose. *Journal of Petroleum Science and Engineering*, 57(3), 294-302.

Dubinin, M. M., Zaverina E. D. and Radushkevich L. V. (1947). Sorption and structure of active carbons, *Journal of Physical. Chemistry*, 21, 1351-1362.

Duke, N. C., Burns, K. A., Swanell, R. P. J, Dalhause, O. and Ropp, R. J. (2000). Dispersant used and a bioremediation strategy as alternate means of reducing impacts of large oil spills on mangroves: The Gladstone field trials. *Marine Pollution Bulletin*, 41(7-12), 403-412.

Duong, H. T., and Burford, R. P. (2006). Effect of foam density, oil viscosity, and temperature on oil sorption behavior of polyurethane. *Journal of Applied Polymer Science*, 99(1), 360-367.

Egbon, E. E., Asia, I. O., Ebhoaye, J. E., Ize-Iyamu, O. K., Okojie, V. U., Egbon, I. E. and Idode, V. O. (2013). Pharmaceutical Industry Wastewater Treatment Using Organic Surfactant Modified Clay. *Civil and Environmental Research*, 3(13), 173-178.

Eman, A. E. (2013). Modified activated carbon and bentonite used to sorbcrude oils emulsified in aqueous solution. *American Journal of Environmental Protection*, 2(6), 161-169. doi: 10. 11648/j. ajep. 20130206. 17

Erhan, D., Kobya, M., Ehf, S. and Ozkan, T. (2004). Adsorption kinetics for Cr (VI) removal from aqueous solution on activated carbon prepared from Agro wastes. *Journal of. water*, 30(4), 533-541.

European Commission (2002). Polyaromatic hydrocarbons-occurrence in food. *Dietary Exposure and Health Effects*, Scientific Committee on Food. 4 December.

Eyong, E. U., Umoh, B., Ebong, P. E., Eteng, M. U., Antai, A. B. and Akpa, A. O. (2004). Haematoxic effects following ingestion of Nigerian crude oil and crude oil polluted shellfish by rats. *Nigerian Journal of Physiological Sciences*, 19(1-2), 1-6.

Fingas, M. and Charles, J. (2001). *Basics of Oil Spill Clean Up*, Second Edition, CRC Press.

Foo, K. Y. and Hameed, B. H. (2010). Insights into the modeling of adsorption isotherm systems, *Chemical Engineering Journal.* 156, 2–10.

French, J.E., Lacks, G.D., Trempus, C., Dunnick, J.K., Foley, J., Mahler, J., Tice, R.R. and Tennant, R.W. (2001). Loss of heterozygosity frequency at trp 53 locus in p53 deficient (+/-) mouse tumors in carcinogens and tissue deficiency. Carcinogenesis, 22910: 99-106.

Freundlich, M. F. (1906). Uber die adsorption in losungen. *Zeitschrift fur Physikalische Chemie*, 57(A), 385–470.

Friends of the Earth Netherlands (FEN) (2009). Oil Spills in the Niger Delta in Nigeria. *Milieu Defensie, 1-2.*

Frost, R., Cannody, D., Yunfei, X. and Kokot, S. (2007). Adsorption of hydrocarbons on organo-clays - implications for oil spill remediation. *Journal of Colloid and Interface Science*, 305(1), 17-24.

Frost, R., He, H., Kloprogge, T., Bostrom, T., Duong, L.,Yuan, P., Xi, Y. and Yang, D. (2006). Changes in the morphology of organoclays with HDTMA+ surfactant loading. *Applied Clay Science*, 31(3-4), 262-271.

García del Cid, M. A., Prolongo, M. G., Salom, C., Sánchez-Cabezudo, M. and Masegosa, R. M. (2014). Influence of Different Organoclays on the Curing, Morphology. and Dynamic Mechanical Properties of an Epoxy Adhesive. *The Journal of Adhesion*, 90(10), 817-834.

Ghalambor, A. (1995). Evaluation and characterization of sorbents in removal of oil spills. *Louisiana Applied Oil Spill Research and Development Program OSRADP Technical Report Series*, Louisiana Oil Spill Coordinators Office,Baton Rouge- Louisiana, 95-006.

Ghiaci, M., Aghabarari, B. and Gil, A. (2011). Production of biodiesel by esterification of natural fatty acids over modified organoclay catalysts. *Fuel*, 90(11), 3382-3389.

Gieg, L. M. and Suflita, J. M. (2005). Metabolic indicators of anaerobic hydrocarbon biodegradation in petroleum-laden environments. *In: Oliver B. and Magot M. (eds.), Petroleum Microbiology*, Washington, DC: ASM Press, 277-300.

Gonzaga, A. C., Sousa, B. V., Santana, L. N. L., Neves, G. A. and Rodrigues, M. G. F. (2007). Study of the different methods in the preparation of Organoclays from the Bentonite with application in the petroleum Industry. *Brazilian Journal of Petroleum and Gas*, 1(1), 16–25.

Gonzaga, A. C., Sousa, B. V., Santana, L. N. L., Neves, G. A. and Rodrigues, M. G. F. (2007). Study of the different methods in the preparation of Organoclays from the Bentonite with application in the petroleum Industry. *Brazilian Journal of Petroleum and Gas*, 1(1), 16–25.

Gorassi, G., Tortora, M., Vittoria, V., Kaempfer, D. and Mülhaupt, R. (2003). Transport properties of organic vapor in nanocomposites of organophilic layered silicate and syndiotactic polypropylene. *Polymer*, 44, 3679–3685.

Greene, G., Mackary, D. and Overall, J. (1975). Cleanup after territorial oil spills in arctic. *Short Papers*, 140-142.

Hackett, E., Manias, E. and Giannelis, E. P., (1998). Molecular dynamics simulations of organically modified silicates. *Journal of Chemical Physics*, 108, 7410–7415.

Hackman, I. and Hollaway, L. (2006). Epoxy-layered silicate nanocomposites in civil engineering. *Composites Part A Applied Science and Manufacturing*, 37, 1161–1170.

Haraguchi, K., Takehisa, T. and Ebato, M., 2006. Control of cell cultivation and cell sheet detachment on the surface of polymer/clay nanocomposite hydrogels. *Biomacromolecules*, 7, 3267–3275.

He, H., Frost, R. L. and Zhu, J. (2004). Infrared study of HDTMA+ intercalated montmorillonite. Spectrochimica Acta. *Part A, Molecular and Biomolecular Spectroscopy*, 60(12), 2853–9. doi:10. 1016/j. saa. 2003. 09. 028

Head, I. M., Jones, D. M. and Larter, S. R. (2003). Biological activity in the deep subsurface and the origin of heavy oil. *Nature,* 2003, 426, 344-352.

Heinz, H., Vaia R. A., Krishnamoorti R. and Farmer B. L. (2007). Self-assembly of alkylammonium chains on montmorillonite: effect of chain length, head group structure and cation exchange capacity. *Chemistry of Materials,* 19, 59-68.

Hitzman, D. O. and Okia, B. (1968). Method of removing oil from polluted water using expanded vermiculite. *US Patent, No. 3414511*.

Ho, Y. S. and McKay, G. (1998). A Comparison of Chemisorption Kinetic Models Applied to Pollutant Removal on Various Sorbents. *Trans IChemE*, 76B, 332-340.

Ho, Y. S., Wase, D. A. J. and Forster, C. F. (1995). *Water Research*, 29, 5, 1327-1332.

Hoidy, W. H., Mansor, B. A., Emad, A. J. A. M. and Nor, A. B. I. (2009). Synthesis and Characterization of Organoclay from Sodium Montmorillonite and Fatty Hydroxamic *Acids American Journal of Applied Sciences*, 6 (8), 1567-1572.

Hosterman, J. W. and Patterson, S. H. (1992). Bentonite and Fuller's earth resources of the United States. *U. S. Geological Survey Professional Paper 1522*. United States Government Printing Office, Washington D. C., USA.

Huassard, M., Gaballah, I., Kanari, N., De Donato, P., Barrés, O. and Villieras, F. (2003). Separation of hydrocarbons and lipid from water using treated bark. *Water Resources*, 37(2), 362–374.

Hulla, L.E., French, J.E. and Dunnick, J.K. (2001). Chromosome 11 allotropes reflect a mechanism of chemical carcinogenesis in heterozygous p-53 deficient mice. Carcinogenesis, 22910: 69-98.

Hussein, M., Amer, A. A., El-Maghraby, A. and Taha, N. A. (2009). Availability of barley straw: application on oil spill cleanup. *International Journal Environmental Science and Technology,* 6(1), 123-130.

Hussein, M., Amer, A. A. and Sawsan, I. I. (2008). Oil spill sorption using carbonized pith bagasse: trial for practical application. *International Journal of Environmental Science and Technology*, 5(2), 233-242.

Iborra, C. V., Cultrone, G., Cerezo, P., Aguzzi, C., Baschini, M. T., Vallés, J. and López-Galindo, A. (2006). Characterisation of northern Patagonian bentonites for pharmaceutical uses. *Applied clay science*, 31(3), 272-281.

Igwe, J. C. and Abia, A. A. (2007). Adsorption isotherm studies of Cd (II), Pb (II) and Zn (II) ions bioremediation from aqueous solution using unmodified and EDTA-modified maize cob. Ecl. Quím.,*São Paulo*, 32(1), 33–42.

Ike, I. A., and Leo, M. (2013). The Changing Face of Global Oil and Gas Production and Its Implication on Nigeria. In SPE Nigeria Annual International Conference and Exhibition. Society of Petroleum Engineers.

International Annual Report on Carcinogens (IARC) (2005). Benzene. *Substance Profile Report on Carcinogens,* CAS: NO 71-43-2.

International petroleum Industry Environmental conservation Association (IPIECA) (2001). *Dispersants and their role in oil spill response*.

International Tankers Owners pollution Federation limited (ITOPF) (2004). *Containment and recovery of floating oil*, http://www. itopf. com/containment. htcm^3. 12 November 2008.

Itodo, A. U. and Itodo, H. U. (2010). Sorption Energies Estimation Using Dubinin-Radushkevich and TemkinSorption Isotherms. *Life Science Journal,* Volume 7, Issue 4, 31-39.

Itodo, A. U., Abdulrahman, F. W., Hassan, L. G., Maigandi, S. A. and Itodo, H. U. (2010). Intraparticle Diffusion and Intraparticulate Diffusivities of Herbicide on Derived Activated Carbon. *Researcher*, 2(2), 74-86.

Itodo, A. U., Happiness, U. O., Obaroh, I. O., Usman, A. and Audu, S. S. (2009). Temkin, R-D, Langmuir and Freundlich sorption Isotherms of industrial dye uptake unto H3PO4 catalyzed poultry waste biosorbent. *Journal of Science and Technology research*; 8(1),52-56.

Jaber, M., Miéhé-Brendlé, J., Delmotte, L. and Dred, R. L. (2005). Formation of organoclays by one step synthesis. *Solid States Sciences*, 7, 610-615.

Jagger, H. (1970). The growth of petroleum production and movement. *Water pollution by oil*.

Jaynes, W. F. and Boyd, S. A. (1991) Clay mineral type and organic compound sorption by hexadecyl trimethylammonium exchanged clays, *Journal of Soil Science Society of America*, 55(1), 43-48.

Jensen, H. V. and Mullin, J. V. (2003). MORICE—new technology for mechanical oil recovery in ice infested waters. *Marine pollution bulletin*, 47(9), 453-469.

Jeong, H. M., Kim, D. H., Jung, J. S., Kim, T. K., Kim, B. K., Kim, Y. S. and Hwang, J. M. (2007). The effect of organoclay on the properties of a reactive hot melt polyurethane adhesive. *Composite Interfaces*, 14(5-6), 467-476.

Johnson, R. F., Manjreker, T. G. and Halligan, J. E. (1973). Removal of oil from water surfaces by sorption on unstructured fibers. *Environmental science and technology*, 7(5), 439-443.

Kakegawa, N. and Ogawa, M. (2002). The intercalation of b-carotene into organophilic interlayer space of dialkyldimethylammonium-montmorillonites. *Applied Clay Science*, 22, 137–144.

Kanaly, R. A. and Harayama, S. (2000). Biodegradation of high-molecular-weight polycyclic aromatic hydrocarbons by bacteria. *Journal of Bacteriology*, 182, 2059-2067.

Kanoh, T., Fukuda, M., Itayemi, E., Kinouchi, T., Nishifiyi, K. and Ohnishi, Y. (1990). Nitro-reaction in mice injected with pyrene during exposure to Nitogen dioxide. *Mutat Resources*, 275, 1-4.

Khan, H. A. (2007). Short Review: Benzene's toxicity: a consolidated short review of human and animal studies. *Human and experimental toxicology*, 26(9), 677-685.

Kim, S.K. (2012). Advanced clay nanocomposites based on in situ photopolymerization utilizing novel polymerizable organoclays. PhD dissertation, University of Iowa. Pp. 75.

Kingston, P. F. (2002). Long-term environmental impact of oil spills. *Spill Science and Technology Bulletin*, 7(1-2), 53-61.

Kirk, R. E. and Othmer, D. F. (2004). *Alkylphenols. Encyclopaedia of chemical engineering*. 5th 2: John Wiley and Sons; New York, pp. 203–233.

Klapyta, Z., Fujita, T. and Iyi, N. (2001). Adsorption of dodecyl- and octadecyltrimethylam-monium ions on a smectite and synthetic micas. *Applied Clay Science*, 19, 5–10.

Klapyta, Z., Gawel, A., Fujita, T. and Iyi, N. (2003). Structural heterogeneity of alkylammonium-exchanged, synthetic fluorotetrasilisic mica. *Clay Minereals*, 38, 151–160.

Kundu, S. and Gupta, A. K. (2006). Arsenic sorption onto iron oxide-coated cement: regression analysis of equilibrium data with several isotherm models and there optimization. *Chemical Engineering Journal*, 122(1-2), 93-106.

Lagaly, G. (1995). Surface and interlayer reactions: bentonites as adsorbents. pp. 137–144. *In:* Churchman, G. J., Fitzpatrick, R. W. and Eggleton R. A. *Clays Controlling the Environment. Proceedings of the 10th International Clay Conference*, Adelaide, Australia. CSIRO Publishing, Melbourne, ISBN 0-643-05536-3

Lane, P. (Ed.). (1995). *The use of chemicals in oil spill response (No. 1252).* Astm International. Pp. 228-229.

Langmuir, I. (1918). The sorption of gases on plane surfaces of glass, mica and platinum", *Journal of the Amerian Chemical Society,* 40(9), 1361-1403.

Lapides, I., Yariv, S. and Golodnitsky, D. (2002). Simultaneous DTG-TG study of montmorillonite mechanochemically treated with crystal-violet. *Jounal of Thermal Analysis*, 67, 99-112.

Lee, B., Hans, J. S. and Rowell, R. M. (1999). Oil sorption by lignocellulosic fibers. *In*: *Kenaf Properties, Processing and Product*, Mississippi State University- Ag and Bio Engineering, Pp. 432-533.

Li, J. and Werth, C. J. (2002). Modeling sorption isotherms of volatile organic chemical mixtures in model and natural solids. *Environmental Toxicology and Chemistry/ SETAC*, 21(7), 1377–83. Retrieved from http://www. ncbi. nlm. nih. gov/pubmed/12109736

Liu, P. and Zhang, L. (2007). Adsorption of dyes from aqueous solutions or suspensions with clay nano-adsorbents. *Separation and Purification Technology*, 58(1), 32–39. doi:10. 1016/j. seppur. 2007. 07. 007.

López-Galindo, A., Viseras, C. and Cerezo, P. (2007). Compositional, technical and safety specifications of clays to be used as pharmaceutical and cosmetic products. *Applied Clay Science*, 36(1), 51-63.

Madejova, J. (2003). FTIR techniques in clay mineral studies. Vibrational Spectroscopy, 31, 1–10.

Magaraphan, R. and Lilayuthalert, W. (2001). Preparation, structure, properties and thermal behavior of rigid-rod polyimide/MMT nanocomposites. *Composite Science and Technology*, 61, 1253-1264.

Mallakpour, S. and Dinari, M. (2011). Preparation and characterization of new organoclays using natural amino acids and Cloisite Na+. *Applied Clay Science*, 51, 353-359.

Mallakpour, S., Dinari, M. and Behranvand, V. (2013). Ultrasonic-assisted synthesis and characterization of layered double hydroxides intercalated with bioactive N, N′-(pyromellitoyl)-bis-l-α-amino acids. *RSC Advances*, 3(45), 23303. doi:10. 1039/c3ra43645d

Manocha, S., Patel N. and Manoch, L. M. (2008). Development and characterization of nano clay from Indian clays. *Defense Science Journal.* 58(4); 517-524.

Masooleh, M. S., Saeed, B., Morteza, T. and Ali, N. (2010). Adsorption of petroleum hydrocarbons on organoclay. *Journal of Applied Chemical Researches*. 4(14), 19-23.

Mehta, G. K., Mark, J., Lee, J. W., Kotov, N., Linderman, J. J. and Takayama, S., 2007. Polyelectrolyte-clay-protein layer films on microfluidic pdms bioreactor surfaces for primary murine bone marrow culture. *Advanced Functional Materials*, 17, 2701–2709.

Merriman, R. J., Highley, D. E. and Camero, D. G. (2003). Definition and characteristics of very-fine grained sedimentary rocks: clay, mudstone, shale and slate. Keyworth, Nottingham: British Geological Survey Commisioned Report. Retrieved from www. bgs. ac. uk/downloads/start. cfm?id=1415

Mobbs, P. (1996). *The Sea Empress Spill: the Potential for Human Health Effects*, Mobbs Environmental Investigations, Cymro, pp. 1-13.

Mortland, M. M., Shaobai, S., and Boyd, S. A. (1986). Clay-organic complexes as adsorbents for phenol and chlorophenols. Clays and Clay Minerals, 34(5), 581-585.

Moyo, F., Tandlich, R., Wilhelmi, B. S. and Balaz, S. (2014). Sorption of hydrophobic organic compounds on natural sorbents and organoclays from aqueous and non-aqueous solutions: a mini-review. *International Journal of Environmental Research and Public Health*, 11(5), 5020–48. doi:10. 3390/ijerph110505020

Muhammad, I. M., El-Nafaty, U. A, Abdulsalam S. and Makarfi, Y. I. (2012). Removal of Oil from Oil Produced Water Using Eggshell, *Civil and Environmental Research*, 2(8), 52-63.

Mullin, J V. and Champ, M A., (2003). Introduction/overview to in-situ burning of oil spills. *Spill Science and Technology Bulletin*, 8(4), 323-330.

Murray, H. H. (2000). Traditional and new applications for kaolin, smectite, and palygorskite: a general overview. Applied clay science, 17(5), 207-221.

Mysore, D., Viraraghavan, T. and Jin, Y. C. (2005). Treatment of oily waters using vermiculite. *Water research*, 39(12), 2643-2653.

Nahla, A. T. (2008). *Study on the use of barley straw for oil spill cleanup*, (unpublished thesis presented to graduate school, Faculty of Engineering, Alexandria University, Egypt).

Naik, N. M. (2009). *Affect of non-mixed condition of oxygen depletion and toxicity in a water body impacted by canola oil spill* (Doctoral dissertation, University of Cincinnati). Retrieved from https://etd.ohiolink.edu/rws_etd/document/get/ucin1238416343/ inline

Naseem, R. and Tahir, S. S. (2001). Removal of Pb (II) from aqueous/acidic solutions by using bentonite as an adsorbent. *Water Research*, 35(16), 3982-3986.

National Oceanic Atmospheric Administration (NOAA) (2004). *Dispersants*, http://www. response. restoration. noaa. gov/oilaids/response/pdfs/methods/disperse. pdf.

Nayak, P. S. and Singh, B. K. (2007). Instrumental characterization of clay by XRF, XRD and FTIR. *Indian academy of science*. 30(3) 235-238

Nenkova, S., Garvanska, R. and Jelev, S. (2004). Fibrous wood sorbent for eliminating oil pollution. *Aulex Research Journal*, 4(30), 157-163.

Nguyen, V. N., Nguyen, T. D. C., Dao, T. P., Tran, H. T., Nguyen, D. B. and Ahn, D. H. (2013). Synthesis of organoclays and their application for the adsorption of phenolic compounds from aqueous solution. *Journal of Industrial and Engineering Chemistry*, 19(2), 640–644. doi:10. 1016/j. jiec. 2012. 09. 018

Nordvik, A. B., Simmons, J. L., Bitting, K. R., Lewis A. and Strøm-Kristiansen T. (1996). Oil and water separation in marine oil spill clean-up operations. *Spill Science and Technology Bulletin*, 3(3), 107-122.

Nounou, M. and Nounou, H. (2010). Multiscale estimation of the Freundlich adsorption isotherms, *International Journal of Environmental Science and Technology*, 7(3), 509–518.

Nwankwere, E. T. O. (2010). *Acetylation of Rice (Oriza Sativa) Husk for Oil Spillage Treatment Using N–Bromo Succinimide as catalyst*. M.Sc. Thesis, Department of Chemistry, Ahmadu Bello University, Zaria.

Nwokoma, D. B., and Anene, U. (2010). Adsorption of crude oil using meshed groundnut husk. Chemical Product and Process Modeling, 5(1).

Odokuma, L. O. and Dickson, A. A. (2003). Bioremediation of a crude-oil polluted tropical rain-forest soil. *Global Journal of Environmental. Science,* 2(1), 29-40.

Ohtsubo, M., Konishi, K., Madama, H., Higashi, T. and Kanayama, M. (2011). Retention and Biodegradation of Oil by Peat Moss. *Science Bulletin of the Faculty of Agriculture, Kyushu University,* 66(2), 11-20.

Oliveira, G. C., Silva, M. M., Rodrigues, M. G. F. and Laborde H. M. (2012). Performance of Natural sodium clay treated with ammonium salt in the separation of emulsified oil in water. *Brazilian Journal of Petroleum and Gas.* 6(4), 171-183.

Olufemi, B. A., Jimoda, L. A. and Agbodike, N. F. (2014). Adsorption of Crude Oil using Meshed Corncobs. *Asian Journal of Applied Science and Engineering*, 3(2), 7–21.

Oshwofasa, B. O. and Anuta, D. E. (2012). Environmental degredation and oil industry activities in the Niger-Delta region. African Journal of Scientific Research, 9(1), 444-460.

Overton, E. B., Sharp, W. D. and Roberts, P. (1994). *Toxicity of petroleum. In Basic Environmental Toxicology, In:* Cockerham, L. G., Shane, B. S., Eds: CRC Press: Boca Raton, FL, pp. 133–156.

Oviasuyi, P. O. and Uwadiae, J. (2010). The Dilemma of Niger-Delta Region as Oil Producing States of Nigeria. *Journal of Peace, Conflict and Development*, 16, 110-126.

Pˇrikryl, R. (2006). Overview of mineralogy of bentonites. Genesis, physicochemical properties, industrial uses and world production. *In: Amer A. A., Mattheus F. A. G.,*

(Ed.). Expansive Soils: Recent Advances in Characterization and Treatment. Taylor and Francis, United Kingdom. pp. 37-51.

Patel, H. A., Somani, R. S., Bajaj, H. C. and Jasra, R. V. (2006). Nanoclays for polymer nanocomposites, paints, inks, greases and cosmetics formulations, drug delivery vehicle and waste water treatment. *Bulletin of Materials Science*, 29(2), 133–145.

Pelletier, E., Delille, D. and Delille, B. (2004). Crude oil bioremediation in sub-Antarctic intertidal sediments: chemistry and toxicity of oiled residues. *Marine Environmental Research*, 57, 311–327. doi:10. 1016/j. marenvres. 2003. 07. 001.

Pichon, C. and Lynch, J. (2005). Synchrotron radiation and oil industry research. *Oil and Gas Science and Technology*, 60(5), 735-746.

Poile, C. A. (1990). Cleaning up oil spills. *Probe Post*, 12(3/4), 13-15.

Powell, T. (1983). Organoclays in Cosmetics. *Journal of the Society of Cosmetic Chemists*, 34(7), 402-402.

Prasad, M. S. and Kumari, K. (1987). Toxicity of Crude Oil to the Survival of the Fresh Water FishPuntius sophore (HAM.). A*cta Hydrochimica et Hydrobiologica*, 15, 29. doi:10. 1002/aheh. 19870150106.

Proffitt, E. (1997). *Managing Oil Spills in Mangrove Ecosystems; Effects, Remediation, Restoration and Modeling*, OCS Study MMS 97-0003, New Orleans U. S Department of Interior, Minerals Management Service, Golf of Mexico OCS Region pp. 76.

Qiu, H., Lv, L., Pan, B., Zhang, Q., Zhang, W. and Zhang, Q. (2009). Critical review in adsorption kinetic models. *Journal of Zhejiang University SCIENCE A*, 10(5), 716–724. doi:10. 1631/jzus. A0820524

Ramos-Vianna, M. M. G., Frano, J. H. R., Pinto, C. A., Valenzuela-Diaz, F. R. and Buchler P. M. (2004). Sorption of oil pollution by organoclays and a coal mineral complex. *Brazilian Journal of Chemical Engineering*, 21(20), 239-295.

Reynolds, J. G., Coronado, P. R. and Hrubesh, L. W. (2001). Hydrophobic aero-gels for oil spill cleanup-synthesis and characterization. *Non-Crystalline Solids*, 292 (1-3), 127-137.

Ribeiro, T., Smith, R. and Rubio, J. (2000). Sorption of oils by the nonliving biomass of a *salviniasp*. *Environmental Science Technology*, 34, 5201–5205.

Rodrigues, L. A. D. S., Figueiras, A., Veiga, F., de Freitas, R. M., Nunes, L. C. C., da Silva Filho, E. C. and da Silva Leite, C. M. (2013). The systems containing clays and clay minerals from modified drug release: a review. *Colloids and Surfaces B: Biointerfaces*, 103, 642-651.

Roopa V., Ramesh K., Rajappa A. and Nandhakumar V. (2014). Equilibrium and Isotherm Studies On the Adsorption of Rhodamine B onto Activated Carbon Prepared from Bark of ErythrinaIndica. *International Journal of Current Research in Chemistry and Pharmaceutical Sciences.*1(2) 23-29.

Ross, D. S. and Ketterings, Q. (1996). Recommended Methods for Determining Soil Cation Exchange Capacity. *In: Recommended Soil Testing Procedures for the Northeastern United States*. 2011th ed., pp. 75–86.

Roulia, M., Chassapis, K., Fotinopoulos, C., Savvidis, T. and Katakis, D. (2003). Dispersion and sorption of oil spills by emulsifier-modified expanded perlite. *Spill Science and Technology Bulletin*, 8(5-6), 425-431.

Royal Dutch Shell Plc (2009). Environment and safety. *In: Annual Report and Form 20-F for the Year Ended December 31, 2008*.

Rožić, L., Grbić, B., Radić, N., Petrović, S., Novaković, T., Vuković, Z. and Nedić, Z. (2011). Mesoporous 12-tungstophosphoric acid/activated bentonite catalysts for oxidation of 2-propanol. *Applied Clay Science*, 53(2), 151-156.

Ruiz-Hitzky, E. and Van Meerbeeck, A. (2006). *In:* Theng, F., Lagaly, B. K. G. (Eds.), *Handbook of Clay Science*. Elsevier, Amsterdam.

Rusu, L. (2010). Application of numerical models to evaluate oil spills propagation in the coastal environment of the Black Sea. *Journal of Environmental Engineering and Landscape Management*, 18(4), 288-295.

Saito, M., Ishii, N., Ogura, S., Maemura, S., and Suzuki, H. (2003). Development and water tank tests of sugi bark sorbent (SBS). *Spill Science and Technology Bulletin*, 8(5), 475-482.

Sakthivel, T., Reid, D. L., Goldstein, I., Hench, L. and Seal, S. (2013). Hydrophobic high surface area zeolites derived from fly ash for oil spill remediation. *Environmental science and technology*, 47(11), 5843-5850.

Sanders, J. M., Bucher, J. R., Peckham, J. C., Kissling, G. E., Hejtmancik, M. R. and Chhabra, R. S. (2009). Carcinogenesis studies of cresols in rats and mice. *Toxicology*, 257(1), 33-39.

Santos, P. S. (1989). *Ciência e Tecnologia de Argilas*. 2 ed. São Paulo: Edgard Blücher. 1, 408. (In Portuguese).

Sarkar, B., Xi, Y., Megharaj, M., Krishnamurti, G. S. R., Rajarathnam, D. and Naidu, R. (2010). Remediation of hexavalent chromium through adsorption by bentonite based Arquad® 2HT-75 organoclays. *Journal of Hazardous Materials*, 183(1-3), 87–97. doi:10. 1016/j. jhazmat. 2010. 06. 110

Satish, M. M. (2003). Vallabh Vidyanagar. *India Sãdhanã,* 28(1-2), 335-348.

Sayed, S. A., El-Sayed, A. S. and Zayed, M. A. (2004). Removal of oil spills from salt water by magnesium, calcium carbonates and oxides. *Journal of Applied Science and Environmental Management*, 8(1), 71-78.

Scheuermann, G. M., Thomann, R. and Mülhaupt, R. (2009). Catalysts based upon organoclay with tunable polarity and dispersion behavior: new catalysts for hydrogenation, C–C coupling reactions and fluorous biphase catalysis. *Catalysis letters*, 132(3-4), 355-362.

Shell petroleum development company (SPDC) (2006). People and the environment. *In*: *Shell Nigeria Annual Report 2006*. Pp 8-9.

Shichi, T., and Takagi, K. (2000). Clay minerals as photochemical reaction fields. *Journal of Photochemistry and Photobiology C: Photochemistry Reviews*, 1(2), 113-130.

Shigenaka, G. (2002). Oil toxicity in mangroves. *In:* Hoff, R. (Ed.) *Oil Spills in Mangroves-Planning and Response Consideration*. National oceanic and atmospheric administration, Seattle, Washington, pp. 23-35.

Shrihari, V. and Das, A. (2009). Adsorption of phenol from aqueous media by an agro-waste (Hemidesmus Indicus) based activated carbon. *Applied Ecology and Environmental Research*, 7(1), 13–23.

Silva, I. A., Sousa, F. K. A., Menezes, R. R., Neves, G. A., Santana, L. N. L. and Ferreira, H. C. (2014). Modification of bentonites with nonionic surfactants for use in organic-based drilling fluids. *Applied Clay Science*. 95, 371-377.

Singh, D. K. and Srivastava, B. (1999). Removal of basic dyes from aqueous solutions by chemically treated Psidium guava leaves. *Indian Journal of Environmental. Health*, 41, 333–345.

Singh, M. and Arbad, B. R. (2014). Characterization of traditional mud mortar of the decorated wall surfaces of Ellora caves. *Construction and Building Materials*, 65, 384–395. doi:10. 1016/j. conbuildmat. 2014. 04. 126

Singh, R. K., Kumar, S., Kumar, S. and Kumar, A. (2008). Biodegradation kinetic studies for the removal of p-cresol from wastewater using< i> Gliomastix indicus MTCC 3869. *Biochemical Engineering Journal*, 40(2), 293-303.

Sirotkina, E. E. and Novoselova, L. Y. U. (2005). Materials for adsorption purification of water from petroleum and oil products. C*hemistry for Sustainable Development*, 13, 359-375.

Site, A. D. (2001). Factors affecting sorption of organic compounds in Natural sorbents/water systems and sorption coefficients for selected pollutants: A review. *Journal of Physical and Chemical Reference Data*, 30(1), 187-439.

Smith, B. (1999). *Infra-Red Spectral Interpretation –A Systematic Approach*. CRC Press, Bocaration London, New York, Washington DC, pp. 243-249.

Smith, M. T., Zhang, L., McHale, C. M., Skibola, C. F. and Rappaport, S. M. (2011). Benzene, the exposome and future investigations of leukemia etiology. *Chemico-biological interactions*, 192(1), 155-159.

Snyder, R. and Hedlim, C. C. (1996). An overview of benzene metabolism (Review). *Environmental Health Perspective,*104(6), 1165-1171.

Soetaredjo, F. E., Ayucitra, A., Ismadji, S. and Maukar, A. L. (2011). KOH/bentonite catalysts for transesterification of palm oil to biodiesel. *Applied clay science*, 53(2), 341-346.

Sokker, H. H., Naeem M. E., Hassan, M. A. and Bahgat E. E. (2011). Sorption of crude oil from aqueous solution by hydrogel of chitosan based polyacrylamide prepared by radiation induced graft polymerization. *Journal of Hazardous Materials*, 190, 359–365.

Srihari, V., Babu, M. and Das, A. (2005). Kinetics of phenol sorption raw agro-based wastes. *Journal of Applied Sciences*, 6(1), 47–50.

Stanley, E. D. (1969). *Oil pollution: Problems and policies*. Washington, D. C.: The Bureau of National Affairs, Inc.

Sulaymon, A. H and Kshash, J. M (2010). Removal Of Oil From Wastewater By Organoclay Prepared From Iraqi Bentonite. *Journal of Engineering,*16 (4), 5778-5798.

Sun, X-F., Sun, R. and Sun, J. X., (2002). Acetylation of Rice Straw for Oil Sorption; With or Without Catalysts. *Journal of Agriculture and Food Chemistry*, 50, 6428.

Suni, S., Kosunen, A. I., Hautata, M., Pasila, A. and Romantschuk, M. (2004). Use of a by-product of peat excavation, cotton grass fiber, as a sorbent for oil spills. *Marine Pollution Bulletin*, 49(11-12), 916-921.

Sunil K. B. and Arti J. (2010). Removal of copper(II) from aqueous solution using spent tea leaves (STL) as a potential sorbent. *Water SA (Online).*36(3).

Sverdrup, L. E., Krogh, P. H., Nielsen, T., Kjær, C. and Stenersen, J. (2003). Toxicity of eight polycyclic aromatic compounds to red clover (Trifolium pretense), ryegrass (Lolium perenne) and mustard (Sinapsis alba). *Chemosphere*, 53, 993–1003.

Tahir, H. and Mushtaque, Z. (2005). Assistment of soil samples after the disaster of tasman spirit near the clifton beach Karachi, Pakistan. *Electronic Journal of Agricultural and Food Chemistry*. EJEAFCHe, 4(6), 1094-1101.

Tamura, K. and Nakazawa, H. (1996). Intercalation of n-alkyltrimethylammonium into swelling fluoro-mica. *Clays Clay Minerals*. 44, 501–505.

Tang, G. Q. and Kovscek, A. R. (2004). An experimental investigation of the effect of temperature on recovery of heavy oil from diatomite. *SPE Journal*, 9(02), 163-179.

Teas, C., Kalligeros, S., Zanikos, F., Stournas, S., Lois, E. and Anastopoulos, G. (2001). Investigation of the effectiveness of absorbent materials in oil spills clean up. *Desalination*, 140(3), 259-264.

Thompson, N. E., Emmanuel, G. C. and Adagadzu, K. J. (2010). Sorption studies of crude oil on acetylated rice husks. *Archives of Applied Science Research*, 2(5), 142–151.

Tiwari, D. K., Behari, J. and Sen, P. (2008). Application of Nanoparticles in Waste Water Treatment. *World Applied Sciences Journal*, 3(3), 417–433.

Tiwari, R. R., Khilar, K. C. and Natarajan, U. (2006). Synthesis and characterization of novel organo-montmorillonites. *Applied Clay Science*, 38(3), 203-208.

Topallar, H. (1998). The Adsorption Isotherms of the Bleaching of Sun ower-Seed Oil. *Turkish Journal of Chemistry*, 22(2), 143–148.

Toyoda, M. and Inagaki, M. (2000). Heavy oil sorption using exfoliated graphite: New application of exfoliated graphite to protect heavy oil pollution. *Carbon*, 38(2), 199-210.

Toyoda, M. and Inagaki, M. (2003). Sorption and recovery of heavy oils by using exfoliated graphite. *Spill Science Tech. B.*, 8(2), 467- 474.

Toyoda, M. and Inagaki, M. (2003). Sorption and recovery of heavy oils by using exfoliated graphite. *Spill Science and Technology Bulletin*, 8(5), 467-474.

Tsutsumi, H., Kono, M., Takai, K., Manabe, T., Haraguchi, M., Yamamoto, I. and Oppenheimer, C. (2000). Bioremediation on the shore after an oil spill from the Nakhodka in the sea of Japan III Field tests of a bioremediation agent with microbiological cultures for the treatment of an oil spill, Marine. *Pollution Bulletin*, 40(4), 320-324.

Uba, C. (2013). "Shell Experiences 137 Oil Spill in Niger Delta – Stolen Oil Hits 150,000 Barrel per Day. " Daily Newswatch, April 12. http://www. mydailynewswatchng. com/shell-experiences-137-oil-spill-in-niger-delta-stolen-oil-hits-150000-barrel-per-day/.

Uddin, F. (2008). Clays, Nanoclays. and Montmorillonite Minerals. *Metallurgical and Materials Transactions A*, 39(12), 2804–2814.

Udoette, U. B. (1997). *Effects of Administration of Qua Iboe Light Crude Oil on Biochemical Parameters in Albino Wister Rats*. Unpublished M. Sc Thesis, Biochemistry Department, University of Calabar.

Umukoro, N. (2013). Socio-Economic Inequality and Health Care in Nigeria: Perceptions of Health Workers from the Niger Delta. Rethinking Development and Inequality, 1.

United Nation Development Program (UNDP) (2006). *Niger Delta Human Development Report 2006*, Abuja, Nigeria, pp. 19-73.

United States Department of Agriculture (USDOA) (2008). *Design Guide for Oil Spill Prevention and Control at Substations*. Rural development utilities programs, bulletin 1724E-302, pp. 73-108.

US Army Corps of Engineering (USACE) (2005). Incidences and environmental effects of oil and gas releases. *In: Known and Potential Environmental Effects of Oil and Gas Drilling Activity in the Great Lakes.* Final report. www.lrc.usace.army.mil/GrtLakes/OilGas/Chapter3.pdf, pp. 26-38.

US Environmental Protection Agency (USEPA) (1994). *Chemicals in the environment: Toluene*. OPPT chemical fact sheet. EPA 749-F-54-021.

US Environmental Protection Agency (USEPA) (2004a). *Booms*, http://www. epa. gov/oilspill/boom. htm.

US Environmental Protection Agency (USEPA) (2004b). *Dispersing agents*, http://www. epa. gov/ oilspill/disperse. htm.

US Environmental Protection Agency (USEPA) (2004c). NRT fact sheet. *Bioremediation in oil spill response*, http://www. epa.gov/oilspill/pdfs/biofact.pdf.

US Environmental Protection Agency (USEPA) (2004d). *Sensitivity of Freshwater Habitats*, Office of Emergency Management, Oil Program, Washington, D. C. Available at http://www.epa.gov/oilspill/freshwat.htm.

Uzunova S., Uzunov, I. and Angelova D. (2013), Liquid-phase sorption of oil by carbonized rice husks: impact of grain size distribution on the sorption kinetics. *Ref Journal of Chemical Technology and Metallurgy*, 48(5), 505-512.

Van der Marel, H. W. and Beutelspacher, H. (1976) *Atlas of Infrared Spectroscopy of Clay Minerals and their admixtures*. Elsevier, Amsterdam. Pp 31-58.

Vee Gee scientific, (2004). *Toluene*. Material and safety Data sheet, M10003.

Venkatathri N. (2006). Characterization and catalytic properties of naturally occurring clay, bentonite. *Bulletin of the catalysis Society of India*, 5(2), 61-72.

Venkatesan, R., Nagarajan, N. R., Paso, K., Yi, Y. B., Sastry, A. M. and Fogler, H. S. (2005). The strength of paraffin gels formed under static and flow conditions. *Chemical engineering science*, 60(13), 3587-3598.

Venkateswaran, P. and and Parimaladevi, V. (2011) Kinetics, Thermodynamics and Isotherm Modeling of Sorption of Triphenylmethane dyes (methyl violet, malachite green andmagenta ii) on to fruit waste, *Journal of Applied Technology in Environmental Sanitation*, 1(3) 273 - 283.

Venosa, A. D., Lee, K., Suldan, M. T., Gracia-Planco, S., Cobanli, S., Moteleb, M. and King, O. W. (2002). Bioremediation and bio restoration of crude oil contaminated fresh wetland on the Saint Lawrence River. *Bioremediation Journal*, 6(3), 266.

Ventikos, N. P., Vergetis, E., Psaratifs, H. N. and Triantafyllou, G. (2004). A high level synthesis of oil spill response equipment and countermeasures. *J. Hazardous Materials*, 107, 51-58.

Vernot, E. H., MacEwen, J. D., Haun, C. C. and Kinkead, E. R. (1977). Acute toxicity and skin corrosion data for some organic and inorganic compounds and aqueous solutions. *Toxicol. Appl. Pharmacol*. 42(2), 417-23.

Viseras, C. and Lopez-Galindo, A. (1999). Pharmaceutical applications of some Spanish clays (sepiolite, palygorskite, bentonite), some preformulation studies. *Applied Clay Science*, 14(1), 69-82.

Volovicheva, N., Vezentsev, A., A. Vezentsev. and Korolkova, S. (2011). Modified Layered Alumosilicate Nanosorbents for Water Treating. *In: Proceedings of the 12th International Conference on Environmental Science and Technology Rhodes*, Greece, 8 – 10 September 2011, pp. 8–10.

Vougaris, D. and Petridis, D. (2002). Emulsifying effect of dimethyldioctadecylammo-nium-hectorita in polystyrene/poly (ethyl methacrylate) blends. *Polymer*, 43, 2213–2218.

Wang, C., Chen, B., Zhang, B., He, S. and Zhao, M. (2013). Fingerprint and weathering characteristics of crude oils after Dalian oil spill, *China. Marine Pollution Bulletin*, 71, 64–68.

Wang, H., Deng, S. X., Shen, Z. R., Wang, J. G., Ding, D. T. and Chen, T. H. (2009). Facile preparation of Pd/organoclay catalysts with high performance in solvent-free aerobic selective oxidation of benzyl alcohol. *Green Chemistry*, 11(10), 1499-1502.

Wang, L. and Sheng, J. (2006). A kinetic study on the thermal degradation of polypropylene/attapulgite nanocomposites. *Journal of Macromolecular Science, Part B: Physics*, 45(1), 1-11.

Wang, W. Zappi, M., Singletary, J., Hall, N. and Karr, L. (2001). *Using chemical priming as a means of enhancing the performance of bio-cells for treating petroleum products containing recalcitrant chemical species*, Environmental technology research and applications laboratory, Mississippi State University.

Wang, Z. and Fingas, M. F. (2003). Development of oil hydrocarbon fingerprinting and identification techniques. *Marine Pollution Bulletin*, 47(9), 423-452.

Wardrop, J. A., Wagstaff, B., Pfennig, P., Leeder, J. and Connoly, R. (1996). *The distribution, persistence and effects of petroleum hydrocarbons in mangroves impacted by the "era" oil spill (September, 1992)*. Final phase one report, Adelaide office of the environmental protection agency, south austrailian department of environmental and natural resources.

Weber, W. and Morris, J. (1963). Kinetics of adsorption on carbon from solution, *J. Sanitery Eng. Div. ASCE*, 89, (SA2), 31-59.

Wei, Q. F., Mather, R. R. and Fotheringham, A. F. (2005). Oil removal from used sorbents using a biosurfactant. *Bioresource technology*, 96(3), 331-334.

Wei, Q. F., Mather, R. R., Fotheringham, A. F. and Yang, R. D. (2003). Evaluation of non-woven polypropylene oil sorbents in marine oil-spill recovery. *Marine Pollution Bulletin*, 46(6), 780–783.

Wilkins-Haug, L. (1997). Teratogen update: Toluene. *Teratology*, 55(2), 145-151.

Xi, Y. (2006). *Synthesis, Characterisation and Application of Organoclays*. Queensland University of Technology. Unpublished PhD Thesis. Pp. 20-55.

Xi, Y., Ding, Z., He, H. and Frost, R. L. (2005). Infrared spectroscopy of organoclays synthesized with the surfactant octadecyltrimethylammonium bromide. *Spectrochimica Acta. Part A, Molecular and Biomolecular Spectroscopy*, 61(3), 515–25.

Xie, W., Gao, Z., Liu, K., Pan, W. P. and Vaia, R. (2001). Thermal characteristic of organomodifiedmontmorillonite. *Thermochimica Acta*, 367-68, 339-350.

Yakout, S. M. and Elsherif, E. (2010). Batch kinetics, isotherm and thermodynamic studies of adsorption of strontium from aqueous solutions onto low cost rice-straw based carbons. *Carbon – Science and Technology*, 1, 144–153.

Yammama, A. G. (1997). *Spillage and emergency*. Workshop on environmental and pollution control, Nigeria Society of Chemical Engineering, Enugu, Nigeria, pp. 25-27.

Yender, R. (2002). Response Oil Spills in Mangroves. *In:* Hoff, R. (Ed.), O*il Spills in Mangroves- Planning and Response Consideration*. National oceanic and atmospheric administration, Seattle, Washington, 36-47.

Yıldız, N., Gönülşen, R., Koyuncu, H., and Çalımlı, A. (2005). Adsorption of benzoic acid and hydroquinone by organically modified bentonites. *Colloids and Surfaces A: Physicochemical and Engineering Aspects*, 260(1), 87-94.

Yue, X., Zhang, R., Wang, H. and Zhang, F. (2009). Sorption and decomposition of crude oil using exfoliated graphite/ZnO composites. *Journal of Physics and Chemistry of Solid*s, 70(11), 1391-1394.

Yun, W. Z. W. T. (1993). A New Paper Filler-Modified Bentonite. *China Pulp and Paper*, 6, 006.

Yürüdü, C., Isci, S., Ünlü, C., Atici, O., Ece I. O. and Güngör, N. (2005). Synthesis and characterization of HAD/NaMMT Organoclay. *Bulletin of Material Science,* 28(6); 623-628.

Zhang, J., Li, L., Xu, J. and Sun, D. (2014). Effect of cetyltrimethylammonium bromide addition on the emulsions stabilized by montmorillonite. *Colloid and Polymer Science*, 292(2), 441-447.

Zhang, J., Zhang, L., Li, Z., Xie, X., Li, J. and Luo, P. (2001). Interaction between the hydrophobically modified water soluble amphoteric cellulose graft copolymer and clay. *Acta Physico Chimica Sinica,* 18(04), 315-320.

Zhang, L., McHale, C. M., Rothman, N., Li, G., Ji, Z., Vermeulen, R., Hubbard, A. E. and Lan, Q. (2010). Systems biology of human benzene exposure. *Chemico-biological interactions*, 184(1), 86-93.

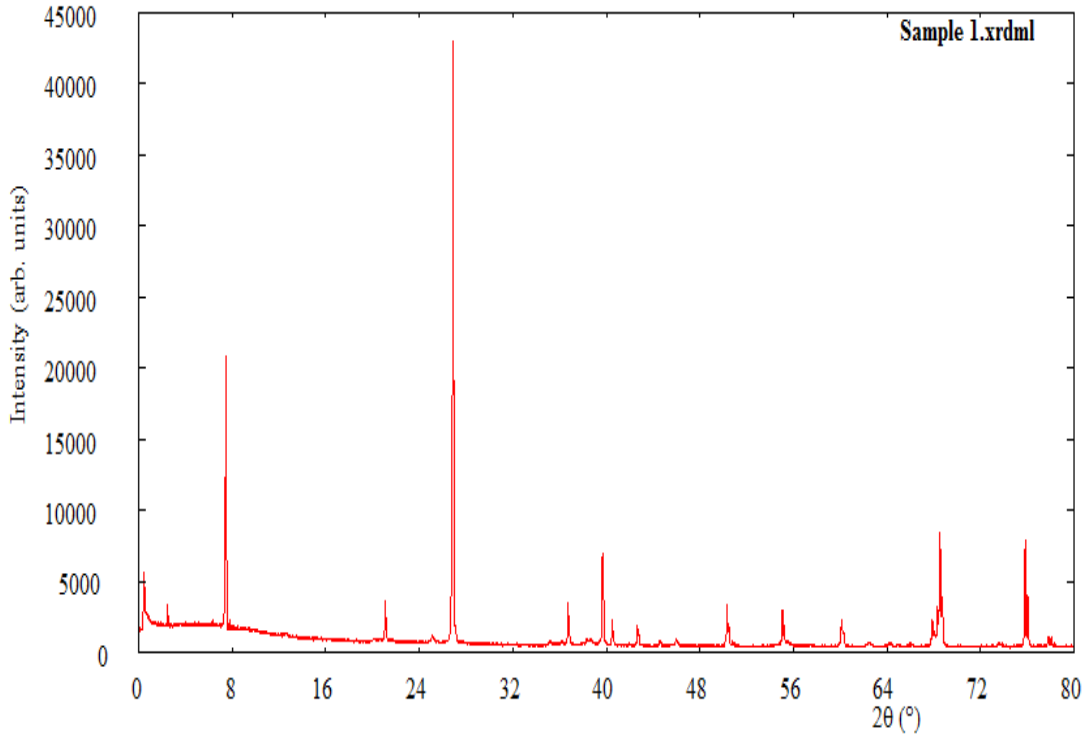
Zhou, Q., Frost, R. L., He, H. and Xi, Y. (2007). Changes in the surfaces of adsorbed para-nitrophenol on HDTMA organoclay-The XRD and TG study. *Journal of Colloid and Interface Science*, 307(1), 50–55.

Zhou, Q., Xi, Y., He, H. and Frost, R. (2008). Application of near infrared spectroscopy for the determination of adsorbed p-nitrophenol on HDTMA organoclay simplications for the removal of organic pollutants from water. *Spectrochimica A: Molecular and Biomolecular Spectroscopy*, 69, 835-841.

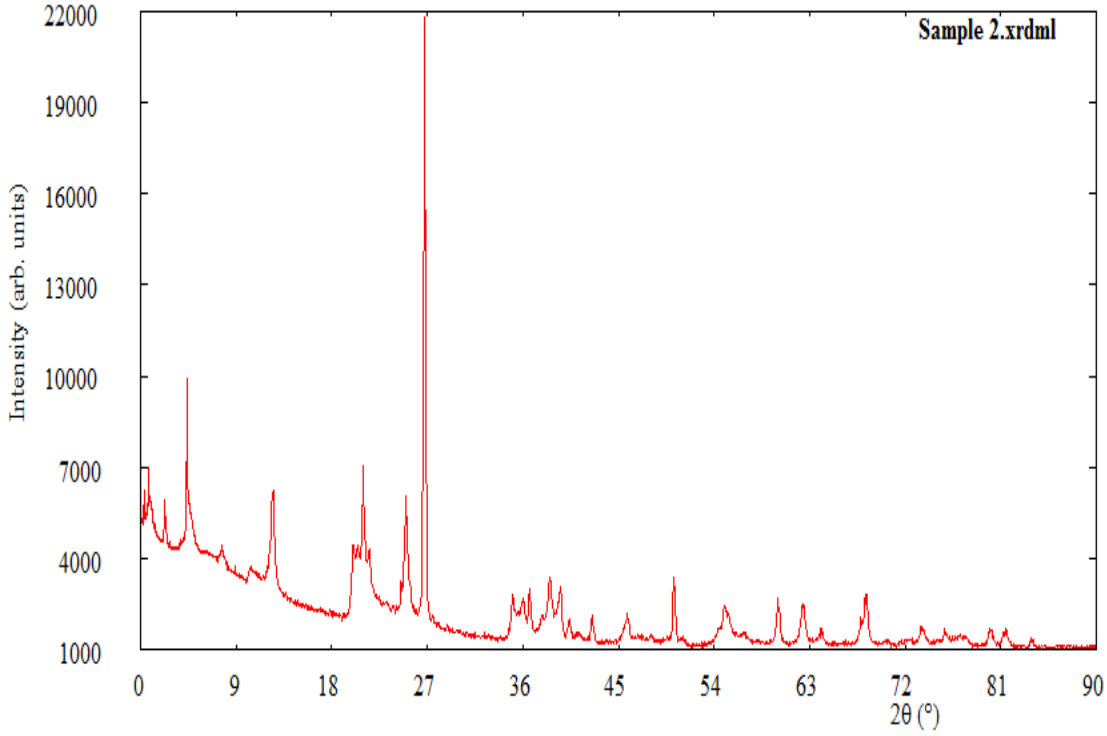
Zhu, J., He, H., Zhu, L., Wen, X. and Deng, F. (2005). Characterization of organic phases in the interlayer of montmorillonite using FTIR and 13C NMR. *Journal of Colloid and Interface Science*, 286(1), 239-244.

Zidelkheir, B. and Abdelgoad, M. (2008). Effect of surfactant agent upon the structure of montmorillonite X-ray diffraction and thermal analysis. *Journal of Thermal Analysis and Calorimetry*, 94, 181-187. DOI: 10. 1007/s10973-008-9053-8.

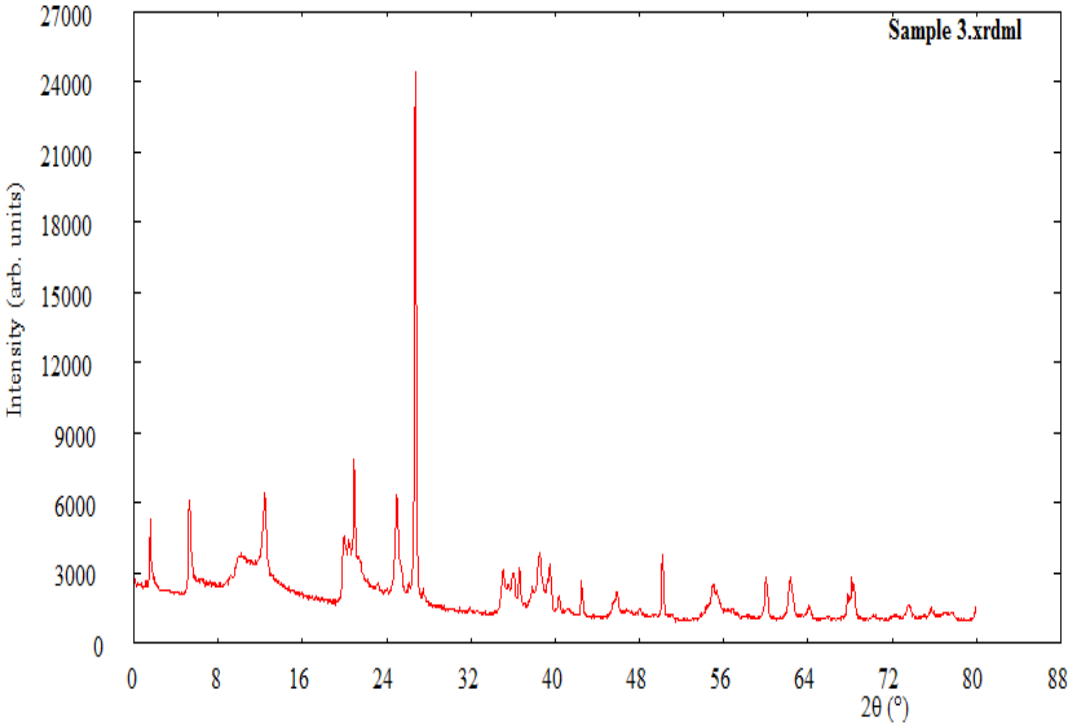
APPENDICES



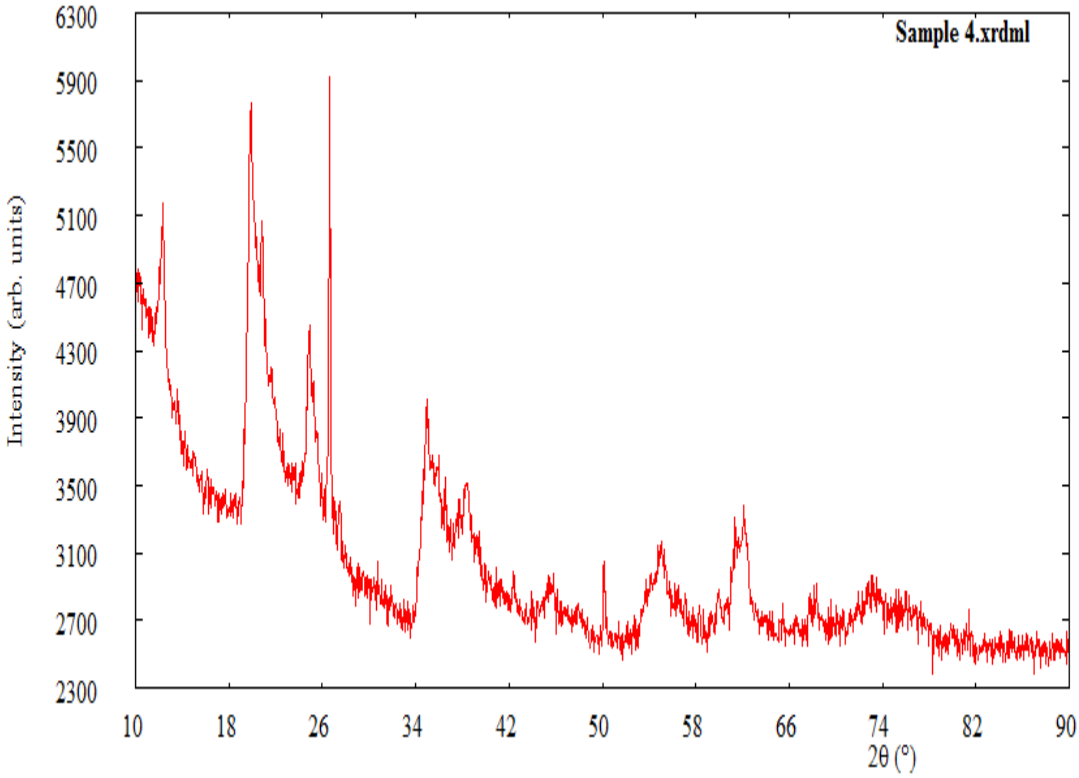
Appendix I: X-Ray diffractogram of sample 1



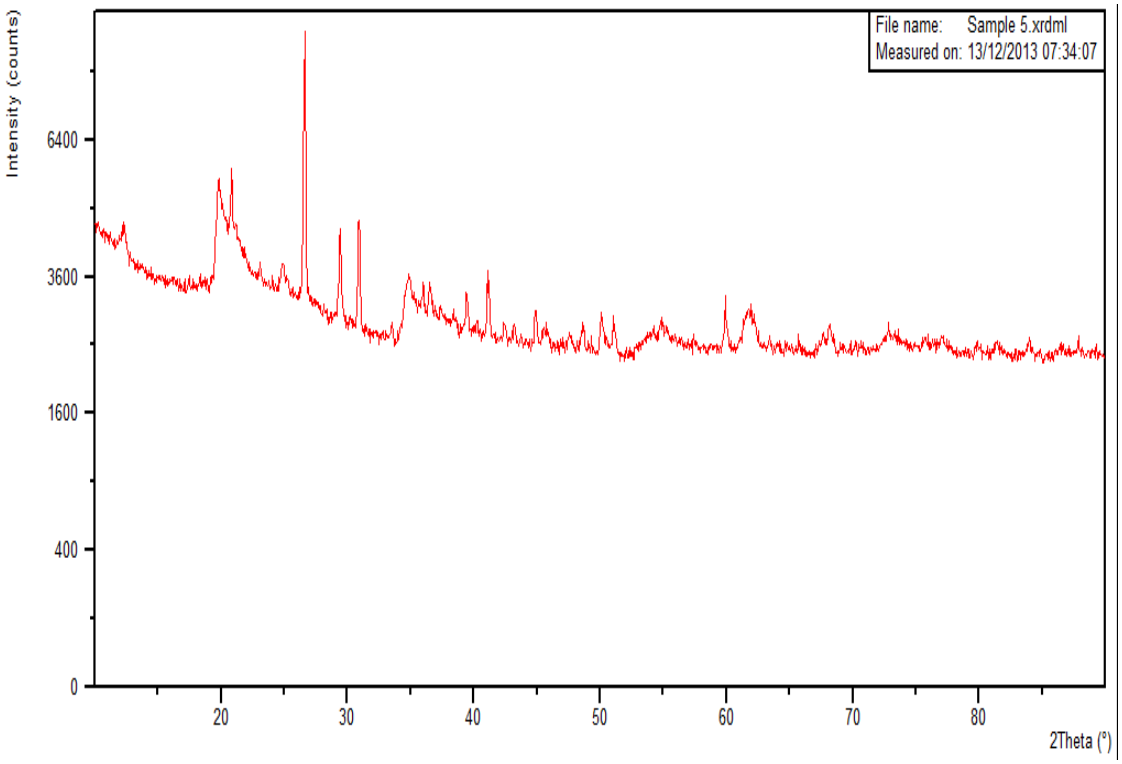
Appendix II: X-Ray diffractogram of sample 2



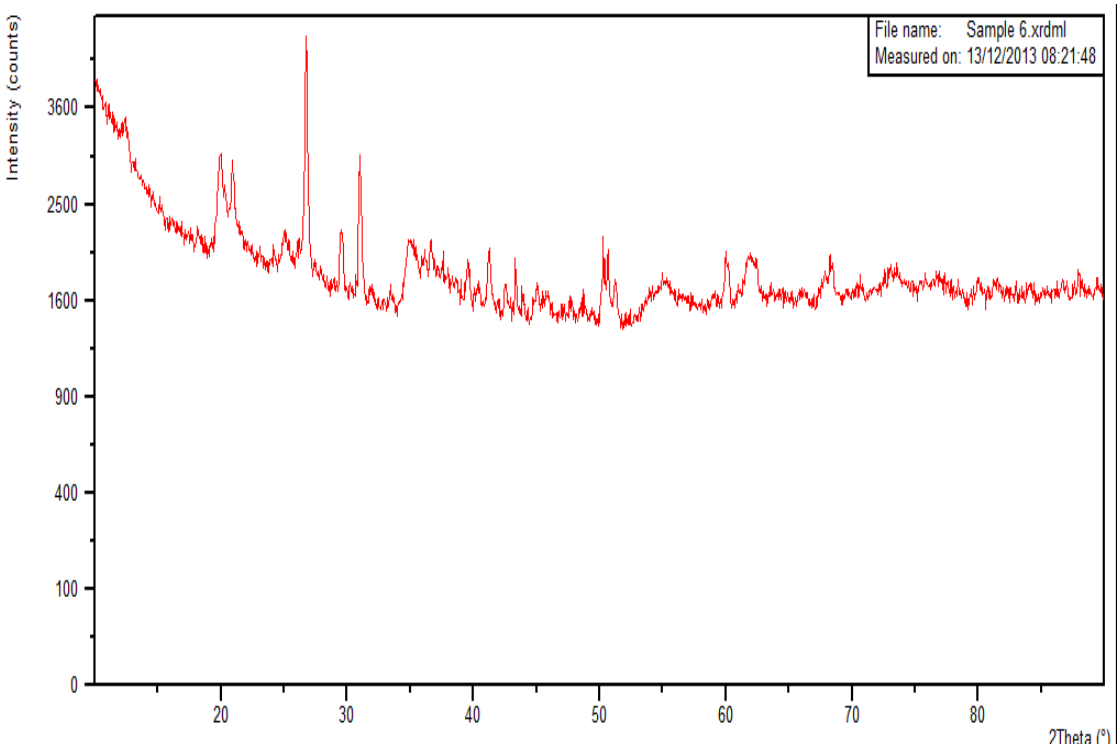
Appendix III: X-Ray diffractogram of sample 3



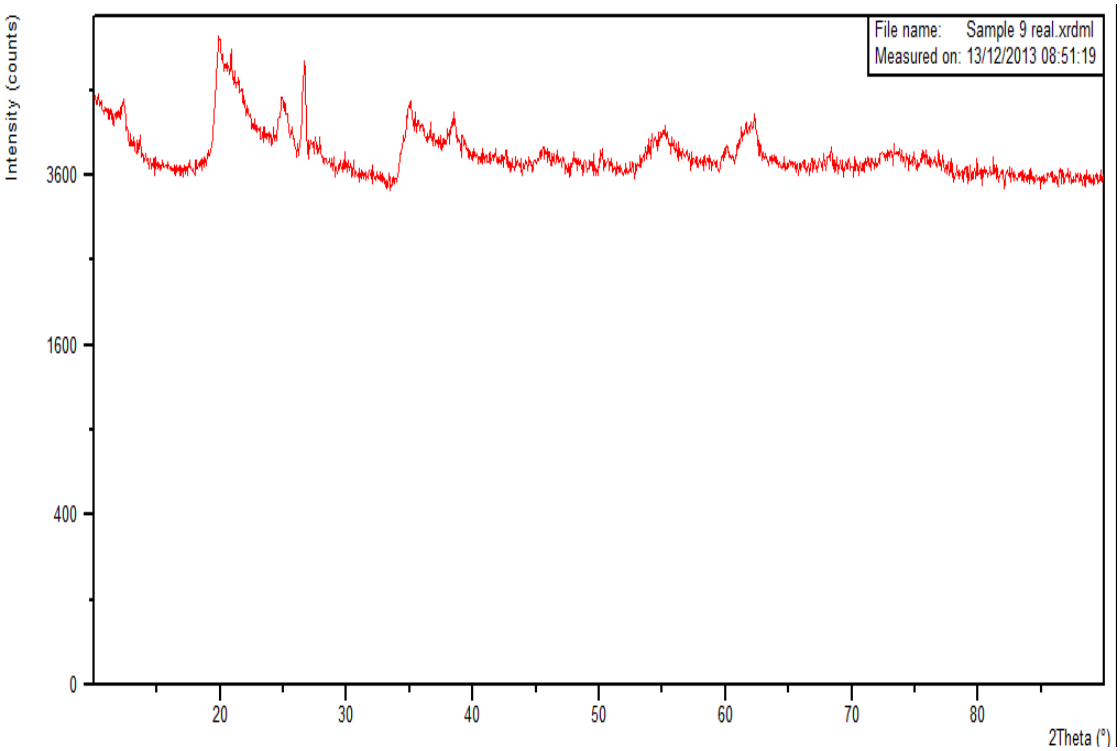
Appendix IV: X-Ray diffractogram of sample 6



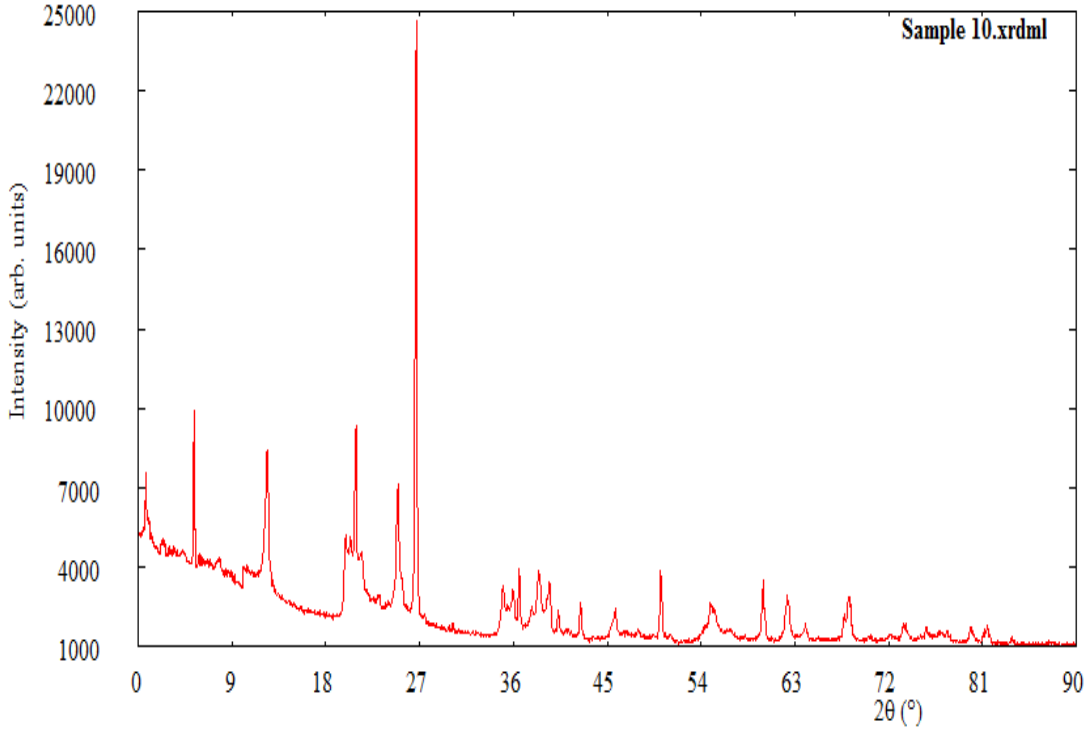
Appendix V: X-Ray diffractogram of sample 5



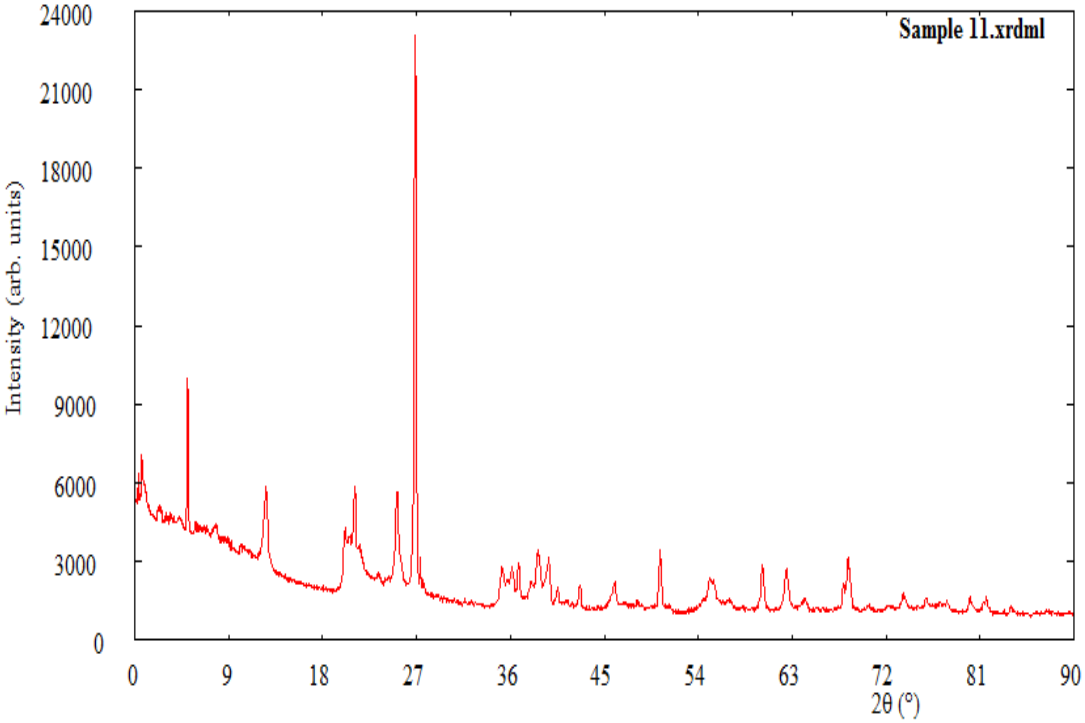
Appendix VI: X-Ray diffractogram of sample 6



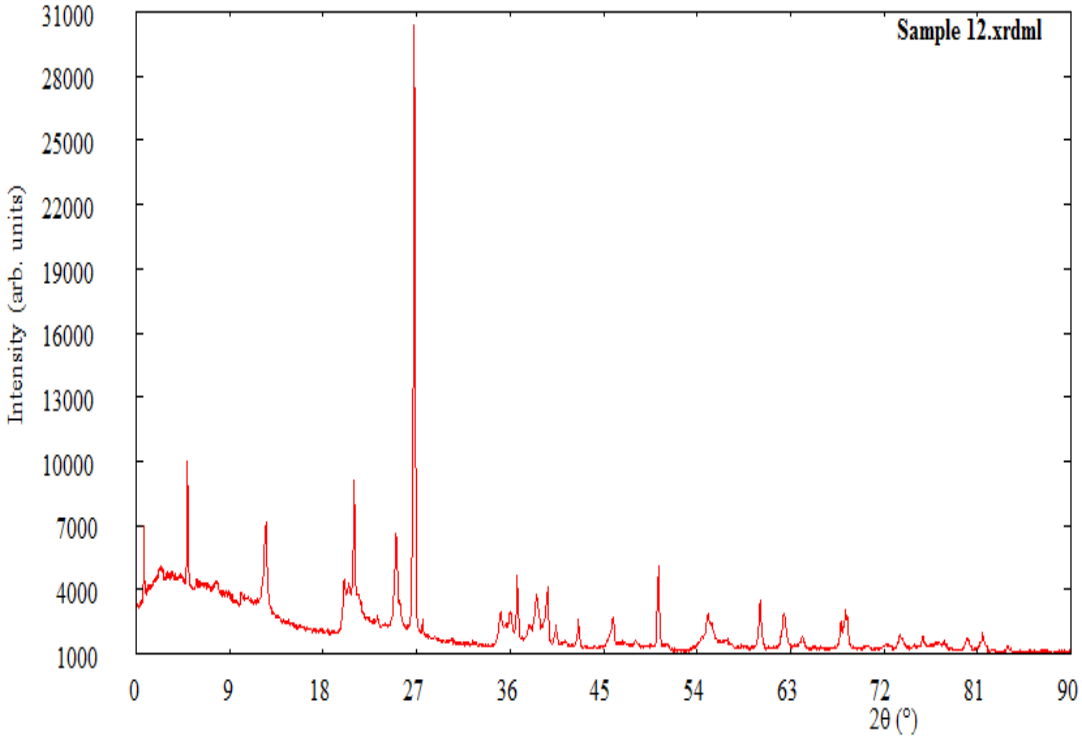
Appendix VII: X-Ray diffractogram of sample 9



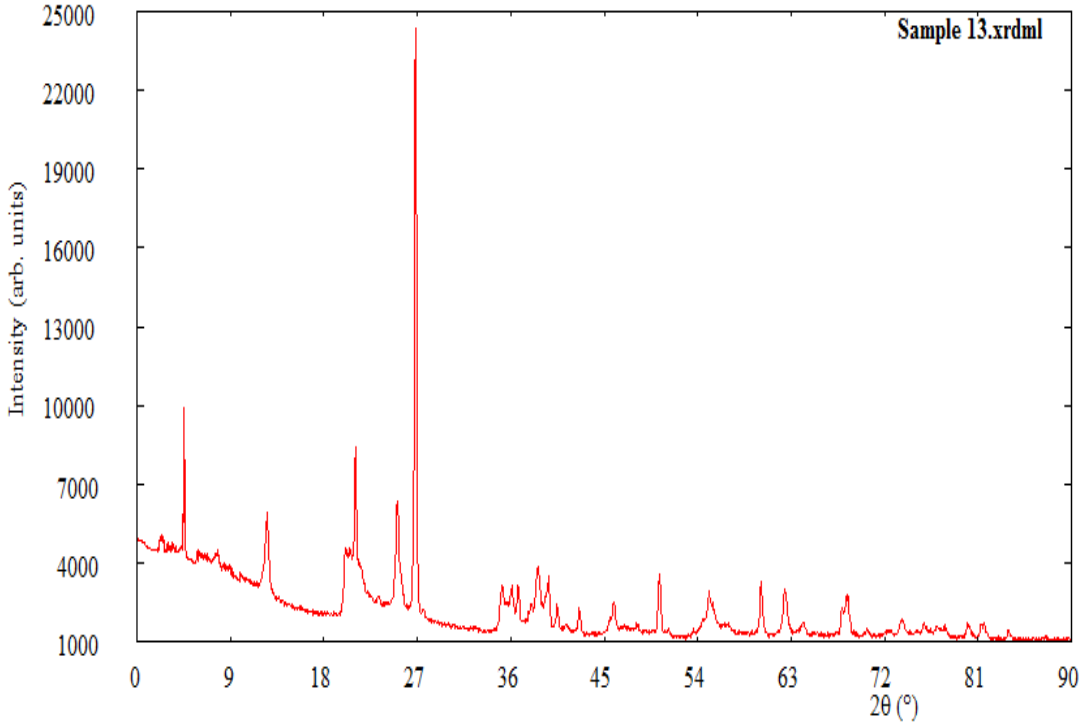
Appendix VIII: X-Ray diffractogram of sample 10



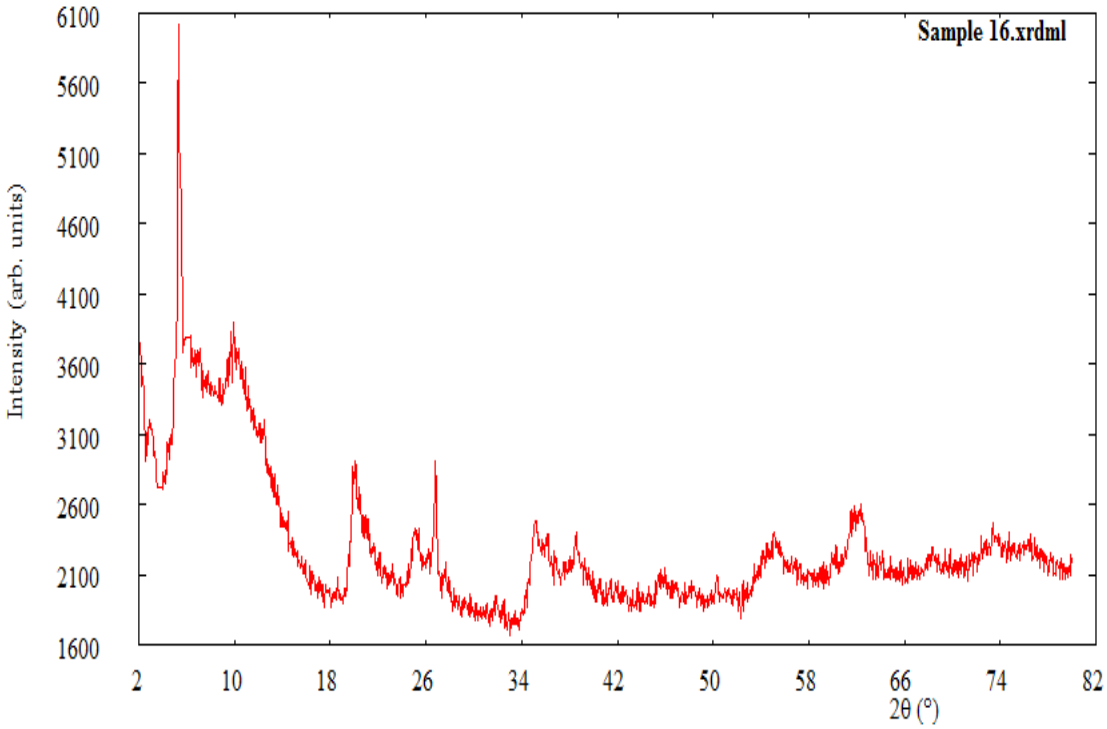
Appendix IX: X-Ray diffractogram of sample 11



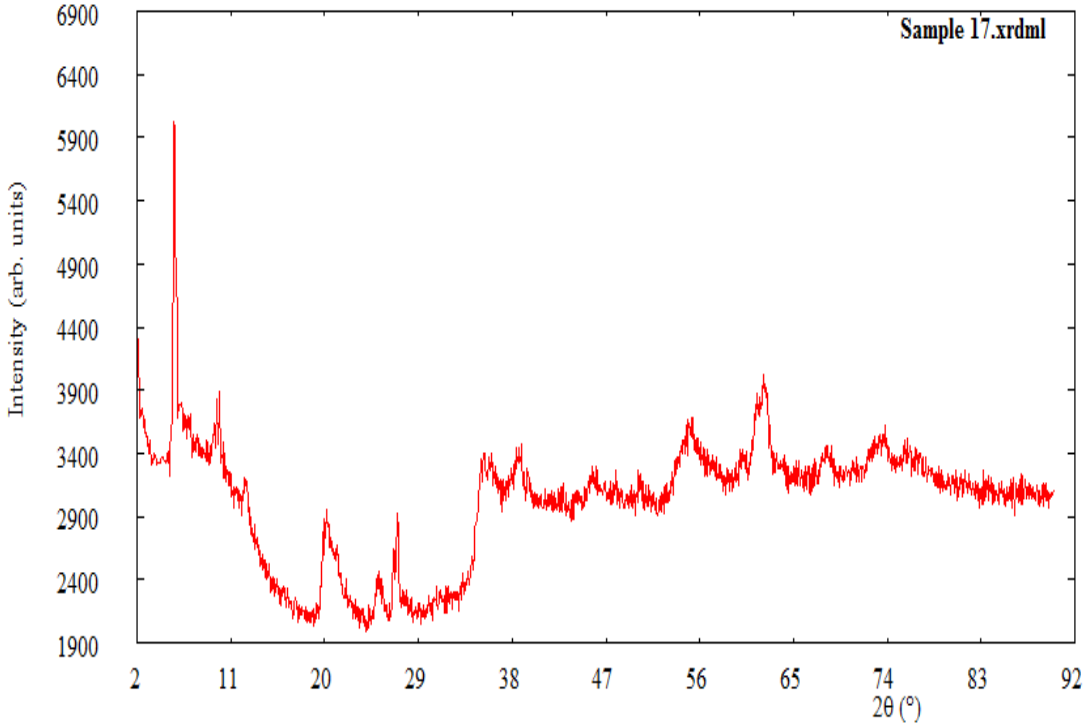
Appendix X: X-Ray diffractogram of sample 12



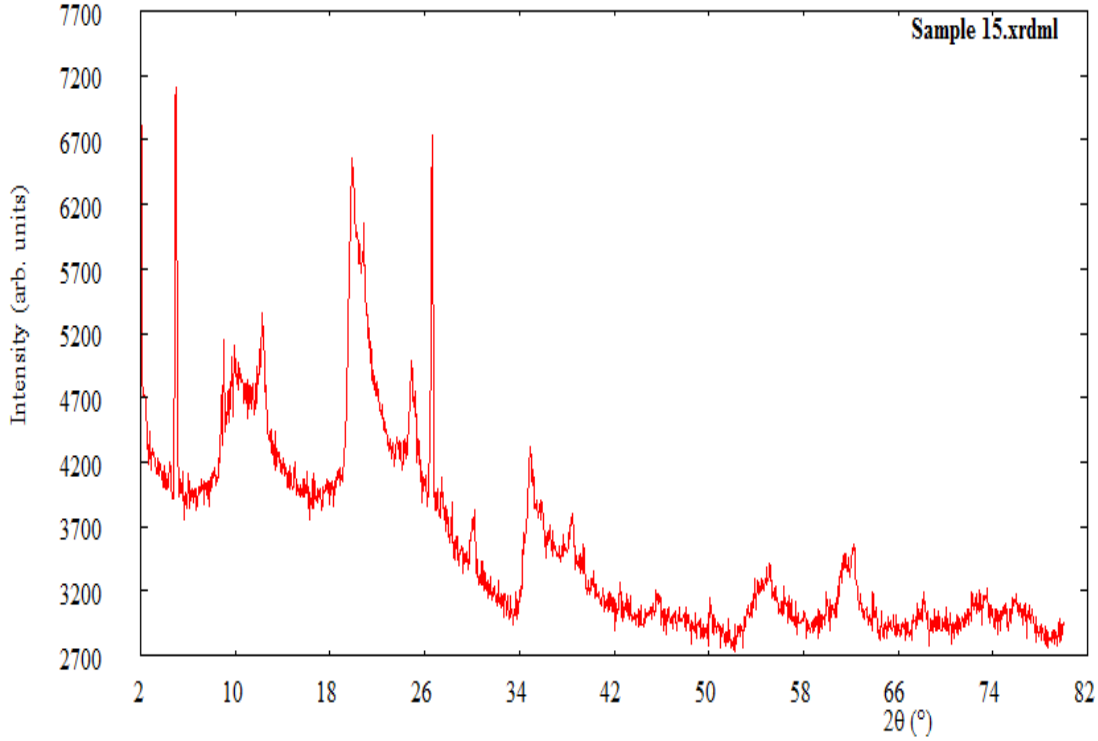
Appendix XI: X-Ray diffractogram of sample 13



Appendix XII: X-Ray diffractogram of sample 16



Appendix XIII: X-Ray diffractogram of sample 17

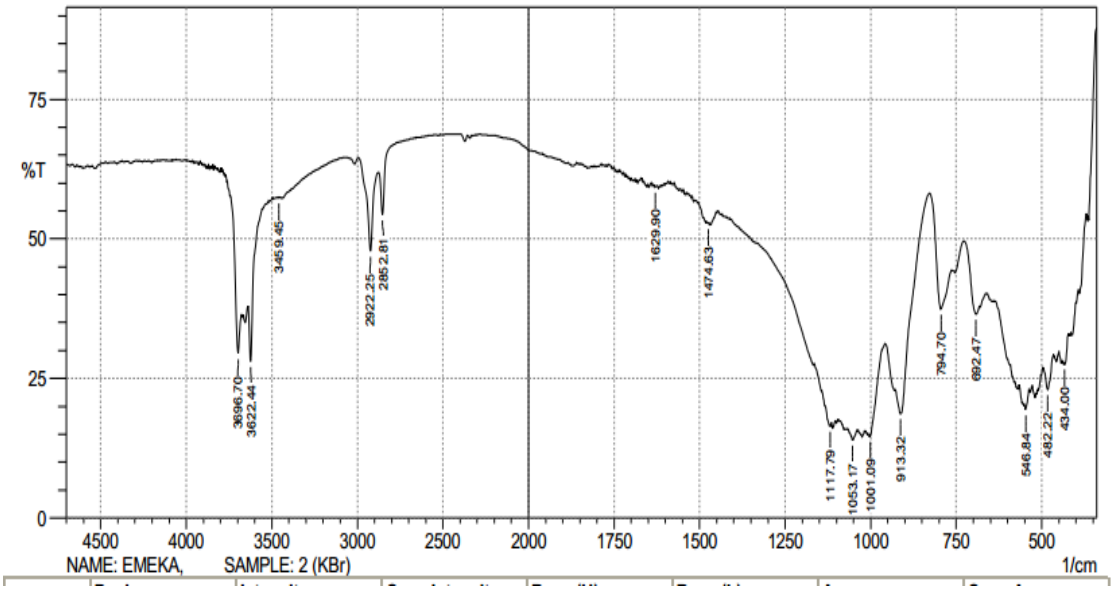


Appendix XIV: X-Ray diffractogram of sample 15

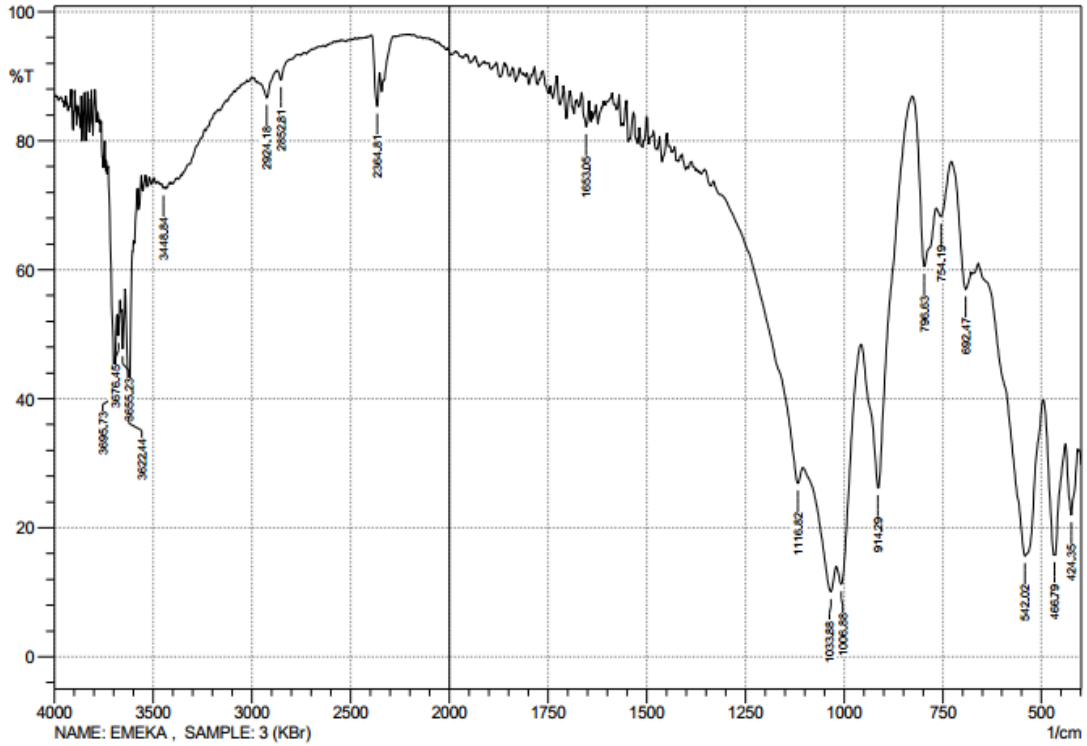
SHIMADZU

FTIR ANALYSIS RESULT NARICT,ZARIA

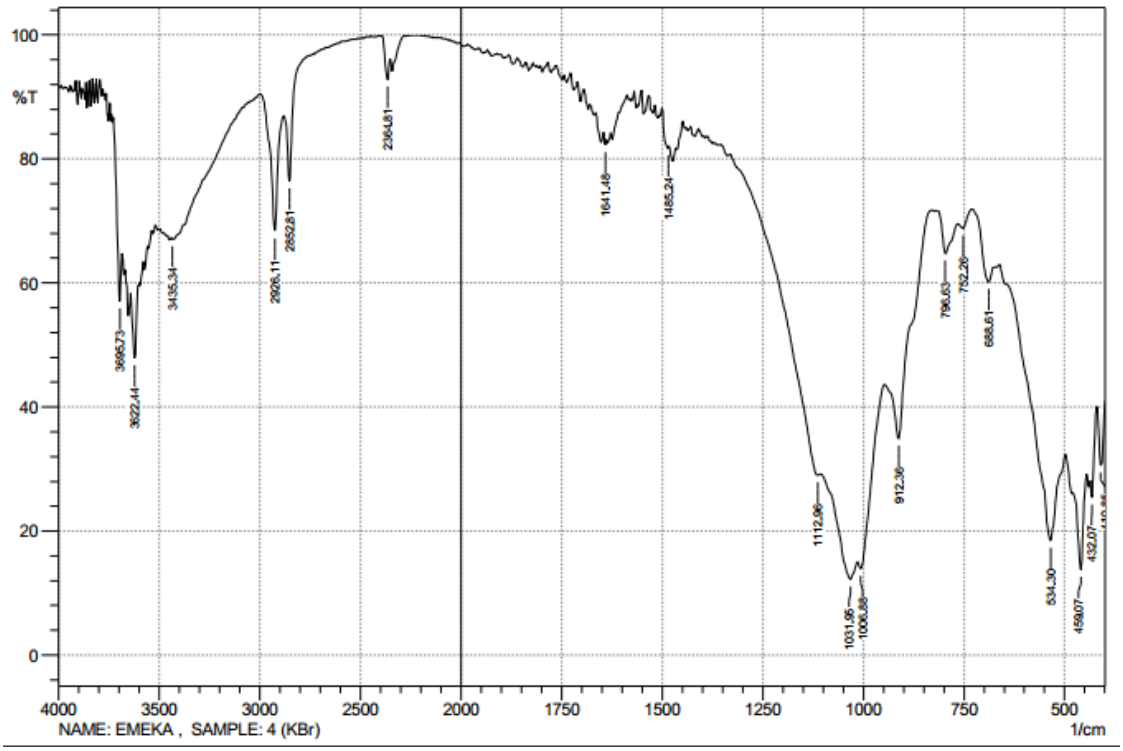
FTIR- 8400S FOURIER TRANSFORM INFRARED SPECTROPHOTOMETER



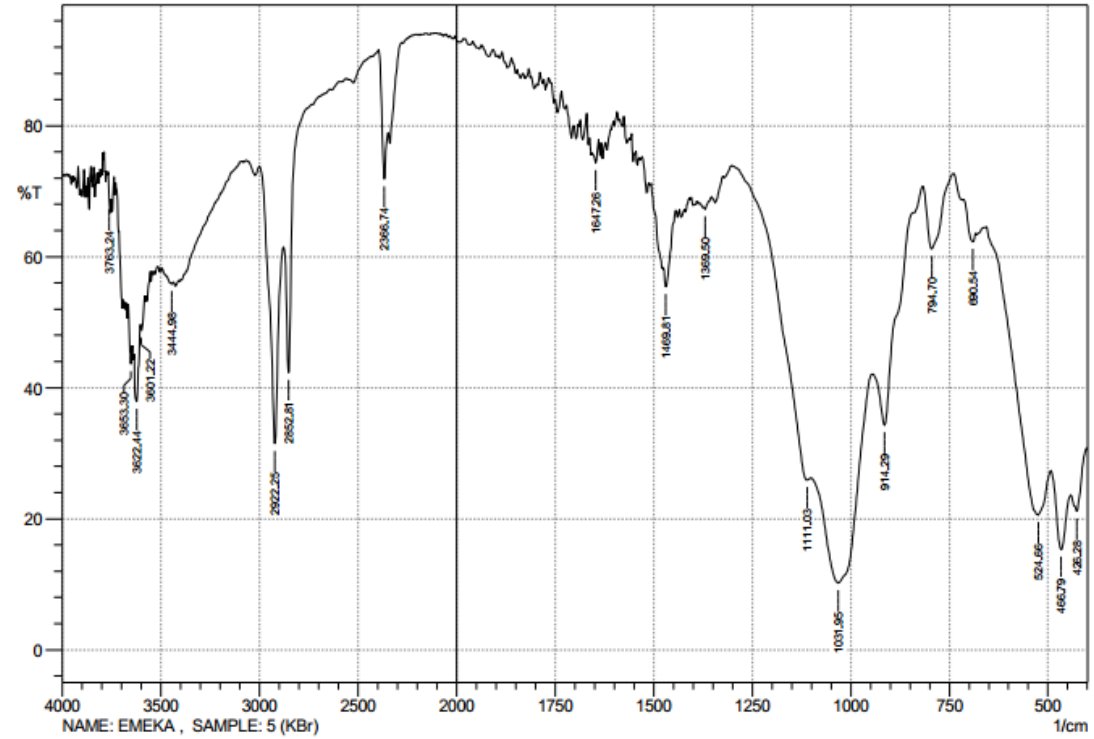
Appendix XV: FTIR Specttra of sample 2



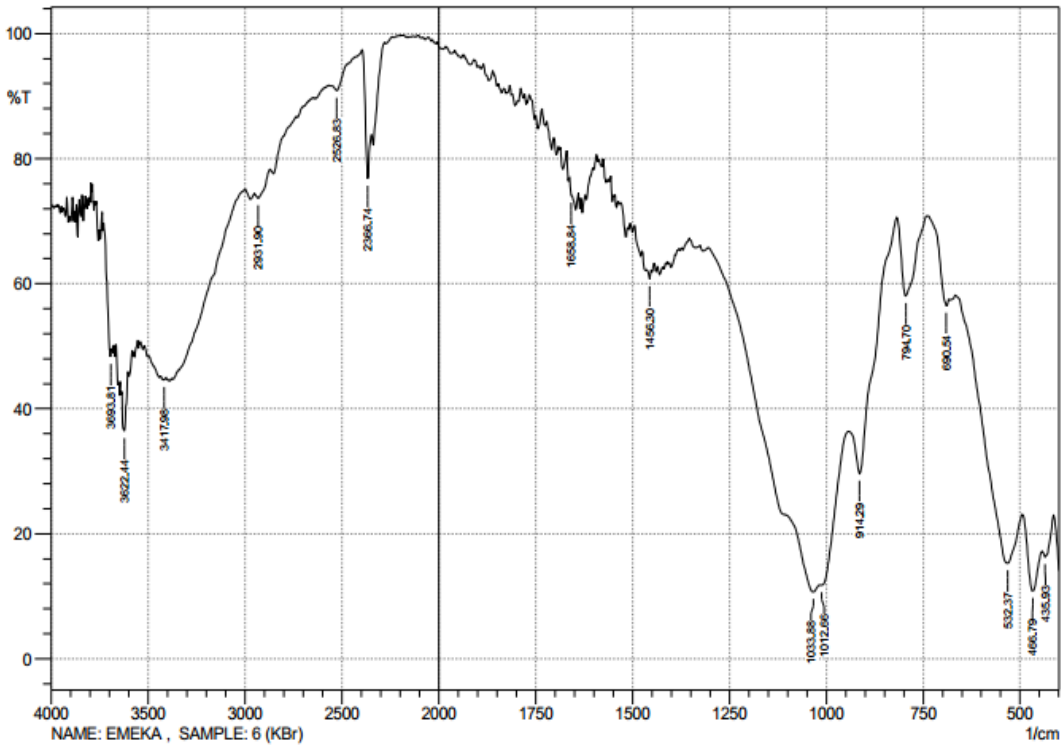
Appendix XVI: FTIR Specttra of sample 3



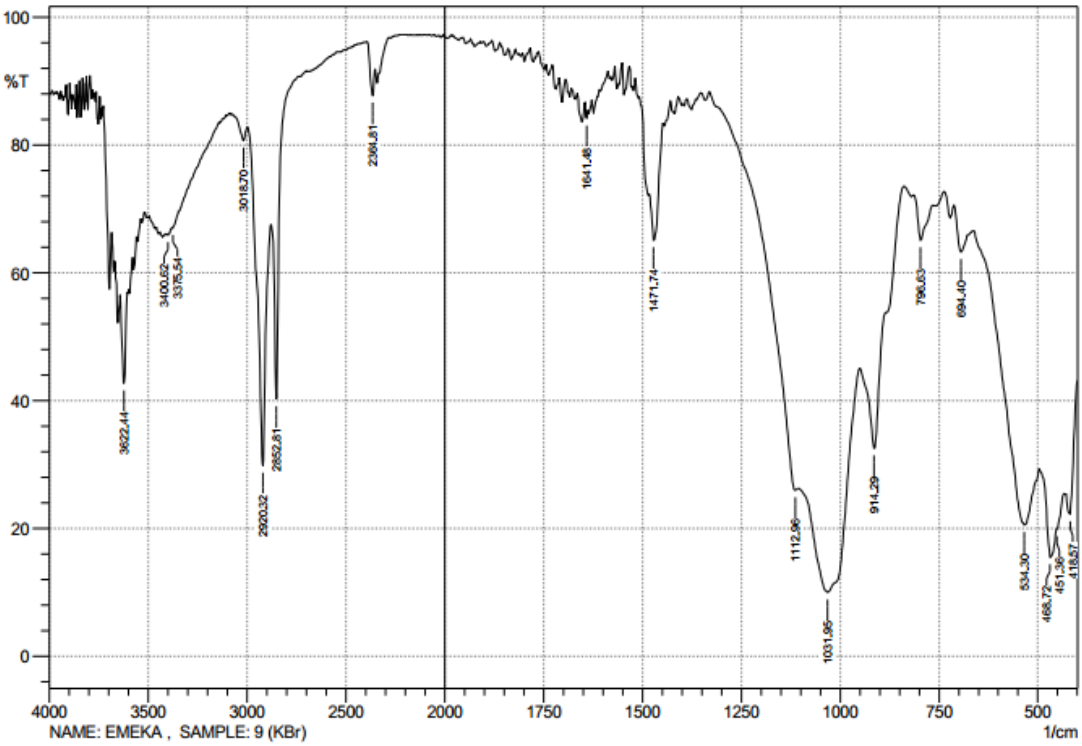
Appendix XVII: FTIR Specttra of sample 4



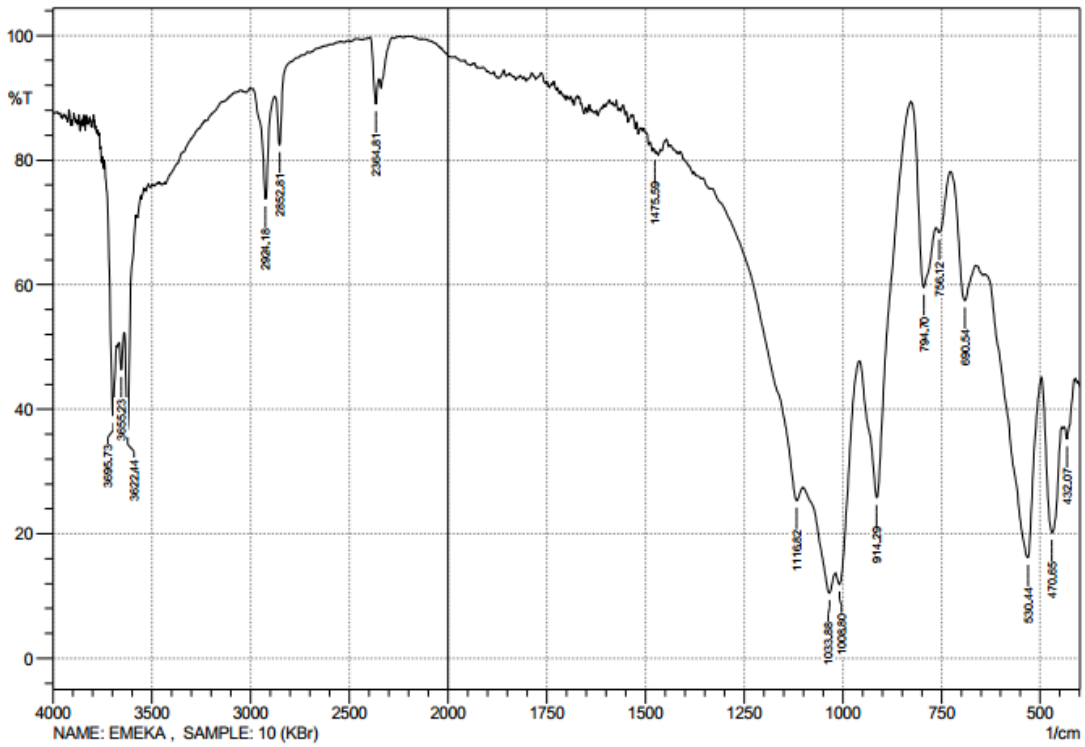
Appendix XVIII: FTIR Specttra of sample 5



Appendix XIX: FTIR Spectra of sample 6



Appendix XX: FTIR Spectra of sample 9



Appendix XXI: FTIR Spectra of sample 10